Negative Pressure Ventilation – *A New Frontier for Ex Vivo Lung Perfusion*

By

Nader Saber Aboelnazar

A thesis submitted in partial fulfillment of the requirements for the degree of

Master of Science

Department

of

Surgery

© Nader Saber Aboelnazar, 2019

Abstract

Lung transplantation is a life-saving therapy for patients suffering from end-stage lung disease; however, there exists a discrepancy between suitable donor grafts and utilization rates. At most, only 40% of offered donor lungs are utilized for transplantation. The majority are deemed unsuitable due to injury encountered during retrieval or cold preservation/transportation. To help mitigate the challenges facing lung transplantation, *Ex Vivo Lung Perfusion* (EVLP) was developed by a Swedish team in 2001. Since its inception, the platform's preservation, evaluation, and reconditioning capabilities has been extensively researched worldwide. EVLP preserves donor lungs under normothermic protective strategies. Over the years, lung grafts have tolerated at least 4-6-hours of EVLP preservation, in clinical settings, and up to 12-hours in preclinical settings. As such, EVLP could be an influential device in the field of lung transplantation – injured/unsuitable donor lungs objectively evaluated for their transplant suitability and a platform for precision repair medicine. However, further research is needed to continue refining EVLP as a preservation and evaluative platform.

Hence, this thesis aims to further elucidate potential enhancement strategies in perfusate and ventilation modalities during EVLP.

In the first project, we sought to investigate an answer to a 10-year old conundrum – what is the optimal perfusate during conventional, positive pressure ventilation (PPV)-EVLP? Our institution is faced with a unique geographical isolation where our patient catchment encompasses a 6 million km^2 area. Patients suffering from end-stage lung disease face odds of ~33% utilization rates of all donated grafts and waitlist mortality rates reported as high as 40%, in 2014. Therefore, our lab sought out to alleviate this burden by developing a portable custom-designed PPV-EVLP. Our platform captures in real-time various lung functional parameters; and as a portable platform

it will ensure safer retrieval of suitable lung allografts. Normothermic preservation reduces the damage insulted to donated organs, compared to limited conventional cold preservation. As such, we began the journey to resolve the aforementioned conundrum with investigations on twenty-four porcine lungs. We assessed the physiological and functional effects of either an acellular or cellular (autologous blood and red blood concentrate) perfusate strategy, on our open left atrium PPV-EVLP platform.

We demonstrated that the utilization of a physiologic perfusate (red blood concentrate or autologous blood) during extended (12-Hours) PPV-EVLP preserves lung compliance and maintains overall lung integrity. An acellular PPV-EVLP strategy significantly injured the organ, resulting in >50% in global edema formation, compared to either cellular based strategy. Moreover, compliance was found to be reduced with acellular treated lungs; but interestingly, compliance was only found to positively correlate with oxygenation and negatively correlate with edema formation, with a cellular based perfusate.

Having explored the optimal perfusate strategy during extended EVLP, in 2015 we theorized that a more physiologic ventilation modality (negative pressure ventilation - NPV) would further optimize our EVLP protocol. To-date, all clinically accepted EVLP platforms differ with regards to their protocol strategies (perfusion and ventilation strategies); however, they unanimously utilize the same ventilation modality, positive pressure ventilation. Despite extensive research demonstrating that positive pressure ventilation can result in ventilator induced lung injury. Our first project elucidated that the greater the mimicry of physiologic conditions in an ex vivo setting, the more we optimize reconditioning during EVLP; hence, preventing further injury to fragile/injured donor lungs. As such, we developed another portable, custom-designed NPV-EVLP platform. For the first time, the effect of ventilation and perfusate were concurrently under

investigation, during extended EVLP. Our second project included thirty-two porcine lungs, allocated randomly and equally into four treatment groups – mode of ventilation (PPV-EVLP versus NPV-EVLP) and perfusate composition (acellular versus red blood concentrate). Additionally, the impact of ventilation strategy was investigated on six unsuitable/injured human donor lungs, using only a cellular based perfusate.

Irrespective of perfusate, the utility of NPV-EVLP compared to PPV-EVLP resulted in significantly attenuated barotrauma and volutrauma, inflammation and edema/lung injury. Additionally, the use of an acellular perfusate demonstrated significant edema formation (irrespective of ventilation strategy). Intriguingly, for the first time, we report human lungs subjected to extended NPV-EVLP demonstrating a "drying" effect – reduction in lung weight form baseline.

Overall, this thesis lays the foundation for future research to come, by establishing our own unique University of Alberta protocol with our innovative NPV-EVLP platform.

Preface

This thesis is an original work by Nader S. Aboelnazar. The research projects conducted in Chapter 4 and 5 received research ethics approval from the University of Alberta Research Ethics Board – Project name "Large animal model of cardiothoracic organ donation after brainstem death", No. AUP00001492, September 15, 2014. The Animal Care and Use Committee of the University of Alberta approved the experimental protocol. All animals received humane care in accordance to the "Principles of Laboratory Animal Care," formulated with the National Society for Medical Research.

Dr. Jayan Nagendran and Dr. Darren H. Freed are Co-Founders of TEVOSOL Inc. Nor me or any other contributors involved in the experiments conducted within this thesis have any financial relationship with a commercial entity that has an interest in the subject presented in Chapter 4 and 5 or other conflicts of interest to disclose. Chapter 4 of this thesis has been published as Aboelnazar NS, Himmat S, Hatami S, White CW, Burhani MS, Dromparis P, Matsumura N, Tian G, Dyck JRB, Mengel M, Freed DH, Nagendran J. "Negative pressure ventilation decreases inflammation and lung edema during normothermic ex-vivo lung perfusion." *Journal of Heart Lung Transplant*. 2018;37:520–30. The technical apparatus (EVLP platforms – NPV and PPV) referred to in Chapters 4 and 5 were designed and created by Dr. Darren H. Freed. I was responsible for conducting the ex vivo lung perfusion runs, cytokine analysis experiments, data collection, and manuscript composition. Dr. Sayed Himmat assisted with experiments and data collection; while statistical analysis of data was conducted by Dr. Sanaz Hatami and histopathology analysis was conducted by Dr. Peter Dromparis. Dr. Christopher W. White and Dr. Mohamad S. Burhani were directly involved in the surgical procedures involving procuring the lungs from the animals. Dr. Jayan Nagendran was the supervisory author and involved with project conceptualizing, and along with Dr. Darren H. Freed, both were involved in editing the published manuscript.

Experiments in Chapter 4 and 5 have been supported by grants from Canadian Institutes for Health Research - Canadian National Transplant Research Program (CIHR-CNTRP), the University Hospital Foundation (UHF), and in part by the Mazankowski Alberta Heart Institute – Gerald Averback Award in Cardiovascular Gene Therapy/Genomics and Vascular Biology.

The end of cover illustration is reprinted with the permission of Alex Konahin (https://www.behance.net/gallery/5118525/Anatomy-).

I dedicate this thesis to my family:

my wife, my parents, my sisters, and beloved grandmother.

Acknowledgements

First and foremost, I would like to extend my sincerest gratitude to my supervisors and mentors – Dr. Jayan Nagendran, Dr. Darren Freed, and Dr. Thomas Churchill. All of whom played independent pivotal roles throughout my personal and academic growth during this project and my time in the lab.

Dr. Jayan Nagendran, I cannot describe how grateful I am for you taking the chance on a recent Bachelor of Science graduate and providing me with the opportunity of a lifetime. From the first moment we sat down and discussed the potential possibilities to come from establishing an ex-vivo lung perfusion at this institute, I had a feeling this could potentially be the opportunity of a lifetime. Nevertheless, it was daunting to think of the steep learning curve ahead, which would involve deeper understanding of medical level lung physiology/pathophysiology, organ perfusion, and lung transplantation. Yet, you always were supportive and most importantly believed that I can step up to the challenge. Your support and motivation during the long perfusion nights in the lab, drove me to believe in my capabilities and the different perspective I brought to the project. As my mind developed from an undergraduate to a graduate level of thinking, so did my confidence in my ability to acquire the higher level of knowledge needed for this project. My personal and academic growth throughout the journey of this project truly would not have been possible, without your unconditional support. Thank you for inspiring me in wanting to become an academic clinician and instilling in me perseverance, work ethics, and confidence. All the lessons and growth I overcame in the lab have been invaluable life lessons, which I surely will carry with me, as I pursue my desired professional/life goals.

Dr. Darren Freed, your mentorship taught me the value of humbleness, work ethics, and the passion for research. Despite your busy schedule and title, your presence in the lab was always appreciated and demonstrated to us trainees the importance of being directly involved in one's projects. I have observed you stay late countless times during perfusion runs, constantly work on enhancing the EVLP platform and other ex-vivo organ platforms. You managed to help instil in us the motivation to think like scientists and 'outside-the-box.' Your innovative mind/thinking is truly an inspiration. I learned a tremendous amount by observing the way you think and finding myself amazed how you manage to find innovate solutions to various issues encountered

throughout the project. Thank you for your mentorship and facilitation in the development of my own inherent passion and sense of curiosity for translational research.

Dr. Thomas Churchill, from the first day and throughout the project, you have demonstrated nothing short of kindness and sincerity to me and all the other trainees in the program. Your exemplary leadership characteristics and genuine attitude to help any student in-need for academic or personal guidance, will always be appreciated. Thank you for your mentorship and all the guidance.

I would like to also acknowledge my gratitude for the Department of Surgery within the Faculty of Graduate Studies for their understanding and support. Also, my appreciation extends to all our funders who funded our experiments.

I am also indebted to my colleagues and friends in the lab. Without you, this project would have not been possible. Specifically, Sanaz Hatami thank you for your extensive help in organizing the lab, ordering analysis equipment, helping with the statistics and the countless guidance throughout my journey in the lab. Sayed Himmat, the brother I never had, thank you for all the help you offered during the long, sometime overnight, perfusion studies. Your friendly demeanor, positive attitude, and curious mind, no doubt helped me keep a positive outlook throughout this journey. I am grateful for all your guidance and your friendship. I wish you the best in your future perfusion endeavours and continuation of this project. Dr. Christopher White, you were and will always be an inspiration to me. Thank you for all the fundamental teachings, which you never hesitated to provide, your support and insight, and most of all, your positive attitude around the lab. You helped me make the necessary step to start thinking like a scientist. Dr. Mohamad Burhani, thank you for the personal guidance and for performing some of the surgical procurements. For our incredible pathology team, Dr. Peter Dromparis and his supervisor Dr. Michael Mengel, thank you for the guidance and all the timely analysis of all our histopathology data. I would also like to extend my gratitude to the medical students who contributed to the early perfusion experiments - Vishnu Vasanthan, Sabin Bozso, Jessica Luc, and Jaskiran Sandha . Last but not least, Almothana Alzamil for his guidance, advice, support during the early stages of this journey.

I am deeply indebted to my father and mother for their unconditional love, support, and faith in me. To my dear father, you truly are my role model and I aspire to one day be half the man

and surgeon you are. Words cannot describe how grateful I am for everything you both have given me. Thank you is an understatement.

Lastly, to my wife, I would like to earnestly express my love and gratitude for believing in my potential, vision, and aspirations. I look forward to experiencing all that will come, from the journey ahead of us.

Table of Contents

Chapter 1 | Background

1.1 | Anatomy of The Respiratory System ……... 2

1.1.1 Gross Anatomy ……... 3

1.1.2 The Respiratory Tree ……..……..... 5

1.1.3 Native Cells of The Respiratory System ……... 12

1.1.4 Pulmonary Circulation ……... 14

1.2 | Physiology of The Respiratory System ……... 16

1.2.1 Respiration Mechanics, Innervation, and Ventilation Rate ……. 16

1.2.2 Lung Compliance ……..... 20

1.2.3 Lung Volume and Capacity …… 22

1.2.4 Homeostasis and Gas Exchange ……. 24

1.2.4.1 Zones of The Human Lung …….. 28

1.2.4.2 Ventilation/Perfusion Mismatch …….. 30

1.3 | Immune Responses …….……. 31

1.3.1 Innate Immune Response …… 31

1.3.1.1 Innate Immune Cells …… 32

1.3.1.2 Innate Immune Receptors …… 34

1.3.1.3 Compliment System ……..… 37

1.3.2 Adaptive Immune Response ……... 38

1.3.2.1 T-Cell Activation ……. 38

1.3.2.2 B/Plasma-Cell Activation ……..... 39

1.4 | Clinical Significance: Disorders of The Respiratory System ……..… 39

1.4.1 Obstructive Disorders ……. 40

1.4.2 Restrictive Disorders ……... 40

1.4.3 Vascular Disorders …….. 41

1.4.4 Acute Lung Injury & Acute Respiratory Distress Syndrome ……. 41

Chapter 2 | Literature Review

2.1 | Lung Transplantation ……. 47
2.1.1 History and Outcomes …… 47
2.1.2 Organ Shortage ……... 49
2.1.2.1 Donor Lung Criteria ……. 49
2.1.2.2 Donor Lung Injury ……... 50
2.1.3 Strategies for Increasing Lung Transplant Volumes …….. 53
2.1.4 Primary Graft Dysfunction ……. 59
2.2 | Lung Preservation Techniques ……. 62
2.2.1 Gold Standard Procurement and Preservation Strategies ……... 62
2.3 | Normothermic Preservation – Ex Vivo Lung Perfusion (EVLP) …… 64
2.3.1 EVLP: Preservation ……..... 64
2.3.2 EVLP: Protocols ……..... 66
2.3.2.1 Toronto Protocol ……..... 66
2.3.2.2 Lund Protocol ……..... 67
2.3.2.3 OCS Lung™ Protocol ……..... 67
2.3.3 EVLP: Evaluation ……..... 68
2.3.3.1 Physiologic Evaluation …… 69
2.3.3.2 Ventilator Induced Lung Injury ……... 71
2.3.4 EVLP: Reconditioning …… 73
2.4 | Summary ……..... 75

Chapter 3 | Rationale, Objectives and Hypotheses

3.1 | Rationale ……..... 79
3.2 | Hypotheses ……... 81
3.3 | Objectives ……...……..... 81

Chapter 4 | Ex-Vivo Lung Perfusion: Cellular Perfusate Preserves Lung Compliance and Lung Integrity

4.1 | Abstract ……..... 83

4.2 | Introduction ……..... 85
4.3 | Materials and Methods ……..... 86
4.3.1 Animal Model ……..... 86
4.3.2 EVLP Treatment Groups ……..... 87
4.3.3 Lung Procurement ……..... 88
4.3.4 Custom EVLP Platform ……..... 88
4.3.5 Initiation of EVLP (U of A Protocol) ……..... 90
4.3.6 Organ Assessment ……..... 93
4.3.6.1 Physiological Parameters ……... 93
4.3.6.2 Inflammatory Markers ……..... 93
4.3.6.3 Histopathological Assessment and Edema Formation ……..…. 93
4.3.7 Statistics …… 94
4.4 | Results ……..... 94
4.4.1 Lung Oxygenation ……..... 94
4.4.2 Pulmonary Vascular Resistance and Pulmonary Arterial Pressure …….. 95
4.4.3 Dynamic Compliance and Plateau Pressure ……. 96
4.4.4 Inflammatory Cytokine Analysis ……. 97
4.4.5 Edema Formation and Lung Injury …….. 98
4.4.6 Unique Perfusate Correlation with Compliance, Pulmonary Vascular Resistance, Oxygenation and Edema …….. 100
4.5 | Discussion ……..... 100

Chapter 5 | Negative Pressure Ventilation Decreases Ventilator Induced Lung Injury during Normothermic Ex-Vivo Lung Perfusion

5.1 | Abstract ……..... 112
5.2 | Introduction ……..... 113
5.3 | Materials and Methods ……..... 113
5.3.1 Perfusate Solutions ……..... 115
5.3.1.1 Porcine Experiments ……..... 115
5.3.1.2 Human Experiments ……..... 116
5.3.2 Ex Vivo Lung Perfusion ……..... 116

5.3.2.1 PPV Platform 117
5.3.2.2 NPV Platform 117
5.3.3 Initiation of EVLP (U of A Protocol) 117
5.3.4 Organ Assessment 120
5.3.4.1 Physiological Parameters 120
5.3.4.2 Inflammatory Markers 121
5.3.4.3 Lung Injury and Edema Formation 121
5.3.5 Statistics 121
5.4 | Results 122
5.4.1 Lung Oxygenation 122
5.4.2 Pulmonary Vascular Resistance and Pulmonary Arterial Pressure 122
5.4.3 Dynamic Compliance and Peak Airway Pressure 123
5.4.4 Inflammatory Cytokine Analysis 125
5.4.5 Lung Injury and Edema Formation 126
5.5 | Discussion 128

Chapter 6 | Summary and Future Directions

6.1 | Summary and Limitations 134
6.2 | Future Directions 138
6.2.1 Re-Transplantation: Porcine and Human Models 138
6.2.2 EVLP: Potential Biomarkers 140
6.2.2.1 Damage-associated molecular patterns 141
6.2.2.2 Glycocalyx 144
6.2.3 EVLP: Potential Therapeutic Avenues 148
6.2.3.1 Von Willebrand Factor 148
6.2.3.2 Drug Therapy 150
6.2.3.3 Gene Therapy 151
6.2.4 NPV-EVLP: A New Frontier 155
6.2.4.1 Expanding the Therapeutic Window (24-Hours) 155
6.2.4.2 Tissue Bioengineering 156
6.2.4.3 Artificial Intelligence: The Lung Whisperer 160

6.3 | Concluding Remarks ……..... 165

Bibliography

List of Figures

Figure 1: Anatomy of the human respiratory system

Figure 2: Anatomy of the alveolar-capillary interface

Figure 3: Lung volumes, capacities and gender differences

Figure 4: Representation of **(A)** internal respiration and **(B)** external respiration

Figure 5: West Zones - pulmonary blood flow

Figure 6: ARDS pathogenesis

Figure 7: ISHLT Kaplan-Meier bilateral and unilateral adult lung transplantation outcomes

Figure 8: Brain death inducing ALI

Figure 9: Organ donation rates in Canada, 2007-2016

Figure 10: Total number of organ donation types in Canada, 2012-2016

Figure 11: Comparison between clinical EVLP protocols

Figure 12: The iron lung ventilator

Figure 13: Advantages and disadvantages of EVLP

Figure 14: **(A)** Simplified experimental protocol and **(B)** custom-built PPV-EVLP platform schematic

Figure 15: Perfusate comparison of lung oxygenations

Figure 16: Perfusate comparison of **(A)** mPAP and **(B)** PVR

Figure 17: Perfusate comparison of **(A)** plateau pressures and **(B)** dynamic compliance

Figure 18: Perfusate comparison of inflammatory cytokine production

Figure 19: Perfusate comparison of lung edema after extended PPV-EVLP

Figure 20: **(A-C)** Representative photomicrographs and **(D-I)** histopathological lung injury scores after extended PPV-EVLP

Figure 21: **(A)** Representation of experimental protocol, **(B)** custom built NPV-EVLP platform schematic and **(C)** functional software interface recording

Figure 22: **(A,B)** Porcine and **(C)** human lung oxygenations (NPV and PPV strategies)

Figure 23: **(A,B,D,E)** Porcine and **(C,F)** human lungs mPAP and PVR (NPV and PPV strategies)

Figure 24: **(A,B,D,E)** Porcine and **(C,F)** human lung P_{AWP} and C_{dyn} (NPV and PPV strategies)

Figure 25: **(A-F)** Porcine and **(G-I)** human lung inflammatory expressions (NPV and PPV strategies)

Figure 26: **(A,B)** Porcine lung bullae and edema formation and **(C)** human lung edema at 12-hours (NPV and PPV strategies)

Figure 27: **(A-F)** Representative photomicrographs and **(G-L)** histopathology human lung injury scores after 12-hours of EVLP (NPV and PPV strategies)

Figure 28: Interactions between DAMPs and TLRs

Figure 29: Electron microscopy of the endothelial glycocalyx layer

Figure 30: Schematic representation of the glycocalyx components

Figure 31: Human lungs undergoing decellularization in a bioreactor

Figure 32: The *Lung Whisperer* – NPV-EVLP

List of Tables

Table 1: Berlin definition of ARDS

Table 2: Risk factors for ARDS

Table 3: Maastricht categories for DCD

Table 4: ISHLT PGD grading

Table 5: EVLP perfusate characteristic

Table 6: **(A)** Initiating reperfusion and **(B)** ventilation strategies for PPV-EVLP

Table 7: Initiation of EVLP (NPV or PPV)

Table 8: NPV and PPV ventilation strategy

Table 9: Unutilized human donor lung characteristics

List of Abbreviations

EVLP	Ex Vivo Lung Perfusion
$EVLP_A$	Acellular-EVLP
$EVLP_B$	Whole/Autologous Blood-EVLP
$EVLP_R$	pRBCs/RBCs-EVLP
PPV	Positive Pressure Ventilation
NPV	Negative Pressure Ventilation
AI	Artificial Intelligence
ALI	Acute Lung Injury
APCs	Antigen Presenting Cells
ARDS	Acute Respiratory Distress Syndrome
BAL	Bronchoalveolar Lavage
BDD	Brain Dead Donor
BOS	Bronchiolitis Obliterans Syndrome
C_{Dyn}	Dynamic Lung Compliance
C_{Stat}	Static Lung Compliance
CF	Cystic Fibrosis
COPD	Chronic Obstructive Pulmonary Disease
CLRs	C-Type Lectin Receptors
CO	Cardiac Output
CRISPER	Clustered Regularly Interspaced Short Palindromic Repeats
CSP	Cold Static Preservation
DAMPs	Damage Associate Molecular Patterns
DBD	Donation after Brain Death
DCD	Donation after Cardiac Death
EEP	End-Expiratory Pressure
EIP	End-Inspiratory Pressure
ERV	Expiratory Reserve Volume
EVLP	Ex Vivo Lung Perfusion

FEV_1	Forced expiratory Volume at 1-Second
FRC	Functional Residual Capacity
FVC	Forced Vital Capacity
GAGs	Glycosaminoglycans
Hct	Hematocrit
HMGB1	High Mobility Group Box-1
HSP	Heat Shock Protein
IC	Inspiratory Capacity
IL-8	Interleukin-8
IL-6	Interleukin-6
IL-1β	Interleukin-1-Beta
IL-10	Interleukin-10
ILD	Interstitial Lung Disease
IPP	Intrapulmonary Pressure
IRAK	Interleukin Receptor Associated Kinase
IRI	Ischemia Reperfusion Injury
IRV	Inspiratory Reserve Volume
ISHLT	International Society for Heart and Lung Transplantation
ITP	Intrapleural/Intrathoracic Pressure
KHB-A	Krebs-Henseleit Buffer with Albumin
LA	Left Atrium
LAP	Left Atrial Pressure
LPD	Low Potassium Dextran
MHCs	Major Histocompatibility Complexes
ML	Machine Learning
MSCs	Mesenchymal Stem Cells
MV/V_E	Minute Ventilation
NF-κB	Nuclear Factor Kappa light-chain
NK	Natural Killer Cells
NLRs	NOD-Like Receptors
NLRP	NOD-Like Receptor Inflammasome

NO	Nitric Oxide
NOD	Nucleotide-Binding Oligomerization Domain
OCS™	Organ Care System™
PA	Pulmonary Artery
PAH	Pulmonary Arterial Hypertension
PAMPs	Pathogen Associated Molecular Patterns
P_aO_2/Fi O_2	Ratio of Partial Pressure of Arterial Oxygen to Fraction of Inspired Oxygen
PAP	Pulmonary Artery Pressure
P_{AW}	Airway Pressure
PCO_2	Partial Pressure of carbon dioxide
PEEP	Positive End-Expiratory Pressure
PGD	Primary Graft Dysfunction
PIP/P_{AWP}	Peak Inspiratory Pressure/Peak Airway Pressure
PO_2/P_aO_2	Partial Pressure of Oxygen/Arterial Partial Pressure of Oxygen
P_{Plat}	Plateau Pressure
pRBCs/RBCs	Packed/Concentrated Red Blood Cells
PRRs	Pattern Recognition Receptors
PVR	Pulmonary Vascular Resistance
Q	Lung Perfusion
RK	Receptor Kinases
ROS	Reactive Oxygen Species
RR/f	Respiratory Rate/Frequency
RV	Residual Volume
sICAM	Soluble Intercellular Adhesion Molecule
sIVCAM	Soluble Vascular Cell Adhesion Molecule
sRAGE	Soluble Receptor for Advanced Glycation End Products
TLC	Total Lung Capacity
TLRs	Toll-Like Receptors
TNF-α	Tumor Necrosis Factor-Alpha
TPG	Transpulmonary Air Pressure Gradient
TPP	Transpulmonary Pressure

V	Lung Ventilation
V_A	Alveolar Ventilation
VC	Vital Capacity
V_D	Dead Air Space/Volume
VEGF	Vascular Endothelial Growth Factor
VILI	Ventilator Induced Lung Injury
V/Q	Lung Ventilation/Lung Perfusion
V_T	Tidal Volume
vWF	Von Willebrand Factor

Chapter 1

Background

1.1| Anatomy of The Respiratory System

The human respiratory system has six fundamental functions:[1,2]

I. Gaseous exchange – important for the cellular fundamental process of cellular respiration and the regulation of the blood's hydrogen ion concentration (pH), along with the kidneys.

II. Production of sound – vibration of the vocal cords during expiration.

III. Olfaction – the integration of the olfactory sensation has been shown to play an importance with interconnections in memory and language; additionally, with social and emotional perception.[3]

IV. Abdominal compression – during parturition, micturition, and defecation.

V. Coughing and sneezing – self-cleaning reflexes.

VI. Defense – Against any airborne microbes entering from the outside environment into the body.

The system is divided into an upper and lower structural division; furthermore, into functional divisions, a conducting and respiratory division. Respiration involves three different, yet inter-related functions, a) ventilation/breathing, b) gaseous exchange, and c) oxygen utilization. External respiration will refer to ventilation and gaseous exchange at the alveoli-capillary/blood interface. While internal respiration refers to the gaseous exchange between the blood and tissue.[1,2] Both external and internal respiration are fundamentally important in maintaining cellular respiration homeostasis: without sufficient oxygen (O_2) the body's tissues cannot produce sufficient amounts of ATP and the accumulation of waste products, including carbon dioxide (CO_2), results in deleterious effects on the tissues.

1.1.1 **Gross Anatomy**

The human lung differs in the number of lobes present for the right and left lungs. The left lung is composed of two lobes (superior and inferior), with the lingual resembling a middle lobe; while the right has three lobes (superior, middle, and inferior) (**Figure 1**).[1,2] The right lung has the horizontal fissure separating the superior and middle lobes, and the oblique fissure separating the middle and inferior lobes. The left lung has only the oblique fissure to separate the superior and inferior lobes (**Figure 1**).[1,2] Each lung can be further divided into bronchopulmonary segments, which possess their own bronchus, arterial supply and venous drainage; thus, each segment is capable of functioning separately, which permits the capability of removing a segment without the rest of the segments getting effected.[1,2]

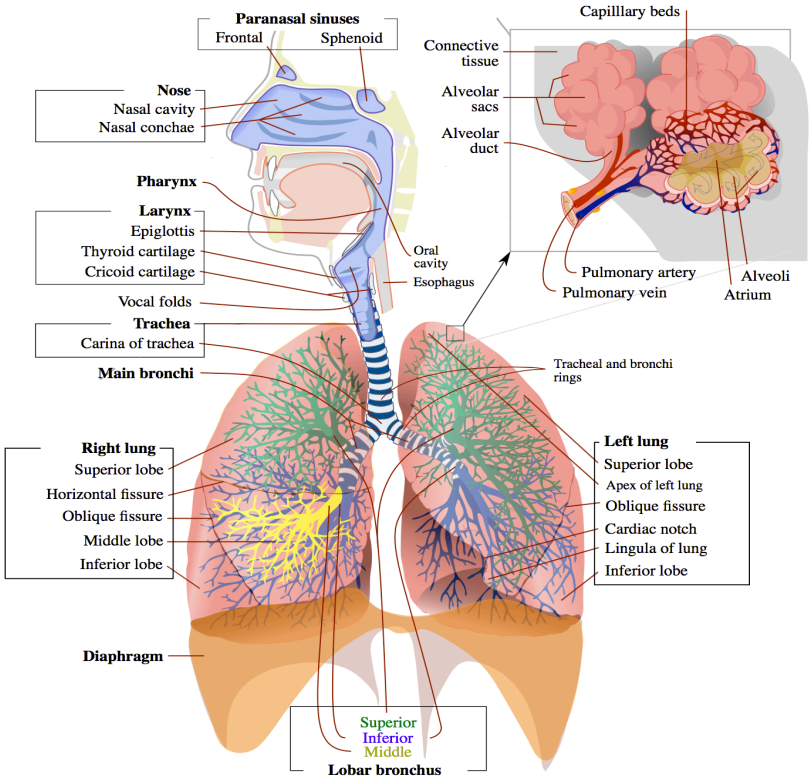

Figure 1: Anatomy of the human respiratory system. Adapted from Ignatavicius *et al.*[4,5]

The right lung is comprised of ten segments: a) superior lobe: apical, posterior, and anterior segments, b) middle lobe: lateral and medial segments, c) inferior lobe: superior, medial basal, anterior basal, lateral basal, and posterior basal segments. On the contrary, the left lung is comprised of eight segments: a) superior lobe: apical posterior, anterior, superior lingular, and inferior lingular segments, b) inferior lobe: superior, anteromedial basal, lateral basal, and posterior basal segments.[6] Each lung contains three borders/surfaces that match the contour of the thoracic cavity:[1]

I. Mediastinal surface: slightly concave with a vertical indentation known as the hilum.
II. Diaphragmatic surface: the inferior base of the lung contacts with the diaphragm.
III. Costal surface: the apex of the lung, has the rounded surface in contact with membranes covering the ribs.

The mediastinum refers to the area between the two lungs, which contains the heart, great vessels, lymphatics, and the esophagus.[1,7,8] The root of the lungs (hilum) occupy a portion of the mediastinal area and it is at this location that the visceral and parietal pleural membranes form a sheath around the primary bronchi, pulmonary vessels, and branches of the vagus nerve, where they enter and exit each lung.[1,7-9] The pleura is a thin double-layered serosa membrane that lines the surface of the lungs and the inside of the chest wall; the pleura are composed of simple squamous epithelium and fibrous connective tissue.[1,7-9] The inner layer, visceral pleurae, adheres to the surface of the lungs, extends to the hilar bronchi and into the major fissures.[1,7-9] The outer layer, parietal pleurae, lines the inner surface of the chest wall and mediastinum. The pleura are separated by an airtight space, intrapleural space (pleural cavity), which contains a lubricating fluid secreted by the two membranes.[1,7-9] This pleural fluid permits the gliding of the visceral and

parietal pleural membranes against each other during inhalation and exhalation; along with aiding in a) maintaining a resting negative intrathoracic/intrapleural pressure (compared to atmospheric pressure), and b) the process of inhalation. The average human lungs can weigh between 900-1000g and approximately 40% of the weight can be attributed to the volume of blood circulating through the lungs.[10,11]

1.1.2 **The Respiratory Tree**

The upper respiratory tract is characterized by the nose and nasal cavity, paranasal sinuses (frontal and sphenoid), and the pharynx; while the lower respiratory tract (tracheobronchial tree) is composed of the larynx, trachea, bronchial tree, alveoli and lungs.[12]

The structural division of the tracts can be further divided into their respective functional division. The conducting zone of the respiratory airway helps transport, warm, humidify, and filter the air that is delivered from the nose to the end of the conducting zone of the lower respiratory tract (terminal bronchioles).[1,13] As air enters the nasal cavity, macro-particulates are immediately filtered by the nasal hairs (vibrissae); dust, pollen, smoke and finer particulates are trapped via the mucus layer. The mucus layer is produced by mucus secreting cells (goblet cells) within the pseudostratified ciliated columnar epithelium (respiratory epithelium), which lines the airway from the nasal cavity/fossae to the bronchioles.[1,4] The nasal cavity consists of three bone like structures (conchae/turbinates) which protrude in the cavity, are highly vascularized, and are lined with a mucus layer. These conchae increase the total surface area for filtering, heating, and humidifying the air that passes into the nasopharynx.[4] The nasal cavity is also responsible for the olfactory sensation via the receptors from the olfactory nerve. The olfactory epithelium is composed of specialized columnar epithelium, which lines the upper medial portion of the nasal cavity.[1,2,4]

The pharynx acts as a passageway for both respiratory and digestive tracts; is further divided based on location and function. The pharynx can be divided into three parts,

a) Nasopharynx – contains the Eustachian (auditory) canals and pharyngeal tonsils (adenoids). The nasopharynx serves only a respiratory function and is located at the base of skull/behind the nasal cavity and above the soft palate.[1,4]

b) Oropharynx – contains the uvula, tonsils (lingual and palatine), and the epiglottis. This location lies behind the oral cavity, below the nasopharynx, extends from the uvula to the level of the hyoid bone, and serves respiratory and digestive functions. As food passes through and is swallowed, the pendulous uvula and soft palate will elevate and close off the nasal cavity; while the epiglottis closes/covers the glottis, to prevent aspiration. The tonsils (nasopharynx/oropharynx) serve as defense against foreign invasion of organisms. The oropharynx is composed of non-keratinized stratified squamous epithelium and is innervated by the pharyngeal plexus (pharyngeal branches of the glossopharyngeal and vagus nerve).[1,4]

c) Laryngopharynx (hypopharynx) – this is an area that represents the caudal part of the pharynx (base of the tongue), which extends and connects the throat to the esophagus. The laryngopharynx is located inferior to the epiglottis and posterior to the larynx. It is a critical common pathway that separates air and food/fluids into the respiratory (larynx; anteriorly) and digestive (esophagus; posteriorly) pathways, respectively. During swallowing, food will have the "right of way", and air passage will temporarily stop. The laryngopharynx is also composed of stratified squamous epithelium and is innervated by the pharyngeal plexus (pharyngeal branches of the glossopharyngeal and vagus nerve).[1,4]

Air continues into the larynx (voice box), which is located above the trachea and represents the beginning and conduit of air to the lower respiratory tract. The larynx serves as a protection to

the trachea against food aspiration and sound production. The larynx is made of six hyaline cartilages: three unpaired and three paired. The three unpaired cartilages consist of:

I. Thyroid cartilage – it is the largest and forms the "Adam's apple". It is connected to the hyoid bone via the thyrohyoid membrane.[1,4,6]

II. Epiglottis – large spoon-shaped elastic cartilage, with hinge-like actions. During swallowing, the pharynx and larynx rise, resulting in the pharynx to widen to receive the food/fluids; while the elevation of the larynx will result in the closing of the glottis against the epiglottis. During breathing and coughing, the epiglottis remains uncovered/opened.[1,4]

III. Cricoid cartilage – a ring of (C) cartilage that forms the lower portion of the larynx and attaches to the top of the trachea. The cricothyroid ligament/membrane joins the thyroid and cricoid cartilages, and is located below the level of the vocal cords.[1,4]

The three paired cartilages consist of:

a) Arytenoid cartilages – of the three paired cartilages, the arytenoid cartilages are the most influential with the position and tension of the vocal cords. Made mostly of hyaline cartilage and located at the posterosuperior border of the cricoid cartilage.[1,4,6]

b) Cuneiform cartilage – aids the arytenoid cartilages, is "club"-shaped pieces of elastic cartilage and is located anterior to the corniculate cartilages.[1,4,6]

c) Corniculate cartilages – also aids the arytenoid cartilages, is "horn"-shaped pieces of elastic cartilage and is located at the apex of each arytenoid cartilage.[1,4,6]

The innervation of the extrinsic laryngeal muscles causes either the elevation or depression of the larynx during/after swallowing. Innervation of the intrinsic laryngeal muscles maintains the

vocal cords patent during breathing; while innervation of respiratory and phonatory muscles causes manipulation of pitch/volume during sound production. These laryngeal muscles are innervated by the superior and recurrent laryngeal nerve branches, which arise from the vagus nerve: the superior laryngeal nerve innervates only the cricothyroid muscle of the intrinsic laryngeal muscles, while the recurrent laryngeal nerve innervates all other intrinsic and extrinsic laryngeal muscles.[1,14] The laryngeal muscles do not completely relax during rapid eye movement (REM) sleep, along with the diaphragm. They also maintain the upper airway open during the negative intrathoracic pressure that is induced during inspiration; which tends to pull the upper airway closed.[1,2,14]

The larynx opens into the trachea which in turn bifurcates at the carina and gives rise to the extensive asymmetrical bronchial tree. The trachea is a cartilaginous and fibromuscular tube that extends from the inferior aspect of the cricoid cartilage (6^{th} cervical vertebra level) to the carina (5^{th} thoracic vertebra level: aortic arch). made of four different tissue layers is considered to be on average 10-12 cm in adults, and varies in diameter between men (1.3 cm – 2.6 cm) and women (1.0 cm – 2.1cm).[9,15] The composition of the trachea permits it to, maintain its rigidity, patency, aid in coughing, protect from frontal injury, moistens/warms and clearance of foreign particulate. The four tissue layers that comprise the trachea:[8,9]

I. Mucosa – the innermost layer of the epithelium which is lined and consists of ciliated pseudostratified columnar epithelium (respiratory epithelium), goblet cells (produce mucins/mucus), and connective tissue. The mucus acts a blanket covering the hair-like cilia that are on the surface of the columnar cells. This serves to maintain the air inhaled moist and warmed as it travels down the bronchial tree, while trapping inhaled foreign particles and preventing them from reaching the alveoli. The entire mucus blanket and trapped foreign particulates trapped will be transferred upward toward the laryngopharynx to be

coughed or swallowed, respectively, in a unidirectional rhythmic beating fashion. This self-clearing mechanism is termed mucociliary escalator/clearance and occurs at an average of 12 mm/min (trachea and large airways) and 1 mm/min (smaller bronchioles).[8]

II. Submucosa – is made of areolar connective tissue that contains seromucous glands, blood vessels, lymph vessels, nerves, collagen, elastic fibers, and trachealis (longitudinal smooth) muscle. The trachealis muscle is present in the posterior wall of the trachea, and anterior to the adjoining esophagus along the tracheoesophageal stripe.[6,8,9] Since the posterior wall of the trachea lacks cartilage, the airway lumen diameter can be reduced, allowing for a more forceful and effective expulsion of irritants during coughing.[1,8,9,15] Moreover, during swallowing, the esophagus is permitted to expand at the tracheoesophageal stripe.

III. Hyaline cartilage – surrounding the submucosa layer, 16-20 incomplete C-shaped rings stack to reinforce the front and sides of the trachea, to protect and prevent collapse of the airway during the negative intrathoracic/pleural pressure induced with inspiration. These incomplete rings are all C-shaped with their ends connected by the trachealis muscle in the posterior wall of the trachea, except for the first ring (cricoid cartilage).[6,8,9] The trachea rings are connected via circular horizontal bands of fibrous tissue called the annular ligaments of the trachea.[6,9]

IV. Adventitia – the outermost layer of the trachea wall, which consists of areolar connective tissue sheath that loosely anchors the trachea to surrounding soft tissues. Therefore, permitting movement within the neck and thorax, which aids the lungs in their expansion and contraction during ventilation.[1,8,9,15]

At the level of the carina, the asymmetrical division of the bronchial tree begins and produces approximately 23 generations of branches. With each division/generation, the

appearance of two or more smaller diameter airways are evident. The primary/main bronchi are the 1st generation and are asymmetrically different from one another. The left main bronchus is considered to have a smaller diameter than the right main bronchus, and since it is situated above the heart, it enters the left lung at 45-55 degrees; compared to the right main bronchus, which is wider, shorter, and enters at an angle of 20-30 degrees into the right lung.[8] Due to this phenomenon, and the forces of gravity, the carina and the right main bronchus are susceptible to aspiration/lodging of foreign objects.[4,8,16] The primary bronchi branch next into five lobar (secondary: 2nd generation) bronchi – three right lobar bronchi and two left lobar bronchi. Those divide further into eighteen segmental bronchi (tertiary: 3rd generation) – ten right segmental bronchi and eight left segmental bronchi. The segmental bronchi give rise to numerous subsegmental bronchi (conducting and respiratory bronchi/bronchioles), which in turn form terminal bronchioles, respiratory bronchiole, alveolar duct, alveolar sac, and finally pulmonary alveoli.[1,8,9,12] As the number of bronchi increases with each generation, the total cross-sectional area increases; despite decreasing airway lumen diameters, this increase in cross-sectional area is significant for easy ventilation of the lobes.[2,8,13]

The structural division of the tracheobronchial tree can be further divided into function. The conducting zone (trachea, primary, secondary, tertiary bronchi, and terminal bronchiole) will act as a conduit for air; and as air is transported through the conducting airways to the respiratory zone (terminal respiratory unit or acini), the air is warmed, moistened, and cleared further from incoming foreign particulates.[1,12,17] The terminal respiratory unit (acini) consist of the respiratory bronchioles, alveolar sacs and ducts, and the abundant alveoli. Each terminal acini is composed of 100 alveolar ducts and 2000 alveoli, and it is here that external respiration (gas exchange) occurs.[8,9,12,17] As the bronchial tree goes through branching generations, the cartilage support

become increasingly interspersed plates and composed of elastic tissue – instead of the C-shaped hyaline cartilage in the trachea. The smooth muscle lining the walls of the airway eventually encircle the bronchioles – the level of the bronchioles lack cartilage.[8,9,12] There is also apparent microanatomical differences in airway epithelium, the higher the branching generation: the epithelium composition changes from a) ciliated pseudostratified columnar epithelium with numerous goblet cells and glands, into b) simple columnar ciliated epithelium (Club/Clara cells), and then into c) simple cuboidal epithelium, with hardly any goblet cells/glands at the bronchioles level.[8,9,18] It is of importance to note that the club cells (bronchiolar exocrine cells) still contain microvilli and may secrete glycosaminoglycans (GAGs) that replace the mucous protective nature, within the bronchiole lining. Club cells tend to increase in an inversely related manner with decreasing levels of goblet cells, and detoxify harmful substances inhaled – using the activity of cytochrome P450 enzymes in their smooth endoplasmic reticulum.[18]

The primary site of gas exchange is at the alveolus level, where each alveolus basal lamina is intimately in contact with an extensive mesh of capillaries from the pulmonary vasculature. The alveolar ducts are lined with simple cuboidal epithelium, while the alveoli are line with simple squamous epithelium.[9,18] The thin alveolar wall (~25 nm) is composed of Type I & II pneumocytes (alveolar cells), phagocytic alveolar macrophages (dust cells), and some alveolar walls contain pores (Pores of Kohn) in their interalveolar septum (**Figure 2**).[1,6,8,9,18] It is via the presence of some collagen and elastic fibers that the alveoli are capable of stretching during inhalation (elastic fibers), and recoil back during exhalation; whereas the pores between neighboring alveoli help equalize air pressures among the alveoli during ventilatory respiration.[2,8,9,12,13]

1.1.3 **Native Cells of the Respiratory System**

The cells that line the respiratory system can be divided into two zones – a) conducting zone and b) respiratory zone.

a) Conducting Zone Cells:[2,7-9,12,13,17-19]

   I. Ciliated pseudostratified columnar epithelium – lines the nasal cavity down to the bronchioles. Warms, humidifies, and clears inhaled particulates via the mucociliary escalator.

   II. Goblet cells – mucus producing cells, which line and defends the entire conductive respiratory zone (upper and lower respiratory tracts) from foreign inhaled particulates. Their presence decreases closer to the terminal bronchioles.

   III. Stratified squamous epithelium (non-ciliated) – lines the oropharynx and laryngopharynx. Protection against abrasiveness of food.

   IV. Simple columnar epithelium (microvilli & non-microvilli) – club/Clara cells present in the bronchiole and terminal bronchiole level. Act as bronchiolar exocrine cells that protect the fine bronchiole lumen via the secretion of GAGs and detoxifying substances.

b) Respiratory Zone Cells:[2,7-9,12,17,19]

   I. Simple cuboidal epithelium – respiratory bronchioles and alveolar ducts are lined with these cells. There may or may not be microvilli on the apex of the cuboidal cells.

   II. Type I pneumocytes – a single thin layer of squamous epithelium, which composes 90% of the respiratory membrane (alveolar epithelium, basal lamina, and capillary endothelium) (**Figure 2**). They play a major role in maintenance and

primary site for simple diffusion of gas exchange with neighboring extensive capillary networks, referred to as the alveolar-capillary interface (**Figure 2**).

III. Type II pneumocytes (septal cells) – occur in much greater numbers than type I pneumocytes, but because of their minute size, they comprise a smaller portion of the total alveolar wall. They are small cuboidal cells with short apical microvilli that attach tightly to neighboring Type I pneumocytes; forming an impermeable seal between alveolar air and connective tissue spaces (**Figure 2**). Type II pneumocytes have the capability to generate both Type I pneumocytes (after injury to the alveolar wall) and Type II pneumocytes. Their most distinguishing feature and important function is the intracellular lamellar bodies that produce, store, and secrete pulmonary surfactant and various other proteins, respectively.

IV. Alveolar macrophages (dust cells) – provide immunologic defense.[7]

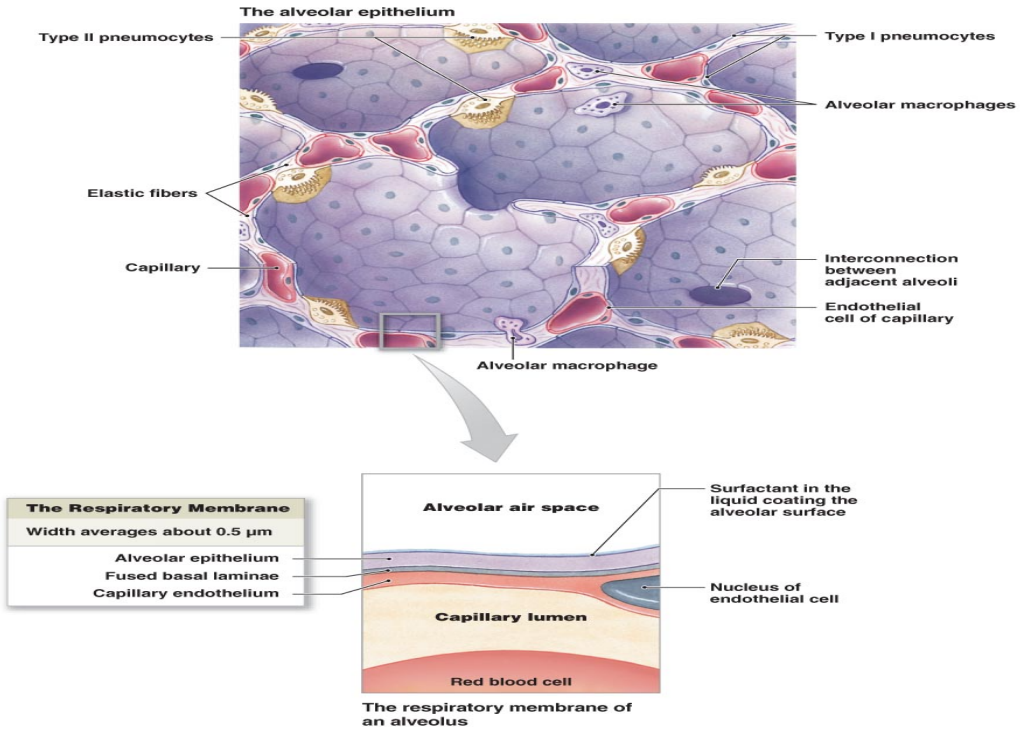

Figure 2: Anatomy of the alveolar-capillary interface. Adapted from Krishnan.[12]

1.1.4 **Pulmonary Circulation**

There are two separate circulatory systems coexisting within the lungs: bronchial and pulmonary systems. The bronchial circulation consists of carrying oxygenated blood that is needed to meet the metabolic demands of the lungs; furthermore, it does not participate in gas exchange. There are two bronchial arteries that serve the left lung, and one bronchial artery that serves the right lung.[1,6-8,17] The left arterial branches arise directly from the thoracic aorta, while the single right arterial branch arises from either a) the thoracic aorta, b) the superior bronchial artery on the left side, or c) any number of the right intercostal arteries.[1,6-8,17] These arteries supply nourishment to the bronchi and connective tissue of the lungs. They enter each lung via the root of each lung, travel, branch with the bronchi, and end approximately at the level of the respiratory bronchioles. They anastomose with the branches of the pulmonary arteries, and together, they supply the visceral pleura of each lung.

On the other hand, venous return is returned to the heart via the pulmonary veins, rather than the bronchial veins. As a result, blood returning to the left atrium of the heart is slightly less oxygenated, than what would be found at the level of the pulmonary capillary beds.[1,6-8,17]

Clinically, signs of chronic pulmonary thromboembolic hypertension consists of visualizing on imaging enlarged and tortuous bronchial arteries.[20] Moreover, with the advancement in modern lung transplantation techniques, bronchial arterial circulation is usually sacrificed during lung transplants – without any clinically significant detriment. Thus, it is the microcirculation arising from the pulmonary circulation, which provides perfusion to the airways.[21]

The pulmonary circulation system arises from the conus arteriosus of the right ventricle of the heart, which branches at the pulmonary trunk as the right and left pulmonary arteries. The right

and left pulmonary arteries will carry venous deoxygenated blood through the root of each lung, in parallel to the bronchial tree, which eventually narrows into arterioles. These arterioles end in a highly vascular capillary network that are meshed around and through the alveoli.[6,8,9] The bifurcation of the pulmonary trunk into the right and left pulmonary arteries follow initially the right and left main bronchi (respectively) – entering each lung at each respective hilum.[2,6,8,9] The pulmonary circulation is considered to be shorter in length and at a lower pressure than the systemic circulation.[22,23] Yet, in comparison with the systemic vessels, the pulmonary arteries also have three layers: intima, media, and adventitia.[6,8]

The pulmonary veins enter the lungs at the same location as the pulmonary arteries (hilum), but unlike pulmonary arteries, travel within the interlobular septa and not in parallel with the airways to carry oxygenated blood back to the left atrium.[24] Also, the pulmonary vein bed serves as a capacitance reservoir between the right and left sides of the heart.[12,16,17]

Any segment of the pulmonary vessels can contribute to active vasomotion, since smooth muscle can be found in the arterial and venous pulmonary vessels.[25-27] The clinical significance of vasoactivity lies in the relationship of ventilation and perfusion (V/Q) – it is a key evaluator of the efficiency of normal lung functional physiology.[7,8,12] The key regulators of the vascular tone and reactivity are the endothelial cells – they possess a number of metabolic activities, one of which is the local production of nitric oxide in the pulmonary circulation (a potent vasodilator).[28] Due to the inherent dual blood supply which supply the lungs (bronchial and pulmonary circulations), the lungs are more resistant to infarction. An occlusion of the bronchial circulation does not cause infarction, but if there is a pulmonary embolism, an infarction can occur – since the pulmonary circulation is occluded and the bronchial circulation cannot fully compensate.[7,8,13]

1.2| Physiology of The Respiratory System

1.2.1 Respiration Mechanics, Innervation, and Ventilation Rate

There are two phases of pulmonary ventilation – a) inspiration (inhalation), and b) expiration (exhalation). Ventilation is simply the exchange of air between the external environment and the alveoli. Air will tend to move via bulk flow by pressure gradients, from an area of high pressure to low pressure.[7,8,13] Pressures in the respiratory system will always be relative to atmospheric pressure (760 mm Hg at sea level). As the body adjusts the thoracic volume, the intrapulmonary pressure (alveolar pressure) will also be adjusted according to Boyle's Law ($P_1V_1 = P_2V_2$ – the pressure (P) of gas is inversely proportional to volume (V) at a constant temperature).[7,8,13] It is these volume changes that lead to changes in the intrapulmonary pressures (IPP), which ultimately determines the ventilation phase, to equalize the pressure. During each phase the body changes the lung dimensions to produce the inhaled/exhaled flow.

a) Inspiration phase:[13,15,16]

   I. A contraction of the diaphragm (inspiratory muscle) downwards, increases the thoracic vertical dimension.

   II. Simultaneously, the external intercostals contract (inspiratory muscles) increasing the side-to-side and anterior-to-posterior dimensions.

   III. Ribs will be elevated (accessory inspiration muscles – interosseous and scalene), sternum raised (accessory inspiration muscles – sternocleidomastoid), and the trapezius and pectoralis minor muscles fix the shoulders. During deep inspiration, the erector spinae and the abdominal muscles are contracted, along with the inspiratory and accessory muscles.

   IV. Thoracic cavity volume increases.

V. Lungs expand due to IPP and intrapleural/intrathoracic pressures (ITP) decreasing ($P \propto 1/V$). This results in a positive transpulmonary pressure (TPP).

VI. Air (gases) flow into the lungs (inhalation) down the pressure gradient, until IPP = 0 mm Hg (equates to atmospheric pressure).

This negative pressure in the intrapleural cavity is a consequence of the interactions between forces acting within the thoracic wall to exert pressure to pull the parietal pleura outward and away from the visceral pleura. On the other hand, the visceral pleura pulls inward and away from the parietal pleura via the elastic fibers within the lungs.[13,15,16] The constant opposite pull between the two pleural membranes causes the ITP to be sub-atmospheric and under normal physiological conditions, ITP < IPP < Atmospheric pressure, with a range that fluctuates from −4 to −10 mm Hg during exhalation and inhalation, respectively. An ITP of −12 to −18 cm H_2O is an inherent ITP that maintains the lungs inflated and prevents collapse, despite the natural elastic recoil of the lungs.[13,15,16] As such, when the lungs are removed from the chest cavity or if atmospheric pressure enters the pleural cavity, all or part of a lung will collapse (pneumothorax). This would mean, TPP = 0 mm Hg (IPP-alveolar pressure = ITP-intrathoracic/pleural pressure): TPP = IPP – ITP.[13,15,16]

Moreover, as the thoracic cavity increases in volume, the lung parenchyma is homogenously pulled from all sides to expand, which causes a partial vacuum within the lung itself. However, it should be noted that this negative pressure (IPP) is not as great as the negative pressure within the pleural cavity (ITP<IPP), otherwise the lungs would pull away from the chest wall.[13,15,16] Air will simply move inward and expand the alveoli when the IPP < atmospheric pressure (760 mm Hg), and it will continue to do so if the IPP remains less than 760 mm Hg. Eventually as the inspiration phase maximizes and begins to shift into passive expiration, the IPP

will equalize/stabilize with atmospheric air pressure; thus, the inward movement of air stops, and expiration begins.[13,15,16] Under physiological conditions TPP will always be positive – ITP always negative and relatively large, while IPP fluctuates from slightly negative to slightly positive as a person inhales and expires, respectively.[13,15,16] Therefore, for any given lung volume the TPP is equal and opposite to the elastic recoil pressure of the lung. When examining TPP vs volume curve (plotted as Volume in function of Pressure), an inherent difference (hysteresis) is present between the inspiratory and expiratory curves. This is due to the lung volume at any given pressure during inhalation will be less than the lung volume at any given pressure during exhalation. This can be attributed to the longer passive process that increases the duration of the exhalation phase compared to inhalation.[13,15,16]

b) Expiration phase:[13,15,16]

I. Inspiratory and accessory muscles relax – diaphragm rises, ribcage descends due to gravity, with the natural recoil in the external intercostal muscles, and contraction of the internal intercostal muscles.

II. Thoracic cavity volume decreases.

III. As the elastic lungs recoil passively, the intrapulmonary volume decreases. Thus, IPP and ITP increases.

IV. Air (gases) flow outwards, but still down its pressure gradient until IPP stabilizes with atmospheric pressure = 0 mm Hg.

During normal/resting breathing, expiration is a passive process that does not require inspiratory and accessory muscles to work – rather it is the relaxing of those muscles that result in the relaxing of the diaphragm, which moves back up towards the lungs and the intrinsic elastic recoil of the lungs assists with the exhalation phase. The internal intercostal muscles can assist

with the inward movement of the ribcage; however, during physical or emotional stress, more frequent and deeper/forced breathing is needed; which can have both inspiration and expiration working as active processes. The accessory inspiration muscles will be contracted, along with several abdominal muscles that are thought to contribute to active exhalation.[13,15,16]

c) Neural Innervation:[13,15-17]

I. Rhythmic ventilation is controlled by the respiratory center located in the central nervous system – composed of the pontine respiratory centers, ventral respiratory group, and dorsal respiratory group. Of those three, ventral respiratory group is the most important. These neurons located in the medulla oblongata and pons of the brainstem generate a smooth ventilation rhythm by sending impulses to the inspiratory muscles to stimulate contraction and relaxation (inspiration and expiration, respectively).

II. As such, normal/resting ventilation is under involuntary central and autonomic nervous system control (parasympathetic – constrict airways, and sympathetic – dilate airways). One can voluntarily increase or decrease breathing rate, but that involves a higher brain function of the cerebral cortex.

III. Neuronal impulses travel along the phrenic nerve to innervate and contract the diaphragm (80% of inhalation) and the external intercostal muscles. The phrenic nerve arises from the cervical plexus through the fourth cervical nerve (C4), with contributions from the third (C3) and fifth cervical (C5) nerves. Hence, trauma involving levels C3-C5 will cause ventilatory dysfunction/paralysis of the diaphragm muscle.

IV. Normal adults have a breathing rate (minute ventilation) of ~12-16 breathes per minute.

V. The stretch receptors within the alveoli send feedback to the medulla oblongata to limit tidal volumes during inspiration and exhalation.

d) Ventilation rate manipulation:[13,15-17]

The respiratory center located in the medulla and pons of the brainstem receive sensitive feedback with regards to the partial pressures of oxygen (PO_2) and carbon dioxide (PCO_2) in the arterial blood. It is via this information that the average respiratory rate is adjusted to maintain these partial pressures constant.

I. Central blood gas chemoreceptors – located on the anterior surface of the medulla oblongata and are sensitive to the increasing partial pressure of CO_2 and the decreasing blood pH. As blood pH decreases (acidic) or CO_2 concentrations increases, a compensatory increase in ventilation rate arises. As such, respiratory acidosis is acutely corrected by involuntary hyperventilation.

II. Peripheral blood gas chemoreceptors – located on the aortic and carotid bodies, they are particularly sensitive to arterial partial pressures of O_2. Although, they also respond to the arterial partial pressures of CO_2.

1.2.2 **Lung Compliance**

Compliance refers to the lungs ability to stretch and expand. The natural tendency of the lungs to recoil, upon the removal of the distending forces, is referred to as elastance (reciprocal of compliance). Clinically, compliance is separated into two different measurements:[13,15-17]

I. Static lung compliance – the change in volume for a given applied pressure, during periods without gas flow or inspiratory pause ($C_{stat} = V_t / P_{plat} – PEEP$). C_{stat} – static

lung compliance; V_t – tidal volume; P_{plat} – plateau pressure; PEEP – positive end expiratory pressure.

II. Dynamic lung compliance – the change in volume for a given applied pressure during periods of gas flow, or during active inspiration ($C_{dyn} = V_t$ / PIP – PEEP). C_{dyn} – dynamic lung compliance; V_t – tidal volume; PIP – peak inspiratory pressure (the maximum pressure during inspiration); PEEP – positive end expiratory pressure.

One should note that since PIP − PEEP is always greater than P_{plat} – PEEP, dynamic compliance will always be lower than or equal to static lung compliance. A low lung compliance indicates a stiffer lung; therefore, requires a greater than average change in intrapleural pressure (ITP) to change the thoracic volume, i.e. inspiration – this is often seen in restrictive lung diseases.[13,15-17] On the contrary, high compliance indicates a pliable lung (one with low elastic recoil); therefore, minimal pressure difference in ITP is needed to bring about change to the thoracic volume – often seen in obstructive lung diseases. Thus, a greater expenditure of energy is required to breathe normally in a person with low lung compliance. These individuals will tend to take shallow and rapid breaths. Lung compliance tends to be the highest at moderate lung volumes, and worse/lower at volumes that are either very low or very high. Lung hysteresis is evident when observing the difference in lung compliance during inspiration and expiration for identical volumes. This difference in compliance (volume/pressure) can be attributed to the additional energy required during inspiration to recruit and inflate additional alveoli. The transpulmonary pressure (TPP) versus volume graph demonstrates this hysteresis by how at any given pressure during inhalation, the corresponding inspired volume will be less than the expired volume at that specific pressure.[13,15-17] There are two major determinants of lung compliance:[13,15-17]

I. Parenchymal elasticity – any thickening of the lung parenchyma due to disease, will decrease lung compliance.

II. Surface tension – the surface of the alveoli cells is typically a moist environment. Since this is the interface where air diffuses and is in contact with the moist alveoli, energy is required to expand the lung parenchyma and to overcome the attractive hydrogen bonding forces of water. The surface tension of water lines the alveoli.

To overcome the forces of surface tension at the respiratory membrane interface, type II pneumocytes secrete surfactant. Surfactant will act as a detergent by disrupting the hydrogen bonding of water that lines the alveoli; thus, decreasing the surface tension, reducing the energy required to expand the lung parenchyma, and most importantly, preventing alveoli atelectasis (collapse).[13,15-17]

1.2.3 **Lung Volume and Capacity**

Lung volumes and capacities refer to the volume of air that is associated with different phases of the respiratory cycle. It has been estimated that the average total lung capacity (TLC) of an adult human lung is ~6L (6000 ml) of air. The average human respiratory rate (RR/f) is 30-60 breaths per minute (bpm) at birth and decreases to ~12-16 bpm in adults.[2,7,13,29]

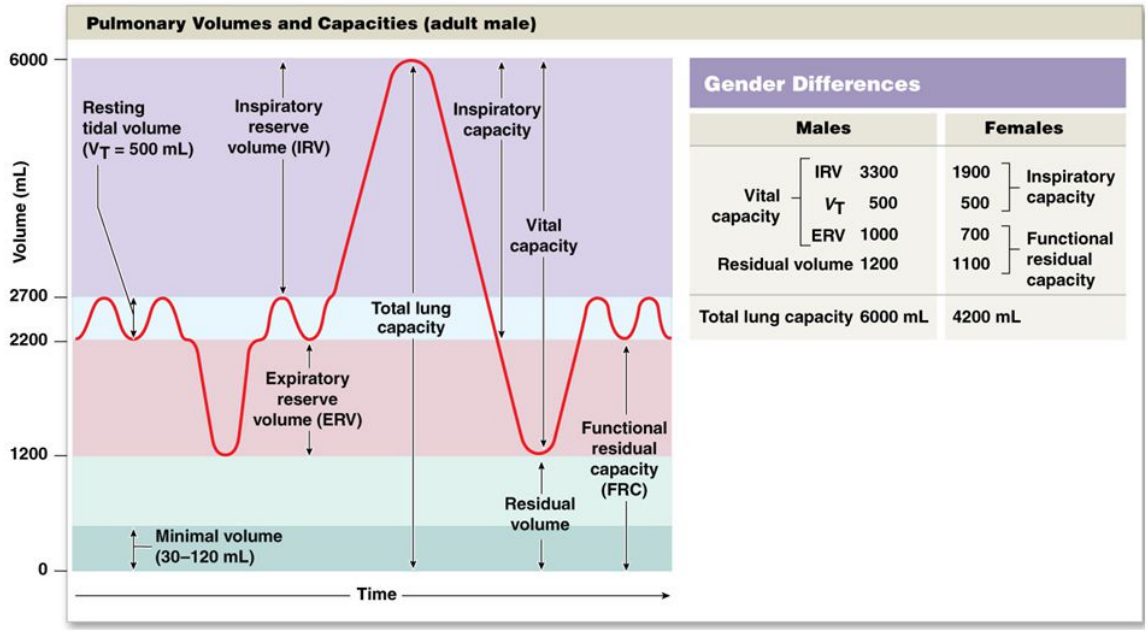

Figure 3: Lung volumes, capacities and gender differences. Adapted from Ganong.[29]

a) Respiratory volumes are measured by a spirometer and differences between gender is illustrated in **Figure 3**:[2,7,13,29]

I. Tidal volume (V_t) – under resting conditions, it is the normal amount of air inhaled or exhaled with each breath (500 ml).

II. Inspiratory reserve volume (IRV) – amount of air that can be forcefully inhaled after a normal tidal volume inhalation (male: 3300 ml; female: 1900 ml).

III. Expiratory reserve volume (ERV) – amount of air that can be forcefully exhaled after a normal tidal volume exhalation (male: 1000 ml; female: 700 ml).

IV. Residual volume (RV) – amount of air remaining in the lungs after a forced exhalation (male: 1200 ml; female: 1100 ml).

b) Respiratory capacities (**Figure 3**):[2,7,13,29]

I. Total lung capacity (TLC) – maximum amount of air contained in the lungs, with maximum inspiration and expiration effort (TLC = V_t + IRV + ERV + RV). Male: 6000 ml; female: 4200 ml.

II. Vital capacity (VC) – maximum amount of air that can be expired after a maximum inspiratory effort (VC = V_t + IRV + ERV). Male: 4800 ml; female: 3100 ml.

III. Inspiratory capacity (IC) – maximum amount of air that can be inspired after a normal expiration (IC = V_t + IRV). Male: 3800 ml; female: 2400 ml.

IV. Functional residual capacity (FRC) – volume of air remaining in the lungs after a normal tidal volume expiration (FRC = ERV + RV). Male: 2200 ml; female: 1800 ml.

Dead air space (V_D) considered to be air that does not participate in gas exchange, due to being trapped in the conducting airways (~150 ml). The respiratory minute ventilaton (V_E/MV) is the total volume of air inhaled and exhaled during each minute – respiratory rate (breathes/min) x tidal volume (volume/breath), $MV = RR \times V_t$ (12 breaths/min x 500 ml = 6 L/min). While alveolar ventilation rate (V_A) represents the volume of the air that enters the alveoli every minute – $V_A = RR \times (V_t - V_D)$.[2,7,13,29]

1.2.4 **Homeostasis and Gas Exchange**

Homeostasis is maintained by gas exchange, internal respiration at the alveoli-capillary level, and by regulation of blood pH. The gas exchange occurs via diffusion of the respiratory gases, oxygen (O_2) and carbon dioxide (CO_2), between inhaled air and the blood. The fundamental purpose of the respiratory system is the equilibration of the varying partial pressures of the respiratory gases between the alveolar air and those in the pulmonary capillary circulation.[2,7,13,29]

Air within the alveoli has a semi-permanent volume of ~2.5-3.0 liters, which surrounds the alveolar-capillary blood. This inadvertently ensures the rapid and efficient equilibration of the partial pressures of the gases between the two compartments. PO_2 = 100 mmHg (13-14 kPa) and PCO_2 = 40 mmHg (5.3 kPa) within the pulmonary and systemic circulation, which are equivalent in tensions within the alveoli.[2,7,13,29] On the other hand, ambient air at sea level corresponds to PO_2 = 160 mmHg (21 kPa) and PCO_2 = 0.3 mmHg (0.04 kPa). This variation in gas tension between ambient air and alveolar air is maintained because of the functional residual capacity that is inherently present within the dead-space – the dead-air space does not contribute to external respiration and can be found within the nose, pharynx, larynx, trachea, bronchi and their branches, until respiratory bronchioles.[2,7,13,29] The nature in which air travels in the mammalian lung is bi-directional flow, combined with the lack of a complete emptying and re-inflation with each breath; which leaves a substantial amount of air, 2.5-3 liters, in the alveoli upon exhalation.[2,7,13,29] This ensures the composition of the alveolar air is only minimally disturbed when the 350 ml of ambient air is mixed with each inhalation. This special "portable atmosphere", within the alveolar air, acts as the functional residual capacity to which the pulmonary circulation and systemic tissues are exposed to, and not to the outside/ambient air.[2,7,13,29]

Gas exchange at the alveolar-capillary interface is dictated by simple diffusion, following Fick's Law – the net diffusion rate of a gas across a fluid membrane is proportional to the difference in partial pressure gradients, proportional to the area of the membrane (alveoli) and inversely proportional to the thickness of the membrane (alveolar-capillary interface). Consequently, a net influx of O_2 from the alveoli into the blood, and a net efflux of CO_2 simultaneously occurs (venous capillary PCO_2 = 45 mmHg (6 kPa); alveolar PCO_2 = 40 mmHg (5.3 kPa)).[2,7,13,29] The net flow fluctuations of each individual gas entering and leaving the alveoli,

necessitates the replacement of about 15% of the alveolar air with ambient air every ~5 seconds.[2,7,13,29] The resulting arterial partial pressures of the respiratory gases are maintained at homeostasis by the close monitoring of the aortic and carotid bodies, as well as by the blood gas and pH sensor on the anterior surface of the medulla oblongata.[2,7,13,29]

The arterial blood gases resemble an accurate reflection of the gas tension composition within the alveolar air. As such, a rise in the arterial PCO_2 and a fall in the arterial PO_2 (lesser extent), will reflexively cause deeper and faster breathing till the gas tensions in the lungs (i.e. arterial blood), return to normal. The converse happens when the PCO_2 falls: the rate and depth of breathing are reduced, till blood gas tensions are restored. There are O_2 and CO_2 sensors within the lungs, but they primarily act to determine bronchiole diameters and pulmonary capillaries – which determines the flow of air and blood (V/Q) to more compliant lung parenchymal.[2,7,13,29] Therefore, a compromise to these homeostats will result in respiratory acidosis or alkalosis. Respiratory acidosis (blood pH <7.35), occurs when the CO_2 is not eliminated from the body at a normal rate; thus, increasing vascular PCO_2. Lung disease or decreased mental status, which results in hypoventilation, may cause respiratory acidosis. On the other hand, respiratory alkalosis (blood pH >7.45), occurs when CO_2 is eliminated too rapidly; thus, decreasing vascular PCO_2. Chronically, these imbalances are compensated by renal adjustments to the hydrogen (H^+) and bicarbonate (HCO_3^-) concentrations in the plasma; the immediate response to pH imbalances is via the hyperventilation syndrome (compensates for acidosis) and hypoventilation syndrome (compensates for alkalosis).[2,7,13,29]

Due to the low solubility of O_2 in water, 98.5% of molecular O_2 is carried in the blood via binding with hemoglobin with erythrocytes. While only 1.5% is dissolved in the plasma. The oxygen bound to the hemoglobin occurs on all four-ferrous iron-containing heme groups (**Figure**

4).[2,7,13,29] When all heme groups are bound to one O_2 molecule, the blood is said to be "saturated" – no further increase in the partial pressure of O_2 will meaningfully increase the oxygen concentration of the blood. Affinity for oxygen continues to increase with each molecule binding until saturation; conversely, release of O_2 molecules to the tissue increases with each oxygen release. The three factors that precipitate release of O_2 from hemoglobin to body tissues are:[2,7,13,29]

I. A decreased O_2 concentration within blood plasma.

II. A decreased blood pH (<7.35).

III. An increased body temperature.

Carbon dioxide is transported in the blood in three forms: a) predominantly, 60-70% converted into HCO_3^- ions within the erythrocytes (via carbonic anhydrase), b) 20-30% binds to amino acids, not heme, within the hemoglobin molecules as carbaminohemoglobin ($HbCO_2$), and c) ~7% dissolved in plasma (**Figure 4**).[2,7,13,29]

The respiratory system intimately attempts to maintain the acid-base balance within the body: $CO_2 + H_2O \Leftrightarrow$ Carbonic Anhydrase (H_2CO_3) $\Leftrightarrow H^+ + HCO_3^-$. The alkali reserve constitutes the bicarbonate ions, which make up a large portion of the blood buffer system. As the CO_2 gets converted to $H^+ + HCO_3^-$, the hydrogen ions bind to the hemoglobin while the bicarbonate ions leave the erythrocytes into the plasma via facilitated diffusion of a counter-transporter; thus, exchanging extracellular chloride ions for intracellular bicarbonate ions. The efflux of bicarbonate ions causes an excess of negative charge, which is relieved via the chloride shift (**Figure 4**).[2,7,13,29]

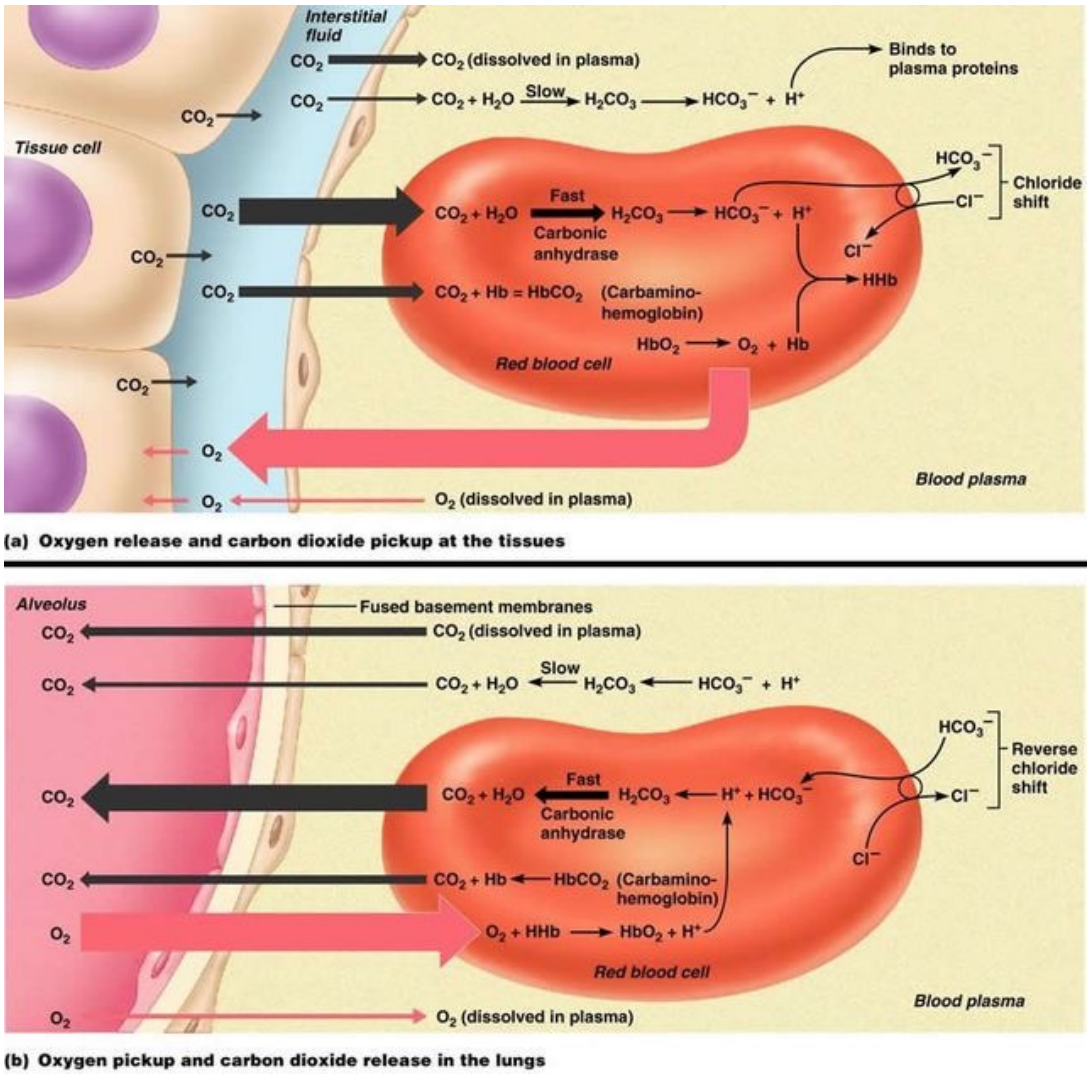

Figure 4: Representation of **(A)** internal respiration and **(B)** external respiration. Adapted from Krishnan.[12]

1.2.4.1 Zones of The Human Lung

The zones of the lung, West Zones, divide the lung into three vertical regions. West zones deepend on the relationship between the pressure in the arteries (Pa), in the veins (Pv), and alveoli (PA).[7,13,30]

- Zone 1: PA > Pa > Pv
- Zone 2: Pa > PA > Pv
- Zone 3: Pa > Pv > PA

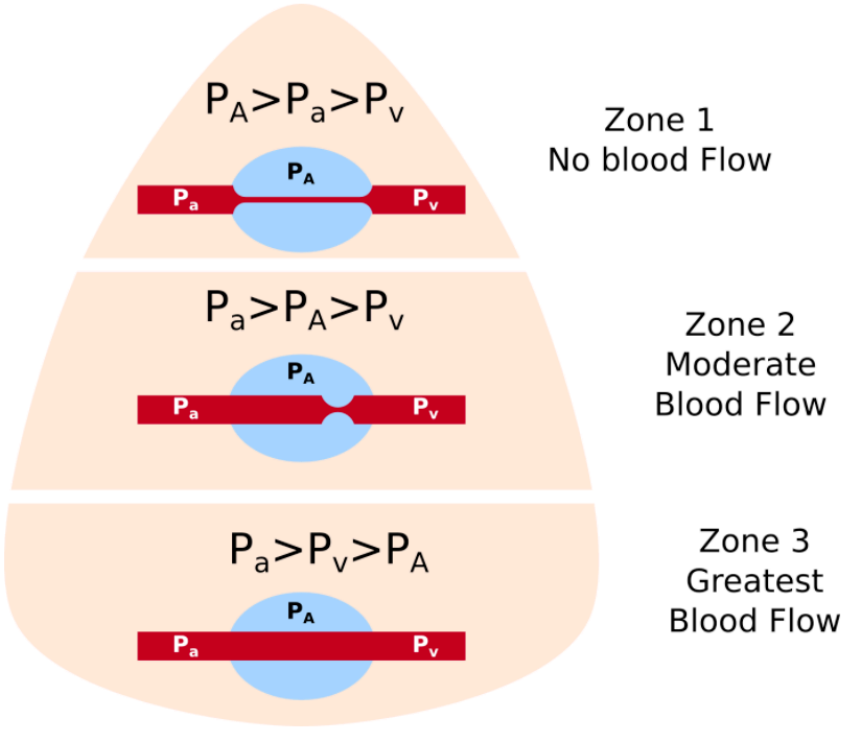

Figure 5: West Zones - pulmonary blood flow. Adapted from Razani.[5,30]

Zone 1 is typically not observed in normal healthy human lungs. In healthy lungs, Pa pressure exceeds PA in all zones, except zone 1 (PA>Pa); therefore, pulmonary blood vessels are completely collapsed by exceeding alveolar pressures, and blood does not flow through these regions.[7,13,30]

Zone 2 blood flows in pulses. There exists no flow, at first, due to obstruction at the venous end of the capillary bed. As the pressures from the arterial side increase, it exceeds alveolar pressures and flow resumes. Flow here is sometimes compared to starling resistor.[7,13,30]

Zone 3 comprises the majority of lungs, in a healthy state. There exists no external resistance to blood flow, thus, blood flows continuously through the cardiac cycle. Flow is determined by the difference in Pa and Pv. Transmural pressure across the wall of the blood vessels

increases down this zone, due to gravity. Consequently, blood vessel walls are stretched further, causing an increase in flow due to lower resistance due to lower resistance.[7,13,30]

1.2.4.2 **Ventilation/Perfusion Mismatch**

Clinical evaluation of lungs is determined by the evaluation of arterial partial pressure of O_2 (P_aO_2). The ventilation (V)/perfusion (Q) ratio is known to be an important determinant of this value, since alveolar air/gases interact with blood to achieve oxygen exchange. In humans, normal V/Q ratio is typically around 0.8, with a normal minute ventilation ~4.2L/min, and normal perfusion rate ~5.5L/min. The overall interaction between ventilation and perfusion brings about the concept of V/Q matching. In extreme cases, if ventilation was to enter only the right lung and the perfusion was to enter the right lung, the overall V/Q would still be 0.8; however, since air is not able to exchange with the perfusion fluid, there exists no gas exchange, and as a result P_aO_2 would be equivalent to the mixed venous PO_2. This demonstrates a complete V/Q mismatch and illustrates the importance of V/Q matching to P_aO_2.[5,7,13,30]

In upright normal lungs, there exists a physiologic V/Q mismatch throughout the lung. Both ventilation and perfusion decline from the bases to the apices. For ventilation, the transpleural pressure at the apex is more negative than at the base. Hence, the lung parenchyma is less expanded at the base, and more compliant. Therefore, as air enters the lung, it preferentially enters the base of the lung first, which results in more ventilation at the base. On the contrary, perfusion distribution of blood flow throughout the lung is affected by gravity and can be explained by hydrostatic pressure differences between the apex and base of the pulmonary arterial system. The apex (zone 1) of the lung is higher than the level of the heart. This results in pulmonary arterial pressures that are relatively low in this zone, while alveolar pressures that exceed Pa: leading to collapse of these vessels during ventilation and development of V>Q and a higher V/Q ratio. In

comparison to the base of the lung (zone 3), V<Q due to Pa exceeding Pv and PA, which results in a comparatively lower V/Q ratio. Since by definition, blood will tend to go to areas where V<Q, the net effect of this physiologic V/Q mismatching (some areas V<Q and others V>Q), P_aO_2 decreases because of the amount of hyperoxic blood coming from V>Q areas cannot correct for the amount of relatively hypoxic blood coming from V<Q areas. This becomes particularly important in pathological conditions seen in common donor pathologies: pneumonia, edema, and aspiration where they all flood the alveoli and leading to increased areas of V<Q (Zone 1). Consequently, V/Q mismatching increases leading to a fall in P_aO_2. Indeed, to mitigate this issue, ICU physicians tend to increase PEEP in patients with these pathological conditions to re-inflate the affected lung units and attempt to reduce V/Q mismatch.[5,7,13,30]

1.3| Immune Responses

1.3.1 **Innate Immune Response**

The immune system has evolved to provide protection from inflammatory insults such as, infections and native damage, and can be subsequently divided into innate versus adaptive (humoral and cell-mediated) immune system. In humans, the blood-brain barrier, blood-cerebrospinal fluid barrier, and other similar fluid-brain barriers separate the peripheral immune system from the neuro-immune system (protects the brain).[31-33] With regards to infection, the immune system can be divided into layers of increasing specificity. Physical barriers prevent pathogens such as bacteria and viruses from entering the organism. Microorganisms/toxins encounter an immediate, but non-specific response, mediated by pattern recognition receptors (PRRs). These PRRs are germline-encoded host sensors, which are proteins expressed by cells of the innate immune system (dendritic cells, macrophages, monocytes, neutrophils, and epithelial

cells). PRRs help initiate that immediate, non-specific innate response, which does not confer long-lasting immunity (memory) against a pathogen; however, the molecules released following specific PRRs will cross-over and activate the adaptive immunity (highly specific with immunological memory).[31-33]

1.3.1.1 Innate Immune Cells

The innate immune system has native leukocytes that include phagocytes (macrophages, neutrophils, and dendritic cells), native lymphoid cells, mast cells, eosinophils, basophils, and natural killer cells. These cells identify and eliminate pathogens through contact or by engulfing the microorganisms; while activating the adaptive immune system.[31-33]

Phagocytosis is an important feature of cellular innate immunity performed by phagocytic cells. Phagocytic cells can roam freely around the body, reside within organ tissues, or lured to specific locations by cytokines. The engulfed pathogen is killed by the activity of digestive enzymes or following a respiratory burst that releases free radicals into the phagolysosome.[31-33]

Neutrophils, normally the most abundant type of phagocytic cells found in the bloodstream (50-60%, total circulating leukocytes) are among the first responders during the acute phase of inflammation (particularly due to bacterial infection). Neutrophils tend to migrate toward the site of inflammation via chemotaxis. Macrophages reside more within tissues, are versatile cells, which produce a wide array of chemicals: including enzymes, complement proteins, and cytokines. Macrophages can act as scavengers that rid the body of worn-out cells and other debris; while also acting as antigen-presenting cells (APC) that activate the adaptive immune system via major histocompatibility complexes (MHCs).[31-33]

Dendritic cells are phagocytic cells that reside within tissues, specifically, tissues that are in contact with the external environment: located mainly in the lungs, skin, nose, stomach and

intestines. Their primary purpose is to serve as a link between the bodily tissues and the innate and adaptive immune systems. They also present antigens to T-lymphocytes via MHCs.[31-33]

Mast cells are predominately found in connective tissues and mucous membranes, with a purpose to regulate the inflammatory response. They are more associated with allergies and anaphylaxis.[31-33]

Basophils and eosinophils, related to neutrophils, secrete various chemical mediators involved in defending against parasites (basophils) and play a role in allergic reactions, such as asthma (eosinophils).[31-33]

Natural killer (NK) cells, are leukocytes that attack and destroy tumor cells or virus infected cells. NK cells are considered lymphocytes that are a component of the innate immune system. They do not directly attack invading microbes, rather, they destroy compromised host cells (tumor cells or virus-infected cells). They recognize such cells by a phenomenon known as "missing self-antigen." This phenomenon describes cells that possess low levels of cell-surface markers called MHC I: arises in viral infections of host cells. NK-cells do not require activation in order to kill cells that are "missing self-antigen." It is through an altered state of MHC make-up on the surface of those tumor/infected cells, which results in NK-cell activation and destruction of those cells. Normally native cells are not recognized and attacked by NK-cells because the express intact self MHC antigens. These antigens are recognized by killer cell immunoglobulin receptors, which essentially halt NK-cells. Briefly, there are two types of MHC molecules that differ in the source of the antigens:[31-33]

I. MHC I – binds peptides from the cell cytosol/

II. MHC II – binds peptides generated in the endocytic vesicles after internalization.

Each T-lymphocyte can recognize ten to hundred copies of a unique sequence of a single peptide among thousands of other peptides that are presented on the very same APCs. These MHC complexes become imperative during predictions of primary graft dysfunction post-allograft lung transplantation.[31-33]

1.3.1.2 **Innate Immune Receptors**

Pattern recognition receptors (PRRs) identify two classes of molecules:[33-37]

I. Damage-associated molecular patterns (DAMPs) – associated with components of host's cells that are released during cell-damage or death. Corresponding to endogenous stress signals that include uric acid and extracellular ATP, among many others.

II. Pathogen-associated molecular patterns (PAMPs) – associated with microbial pathogens, toxins, bacterial carbohydrates (lipopolysaccharide), nucleic acids (bacterial or viral DNA/RNA), bacterial peptides (flagellin), peptidoglycans and lipoteichoic acids (gram-positive bacteria), lipoproteins and fungal glucans and chitin.

PRRs exist as several subgroups that are classified according to their ligand specificity, function, and localization. Based on their localization, PRRs are divided into either membrane-bound PRRs (Toll-like receptors, TLRs; receptor kinases, RK; C-type lectin receptors, CLRs), and cytoplasmic PRRs (NOD-like receptors, NLRs; RIG-I-like receptors, RLRs).[33-37]

<u>Membrane-bound PRRs</u>:[33-38]

I. RK – commonly associated with kinases called interleukin-1 receptor-associated kinase (IRAK) and receptor-interacting protein (RIP) kinase family. Both IRAK and RIP do not auto-phosphorylate the activation loop.

II. TLRs – transmembrane proteins that recognize extracellular/endosomal PAMPs. First discovered in *Drosophila*, trigger the synthesis and secretion of cytokines and other host defense activations that are necessary for both humoral and cell-mediated immune responses. There are twelve functional members of the TLR family that have been described in humans, to-date; each of the TLR shown to interact with a specific PAMP. The interaction of TLRs with their specific PAMP is mediated through either MyD88-dependent pathway or TRIF-dependent signaling pathway. MyD88-dependent pathway is induced by various PAMPs that stimulate TLRs present on macrophages and dendritic cells: inducing secretion of pro-inflammatory cytokines and co-stimulatory molecules via the signaling pathway of this triggers signaling through the NF-κB and the MAP kinase pathways. MyD88 attracts the IRAK4 molecule, IRAK4 recruits IRAK1 and IRAK2 to form a signaling complex. This singling complex reacts with TRAF6, which leads to TAK1 activation and consequently the induction of inflammatory cytokine production/release. On the other hand, TRIF-dependent pathway is induced by macrophages and dendritic cells, after TLR3 and TLR4 stimulation. Of the known twelve TLRs, all but one (TLR3) signals via MyD88 to induce inflammation: TLR3 specifically utilizes TRIF for signal transduction, while TLR is unique since it can signal via either MyD88 or TRIF. TLRs are instrumental with the propagation/activation of the innate and adaptive immunity.

III. CLRs – different cells of the innate immune system express a myriad of CLRs. Despite most classes of human pathogens covered by CLRs, they are major receptors for recognition of fungi.[39] However, other PAMPs have been identified as targets of CLRs such as mannose: the recognition motif for many viruses, fungi, and mycobacteria. In

addition, acquired non-self-surface neoantigens carrying “internal danger source”, or “self-antigen turned non-self”, are identified and destroyed via complement fixation, cytotoxic attacks, or sequestered (phagocytosis) by the immune system by virtue of the CLRs. CLRs are vast, vary based on structure and phylogenetic origin, and have complex variations of signaling involved in CLR induced immune response. However, there exists a major connection between TLR and CLR signaling, which are TLR-dependent and TLR-independent.

Cytoplasmic PRRs:[40]

NLRs – recognize bacterial peptidoglycans, mount a pro-inflammatory and antimicrobial immune response. Among other proteins the most important are MHC II and IPAF. These proteins recognize PAMPs and DAMPs that activate inflammatory caspases (e.g. Caspase 1), which in-turn cleaves and activates important inflammatory cytokines such as interleukin-1 (IL-1), and/or the NF-κB signaling pathway (augmenting production of pro-inflammatory cytokines). From the vast numbers of existing NLR members, nucleotide-binding oligomerization domain (NOD) proteins (NOD1 and NOD2) are the most significant. They detect conserved microbial peptidoglycans in the cytoplasm of the cell; therefore, representing another level of immune response after membrane-bound receptors (TLRs and CLRs).

I. NOD1 recognizes a specific peptidoglycan molecule (meso-DAP), which is a constituent only of gram-negative bacteria.

II. NOD2 recognizes intracellular muramyl dipeptide, which is a peptidoglycan constituent of both gram-positive and negative bacteria.

NODs transduce signals via NF-κB and the MAP kinase pathways via serine-threonine kinase (RIP2). An interesting cooperation exists between TLRs and NLRs, particularly between TLR4 and NOD1 in response to *Escherichia coli* infection.[41]

III. NLRPs are similar to NODs, acting as a regulatory domain and involved in recognition of microbial pathogens. NLRP3 and NLRP4 have been shown to be specific for inflammasome activation.[42] For effective immune response, NLRP3 inflammasome has been demonstrated to be essential for a response induction.

IV. RLRs are RNA helicases, shown to participate in intracellular recognition of double/single-stranded viral RNA, the activation of antiviral gene programs, and have been experimented in exploiting therapy for viral infections. RLRs will often interact and cross-communicate with TLRs in the innate immune response by initiating the release of pro-inflammatory cytokines and type I interferon (IFN I); while acting in the regulation of the adaptive immune response.[43-45]

1.3.1.3 **Compliment System**

This system's name is derived from its twenty different proteins functionally able to "complement" the killing of pathogens by antibodies. This biochemical cascade acts as a major humoral component of the innate immune response. Upon the activation by complement binding to antibodies to microbes directly or through complement proteins to carbohydrates on microbe surfaces, a rapid killing response is triggered. The intensity and speed of the response is a result of signal amplification occurring after sequential proteolytic activation of complement molecules, acting as proteases. This catalytic cascade is amplified and controlled by positive feedback. Throughout the process peptides are produced, which attract immune cells, increase opsonization of pathogen surfaces, and increase in vascular permeability.[46,47]

1.3.2 **Adaptive Immune Response**

An antigen-specific and stronger response, this evolved immune system recognizes specific "non-self" antigens during antigen presentation; while eliciting antigen specific tailored responses, specific pathogens or pathogen-infected cells. To mount these tailored responses and the speed to recognize and dismantle an infection, the production of immunological memory cells is imperative. The specialized adaptive immune leukocytes, B/T-lymphocytes, both carry "self" receptors and recognize specific pathogenic antigens presented on MHCs molecules of other cells. T-lymphocytes are subdivided in two major subtypes: killer T-lymphocytes and Helper T-lymphocytes. Killer T-lymphocytes recognize antigens coupled to MHC I molecules, while helper T-lymphocytes and regulatory cells recognize antigens coupled to MHC II molecules. In contrast, B-lymphocytes have antibody molecules (antigen-specific receptor) on their surfaces that recognize whole pathogens without the need for antigen processing.[31-33,48]

1.3.2.1 **T-Cell Activation**

Killer T-lymphocytes recognize various antigens and directly kill virus infected cells, or cells that are recognized as damaged/dysfunctional. They are activated when their T-cell receptor (TCR) binds to a specific antigen on a MHC I complex from an antigen-presenting cell. The recognition of this MHC:antigen complex is aided by the co-TCR known as CD8. Once activated, killer T-cells release cytotoxins (e.g. perforin) that target cell plasma membrane. These induced pores disturb the native ionic gradients, hydrostatic gradients and permit the entry of granulysin (protease), which trigger apoptosis. Activation is tightly controlled, requires a strong MHC:antigen activation signal, or an additional activation signal from helper T-cells.[31-33,48]

Helper T-cells are known to regulate both the innate and adaptive immune response, while determining the appropriate immune response toward a particular pathogen. These cells possess

no cytotoxic activity. Their specific MHC II:antigen activation is recognized by the TCR known as CD4 on helper cells. Helper cells are known to have weaker associations with the MHC II:antigen; thus, requiring a greater activation number of CD4 TCRs and longer duration of engagement with an APC. Activation of a helper T-cell releases cytokines that enhance microbicidal function of macrophages and the activity of killer T-cells. (14) In addition, CD40 ligands are upregulated and expressed on helper T-cell surfaces, providing extra-stimulatory signals required to activate antibody-producing B-cells.[31-33,48]

1.3.2.2 **B/Plasma-Cell Activation**

The antigen/antibody complex, from pathogens, are up-taken and processed by proteolysis to produce peptides, which are displayed as antigenic peptides on its surface MHC II molecule. This attracts matching helper T-cells, which then release lymphokines that activate B-cells. The activation of B-cells produces and secretes independent plasma cells, millions of copies of antibodies. These plasma cells circulate in blood plasma and lymph, binding to any recognizable specific pathogenic antigen: the cells are marked for destruction by complement activation, uptake and destruction by phagocytes, or direct neutralization.[31-33,48]

1.4| Clinical Significance: Disorders of The Respiratory System

Chronic respiratory diseases affect the tracheobronchial tree and other anatomical structures of the lungs (pleura, pleural cavity, and nerve innervation). These range from mild and self-limiting (e.g. common cold), to life-threatening entities like bacterial pneumonia (community acquired, or hospital/ventilator acquired), pulmonary embolism, acute asthma, and lung cancer. Chronic respiratory diseases are characterized by high inflammatory cell recruitment (neutrophil) and/or destructive infection (e.g. *Pseudomonas aeruginosa*). Advanced chronic obstructive

pulmonary disease (COPD), interstitial lung disease (ILD), cystic fibrosis (CF), emphysema due to alpha-1 antitrypsin deficiency, and pulmonary arterial hypertension (PAH), account for ~85% of all cases indicated for lung transplantation.[49]

1.4.1 **Obstructive Disorders**

Characterized by expiratory airflow obstruction, is a consequence of inflammatory narrowing to the bronchi and bronchiole. As such, gas trapping is a common factor that aides in the diagnosis of obstructive disease. Spirometry measurement of decreased expiratory flow via forced expiratory volume at 1 second (FEV_1) to forced vital capacity (FVC) less than 70%. Types of obstructive lung disease include: COPD (chronic bronchitis and emphysema), asthma, and bronchiectasis. Advanced COPD, with the greatest risk factor being smoking, is a gradual progressive condition that has been documented to account for 32% of all indications for lung transplantation.[49]

1.4.2 **Restrictive Disorders**

Characterized by reduced lung volumes (TLC), restrictive disorders can arise due to alterations in intrinsic lung parenchyma or extrinsic causes. Intrinsic diseases cause inflammation, scarring of lung interstitium, or infiltration of alveoli with exudate and debris. Interstitial lung disease (ILD) being the second most common indication for transplantation (30%), has varying aetiologies from infection (e.g. interstitial pneumonia)/environmental exposures (e.g. pneumoconiosis) to idiopathic pulmonary fibrosis. While extrinsic restrictive disorders have extrapulmonary aetiologies – pleural thickening, non-muscular diseases of the chest wall (e.g. kyphoscoliosis), and neuromuscular disorders (e.g. myasthenia gravis).[50]

1.4.3 **Vascular Disorders**

Pulmonary vascular diseases are conditions that affect the pulmonary circulation. The aetiologies of vascular diseases are pulmonary embolism, pulmonary arterial hypertension, pulmonary edema and pulmonary hemorrhage. Pulmonary embolism occurs due to deep vein thrombosis that usually embolize from the lower extremities and lodge in the pulmonary circulation. Pulmonary arterial hypertension is most commonly associated with idiopathic elevations in pulmonary circulation pressure. However, other co-morbidities (e.g. COPD) can cause pulmonary hypertension, which left untreated can result in cor pulmonale. Pulmonary edema and hemorrhage are the sequalae of acute lung injury (ALI) and acute respiratory distress syndrome (ARDS).[50,51]

1.4.4 **Acute Lung Injury and Acute Respiratory Distress Syndrome**

ALI and ARDS describe clinical syndromes of acute respiratory failure, which have been substantially associated clinical morbidity and mortality.[51] It was Ashbaugh and colleagues, in 1967, who first coined the phrase "acute respiratory distress syndrome (ARDS)" to describe a cohort of 12 critically ill patients with acute respiratory failure.[52] It was not until 1994, after decades of varying definitions, that the American-European Consensus Conference Committee recommended that the clinical requirement to diagnose the syndromes needed have the following criteria:[53]

I. An acute onset of diffuse bilateral pulmonary infiltrates by chest radiograph.

II. $PaO_2/FiO_2 \leq 300$ mm Hg for ALI and ≤ 200 mm Hg for ARDS (PaO_2/FiO_2 – ratio of partial pressure of arterial oxygen to fraction of inspired oxygen).

III. a pulmonary artery wedge pressure ≤ 18 mm Hg or no clinical evidence of left atrial hypertension.

These criteria provided two primary advantages, simplicity of clinical applicability and the ability to quantify the severity of lung injury. This established clinical definition of ARDS has been widely adopted both clinically and for research purposes, until the proposed/updated Berlin definition in 2012. The Berlin definition breaks tradition by establishing three risk strata that are based on degree of hypoxemia, assessed at a minimum positive end-expiratory pressure (PEEP) (**Table 1**).[54,55]

Table 1: Belin definition of ARDS. Adapted from Ferguson *et al*.[55]

Criteria	Rationale
Onset within 7 days after a known clinical insult or new or worsening respiratory symptoms	Observational data suggest that ARDS will develop within 72 hr in the majority of patients at risk for the syndrome and within 1 wk in nearly all patients at risk
Bilateral opacities that are "consistent with pulmonary edema" on chest radiographs or chest CT	There is poor interobserver reliability in interpreting the chest radiograph for the presence of edema. To address this issue, the Berlin definition offers more explicit criteria (e.g., opacities should not be fully explained by effusions, lobar or lung atelectasis, or nodules or masses), with illustrative radiographs provided
Categorization of ARDS severity	A patient-level meta-analysis validated three thresholds for hypoxemia, all consisting of a Pao_2:FIo_2 ratio ≤300 mm Hg
Mild	Pao_2:FIo_2, 201 to 300 mm Hg; mortality, 27% (95% CI, 24–30)
Moderate	Pao_2:FIo_2, 101 to 200 mm Hg; mortality, 32% (95% CI, 29–34)
Severe	Pao_2:FIo_2, ≤100 mm Hg; mortality, 45% (95% CI, 42–48)
Minimum PEEP setting or CPAP, 5 cm of water; Pao_2:FIo_2 assessed on invasive mechanical ventilation (CPAP criterion used for the diagnosis of mild ARDS)	Estimates of FIo_2 are not accurate with oxygen-delivery systems other than invasive or noninvasive ventilation (with a tight-fitting mask), with the exception of nasal high-flow oxygen delivery systems (at flow rates ≥45 liters per minute); requiring higher PEEP settings does not increase predictive validity of the Berlin severity strata and adds complexity

The Berlin clinical criteria helped update, broaden the diagnostic thresholds and additionally, discouraging the term "acute lung injury." Moreover, prior definitions have excluded volume overload or heart failure, but recent evidence suggests that these problems may coexist up to 33% of patients with ARDS.[54,55]

The diffuse alveolar compromise of the pulmonary system leading to ARDS, usually within 7-days after clinical recognition of a known risk factor (**Table 2**), has been described by Katzenstein *et al* (1976) as the development of capillary congestion, atelectasis, intra-alveolar

hemorrhage, and alveolar edema; with hyaline-membrane formation, epithelial-cell hyperplasia, and interstitial edema following days later.[56]

Table 2: Risk factors for ARDS. Adapted from Ferguson *et al*.[55]

Direct lung-injury risk factors
Pneumonia (bacterial, viral, fungal, or opportunistic)*
Aspiration of gastric contents*
Pulmonary contusion
Inhalation injury
Near drowning
Indirect lung-injury risk factors
Sepsis (nonpulmonary source)*
Nonthoracic trauma or hemorrhagic shock
Pancreatitis
Major burn injury
Drug overdose
Transfusion of blood products
Cardiopulmonary bypass
Reperfusion edema after lung transplantation or embolectomy

* Pneumonia, aspiration of gastric contents, and sepsis together account for more than 85% of cases of ARDS in recent clinical trials.

The pathogenesis of endothelial dysfunction, resulting in ARDS injury (**Figure 6**), is initiated either directly or indirectly (**Table 2**) to the delicate alveolar-capillary interface. In the exudative phase of ARDS, the lung's initial response to injury, is characterized by a marked innate immune and cell-mediated damage to the alveolar endothelial and epithelial barriers. Resident alveolar macrophages are activated, leading to release of potent pro-inflammatory cytokines and chemokines. The increased inflammation state promotes the recruitment of neutrophils and

monocytes, which in turn result in the activation of alveolar epithelial cells and effector T-cells. Thus, the sustained inflammatory state results in tissue injury.[54,57]

This deleterious cyclical effect of endothelial activation and microvascular injury contribute to the alveolar-capillary barrier disruption in ARDS; which is further augmented by the release of extensive inflammatory biomarkers and further mechanical stretching (**Figure 6**). However, there is a repair processes that gets initiated during the proliferative phase of ARDS. This phase is essential for the host survival. Once epithelial integrity has been re-established, the reabsorption of alveolar/interstitium protein-rich edema and provisional matrix aid in restoring the native alveolar architecture and function.[54,57] The final phase of ARDS, the fibrotic phase, does not occur in all patients; however, the onset of this phase has been linked to prolonged mechanical ventilation, resulting in ventilator induced lung injury (VILI) and increased mortality.[51,54,57]

Matthay and Zimmerman (2005) summarize the natural progression of ALI/ARDS, with predisposing clinical risk factors and repair versus deleterious evolution.[58] They noted that the outcomes of persistent and progressive injury include multiple organ failure, pulmonary vascular obliteration with pulmonary hypertension, fibrosing alveolitis, and death.[58] It should be noted, that the genetic, cellular, molecular and iatrogenic factors contributing to each of these severe outcomes have been investigated over the years, but require further elucidation. Moreover, over the years, there has been extensive evidence-based research (in-vitro or ex-vivo) with the hope to therapeutically favor and influence repair of the alveolar-capillary membrane during experimentally designed ALI/ARDS models.[59-62]

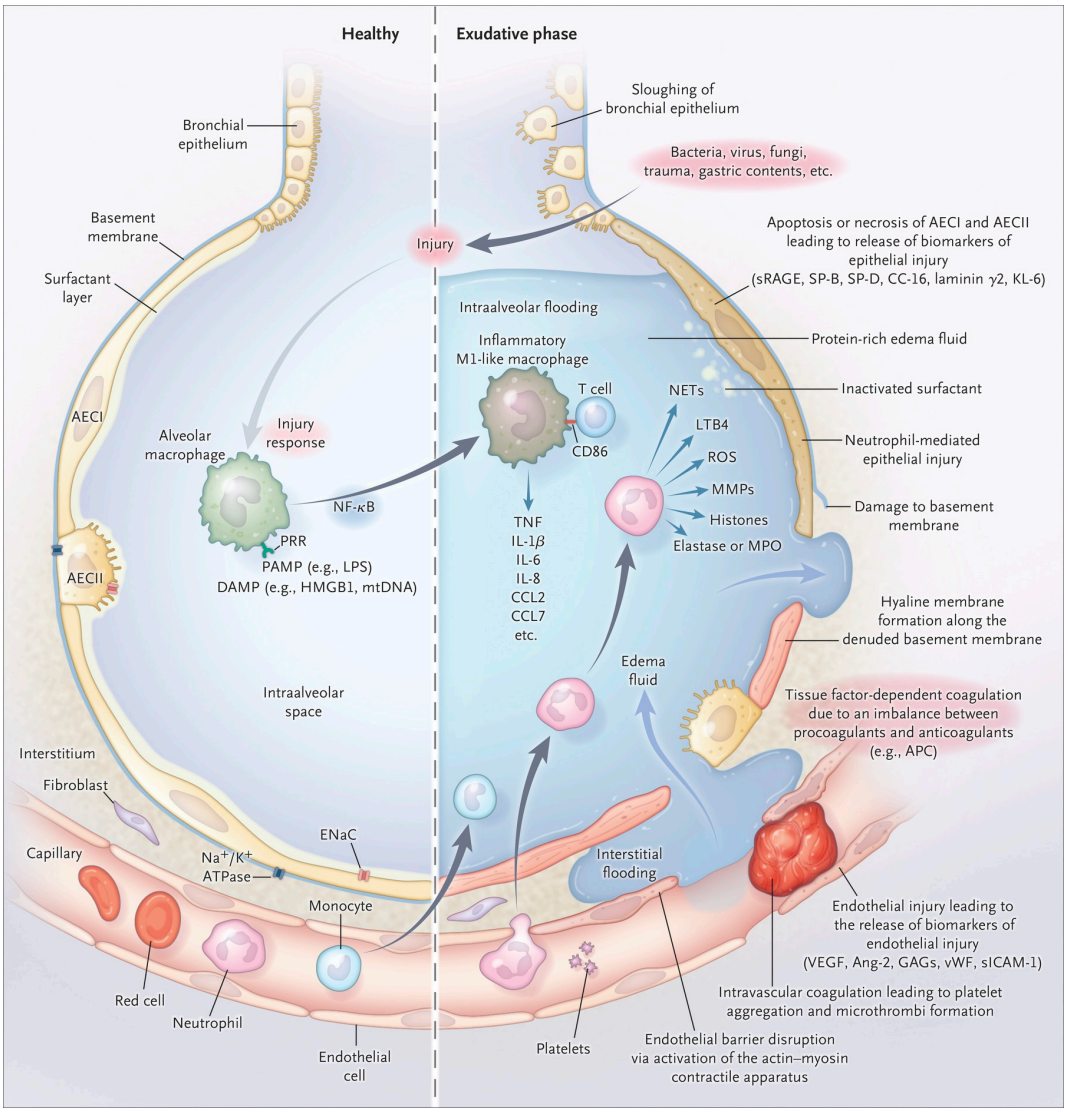

Figure 6: ARDS pathogenesis. Adapted from Thompson et al.[54]
TNF: Tumor necrosis factor; AECI: Type I alveolar epithelial cell; AECII: Type II alveolar epithelial cell; APC: Activated protein C; CC-16: Club cell/Clara cell secretory protein 16; CCL: Chemokine ligand; DAMP: Damage-associated molecular pattern; PAMP: Pathogen-associated molecular pattern; PRR: Pattern recognition receptor; GAG: glycosaminoglycan; HMGB1: High-mobility group box 1 protein; LPS: Lipopolysaccharide; LTB4: Leukotriene B4; MMP: Matrix metalloproteinase; MPO: Myeloperoxidase; mtDNA: Mitochondrial DNA; NF-κB: Nuclear factor kappa light-chain enhancer of activated B cells; ROS: Reactive oxygen species; sICAM: Soluble intercellular adhesion molecule; SP: Surfactant protein; sRAGE: Soluble receptor for advanced glycation end products; VEGF: Vascular endothelial growth factor; vWF: Von Willebrand factor.

Chapter 2

Literature Review

2.1| Lung Transplantation

Solid organ transplantation is considered one of the major medical achievements of the twentieth century. The first successful long-term lung transplantation was achieved 30 years ago by Dr. Joel Cooper and his team in Toronto.[63] Today, lung transplantation has matured into a successful therapy for selected patients with end-stage lung disease. The Registry of International Society for Heart and Lung Transplantation reports ~60,100 adult lung transplants have been performed globally between 1985 and 2016.[49] Indications for lung transplantation vary from patients have the most common types of end-stage lung disease, such as, COPD, ILD/Pulmonary fibrosis, cystic fibrosis, and pulmonary hypertension; to the rarer end-stage lung diseases from connective tissue disorders, lymphangioleiomyomatosis, and sarcoidosis.[49]

2.1.1 **History and Outcomes**

Early first attempts in lung transplantation occurred in the 1946 when Demikhov, a Soviet scientist, attempted to perform a single lung transplantation in a canine; however, ultimately failed due to bronchial dehiscence.[64] Subsequently, in 1950, Metras reported the first successful canine lung transplant and the first bronchial artery and left atrial anastomoses.[65] The first successful human lung transplant, post-op survival 18 days, occurred June 11, 1963.[66] Derom and colleagues, 1971, however, were the first to report out of Belgium a long-term post-op survival (10.5 months).[67] Survival rates like these were not heard of until the advent of immunosuppression, cyclosporine, and better understanding behind poor bronchial anastomoses.[68] In 1983, Goldberg under the guidance of Dr. JD Cooper, elucidated the significance behind the utilization of cyclosporine and its association with improved bronchial anastomoses.[69] Shortly after, 1986, Dr. JD Cooper and team, report the first successful single-lung transplantations for two patients with pulmonary fibrosis.[63] His team, based out of Toronto, continued to perform successful double-lung

transplants, and laid the foundation for the bilateral sequential transplantation technique (remains mostly utilized to-date) – this improved airway healing and had the additional benefit of avoiding cardiopulmonary bypass, if desired.[70]

Despite lung transplantation demonstrating increasing survival rates, patient satisfaction, and overall improved perception of quality of life,[71,72] survival following lung transplantation is 59% (bilateral transplantation) and 48% (unilateral transplantation) at 5-years.[49] At 10 years, survival rates have been reported to almost drop by half, respectively.[49] Majority of reported death following lung transplantation varies with time post-operation – 30-day mortality is mostly related to surgical issues, donor lung preservation, infectious causes, malignancy, bronchiolitis obliterans syndrome (BOS), and primary graft dysfunction (PGD).[49] This is illustrated in **Figure 7**, portraying the current survival curves of bilateral/single lung transplant recipients.

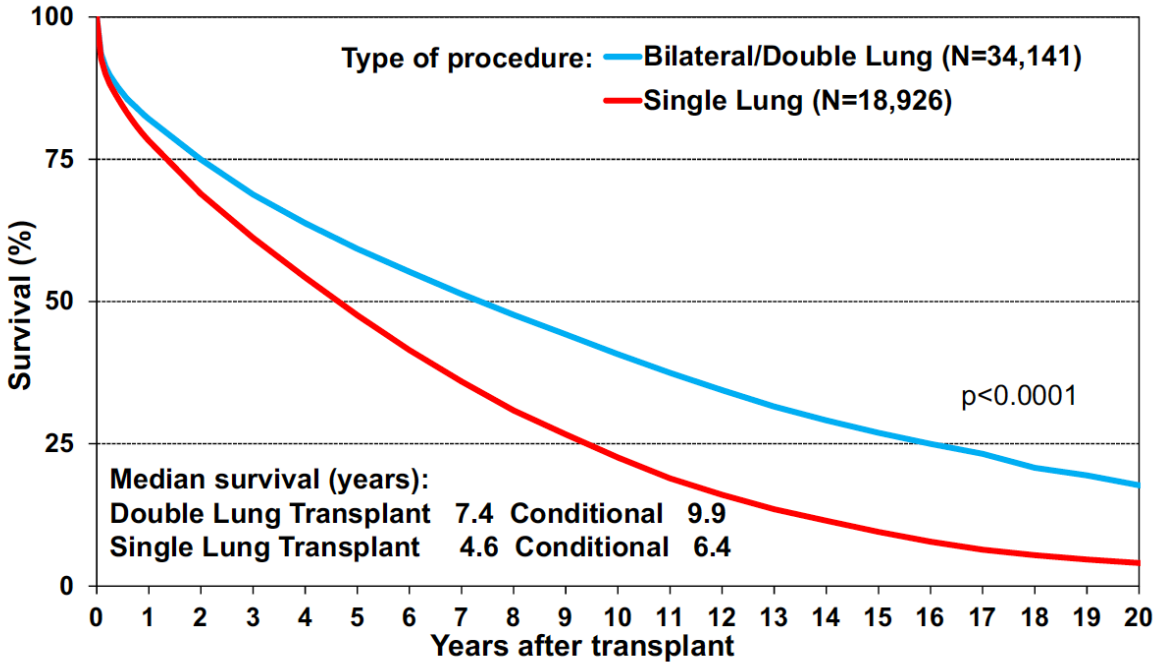

Figure 7: ISHLT Kaplan-Meier bilateral and unilateral adult lung transplantation outcomes. Adapted from Chambers *et al.*[49]

2.1.2 **Organ Shortage**

As the success of lung transplantation increases over the years, the number of patients being listed for lung transplantation has steadily been increasing. Consequently, similar to solid organ transplantation, lung transplantation experiences a shortage of suitable donor lungs, resulting in reported waitlist mortality rates of up to 40%.[73] However, unlike most other solid organ transplants, suitable donor organ shortages in lung transplantation is further compounded by a low utilization rate of 20%.[73] The low utilization rate can be attributable to stringent donor organ acceptance criteria aimed to optimize post-transplant outcomes.[73,74] Moreover, increased susceptibility of donor lungs to injury during brain death, organ procurement, and organ preservation/transportation further contribute to the observed low utilization rate. Currently, clinical standard for organ preservation and transportation includes cold static preservation (CSP); which aims to slow tissue metabolism and minimize oxidative stress.[51,75,76] However, Thabut and colleagues reported in 2005 that the duration of CSP correlates with post-transplant mortality, which has limited maximum acceptable cold ischemic times to 6-12 hours.[77]

2.1.2.1 **Donor Lung Criteria**

Currently, there exists a conservative ideal donor lung criteria list outlined by International Society for Heart and Lung Transplantation (ISHLT):[78]

I. Age <55 years
II. ABO compatibility
III. Clear chest radiograph
IV. PaO_2 >300 on FiO_2 = 1.0, PEEP 5 cm H_2O
V. Tobacco history <20 pack-years
VI. Absence of chest trauma
VII. No evidence of aspiration/sepsis
VIII. No prior cardiopulmonary surgery
IX. Sputum gram stain – absence of organisms
X. Absence of purulent secretions at bronchoscopy

Upon offering of donor lungs to an institution, blood samples are obtained for matching of blood type and minimizing risk of donor-transmitted diseases. Donor size is considered, and a potential recipient is chosen based on size and blood type. A chest x-ray is performed to exclude gross parenchymal or pleural abnormalities; while a bronchoscopy excludes gross infection or anatomical abnormalities. Finally, an oxygen exchange challenge of the donor lungs is performed, and an overall consensus is arrived at based on all the examination findings for the suitability of the organ.[79] On the other hand, at retrieval, the surgeon performs a gross physical evaluation by macroscopic observation and palpation to assess lung compliance and edema. Palpation can exclude intrinsic lung disease, pneumonic infiltrates, nodules, or areas of contusion. During deflation, observing the lungs assesses pulmonary compliance.[80] Consequently, the utilization of this evaluative process is highly clinical and subjective in nature; which raises the question, how likely are suitable organs discarded?

2.1.2.2 **Donor Lung Injury**

To-date, brain death donors (Donation after Brain Death – DBD) are the largest pool of donor organs for transplantation. In DBD, these patients have a cessation of neurologic function that results in a legal definition of death, but their organs remain viable due to preserved cardiac function and ICU support.[81] This situation and type of donors may seem ideal for organ transplantation; however, many factors can contribute to donor lung injury: direct trauma, aspiration, pneumonia, atelectasis, oxygen toxicity, volume overload and ventilator induced lung injury (VILI) all are common causes of organ injury. Moreover, it has been well recognized that the process of brain death results in a deleterious effect on organs, due to the significant ‘cytokine and catecholamine storms’ associated with this process.[80]

The cytokine storm represents a systemic pro-inflammatory response, following brain death. In rodent models[82] and DBD patients,[83] an increase in pro-inflammatory cytokines have been found in various organs, including the onset of lung injury similar to ARDS, as a result of this systemic inflammation. The increase in circulating pro-inflammatory cytokines activates the induction of cell adhesion molecules on pulmonary endothelial and epithelial surfaces; while activating the recruitment of neutrophils and monocytes, propagating the inflammatory injury to the lungs (**Figure 8**).[32,84]

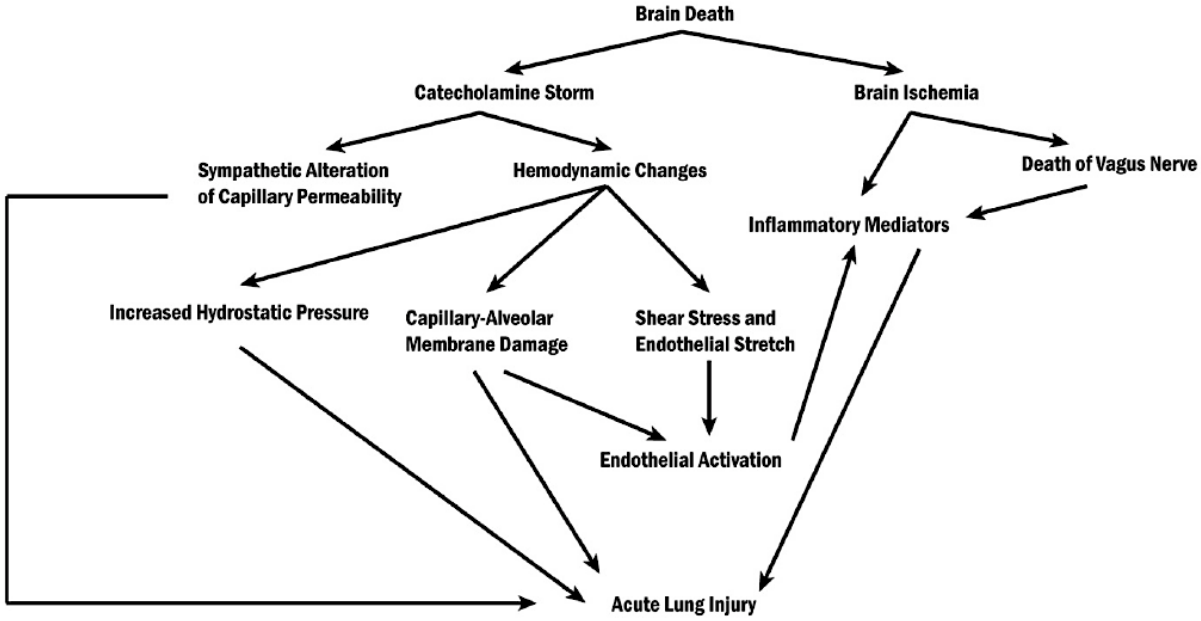

Figure 8: Brain death inducing ALI. Adapted from Avlonitis *et al*.[84]

It has been illustrated in the literature the association of interleukin (IL-8) levels significantly higher during ischemia and post-reperfusion, in patients who developed severe primary graft dysfunction.[85,86] Similarly, Fisher and colleagues in 2001, reported higher concentration of IL-8 in bronchoalveolar lavage (BAL), from 26 human donor lungs used for transplantation, correlated with severe graft dysfunction and early post-operative deaths.[87] It was

not until 2006, when Kaneda et al studied a vast array of pro-inflammatory cytokines (IL-6, IL-8, TNF-α, IL-1β, IL-10, and interferon-γ), using real time reverse transcriptase polymerase chain reaction (RT-PCR), assessing their expression in human donor lungs at the end of cold ischemia: finding that the IL-6/IL-10 ratio being most predictive of recipient 30-day mortality.[88]

Moreover, the catecholamine storm, which arises after the cytokine storm, augments further damage to the integrity of the alveolar-capillary interface. In the vast majority of cases, donors become brain dead following a rise in intracranial pressure, due to either massive intracranial hemorrhage or head trauma.[89] In an attempt to protect cerebral perfusion during brain death, the body releases a large amount of catecholamines. This can be attributed due to increasing ischemia spreading to the medulla, vagal nuclei becoming more ischemic, and as a result unopposed sympathetic stimulation and the rise of the 'catecholamine storm.' This surge causes significant systemic hypertension, resulting in elevated left-sided heart pressures, and consequentially interstitial edema (sometimes alveolar hemorrhage) in the lungs: known as a state of neurogenic pulmonary edema.[90,91] The mechanism for neurogenic pulmonary edema (common injury in DBD) has been attributed to the sudden and profound increase in systemic vascular resistance, induced by the catecholamine storm, leading to decreased left ventricular output and increased left atrial and pulmonary capillary pressure. This marked increase in atrial and pulmonic capillary pressures increases both hydrostatic and permeability injury to the pulmonary epithelium: as a consequence pulmonary edema forms.[92] It should be noted that the catecholamine storm can also induce inflammation either from a) shear stress on endothelial cells during the hypertensive state, b) change to anaerobic metabolism, or c) transient gut ischemia.[83,93]

The importance of vagal tone over the control of inflammation has been recently elucidated.[94] This theory was tested by Hoeger *et al* in 2010, with a brain dead rat model, showing

vagus nerve stimulation (following the induction of brain death) can reduce circulating TNF-α concentrations and lead to down-regulation of a variety of pro-inflammatory genes in the intestinal tissue. Most importantly, vagal stimulation significantly decreased the expression of E-selectin and IL-1β in renal tissue, when transplanted, recipients of those kidney grafts had superior early renal function.[95] The innate immune system has also been implicated as a key mechanism, interacting with vagal stimulation. The vagus nerve inhibits the release of (high mobility group box-1) HMGB1, an intranuclear protein, which is released extracellularly during tissue damage.[96] As discussed in the previous chapter, TLRs play a key role as receptors for tissue damage biomarkers, such as activated HMGB1.[97] In a recent study conducted by Rostron *et al* (2010), inflammatory cytokine release following brain death in a rat model, was significantly reduced when TLR2 and TLR4 receptors were desensitized prior to the induction of brain death – further strengthening the evidence for an interactive role between the vagus nerve and innate immune system, in post-brain death inflammation.[98]

Consequently, if lungs incur the deleterious onset of neurogenic pulmonary edema, it generally precludes the use of those donor lungs for transplantation – primarily due to the significant poor oxygenation observed. This is definitely one area that is open for potential therapeutic models, such as *Ex-Vivo Lung Perfusion* (EVLP). Lungs would be removed from the inflammatory milieu of DBD and provided an ex-vivo window, via EVLP, to be carefully preserved, assessed, reconditioned, and potentially removing extravascular edema.[99]

2.1.3 **Strategies for Increasing Lung Transplant Volumes**

To help alleviate the utilization rate of offered donor organs in lung transplantation, strategies have been developing over the years not only to increase the absolute number of organ donors, but also to increase the utilization rate of organs.

I. *Improving Organ Donation Rate*

Deceased organ donation rate in Canada was approximately 14 per million population in 2007. However, between 2007 and 2016 (**Figure 9**), deceased donor rates increased by 42% (from 14 to 21 donors per million population).[100,101] Interestingly, a Canadian study conducted by Ipsos-Reid found that despite 95% of respondents are in support for organ donation, only 27% have actually registered to donate their organs.[102]

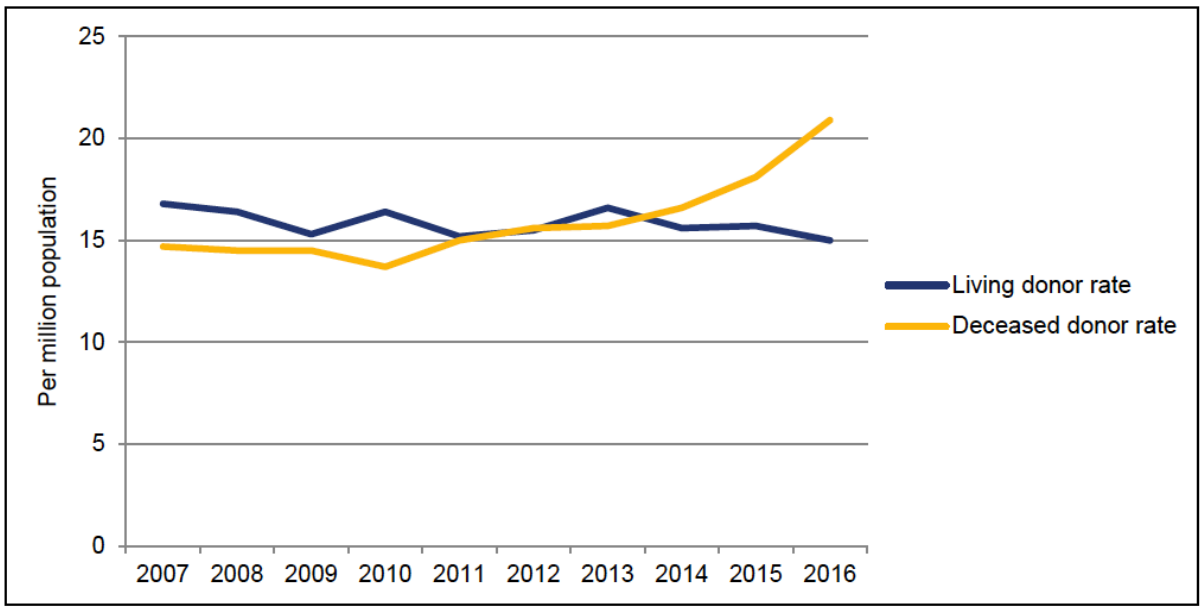

Figure 9: Organ donation rates in Canada, 2007-2016. Adapted from Norris S.[100]

The increase in deceased donor rates seen over the years can be attributable to four changes:

i. Parliament proposing to nationalize aspects of organ donation under the Canadian Blood Services in 2007. Since accepting responsibility for Canada's organ and tissue donation and transplantation system, the Canadian Blood Services developed with all jurisdictions/provinces, the Canadian Transplant Registry. This national database of intended donors has mandated the declaration of a citizen to consent to organ donation, usually at time of renewal of a driver's license or health card.[103]

ii. The government has considered mandating required referral and required request, whereby required referral requires physicians to report all brain deaths and required request obligates physicians to approach all families of potential organ donors.[100]

iii. Professional training of healthcare allies in donor recruitment to assist in capturing more potential donors: particularly in rural hospitals where organ donor coordinators may not be stationed.[100]

iv. Since 2006, there has been an increase interest in exploring an alternative source of donors – cardiorespiratory determined death (DCD).[101,104]

Up to 2006, donations from deceased donors came in large from brain death donors. The Canadian Institute for Health Information (CIHI) refers to these donors as DBD or "neurologically determined death" (NDD). However, the number of deceased donors that have been recruited under certain circumstance after cardiac death (DCD) have steadily increased (**Figure 10**) – in 2006 there were four DCD donors only from Ontario.[101,104] By 2010, all provinces, except Manitoba and Saskatchewan, were considering DCD donors and 45 DCD donors were obtained that year. In 2016, DCD category accounts for almost 25% of all deceased donors.[101,104]

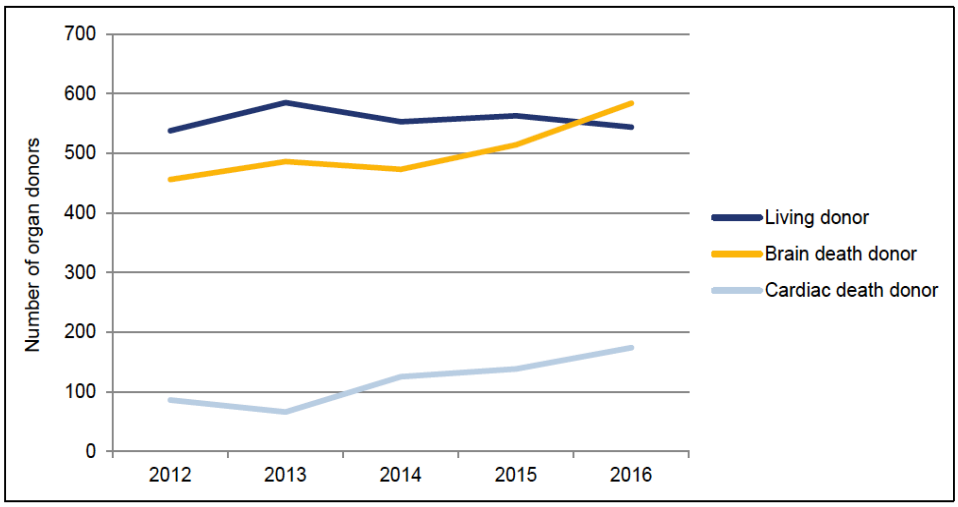

Figure 10: Total number of organ donation types in Canada, 2012-2016. Adapted from Norris S.[100]

II. *Alternate Donor Source*

Some transplant programs began re-exploring the use of DCD as alternative source for donor lungs.[105,106] Since most patients die due to cardiac arrest, the utilization of DCDs could potentially open a new pool of organ donors, which ultimately can meet the entire shortage demand. The first clinical lung transplantation by Hardy utilized a DCD who died from a myocardial infarction.[66] This was acceptable practice in 1963 since the concept of brain death was not yet legally established. In 1970s, brain death criteria reached general acceptance status, which resulted in a shift that the majority of organs harvested would be from DBD with intact circulation.[107,108]

It was not until the early nineties that renewed interest in potential use of lungs from DCD following a series of canine experiments.[109,110] Egan and colleagues demonstrated that lung cells are capable of remaining viable for a certain period after circulatory arrest.[111,112] The lung is the only solid organ which is not dependent on perfusion for aerobic metabolism; rather, it uses a mechanism of passive diffusion through the alveoli for substrate delivery.[113-116]

The First International Workshop on DCDs in Maastricht of the Netherlands in 1995 defined four types of donors, referred to as "Maastricht Categories" (**Table 3**).[117] Categories I (**dead on arrival**) and II (**unsuccessful resuscitation**) comprise the ***uncontrolled*** donors. Categories III (**awaiting cardiac arrest**) and IV (**cardiac arrest in Brain-Death**) include the ***controlled*** donors. Category V (**cardiac arrest in a hospital inpatient**) has recently been added.[118]

Table 3: Maastricht categories for DCD. Adapted from Sanchez-Fructuoso *et al.*[118]

I	Dead on Arrival to Hospital	**Uncontrolled**
II	Unsuccessful Resuscitation	
III	Awaiting Cardiac Arrest	**Controlled**
IV	Cardiac Arrest Following Brain-Death	
V	Cardiac Arrest in a Hospital Inpatient	**Uncontrolled**

Several centers worldwide have adopted DCD programs in their perspective clinical routine for lung transplantation. The most reported series deal with controlled Category III donation, after withdrawal from life support.[114,116,119,120] To-date, the reported experience with this category amounts to more than 100 patients worldwide.[80] Interestingly, the majority of reported cases using Category III DCDs have comparable results to the cases of lung transplantations that utilized DBD.[121]

Theoretically, lung utilization from DCDs hold advantages, given the injuries acquired by potential DBDs. Studying microarray data from DCD and DBD lungs, Keshavjee and team (2011) demonstrated significantly increased inflammatory features with DBD lungs compared to DCD lungs. Furthermore, pathway analysis demonstrated distinct DBD lungs enriched with gene-sets corresponding to pathways of innate immunity, cytokine interaction, intracellular signaling, cell communication and apoptosis.[122]

The above two strategies focused on increasing the absolute quantity of organ donors. The next strategy aims to increase the utilization of the current pool of organ donors, by expanding the current donor pool.

III. *Extension of Current Acceptable Donor Criteria*

Best transplant outcomes will occur when ideal organs are carefully matched to ideal recipients; however, one must consider the shortage of donor organs and the consequence of high waitlist morbidity and mortality rates. Therefore, a common strategy to maximize the utilization of donated lungs considered 'suitable' for transplantation has been to use an "extended criteria:" these organs fall outside the accepted ISHLT standard criteria, designated as marginal organs.[123,124] It has been estimated that ~40% of currently rejected donor lungs could be considered 'safe to transplant', if a more detailed and accurate evaluation was available to identify these marginal/extended criteria lungs.[125] Liberalization of donor criteria in centers that adopted the extended criteria included lungs utilized from donors with:[123,124]

i. Age >55 years
ii. >20 pack year smoking history
iii. >4 days on ventilator
iv. Positive gram stain on BAL

Yet, contraindicated organs that risked disease transmission, active extra-central nervous system malignancy and positive serology for HIV, remain unutilized.[124]

The experience using marginal/extended criteria lungs has been published showing mostly equivalent short-term outcomes.[126-131] Bronchoscopy and chest radiograph evaluation remain the most subjective of the ISHLT criteria; but, it is within these two criteria that there is evidence of increased risk of post-operative death. Pierre *et al* (2002) reported their experience with 63 extended donors, and part of the extended criteria included chest radiographic infiltrates and purulent secretions on BAL. They concluded that there was statistically significant higher 30- and 90-day mortality when compared with recipients of standard criteria donors during the same time-

frame. This experience demonstrated that donor lungs with truly purulent secretions and bilateral infiltrates are considered high risk for recipient mortality and clearly should not be utilized.[130] Moreover, subgroup analysis suggests that lungs with purulent secretions and a $PaO_2 < 300$ mm Hg had a negative impact on recipient outcome.[129] Another factor that should be considered with extended criteria lungs is graft ischemic time. Gabbay *et al* (1999) reported that graft ischemic times were predictive of recipient P/F ratio, and they did not transplant marginal lungs with ischemic times greater than six-hours.[132]

Overall, for centers with long waiting lists and limited donor pools, there should be a thoughtful use for extended criteria donor lungs.

2.1.4 **Primary Graft Dysfunction**

At a fundamental level, transplant clinicians fear primary graft dysfunction (PGD), which might be another contributing factor toward the current low utilization rate of donor lungs. When an injured or inflamed lung is transplanted into a recipient, a type of ALI occurs within 72-Hours of transplantation, known as PGD.[133] Currently, PGD affects 11-25% of lung transplant recipients and is the leading cause of 30-day/early mortality.[134] Clinically, PGD can be diagnoses based on severe hypoxemia, lung edema, and diffuse pulmonary infiltrates on chest X-ray. Pathologically, PGD represents a diffuse alveolar damage picture. In addition to the acute deleterious effects of PGD, recipients that survive PGD appear to be at higher risk for development of chronic graft dysfunction and BOS.[135] Hence, prevention PGD is of the utmost concern for both short and long-term post-transplant outcomes.

The pathogenesis of PGD is multifactorial, but it can be thought of as the sustained summation of insults to the donor lung, pre-transplant. Of these insults, ischemia-reperfusion injury (IRI) is thought to play the largest role in the development of PGD.[136,137] IRI affects the

transplanted lung by stimulating mechanisms of inflammation and generation of reactive oxygen species (ROS).[136,137] During the process of ischemia and reperfusion, resident macrophages within the lung are simultaneously activated and subsequently release cytokines and chemokines in a major and complex pro-inflammatory response.[138] Leading to a direct recruitment of neutrophils and leukocytes by chemokines signalling and the indirect recruitment by upregulated adhesion molecules and activated complement pathways. These recipient neutrophils and T-cells[139] augment the inflammatory response and cause further injury to the alveoli. Concurrently, this marked pro-inflammatory state acts as a strong co-stimulation for development of adaptive immune reactions towards the graft, possibly through DAMPs. Thus, the inflammatory process that occurs during IRI and leads to PGD, appears to follow a biphasic pattern: the initial phase caused by macrophage activation and the second phase caused by responding neutrophils. Animal experiments with clodronate or gadolinium (macrophage depletion) have demonstrated reduced PGD onset.[140]

Reactive oxygen species are another major contributory cause of lung injury and PGD, following ischemia. During cold storage, on ice, anoxia results in ATP degradation and the production of hypoxanthine.[136,137] During ischemia, xanthine dehydrogenase, the enzyme responsible for the conversion of hypoxanthine to xanthine, is converted to xanthine oxidase. At reperfusion, xanthine oxidase converts hypoxanthine to xanthine with superoxide, a ROS by-product. As a consequence, direct injury occurs to the alveolar-capillary interface; thereby, damaging the alveolar air-fluid barrier. In addition, NADPH oxidase found on capillary endothelial and neutrophil cells can generate another source of ROS during reperfusion, adding to the alveolar injury. Clinically, it is by these two mechanisms that the formation of alveolar infiltrates and failure of gas exchange is seen, hours following transplantation.[136,137]

As one can appreciate, PGD is quite similar to ALI/ARDS, where increased permeability of the microvasculature due to inflammation leads to alveolar edema and diffuse alveolar damage. Therefore, the currently utilized PGD scoring system is analogous to that used to score ARDS, where P/F ratios and chest infiltrates are key components and asses at time-points up to 72-Hours (**Table 4**). It was validated that with this scoring system, grade 3 PGD within 48-Hours of transplant resulted in higher short and long-term mortalities and long hospital length-of-stay.

Table 4: ISHLT PGD grading.[134]

Grade	P/F Ratio	Chest X-Ray
0	>300	Normal
1	>300	Diffuse Allograft Infiltrates
2	200-300	Diffuse Allograft Infiltrates
3	<200	Diffuse Allograft Infiltrates

To better predict recipients susceptible to PGD, many centers have retrospectively reviewed their experience.[141] Unfortunately, the data from different studies conflict: due to limited number of patients at single centers and collection of data over different eras of lung transplantation. Nonetheless, age >45 years, prolonged ischemic times, and pulmonary arterial hypertension at time of transplant, have demonstrated an increase in development of PGD, in the majority of studies.[141]

Treating PGD is supportive and similar to the strategy employed for ARDS patients. This is accomplished via low tidal volume ventilation, combined with careful fluid administration, in attempt to reduce VILI and capillary leak.[142] As more research goes into therapeutic measures to

best treat PGD, at this point in time, the best treatment for PGD remains prevention through careful selection of donor lungs.

2.2| Lung Preservation Techniques

In the current clinical paradigm of lung transplantation, it is at the time of donor surgery that the decision to utilize or reject the organ for transplantation is made. Once the decision is made to utilize, the lungs are procured from the donor and undergo obligate ex vivo cold static preservation (CSP) – the lungs are placed in ice with the aim to slow tissue metabolism and minimize the formation of oxidative stress. Most often, the recipient operation begins in parallel with the decision to utilize the lungs; thus, minimizing further injury to the organ while it is under cold ischemic.

2.2.1 Gold Standard Procurement and Preservation Strategies

There are many strategies employed at time of procurement to better preserve the donor lung.[143] First, the utilization of a protective ventilation strategy (tidal volume = 6-8ml/kg, PEEP = 5 cm H_2O and FiO_2 <0.5) helps avoid further injury from barotrauma; while full anticoagulation of the donor (300 U Heparin/kg) is conducted to minimize the risk of intravascular clot formation.[51]

Upon assessment of the donor, aortic cross-clamp is induced in the donor. This results in the heart to arrest and the organ (lungs) recovery begins. 500μg of prostaglandin E1 (PGE_1) is given in the pulmonary artery to lower the pulmonary vascular resistance – PGE_1 acts as vasodilator in the pulmonary vasculature. PGE_1 have also been reported to help reduce PGD by downregulating pro-inflammatory cytokine expression.[144]

The vasculature of the lungs is extensively flushed with a cool extracellular low-potassium solution. Flushing serves three purposes, a) cool the organ, b) remove blood from the pulmonary

vasculature (minimize clot formation), and c) removal of demarginated inflammatory and immune cells. Early experience in lung transplantation utilized an extracellular low-potassium solution and was found to benefit lung preservation, compared to the utilization of intracellular type solution used in other organs.[145] The addition of dextran-40 has been studied and believed to serve two purposes. First, as a carbohydrate it acts as an osmotic agent, helping to keep fluid within the intravascular space. Second, acting as an endothelial scavenger, it is believed to reduce the aggregation of erythrocytes and thrombocytes.[115] Thus, it is theorized that the addition of this ingredient to the existing extracellular low-potassium solution will help preserve flow through the microvasculature, after reperfusion, particularly in the bronchial microcirculation; thus, may play a role in reducing bronchial anastomotic complications.[115,145] Another ingredient added to the flush solution is glucose. Since the lungs are stored inflated with oxygen, a unique situation arises during CSP where the lungs are ischemic but not hypoxic. Glucose is believed to help support the aerobic metabolism during lung preservation under CSP. Approximately 50-60 ml/kg of flush solution is administered anterograde (pulmonary artery) and retrograde (pulmonary vein).[115,145]

A delicate balance is desired for flush pressure – too high of a pressure leads to injury to the pulmonary vasculature, and too low leads to inhomogeneous flushing. In practice, the flush solution is hung at 30 cm above the patient and driven by gravity.[115,145]

Over the years, studies have demonstrated the improving post-transplant outcomes, with the use of low-potassium dextran-glucose flush solution (LPD-glucose/Perfadex). In a retrospective study conducted in Oto *et al* (2006), recipients of lungs stored with Perfadex/LPD had overall lower rates of PGD, days on ventilator, and 30-day mortality in comparison to other intracellular-type (high potassium) flush solutions.[146] However, a more recent retrospective study conducted by Gohrbrandt *et al* (2015) demonstrated non-significant difference in 3-year survival

rates between LPD and Celsior (LPD: 66.5% vs. Celsior: 72.0%); while demonstrating that there is a trend toward better survival and increased freedom from BOS observed with the Celsior cohort. This illustrates that lung preservation solution are undergoing continued research and other solutions might be as safe, effective, and carry advantages just like the LPD-solution.[147]

Following flush, lungs are procured, inflated to an airway pressure of 20 cm H_2O with 50% oxygen and stored on ice. Inflation of the lungs provides oxygen to the lung parenchyma for aerobic metabolism; furthermore, it preserves the alveolar structure during storage. This was validated by van Raemdonck *et al* (1997) showing that inflation of the lungs, even with nitrogen, is still superior to atelectatic storage.[148]

Upon removal of the lungs from the body, reduction of the metabolic rate is commenced by cooling them in ice (CSP); which remains the cornerstone strategy for lung preservation over 30 years. Despite studies in a rate model demonstrating the optimal temperature for lung preservation under CSP being approximately 10 degrees Celsius,[149] to simplify transport logistics, ice (4 degrees Celsius) is commonly used. However, it has been reported that PGD and 30-day mortality rates are augmented with cold ischemic times longer than 8-hours.[77,150]

2.3| Normothermic Preservation – Ex Vivo Lung Perfusion (EVLP)

2.3.1 **EVLP: Preservation**

Physiological normothermic ex-vivo lung perfusion is a novel method that maintains the organ in a more physiological protective condition, outside the body, during preservation. EVLP will help increase the utilization of donor lungs by allowing trained professionals to accurately evaluate and assess the functionality of lungs during the transport period. While the lungs are on EVLP, they will be maintained under normothermic physiological conditions to help alleviate the

deleterious ischemia reperfusion injury that is observed with CSP; furthermore, permitting the treatment/reconditioning of the lungs prior to transplantation. Currently with CSP, lungs have no way to be truly assessed for injury that occurs during the transport period, which can range from 6-8 hours. Thus, transplanting lungs that have sub-optimal functions can result in poor post-lung transplantation outcome and increase the severity of primary graft dysfunction.

Ex-vivo perfusion of organs began with the work of Carrel and Lindbergh in 1935.[151] They have documented twenty-six perfusions of whole organs: ovary, thyroid, kidney and heart. Organs that were perfused were functional for several days with active cellular proliferation. Since the advent of Carrel and Lindbergh's work on ex-vivo perfusion, ex-vivo systems were limited to the study of organ physiology, including lungs.[152] It was not until 2001 that Dr. Stig Steen first described the use of EVLP in clinical lung transplantation.[153] Using a proprietary lung-perfusion solution (STEEN Solution™), put together in their lab, the group was able to re-assess uncontrolled DCD lungs.[154] With the help of EVLP, their successful reconditioning of these DCD lungs (an unutilized donor pool) resulted in a cascade of research to revisit the possibility to utilize donor lungs from the DCD pool.

It was not until further modifications of the EVLP system and perfusion technique by the University of Toronto group, which allowed perfusion of pig lungs on EVLP from only 4-6 hours[154] to a prolonged 12-hour ex-vivo perfusion, with promising functional data.[155] The group went on to determine the impact of prolonged EVLP using injured ischemic donor pig lungs. To mimic the clinical scenario, where lungs undergo a period of cold ischemia during transportation, pig lungs were preserved under CSP for 12 hours and subsequently divided into two groups: cold static preservation (the current gold standard) or normothermic EVLP for a further 12 hour of perfusion (total 24 hours of preservation).[156]

It became evident that unlike CSP, normothermic EVLP demonstrated noticeable improvement in regard to overall lung function: less edema formation post-transplantation, better alveolar-epithelial cell tight junction integrity, enhanced metabolic function, and improved oxygenation.[154,157-159]

2.3.2 **EVLP: Protocols**

Currently, there exists' three different EVLP protocols utilized around the world: 1) Toronto protocol, 2) Lund Protocol, and 3) Organ Care System™ (OCS) protocol. These protocols vary with their perfusion and ventilation settings, and in the equipment used for their circuits (**Figure 11**). In general, after cold pulmonary flush and retrieval using an extracellular solution (low-potassium dextran solution, LPD, known as Perfadex®), the donor lungs will be instrumented in the donor hospital or recipient hospital (experiencing a period of cold ischemia during transport), then placed on the EVLP platform for either immediate or delayed normothermic perfusion, respectively. Interestingly, Mulloy *et al* (2012) investigated the best timing for EVLP: at the donor hospital immediately after cold pulmonary flush or at the recipient hospital after transport and a period of cold storage (delayed EVLP).[160,161] It was found that lower levels of inflammatory markers on bronchoalveolar lavage were present, less histologic lung injury, and superior post-transplant oxygenation were seen in the group of delayed EVLP (4-hours of cold storage followed by 4-hours of EVLP).[160,161]

2.3.2.1 **Toronto Protocol**

The Toronto group uses an acellular perfusate, Steen Solution™ (XVIVO Perfusion, Goteborg, Sweden), which was originally described by Stig Steen and coworkers from the Lund University.[154] This proprietary solution is an extracellular-buffered solution with the addition of human albumin (maintains physiologic colloid pressure) and dextran-40.[161,162] Once the LA

cannula is filled with Steen Solution™ (XVIVO Perfusion, Goteborg, Sweden), perfusion commences at 10% of the calculated cardiac output flow, and incrementally increased till a final 40% cardiac output flow for the remainder of the perfusion run, by 50 minutes from the start of perfusion.[156,158,161,163] Ventilation is initiated once the perfusate temperature reaches 32°C at an immediate 7ml/kg tidal volume, positive end-expiratory pressure (PEEP) of 5 cm H_2O, respiratory rate (RR) of 7 breathes/min, and with an inspired fraction of oxygen (FiO_2) of 21% (**Figure 11**).[156,158,161,163] Unlike the other two protocols, the Toronto method elects to have a closed left atrium and by adjusting the height of the reservoir manually to maintain a positive LA pressure between 3-5 mm Hg.[156,158,161,163] Finally, the Toronto group carefully monitors and maintains the mean pulmonary arterial pressure (PAP) to stay below 15-20 mm Hg, which is flow dictated. This is believed to avoid development of hydrostatic pulmonary edema.[163]

2.3.2.2 Lund Protocol

The Lund group utilizes a cellular perfusate: Steen Solution™ (XVIVO Perfusion, Goteborg, Sweden) mixed with packed red blood cells (pRBCs) to obtain a hematocrit of 14%.[162] In the Lund technique, ventilation begins at a tidal volume of 3ml/kg at 32°C and gradually increases by 1L/min, for each degree, until it reaches 5-7ml/kg at 37°C. Other parameters that differ from the Toronto protocol include, the open LA system at 100% cardiac output flow, respiratory rate (RR) of 20 breaths/min, and a FiO_2 of 50% (**Figure 28**).[161,162,164]

2.3.2.3 OCS Lung™ Protocol

The OCS Lung™ protocol is based on a cellular perfusate like the Lund protocol; however, in this protocol the perfusate is composed of an OCS™ Solution® (Transmedics) or Perfadex® (XVIVO Perfusion AB, Goteborg, Sweden) and pRBCs to achieve a hematocrit between 15-25%.[161,165] Both of these solutions are LPD based solutions, without the addition of human albumin

(unlike Steen Solution™) . Perfusion flow is set to 2-2.5 L/min, PAP maintained ≤20 mmHg, with an open LA system, initiating ventilation at 34°C and 6ml/kg, a RR of 10 breaths/min, PEEP of 5-7 cm H_2O, and an FiO_2 of 12%.[161,163,165] The variations among these protocols have been summarized below in (**Figure 11**).

Parameter	Toronto	Lund	OCS*
Perfusion			
Target flow	40% CO	100% CO	2.0–2.5 l/min
PAP	Flow dictated	≤20 mmHg	≤20 mmHg
LA	Closed	Open	Open
Perfusate	Steen™ solution	Steen™ solution + RBC's hct 14%	OCS™ solution + RBC's hct 15–25%
Ventilation			
Start temp (°C)	32	32	34
Tidal volume	7 ml/kg bw	5–7 ml/kg bw	6 ml/kg bw
RR (bpm)	7	20	10
PEEP	5 cm H_2O	5 cm H_2O	5–7 cm H_2O
FiO_2 (%)	21	50	12

Figure 11: Comparison between clinical EVLP protocols. Adapted from Machuca et al.[163]
CO – cardiac output; FiO_2 – inspired fraction of oxygen; hct – hematocrit; LA – left atrium; PAP – pulmonary artery pressure; RBC's – red blood cells; PEEP – positive end-expiratory pressure; Temp – Temperature; *OCS – Organ Care System™ (Transmedics).

2.3.3 **EVLP: Evaluation**

To-date, the judgement of the surgeon remains one that is greatly dependent on clinical lung evaluation. Prior to retrieval, some objective evaluation is conducted in the means of chest x-rays and ICU bronchoscopy; however, the majority of the evaluation leading to the decision of utilization occurs at one timepoint, organ retrieval. Inadvertently, lungs which may have some underlying injury may simply have not expressed the signs (edema and/or lower P/F ratios) and still be utilized. Furthermore, donor physiology at retrieval may not be entirely conducive to

accurate lung evaluation, since blood pressure is often labile and under recruitment of the lung parenchyma, may give falsely low P_aO_2.

2.3.3.1 **Physiologic Evaluation**

Ex vivo lung perfusion (EVLP) permits the potential of lung evaluation under more physiologic conditions, at controlled perfusion flow, and ventilation strategies. More significantly, the decision for utilization or unsuitability can be delayed until EVLP assessment at the recipient hospital, drastically improving decision-making. However, the understanding of physiology during EVLP and which functional parameters correlate with accurate markers of lung health during ex vivo evaluation, still requires elucidation. P_aO_2 has been the main clinical evaluation of lungs for decision making of suitability for transplantation. The pulmonary ventilation (V) to pulmonary blood perfusion (Q) ratio is an important determinant of this value – air must interact with fluid to achieve oxygen exchange.[13] In humans, normal V/Q ratio is typical ~0.8, with normal minute ventilation ~4.2L/min and normal perfusion rate ~5.5L/min. However, with V/Q mismatching, P_aO_2 falls towards equivalence to mixed venous PO_2. As described by West, there exists a physiologic V/Q mismatch across the normal upright lung. Both ventilation and perfusion decline from the bases to the apices of the lung (West Zones 1,2, and 3).[13] The apex of the lung is slightly V>Q with a concomitant area at the base that is V<Q. By definition, blood perfusion will follow the path of least resistance and perfuse areas where V<Q – the net effect is a mismatch with areas V<Q and other areas V>Q. The amount of hyperoxic blood coming from V>Q areas cannot correct for the amount of relatively hypoxic blood coming from V<Q areas. This plays an important concept when pathological conditions arise in the lung. Common donor pathologies such as pneumonia, edema, and aspiration all flood the alveoli leading to increased areas of V<Q. Consequently, V/Q mismatching occurs and the reported P_aO_2 and P/F ratio can result in unsuitable

donor lungs. Hence, why clinically, physicians increase PEEP in patients with these conditions to re-inflate the affected lung units, attempt to reduce V/Q mismatch, and obtain a more reliable P/F value.[54,58]

Traditionally, two foundational clinical trials have described the variables that investigators should consider when deciding the utility of lungs – oxygenation and lung compliance.[166,167] Nonetheless, donor quality gas exchange is still considered the most important single parameter to gauge lung quality. However, it has been shown that the value of PO_2 during EVLP, especially with an acellular perfusate, should be questioned on the grounds that only a few molecules of oxygen are required to increase it significantly in plasma-like solutions. Moreover, animal pre-clinical models demonstrated the deterioration of lung compliance, earlier than PO_2 during the evolution of ALI.[168,169] Sanchez *et al* (2012), provide the explanation behind this observation by stating that the loss of capillary barrier function, with consequent accumulation of interstitial and intra-alveolar fluid, typically precedes a fall in systemic oxygen saturation.[168] This was further confirmed by the Toronto group with their pre-clinical studies showing oxygenation alone is not a predictor of donor lung function post-transplantation; while other functional parameters, including compliance, decrease on EVLP, if lungs are incurring injury.[156]

The literature is in discordance with regards to what can be considered the optimal perfusate during EVLP evaluation – a cellular or acellular perfusate?[99,170,171] Cellular based perfusates (pRBCs or autologous whole blood) might better mimic physiological conditions further, seen after donor lungs have been transplanted and reperfused.[99,161,165,172,173] On the other hand, others have claimed that the use of an acellular perfusate is more favorable during EVLP, since cellular based perfusates might be subjected to destruction over extended EVLP runs (12 hours); thus, exacerbating lung edema/injury.[155]

2.3.3.2 **Ventilator Induced Lung Injury**

As EVLP continues to gain interest in the transplant world, ensuring that the protocols established are refined and suited to provide the best results for reconditioning marginal lungs, is imperative. Two key components that govern any EVLP platform are a) perfusion parameters and b) ventilation parameters. As described earlier, which perfusate produces more favorable reconditioning environment for ex vivo repair and evaluation. Moreover, all three clinically trailed EVLP platforms have varying perfusion protocols.[163] On the other hand, the difference in ventilation protocols between Toronto, Lund, and OCS platforms are fairly consistent. All three clinical EVLP platforms employ positive pressure ventilation (PPV) as a modality of ventilation. They all utilize ventilation settings expected to protect reconditioning lungs from ventilator-induced lung injury (VILI) – tidal volume of 5-7 ml/kg and PEEPs of 5-7 cm H_2O.[163] The rationale behind these settings is that tidal hyperinflation of patent alveoli and tidal recruitment of collapsed alveoli may cause VILI.[174] Nonetheless, patients with ARDS have demonstrated that injured lungs may still develop VILI even with protective tidal volumes limited to 6 ml/kg.[175-177] Furthermore, over the years of experimental studies of PPV-EVLP, it has been widely reported the potential deleterious effects of VILI with extended PPV-EVLP is associated with increasing pro-inflammatory markers, DAMP expressions, and ALI formation. Which is contrary to the purpose of PPV-EVLP, that is to preserve and recondition lungs.[178-183]

Alternatively, negative pressure ventilation (NPV) was historically utilized in the "iron lungs" to treat patients that suffered from respiratory failure induced by poliomyelitis (**Figure 12**).[184,185] The first negative pressure ventilator was described by Scottish physician named Dr. John Dalziel in 1832. Several prototypes followed, however, the first widely utilized and developed iron lung machine did not appear until 1928, invented by professors Philip Drinker and

Louis Shaw Jr. from Harvard School of Public Health.[186] Known as the "Drinker respirator", this iron lung machine was powered by an electric motor with air pumps from two vacuum cleaners. The pumps alternated the pressures within the rectangular, airtight metal box (where the patient lays supine), pulling air in and out of the lungs in a non-invasive ventilatory technique.[187]

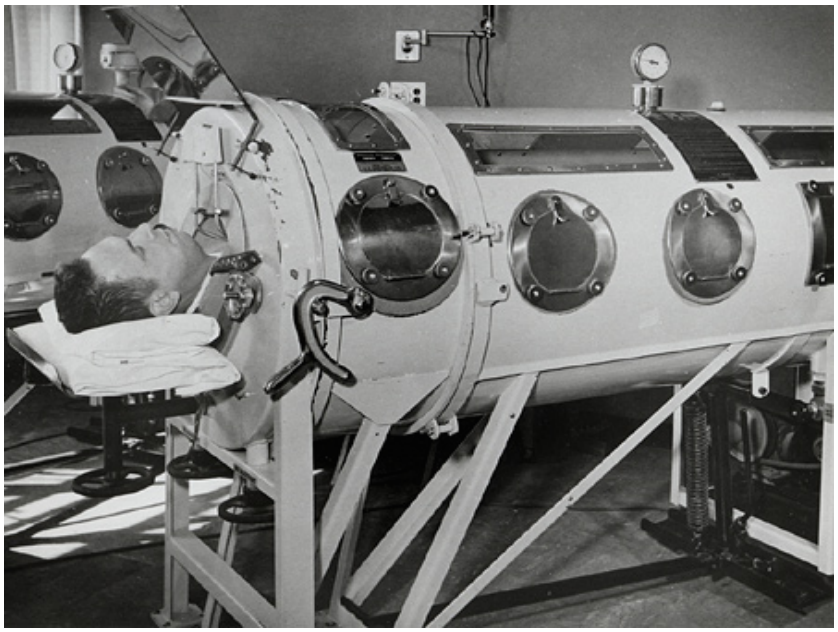

Figure 12: The iron lung ventilator. Adapted from Kenneth.[187]

One can theorize that the utilization of an NPV strategy during EVLP would minimize VILI observed with PPV-EVLP since the production of a negative intrathoracic pressure would equally be distributed over the pleural surface of the lungs relative to alveolar pressure; as a consequence, resulting in a more uniform ventilation throughout the lung parenchyma. There has been no prior investigation into the utility of NPV during EVLP, until 2008. Grasso *et al* (2008), utilizing a rabbit model, demonstrated that the application of short term NPV-EVLP over PPV-EVLP improved oxygenation, decreased overall atelectasis and improved ALI.[188]

Therefore, further refinement to current EVLP platforms should consider investigating ventilation modality, not only ventilation settings. Ventilation modality may improve donor lung preservation strategies, reconditioning, and safely extend EVLP's therapy window beyond the current clinical limit, 4-6 hours.[161]

2.3.4 **EVLP: Reconditioning**

As EVLP strategies are investigated further and refined, extending the therapeutic window will open possibilities for more precision medicine – cell and gene therapy. Given that a large portion of potential donor lungs are injured via a variety of mechanisms (brain death, contusion, infection, aspiration, atelectasis, and edema), there is potential for targeted therapies for each insult. With the safety of an isolated ex-vivo setting, without systemic organ toxicity, one can speculate the truly revolutionary impact EVLP (as a platform) will introduce for novel therapies. Moreover, EVLP possesses the potential to expand the current limited donor lung pool, and drastically changing current waitlist mortality rates. Consequently, since the introduction of EVLP groups around the world have been investigating interventions towards common mechanisms of lung injury.

Donation from DBD, being the largest currently utilized organ donors, can be accompanied by a pro-inflammatory milieu and neurogenic edema. Steen *et al* (2009) demonstrated that a series of 4 human lungs were bronchiolitis obliterans syndrome free, 1-year post-transplantation, after reconditioning on EVLP. Furthermore, the authors claim that the use of their proprietary high oncotic perfusate (STEEN Solution), may have assisted in the removal of lung edema following EVLP.[99]

Since then, almost a decade of EVLP therapeutic approaches has shown quite the advancement in drug, gene, and stem cell therapy. In theory, EVLP allows administration of most

effective therapies, while avoiding systemic toxicity. Notable clinical applications were reported by Luc *et al* (2014), Mazankowski Alberta Heart Institute utilizing the portable OCS Lung™, successfully reconditioning DCD donor lungs that had a large pulmonary embolus with therapeutic thrombolysis medication; followed by successful transplantation of the treated lungs and positive clinical outcomes.[189] Nakajima *et al* (2016) demonstrated that the treatment with broad spectrum antibiotics of rejected human donor lungs due to infection found all antibiotic-treated lungs having a significantly decreased bacterial counts in BAL. Moreover, perfusate endotoxin levels after extended EVLP (12-hours) were also significantly lower than the control group. Overall, the strong correlation associated with endotoxin concentrations at 12-hours and pro-inflammatory markers was observed on a functional level of the all the antibiotic treated donor lungs – significant improvement in oxygenation, compliance, and reduction in pulmonary vascular resistance (PVR).[190]

Similar to pharmacological therapy, gene therapy is feasible during EVLP. However, to assess the true nature with regards to safety and efficacy of this therapy, extended EVLP (12 to 24-hours) strategies are needed. Cypel *et al* (2009) report an encouraging and potentially impactful pilot study of IL-10 gene transfection with adenovirus (AdhIL-10), over extended 12-hour EVLP. Clinically ten-multiorgan human donor lungs, unsuitable for transplantation, were evaluated with or without intra-airway delivery of AdhIL-10 gene therapy. The treated lungs showed significant improvement in oxygenation and PVR, a favorable shift from pro-inflammatory to anti-inflammatory cytokine expression – resulting in a reported recovery of alveolar-endothelium integrity.[191]

Interestingly, since the inception of EVLP in 2001, the past 17-years has demonstrated Moore's law – with evolving technologies and their interdisciplinary integration in various

disciplines, including medical research.[192] Most notable are the advancement in tissue decellularization, bio-regeneration of whole rodent organs, and stem cell therapy, provide promising clinical utilizations for treating complicated lung diseases;[193-196] while opening up the idea of a new form of bio-engineered autologous donor bank.[197] In the field of lung transplantation, mesenchymal stem cells (MSCs) have been well investigated due to their multipotent capabilities and their ability to secrete paracrine factors; which regulate endothelial and epithelial permeability, immunoreaction, and attenuate the deleterious inflammatory cascade.[198,199] The beneficial effects of MSCs have been confirmed and reported by various groups investigating their effect on types of ALI. The Toronto group reported in 2016 that the intravascular administration of MSCs, compared to intrabronchial, in porcine lungs on 12-hours of EVLP showed decreased concentration of circulating porcine IL-8 levels and marked increased in human vascular endothelial growth factor (VEGF) concentrations – concluding that MSCs might have potential therapeutic roles against ischemia-reperfusion injury (IRI).[200] Furthermore, stem cell therapy has shown potential in replacing damaged multi-ciliated airway cells, with new functioning cells differentiate from stem cells – a potential avenue for EVLP repair of cystic fibrotic donor lungs.[201] Nevertheless, further studies are needed to integrate this stem cell functionality with EVLP. If successful, the integrity and functionality of various lung grafts could be improved significantly.

2.4| Summary

Lung transplantation continues to be a promising therapy for end-stage lung disease. Yet, it is limited by low donor rates and poor donor lung utilization rates. EVLP has demonstrated significant growth and promising outcomes in the setting of improving conversion donor rates and potentially alleviating donor shortages. As the success of EVLP continues in clinical lung

transplantation, this will significantly advance translational research in various domains of lung pathology and repair. Hence, it is equally essential to recognize both the advantages and disadvantages inherent with EVLP as a novel evaluative and reconditioning platform (**Figure 13**).

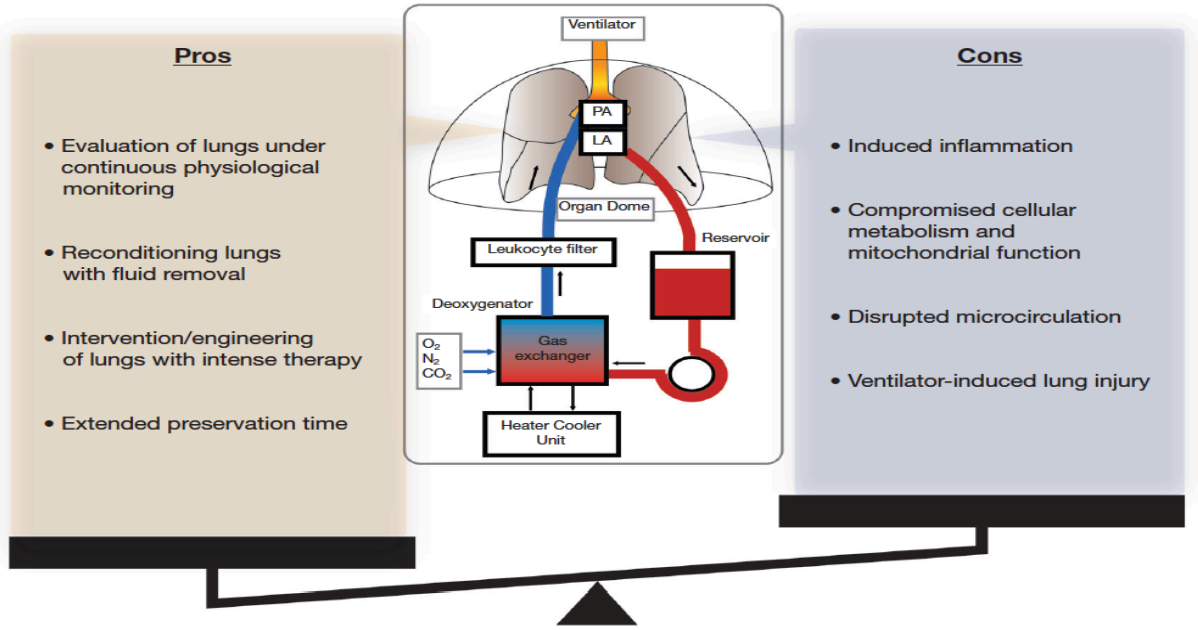

Figure 13: Advantages and disadvantages of EVLP. Adapted from Tane *et al.*[202]

Normothermic EVLP permits the evaluation of lung grafts in real time via multiple functional parameters and mimicking in-vivo physiological conditions; as such, the relationship between which functional parameters can give insight on graft health during ex vivo reconditioning, is imperative.

Ultimately, the goal is to reduce inflammation, bullae and edema formation; while providing adequate time for ex vivo reconditioning. In order to achieve the goal of optimized EVLP reconditioning of marginal or sub-optimal donor lungs, optimal perfusate and ventilation strategies with EVLP platforms need further investigations. Accordingly, this thesis focuses on pre-clinical and clinical investigations of the optimal perfusate and ventilation modalities needed

to successfully preserve, assess, and evaluate porcine and human lungs on custom-designed, portable, extended PPV & NPV-EVLP platforms.

Chapter 3

Rationale, Hypotheses and Objectives

3.1| Rationale

Even with the most aggressive lung transplant programs, they utilize at most 40% of offered donor lungs for transplantation. The remainder are deemed unsuitable for transplantation. With the development of extended normothermic ex vivo lung perfusion, there exists great alternate potential for:

1. Objective evaluation of donor suitability
2. Individualized medicine – repair of injured human donor lungs during preservation phase, on EVLP.

As development of this paradigm succeeds, this would have immense changes on lung transplant volumes and reducing waitlist times and mortality rates significantly.

With regards to the University of Alberta-Mazankowski Hospital Transplant Program, the centre is one of the largest in western Canada. Unique to this centre than other transplant centres around the world, is its geographical isolation and large catchment area – serving a catchment area >6 million Km^2 and >7 million Canadians. Thus, better effective methods related to lung preservation and transportation, to minimize the deleterious effects of cold ischemic times and post-transplantation complications, would alleviate some of the lung transplant challenges faced at this transplant program. Currently, the centre accepts ~27% of all lungs donated, consequently resulting in a waitlist mortality rate of ~33%. University of Alberta Hospital Transplant Program decided to join the INSPIRE lung international trial to evaluate the use of a portable EVLP system (OCS Lung™) for centres with challenging large catchment areas.[203] Bozso *et al* (2015), report promising retrospective cohort results for three bilateral lung transplants from controlled DCD donors (Maastricht category III); following organ preservation and reconditioning using the portable OCS Lung™ EVLP device at the University of Alberta transplant centre. Lung graft

function remained stable, with improvement in P/F ratios, following EVLP. Warm organ ischemic time was <30 minutes, mechanical ventilation was discontinued within 48-hours, and no patient stayed in the intensive care unit longer than eight days. Post-transplant, PGD 3 had resolved for two of three recipients by 72-hours. There was 0% mortality for all recipients 90-days post-transplant.[204] In 2018, the INSPIRE trial was completed and results published in the journal of *Lancet Respiratory Medicine*. It is quite the significant study since it stands to be the largest international clinical trial to-date, conducted as a prospective, randomized controlled, non-inferiority study. Warnecke and colleagues set the primary effectiveness end-point as a composite of patient and graft survival at day 30 and absence of PGD grade 3 within the first 72-hours. The study showed the OCS group met the non-inferiority test, when compared to the static cold storage group (4°C) – for primary end-point, freedom from severe PGD 3 within 72-hours and freedom of death within 30-days of transplant.[205] Moreover, data from the INSPIRE Trial demonstrates ischemic times >5 hours have strong correlation with the development of PGD 3, in early post-transplant period, and the development of bronchiolitis obliterans syndrome (BOS) at two years.[206] The investigators state that this finding may have strong implications in the development of chronic lung allograft dysfunction. Given that chronic lung allograft dysfunction stands to be the major cause of disability and death after lung transplant.[49] Alleviation of PGD 3, in early post-transplant period, has been recognized to be crucial determinant of chronic lung rejections and long-term survival; however, further study follow-up are needed.[207,208]

Other corroborating clinical studies demonstrating clinical efficacy and promising utility of EVLP to increase donor rates and expand the current limited donor pool are the Toronto led clinical HELP trial,[158,166] the DEVELOP-UK trail,[178] the U.S. NOVEL trial,[167] and the

international EXPAND lung trial.[209] Nevertheless, debate continues with regards to the optimal perfusate composition (cellular versus acellular),[170,171,210,211] and ventilation strategies.[154,155]

Therefore, due to the aforementioned promising results of EVLP as a novel platform in alleviating specific challenges encountered with transplant centers serving large catchment areas and geographical isolation, we sought out to create our own portable custom-designed EVLP platform.

3.2| Hypotheses

1. Cellular based perfusates will demonstrate more favorable lung outcomes, during extended 12-hour PPV-EVLP.
2. A Negative pressure ventilation strategy during (NPV)-EVLP will lead to less ventilator induced lung injury, compared to conventional positive pressure ventilation (PPV)-EVLP.

3.3| Objectives

1. To evaluate the optimal perfusate composition (cellular versus acellular) in a large porcine model, during extended PPV-EVLP.
2. To evaluate the safety and efficacy of the utilization of a novel ventilation modality, NPV-EVLP, in a large porcine model and unutilized marginal human lungs.
3. To assess the functional physiologic parameters, inflammatory cytokine expression, histopathology, and edema formation during PPV/NPV-EVLP.
4. To elucidate potential evaluative parameter(s) for organ health, during PPV/NPV-EVLP

Chapter 4

Ex-Vivo Lung Perfusion: Cellular Perfusate Preserves Lung Compliance and Lung Integrity

4.1| Abstract

Introduction: Normothermic Ex Vivo Lung Perfusion (EVLP) is an accepted technique, used clinically to evaluate and increase the utilization rate of unsuitable donor lungs, for lung transplantation. Here we sought out to identify the optimal perfusate composition that should be utilized for extended EVLP.

Materials and Methods: Twenty-four porcine lungs underwent 12-hours of EVLP utilizing a custom-built portable platform. Lungs were allocated equally to either perfusate composition: acellular ($EVLP_A$), whole blood ($EVLP_B$), or red blood concentrate ($EVLP_R$), n=8/perfusate. Physiological parameters, edema formation, and lung injury were assessed; and whether any perfusate demonstrates a unique association among the assessed parameters.

Results: With regards to aerodynamic parameters, cellular based perfusate groups showed a significantly improving trend in compliance over EVLP, compared to the deteriorating trend of the acellular group; with the $EVLP_R$ group having significantly higher lung compliance at the end of EVLP, compared to the acellular group (30.9 ± 2.3 ml/cm H_2O vs. 21.3 ± 1.4 ml/cm H_2O; respectively, p=0.03). Lung oxygenation did not differ significantly between perfusates and was >400 mm Hg for all groups. The acellular group had a significantly lower pulmonary arterial pressure and vascular resistance, compared to the cellular perfusates. TNFα concentrations were significantly higher for $EVLP_B$, while $EVLP_A$ and $EVLP_R$ did not differ. There was no significance in IL-6 concentrations between all three perfusates. The acellular group had significantly higher IL-8 levels at the end of EVLP, compared to the cellular perfusates. $EVLP_A$ demonstrated significantly worse histological interstitial edema, while the cellular perfusates did not differ. This was further corroborated with the acellular group showing >50% in lung edema formation after

12-hours ($p=0.002$); while the cellular perfusates did not differ significantly. As for perfusate correlative investigations, only the cellular based perfusates demonstrated significant positive correlation with compliance and oxygenation ($EVLP_R$: $r = +0.926$, $p<0.05$; $EVLP_B$: $r = +0.844$, $p<0.05$). The acellular based perfusate ($EVLP_A$) demonstrated a significant negative correlation only with oxygenation and PVR ($r = -0.934$, $p<0.05$) and compliance and PVR ($r = -0.884$, $p<0.05$). On the other hand, autologous blood based perfusate ($EVLP_B$) was the only cellular perfusate strategy that also demonstrated significant negative correlation with oxygenation and PVR ($r = -0.873$, $p<0.05$) and compliance and PVR ($r = -0.976$, $p<0.05$). Moreover, $EVLP_B$ was the only perfusate strategy to show significant negative correlation with oxygenation and edema formation after 12-hours of EVLP ($r = -0.833$, $p<0.05$). All other assessed parameters showed no significant association, for any of the perfusates.

Conclusions: During extended EVLP, a cellular based perfusate appears to preserve lung compliance and maintain overall lung integrity. Nonetheless, survival models are needed to investigate which evaluative parameter will reliably predict lung health over extended EVLP and donor lung function after transplantation.

4.2| Introduction

Human lung transplantation has been widely accepted as a modality of treatment for advanced stage lung disease.[212] The annual report from the Registry of the International Society for Heart and Lung Transplantation (ISHLT) states more than 45,000 LTx cases performed worldwide since the 1990s.[212-214] Over the years, the volume of lung transplantation has steadily plateaued – with a progressive increase in demand, a growing recipient waitlist, and a shortage of suitable organs, donor lung utilization is merely 15%.[215-217] Currently, more than 80% of donor lungs are potentially injured and therefore deemed unsuitable for transplantation.[158]

The gold standard in lung graft preservation for over 30 years has been exclusively cold static preservation (CSP).[218] It was not until the development of normothermic ex-vivo lung perfusion (EVLP) by Prof. Steen's group in Lund, which ushered the emergence of a new platform that can be used to help preserve, assess, evaluate and recondition donor lungs under physiological conditions; therefore, improving donor lung suitability for transplantation and expanding the current donor pool.[219-221]

Currently, there are three main clinically investigated EVLP platforms:

a) The Toronto XVIVO Perfusion System (XPS), uses the Toronto protocol: an acellular based perfusate (Steen Solution™).[155]
b) Vivoline, uses The Lund protocol: Steen Solution™ and cellular perfusate (packed Red Blood Cells, pRBCs).[162]
c) Organ Care System (OCS, Transmedics), uses the Transmedics Protocol: OCS™ Solution® or Perfadex® (XVIVO Perfusion AB, Goteborg, Sweden) and pRBCs.[221]

These differing, positive pressure ventilated, (PPV)-EVLP platforms have been extensively studied and shown successful preservation, assessment, and potential repair of donor lungs.[99,158,161,165] Unfortunately, there exists a dichotomy between clinical EVLP (4-8 hours) and pre-clinical experimental EVLP (12 hours).[155,165,204]

Controversy persists among literature between cellular versus acellular perfusates during EVLP.[99,170,171] It is argued, that the use of a cellular based perfusate (pRBCs or whole blood) might better mimic the physiological conditions seen after the lungs are re-transplanted. [99,161,165,172,173] While others claim that the use of red blood cells within a perfusate would result in their destruction over time and may exacerbate lung edema.[155]

Therefore, here we investigate if there is an optimal perfusate that will reproducibly extend perfusion on EVLP up to 12 hours, while maintaining macro/microscopic lung integrity. Differences in lung hemodynamics, aerodynamics, pro-inflammatory cytokines, histomorphology, global edema formation, and perfusate specific parameter associations were analyzed. We hypothesize that the utilization of a cellular based perfusate during EVLP will further protect lung integrity.

4.3| Materials and Methods

4.3.1 **Animal Model**

Twenty-Four domestic female pigs (42 ± 5 kg body weight) were used for this study. Porcine lungs underwent normothermic PPV-EVLP for 12 hours using a custom-built portable platform, with minimal ischemia time. Each animal was randomly allocated to three treatment groups, according to perfusate composition: a) acellular (n=8), b) autologous whole blood (n=8), and c) pRBCs (**Figure 14A**).

All experiments were conducted in accordance with the NIH 'Principles of Laboratory animal care', guidelines of the Canadian Council on Animal Care (CCAC), and under a protocol approved by the Animal Care and Use Committee at the University of Alberta.

4.3.2 **EVLP Treatment Groups**

Acellular perfusate group ($EVLP_A$): 2L of Krebs-Henseleit buffer (KHB) with 8% bovine serum albumin (KHB-A).

Whole Blood group ($EVLP_B$): 1L KHB-A + 1L autologous donor whole blood

Packed Red Blood Cell group ($EVLP_R$): 1.5L KHB-A + 0.5L pRBCs

For each experiment, the standard KHB/acellular solution was made fresh (**Table 5**),[222-224] and was used to mimic the published hyperoncotic pressure and buffered extracellular properties of STEEN Solution™ (XVIVO Perfusion, Gothenburg, Sweden).[162,225]

Table 5: EVLP perfusate characteristic.

	Perfusate		
Variables	**AC** (n=8)[a]	**pRBC** (n=8)[a]	**WB** (n=8)[a]
pH	7.40 ± 0.03	7.35 ± 0.03	7.40 ± 0.05
Hct (%)	n/a	13.0 ± 2.0	13.5 ± 1.5
Na^+ (mmol/l)	130.5 ± 2.9	135.7 ± 2.9	136.0 ± 3.9
K^+ (mmol/l)	3.9 ± 0.4	4.2 ± 0.2	4.4 ± 0.4
Ca^{2+} (mmol/l)	2.1 ± 0.3	2.2 ± 0.3	2.3 ± 0.2
Cl^- (mmol/l)	98.8 ± 3.6	101.2 ± 1.8	98.3 ± 3.7
Osmolarity (mOsm/kg)	272.1 ± 7.2	279.5 ± 6.4	275.6 ± 6.9
Oncotic Pressure (mm Hg)	31.6 ± 0.9	26.8 ± 0.6	27.0 ± 1.5

AC – Acellular perfusate; **pRBC** – Packed red blood cells perfusate; **WB** – Whole blood perfusate; **Hct** – Hematocrit; **Na^+** – Sodium; **K^+** – Potassium; **Ca^{2+}** – Calcium; **Cl^-** – Chloride; n/a – Not applicable.
[a]Data expressed as mean ± standard error.

Packed red blood cells were obtained via the collection of autologous whole blood, following donor exsanguination, washed with 1L of 0.9% saline, and concentrated using the Sorin Xtra cell saver (Sorin Group Canada Inc., Burnaby, BC). The described volumes for the cellular groups provided a constant desired hemoglobin concentration of 40-50 g/liter or a hematocrit of 12-15% (**Table 5**).

4.3.3 **Lung Procurement**

The donor lung procurement procedure was identical in all groups and is described in detail else-where.[226,227] Pigs' anesthesia was induced via an intramuscular injection of Ketamine (20 mg/kg), Atropine sulphate (0.05mg/kg) and xylazine (0.9mg/kg). Orotracheal intubation was established, and general anaesthesia was maintained with 1-3% isoflurane. A median sternotomy was performed and systemic heparinization was given at 400U/kg, intravenously. Then a 2-stage venous cannula was placed into the right atrium, through which autologous whole blood was exsanguinated and collected. Cardiectomy and bilateral pneumonectomy followed promptly after exsanguination. Trachea was clamped at a peak airway pressure of 20 cm H_2O, positive end expiratory pressure (PEEP) 7 cm H_2O, and lungs were explanted en-bloc. Our portable EVLP circuit minimizes the duration of ischemic time.

4.3.4 **Custom EVLP Platform**

The custom EVLP platform was primed with 2 Liters of the respective experimental perfusate (**Figure 14A**), 10,000 IU Heparin, 500 mg of methylprednisolone, and 3.375 g of piperacillin/tazobactam. The lungs were placed in the standard organ chamber (XVIVO Perfusion, Gothenburg, Sweden) and had the open left atrium drain the perfusate into a hard-shell reservoir. A centrifugal pump (Medtronic, Minneapolis, MN, USA) generated continuous flow to the pulmonary artery (PA) from the reservoir; prior to entering the PA, perfusate passed through a

membrane de-oxygenator (Sorin PrimO2X, Sorin Group Canada Inc., Burnaby, BC) and heat exchanger (PolyScience, Illinois, USA), and a M27 PH.I.S.I.O adult arterial filter (Sorin Group Canada Inc., Burnaby, BC), **Figure 14B**. The specially designed circuit has a corresponding custom software package, which wirelessly controlled our desired pulmonary arterial flow and pressure. Data was collected and stored at 10s intervals, utilizing a flow probe (BIO-Probe Transducer Model TX 40, Medtronic, Minneapolis) and pressure transducer (Edwards Lifesciences, Dominican Republic). Compressed medical air and hypoxic sweep gas mix (89% N_2, 8% CO_2, 3% O_2) were used to maintain the pulmonary arterial PO_2 and PCO_2 within physiologic parameters.

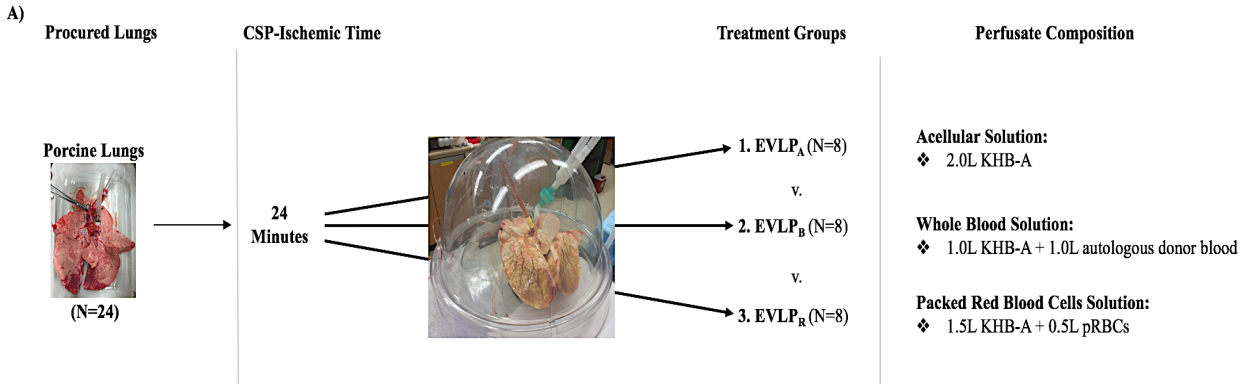

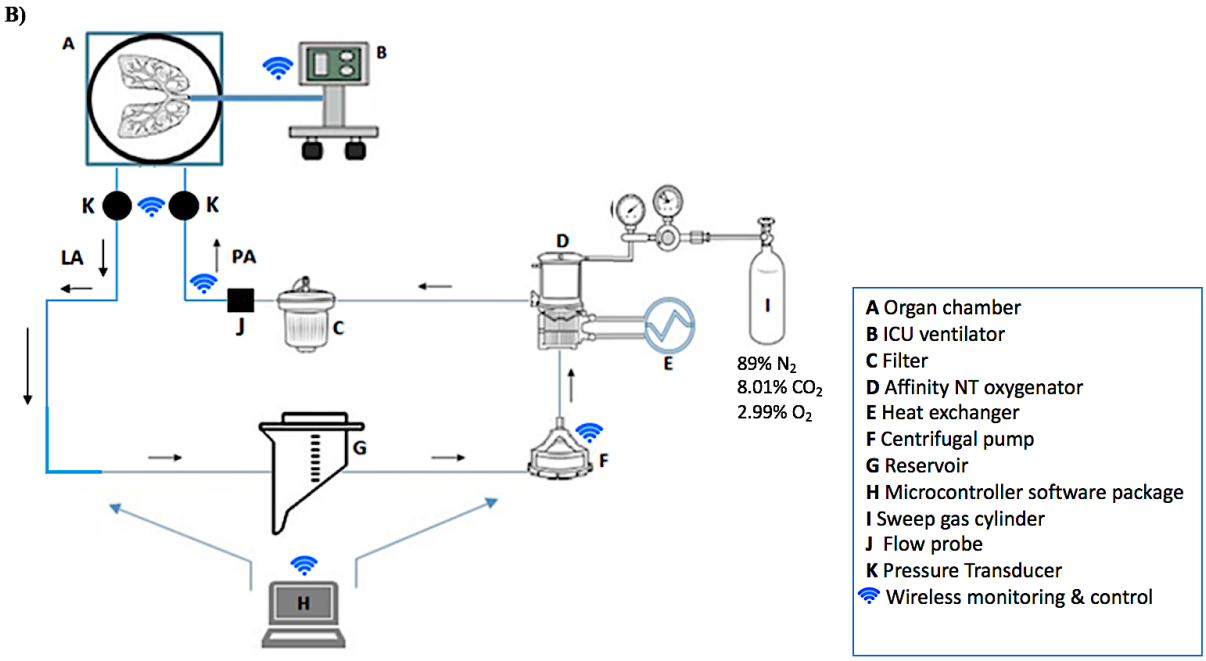

Figure 14: (A) Simplified experimental protocol. **(B)** Custom-built PPV-EVLP platform schematic. **(A)** Porcine lungs (N=24) underwent normothermic EVLP for 12 hours. Lungs were subjected to a minimum amount of cold storage preservation (CSP) ischemic time of 24.0 ± 5.0 minutes: from the time of donor exsanguination to connecting pulmonary arterial cannula and initiating gradual reperfusion on the custom built portable EVLP platform. Porcine lungs were randomly divided into 3 treatment groups, based on perfusate composition: a) $EVLP_A$: acellular based solution made of Krebs-Henseliet and 8% bovine serum albumin (KHB-A), b) $EVLP_B$: autologous donor whole blood mixed with KHB-A, and c) $EVLP_R$: packed red blood cells mixed with KHB-A. **(B)** With the open left atrial system, oxygenated perfusate exits the lungs, drains naturally into a hard-shell reservoir (G), then pumped via the centrifugal pump (F) to the oxygenator/heat exchanger (D,E); which in turn warms the perfusate to normothermia (computer controlled/adjusted) and deoxygenates it with a hypoxic gas mixture (I). Prior to re-entering the lungs via the pulmonary arterial cannula (PA) for re-oxygenation, the perfusate passes through an arterial line filter (C).

4.3.5 **Initiation of EVLP** (U of A Protocol)

Using the portable platform, reperfusion of explanted porcine lungs was initiated at 5% cardiac output and 20-25°C, after minimum amount of ischemic time (24 ± 6 minutes); which was calculated after the initiation of exsanguination. The lungs had the pulmonary artery cannulated, the left atrium left open to drain passively into the reservoir, and trachea intubated with an 8mm endotracheal tube. Anterograde flow was gradually increased to 10% of predicted cardiac output (CO: 70 ml/kg/min) and then incrementally increased by 10% CO every 20-minutes to achieve a

preservation mode flow of 30% CO by 1-hour of EVLP (**Table 6A**). During this time, the perfusate solution was also gradually warmed to 38°C, which is physiologic temperature for porcine lungs.[228-231]

Table 6: **(A)** Initiating reperfusion and **(B)** ventilation strategies for PPV-EVLP.

A)	**Perfusion Time (Minutes)**					
	0	10	20	20-40	40-50	60 (T1)
Perfusion Temperature (ºC)	20-25ºC	25ºC-30ºC	32ºC	32ºC-34ºC	34ºC-36ºC	38ºC
PA Flow (% Cardiac Output, CO; CO = 70 ml/kg/min)	5%	10%	10%	20%	30%	30%
Ventilation	None	None	Initiate Preservation Mode			Recruitment Phase
Medical Gas Mixer	None	None	None	None	None	Start
Left Atrial Pressure (mm Hg)	0	0	0	0	0	0

B)	Ventilation Mode	
	Preservation	**Evaluation**
Temperature (ºC)	38ºC	38ºC
Pulmonary Artery Flow	30% of estimated Cardiac Output; CO=70ml/kg/min	50% of estimated Cardiac Output; CO=70ml/kg/min
Ventilation Parameters:		
Mode	Pressure Control	Pressure Control
Desired Inspiratory Tidal Volume	6 ml/kg	10 ml/kg
Frequency	7-8 bpm	10-12 bpm
P_{AWP}	< 20 cm H_2O	< 25 cm H_2O
PEEP	7 cm H_2O	5 cm H_2O
FiO_2	21%	21%
Pressure Parameters:		
PAP	< 20 mm Hg	< 20 mm Hg
LAP	0 mm Hg	0 mm Hg
Medical gas mixer	89% N_2, 8% CO_2, 3% O_2	83% N_2, 8% CO_2, 3% O_2
Medical gas mixer (L/min) titrated to PCO_2	35-50 mm Hg	35-50 mm Hg
P_{AWP}: peak airway pressure; **PEEP**: positive end-expiratory pressure; **FiO_2**: fraction inspired of oxygen; **PAP**: mean pulmonary artery pressure; **LAP**: left atrial pressure; **PCO_2**: partial pressure of carbon dioxide in pulmonary arterial circulation		

For all treatment groups, donor lung ventilation was undertaken via positive pressure-control ventilation and flow-controlled perfusion. Once perfusate temperature reached 32°C, preservation mode ventilation was initiated (**Table 6B**). Mechanical ventilation was performed using a standard intensive care unit positive pressure ventilator (SERVO-I, Maquet Critical Care AB, Solna, Sweden). Recruitment maneuvers were performed for the first 3-hours of EVLP by maintaining the PEEP at 7 cm H_2O with inspiratory holds performed every 30 minutes for three consecutive breaths (5-10 seconds/breath), before initiation of organ evaluation.

The desired preservation and evaluation modes of ventilations, and vascular pressure parameters are described in **Table 6B**. Evaluation was conducted serially every 2 hours (beginning with 3-hours (T3) of EVLP, until T11), with upper peak airway pressure limit set to 25 cm H_2O, and by raising preservation settings to the ventilation parameters described in **Table 6B**. Sweep

gas flow rate was titrated through the hollow fiber de-oxygenator to maintain a physiologic pH of 7.35-7.45 and PCO_2 (35-50 mm Hg). While Insulin (2.0 U/h) and glucose (1.0 g/h) were infused over the duration of EVLP.

4.3.6 **Organ Assessment**

4.3.6.1 Physiological Parameters:

Pulmonary artery pressure, pulmonary vascular resistance, dynamic compliance, peak airway pressure, and the ratio of partial pressure of arterial oxygen to the percent oxygen in of inspired air, were all recorded during the evaluative time points.

4.3.6.2 Inflammatory Markers:

Cytokine profiles (tumor necrosis factor-α – TNFα; interleukin-6 – IL-6; interleukin-8 – IL-8) were analyzed using species specific enzyme-linked immunosorbent assay kits (R&D Systems, Minneapolis, MN, USA).

4.3.6.3 Histopathological Assessment and Edema Formation:

All lungs were weighed before and after EVLP, and edema formation was calculated as a percentage of the initial organ weight (weight gain (%) = (End_{weight} (g) - $Start_{weight}$ (g)/ $Start_{weight}$ (g)) * 100%).

Porcine peripheral lung tissue biopsies were collected following 12-hours of EVLP. Biopsies were fixed in 10% buffered formalin for 24 Hours, embedded in paraffin, sectioned at 5-μm thickness, stained by hematoxylin-eosin, and examined for pathological changes with light microscopy. A blinded pulmonary pathologist graded the lung sections in a randomized fashion to assess the histopathological grading of acute lung injury as previously described.[232,233] Interstitial

and perivascular neutrophil infiltration was scored via a density count; while the remaining standard criteria were scored from 0-3: 0 = absent (0%), 1 = mild (<25%), 2 = moderate (25%-75%), and 3 = severe (75%-100%).

4.3.7 **Statistics**

Data were analyzed with IBM SPSS Statistics v16.0 (SPSS Inc., Chicago, USA). All results are expressed as mean ± standard error and $p<0.05$ was considered statistically significant. For comparisons between evaluative time-points between treatment perfusates, a one-way ANOVA was utilized with Bonferroni's correction applied for multiple comparisons. While repeated measures ANOVA was utilized to test significance within a perfusate group – trend over time. Relationships between functional, edema formation, inflammatory cytokines, and histopathology, for each perfusate group were characterized with Pearson's correlation coefficients.

4.4| Results

4.4.1 **Lung Oxygenation (PO_2/FiO_2 or P/F ratio)**

Lung oxygenation had acceptable criteria throughout perfusion (P/F ratio > 350 mm Hg) for all three treatment groups, with no significance between perfusate composition ($EVLP_A$: 545.4 ± 16 mmHg; $EVLP_B$: 468 ± 23 mmHg; $EVLP_R$: 509 ± 26 mmHg, $p>0.05$; **Figure 15**). Only the cellular based perfusates demonstrated significantly improving oxygenation over the course of EVLP ($^{\#}p<0.05$; **Figure 15**).

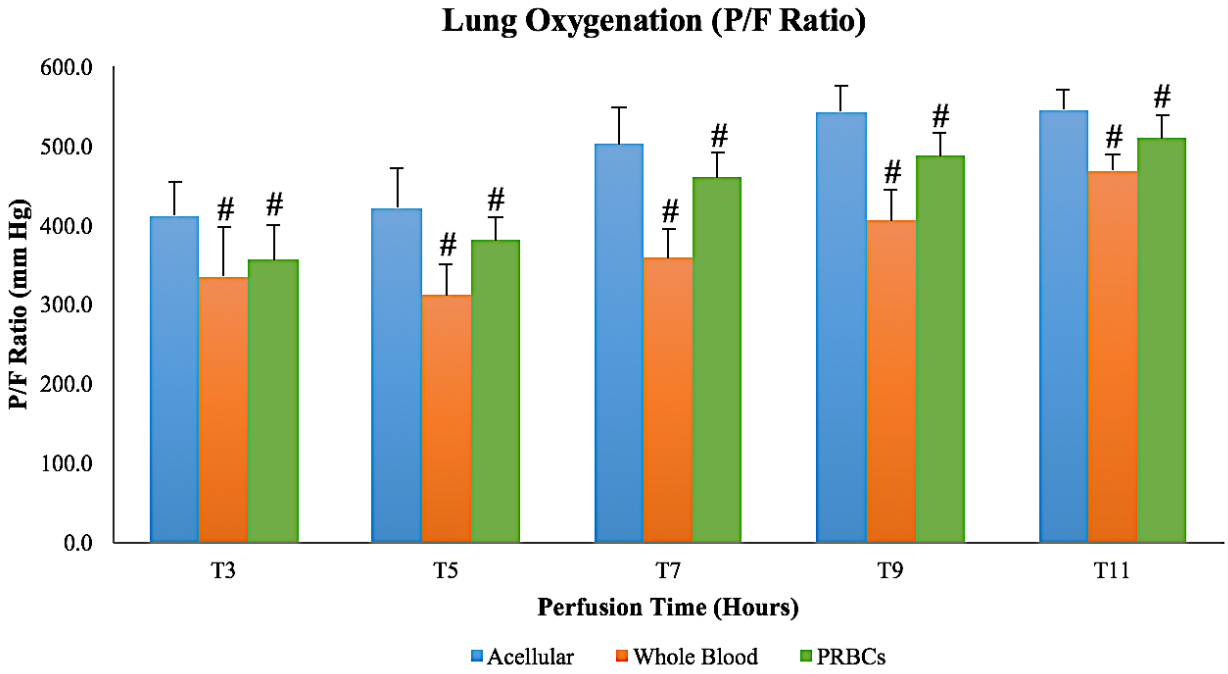

Figure 15: Perfusate comparison of lung oxygenations.
Acceptable lung oxygenation throughout the duration of EVLP for all perfusates. Results shown as mean ± SE. There was no significant difference in lung oxygenation (PO_2/FiO_2 or P/F ratio) between perfusates at T11. However, only the cellular based perfusates ($EVLP_B$: whole blood; $EVLP_R$: pRBCs) demonstrated a significant improvement in oxygenation over time ($^{\#}$**p < 0.05**).

4.4.2 Pulmonary vascular resistance (PVR) and mean Pulmonary arterial pressure (mPAP)

All three perfusates showed a significant decline in mPAP and PVR, over the course of EVLP ($^{\#}p<0.05$; **Figure 16A,B**). With regards to mPAP, an acellular based perfusate was significantly lower at T11, compared to either cellular based perfusates ($EVLP_A$: 6.7 ± 0.6 mm Hg; $EVLP_B$: 9.3 ± 0.8 mm Hg; $EVLP_R$: 10.3 ± 0.8 mm Hg; **Figure 16A**, *p<0.05). Similarly, for PVR, an acellular perfusate was significantly lower at T11 ($EVLP_A$: 282.4 ± 33.7 dynes*s/cm^5; $EVLP_B$: 423.2 ± 53.2 dynes*s/cm^5; $EVLP_R$: 395.5 ± 49.8 dynes*s/cm^5; **Figure 16B**, *p<0.05).

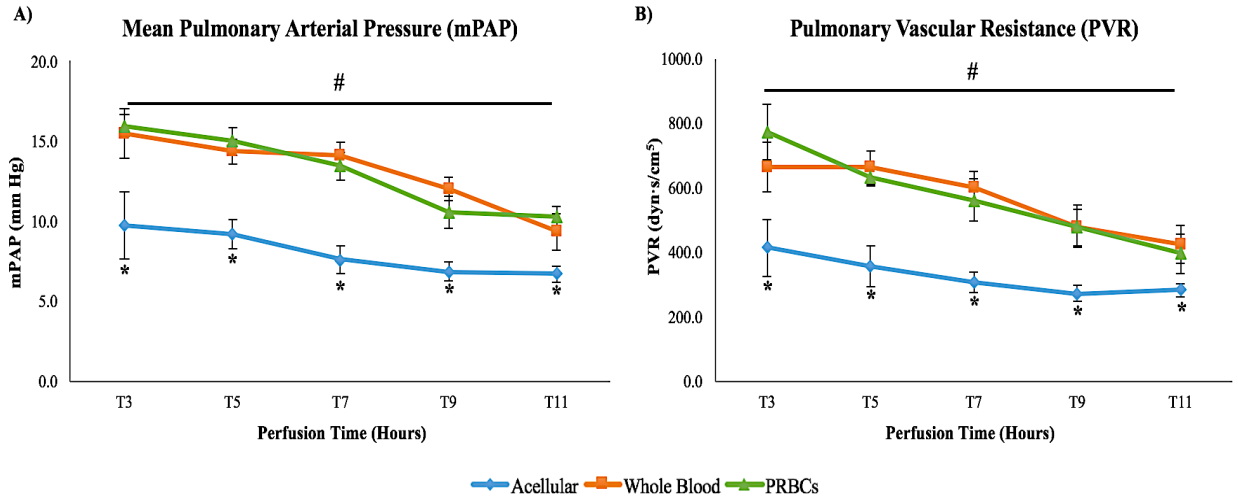

Figure 16: Perfusate comparison of **(A)** mPAP and **(B)** PVR.
An acellular perfusate had significantly lower mPAP and PVR, compared to either cellular based perfusate throughout EVLP. Results shown as mean ± SE. **(A)** Mean pulmonary arterial pressure was significantly lower for the acellular perfusate ($EVLP_A$) throughout EVLP at all time-points, compared to the cellular based perfusates ($EVLP_R$ or $EVLP_B$, ***p < 0.05**). However, all three perfusates significantly declined over the course of perfusion ($^{\#}$**p < 0.05**). **(B)** Pulmonary vascular resistance followed a similar significant decreasing trend for all three perfusates ($^{\#}$**p < 0.05**). With both cellular based perfusates ($EVLP_R$ and $EVLP_B$) showing higher T11 pressures than the acellular perfusate ($EVLP_A$, ***p < 0.05**).

4.4.3 Dynamic Compliance (C_{dyn}) and Plateau Pressure (P_{Plat})

Only cellular based perfusates demonstrated significantly improving trends in compliance over the course of EVLP ($^{\#}p<0.05$); while the same trend was not observed in the acellular based perfusate ($p>0.05$), **Figure 17B**.

Between perfusates, only $EVLP_R$ had a significantly higher compliance compared to $EVLP_A$ at T11 (30.9 ± 2.3 ml/cm H2O vs. 21.3 ± 1.4 ml/cm H_2O, respectively, $^{*}p = 0.03$; **Figure 17B**).

Plateau pressures where not significantly different between any of the perfusates at T11 and demonstrated stable trends throughout EVLP ($EVLP_A$: 19.0 ± 1.2 cm H_2O; $EVLP_B$: 16.8 ± 1.3 cm H_2O; $EVLP_R$: 15.8 ± 1.0 cm H_2O, $p>0.05$; **Figure 17A**).

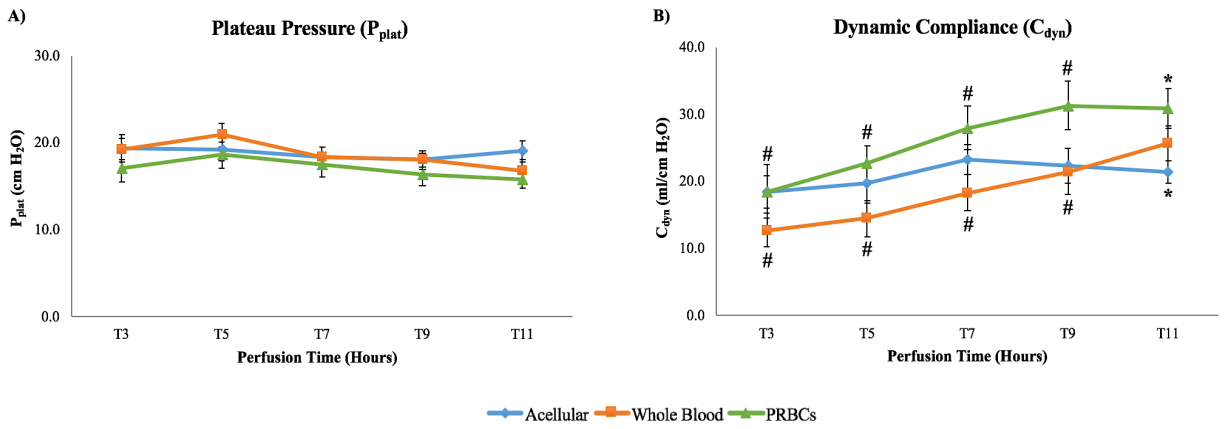

Figure 17: Perfusate comparison of **(A)** plateau pressures and **(B)** dynamic compliance.
Stable plateau pressures for all three perfusates with significantly better compliance for $EVLP_R$ compared to $EVLP_A$. Results shown as mean ± SE. **(A)** All three perfusates showed a stable trend of plateau pressure, with no significant difference between them at T11 ($p = 0.10$). **(B)** Dynamic compliance significantly improved over time with the cellular based perfusates ($EVLP_R$ and $EVLP_B$, $^{\#}$**$p < 0.05$**). While the acellular perfusate demonstrated a deterioration in lung compliance after T7, compared to either $EVLP_R$ and $EVLP_B$ ($p = 0.055$). At T11, $EVLP_R$ had significantly better lung compliance than $EVLP_A$ (***$p = 0.03$**).

4.4.4 Inflammatory Cytokine Analysis

Pro-inflammatory cytokines (TNFα, IL-6, IL-8) showed similar trends between all three perfusate groups throughout EVLP. All three perfusates had significantly increasing IL-6 and IL-8 concentration trends with time during EVLP ($^{\#}p<0.05$; **Figure 18B,C**); while with TNFα, all three perfusates had increasing concentrations until T3, then declined over time ($^{\#}p<0.05$; **Figure 18A**).

$EVLP_B$ had significantly higher concentrations of TNFα compared to $EVLP_R$ and $EVLP_A$, at all time-points ($^{*}p<0.05$; **Figure 18A**); while $EVLP_R$ and $EVLP_A$ showed no significant difference between each other ($p>0.05$; **Figure 18A**).

There was no significance between perfusates at T11 with IL-6 concentrations ($p>0.05$; **Figure 18B**). On the other hand, the acellular based perfusate demonstrated significantly higher IL-8 concentrations at T11, compared to either cellular based perfusate ($EVLP_A$: 3158 ± 312 pg/ml; $EVLP_B$: 1892 ± 296 pg/ml; $EVLP_R$: 1503 ± 150 pg/ml, $^{*}p<0.05$; **Figure 18C**).

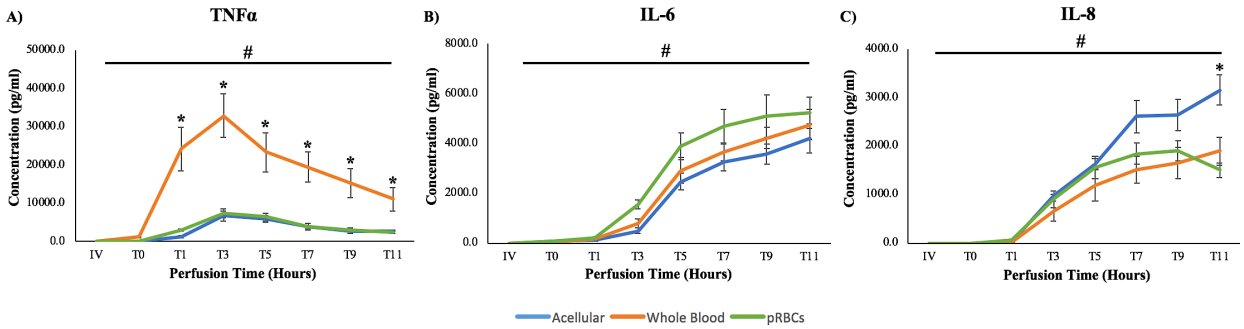

Figure 18: Perfusate comparison of inflammatory cytokine production.
All three perfusates followed similar trends with each respective pro-inflammatory cytokine. Results shown as mean ± SE. **(A)** $EVLP_B$ (whole blood) perfusate shows significantly higher concentrations of TNFα compared to $EVLP_R$ and $EVLP_A$, throughout the duration of EVLP (***p < 0.05**). Interestingly, all three perfusates had TNFα concentrations peak at T3, then decrease over time ($^{\#}$**p < 0.05**). **(B)** When comparing IL-6, there was no significant difference between the perfusates at any time-point; however, all three demonstrated an increasing trend in concentration over time ($^{\#}$**p < 0.05**). **(C)** The acellular perfusate ($EVLP_A$) showed significantly higher concentrations of IL-8 at T11, compared to either cellular based perfusate ($EVLP_R$ and $EVLP_B$, ***p < 0.05**). Like IL-6 trends, all three perfusates demonstrated increasing concentrations over the duration of EVLP ($^{\#}$**p < 0.05**).

4.4.5 **Edema Formation and Lung Injury**

Lungs perfused with an acellular based perfusate demonstrated significantly higher edema formation after 12 hours of EVLP, than lungs that were perfused with either cellular based perfusates ($EVLP_A$: 79.3 ± 13.0%; $EVLP_B$: 21.2 ± 5.8%; $EVLP_R$: 30.1 ± 9.2%, *p=0.002; **Figure 19**). The cellular based perfusates did not differ significantly (p=0.82; **Figure 19**).

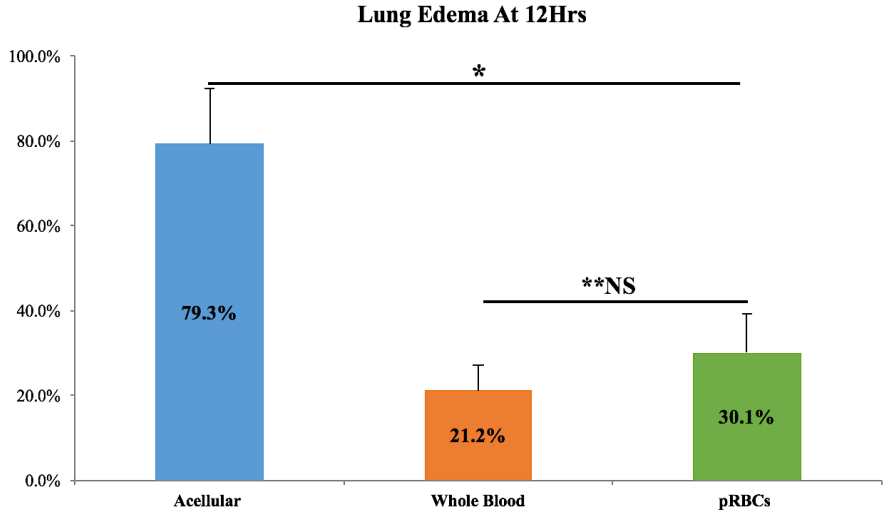

Figure 19: Perfusate comparison of lung edema after extended PPV-EVLP.

Macroscopic evidence of increased lung injury, by way of edema formation, with an acellular perfusate compared to the cellular based perfusates. Results shown as mean ± SE. A significantly higher edema formation was observed with the utilization of an acellular perfusate ($EVLP_A$) compared to either cellular based perfusates ($EVLP_R$ and $EVLP_B$, ***p < 0.001**). While both cellular based perfusates did not significantly differ, despite $EVLP_R$ showing slightly higher edema formation than $EVLP_B$ (**p = 0.82).

With regards to histopathology, there was no significant difference between perfusates, except with interstitial edema and inflammation at T12 (**Figure 20A,B,C,D,E**). The acellular perfusate showed significantly higher lung injury score compared to either cellular perfusate groups ($EVLP_A$: 1.5 ± 0.2; $EVLP_B$: 0.5 ± 0.2; $EVLP_R$: 0.7 ± 0.2, *p=0.04; **Figure 20D**). Yet, the cellular based perfusates did not differ significantly (p=0.95; **Figure 20D**). With regards to interstitial inflammation, out of the two cellular perfusates, only $EVLP_R$ showed significantly lower interstitial inflammation compared to either $EVLP_A$ or $EVLP_B$ (0.7 ± 0.2; 1.3 ± 0.2; 1.5 ± 0.3, respectively, *p = 0.03; **Figure 20E**).

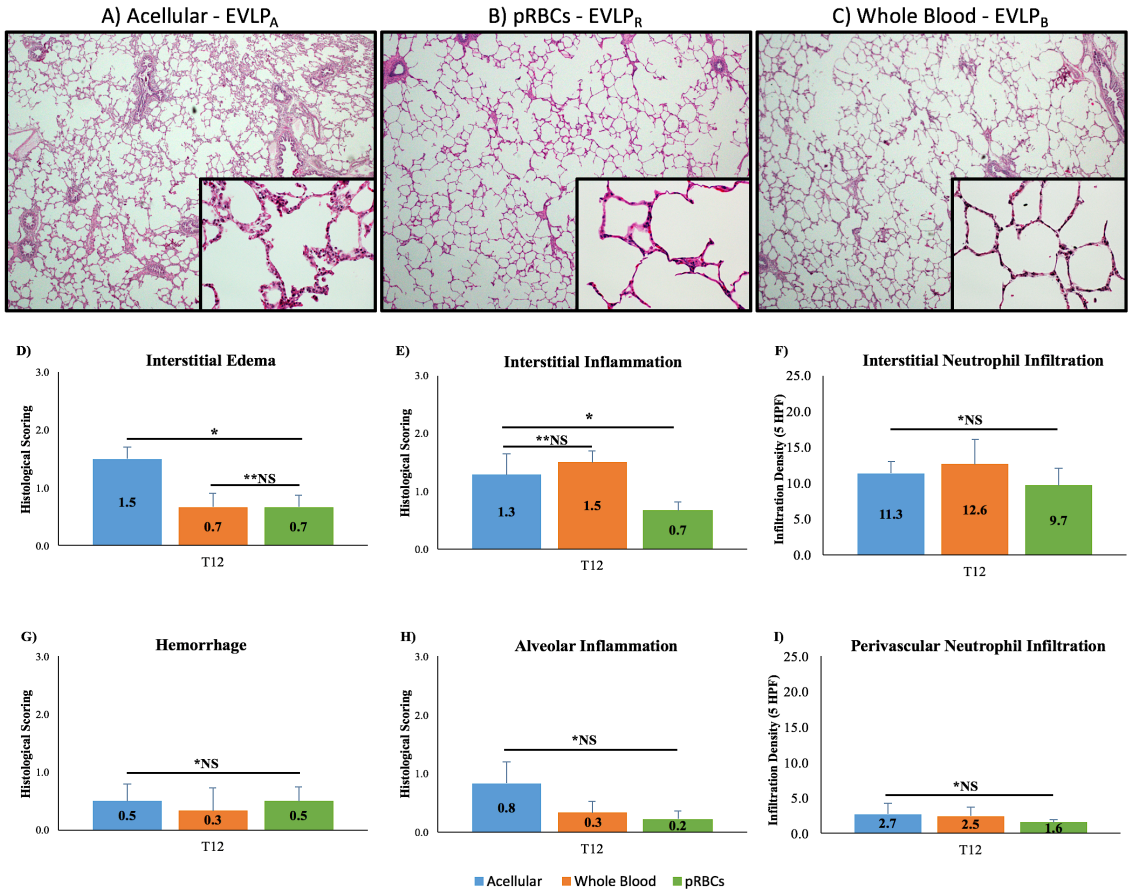

Figure 20: (A-C) Representative photomicrographs and **(D-I)** histopathological lung injury scores after extended PPV-EVLP.
(A,B,C,D) low magnification (4x) H&E staining with a 40x H&E micrograph inset, demonstrating significantly more interstitial edema with an acellular based perfusate ($EVLP_A$) compared to either cellular based perfusates ($EVLP_R$ and $EVLP_B$, ***p = 0.04**). $EVLP_R$ and $EVLP_B$ did not differ significantly ($^{**}p = 0.95$). **(E)** $EVLP_R$ had significantly lower interstitial inflammation compared to either $EVLP_A$ or $EVLP_B$ (***p = 0.03**). $EVLP_A$ and $EVLP_B$ did not differ significantly ($^{**}p = 0.66$). **(F,G,H,I)** There was no statistical difference with the histological analysis of hemorrhage, alveolar inflammation, and neutrophilic infiltration ($^{**}p = 0.83$).

4.4.6 Unique Perfusate Correlation with C_{dyn}, PVR, Oxygenation and Edema

Only the cellular based perfusates demonstrated significant positive correlation with compliance and oxygenation ($EVLP_R$: r = +0.926, *p<0.05; $EVLP_B$: r = +0.844, *p<0.05). On the other hand, the acellular based perfusate ($EVLP_A$) demonstrated significant negative correlation only with oxygenation and PVR (r = -0.934, *p<0.05) and compliance and PVR (r = -0.884, *p<0.05). Autologous blood based perfusate ($EVLP_B$) was the only cellular perfusate strategy that also demonstrated significant negative correlation with oxygenation and PVR (r = -0.873, *p<0.05 and compliance and PVR (r = -0.976, *p<0.05). Moreover, $EVLP_B$ was the only perfusate strategy to show significant negative correlation with oxygenation and edema formation after 12-hours of EVLP (r = -0.833, *p<0.05). No other evaluative parameters, for any of the perfusates, demonstrated significant associations.

4.4| Discussion

This study demonstrated the feasibility of our portable custom-designed PPV-EVLP platform to reproducibly achieve prolonged (12-hours) physiologic organ preservation and evaluation. The central aspect of this study was to establish our own protocol, with a portable EVLP platform, and identify an optimal perfusate in a pre-clinical large porcine model. At the University of Alberta Mazankowski institute, our patient catchment consists of more than >7 million Canadians, a geographical coverage of 6 million km^2, and a current donor lung utilization

rate of 27%. With the currently low donor utilization rate, the waitlist mortality rate for patient in need of a suitable donor lung transplantation stands at 33%. As such, we sought out to develop our own EVLP model; while investigating further the inherent differences that exists between the utilization of a cellular ($EVLP_R$ and $EVLP_B$) versus acellular based perfusate during normothermic EVLP, over 12-hours of physiologic perfusion.

Our protocol reinforces the importance of a slow incremental change in hemodynamic and temperature changes during the first hour of organ reperfusion (**Table 6A**); which has been attributed to the success of Toronto's prolonged (12-hour) EVLP technique.[155] Furthermore, our predefined evaluative ventilation parameters (**Table 6B**) resemble parts from both the Toronto and Lund protocols.[155,159] A central aspect of this study is the fact that the acellular and cellular perfusate compositions (**Table 5**) were directly compared using identical settings (**Table 6 & Figure 14**) – porcine lungs endured minimum cold ischemic times (<30 minutes), randomly allocated to one of three perfusate groups on a portable EVLP platform with an open left atrium system, challenged under normothermic conditions with a physiological flow of 35 ml/kg/min, and evaluated with a desired inspired tidal volume of 10ml/kg. The only other studies that have investigated cellular and acellular perfusates following an identical protocol setting were published in 2015 by Becker *et al*., Roman *et al*., and in 2017 by Loor *et al*.[170,171,234]

Becker *et al*., challenged porcine lungs with a perfusion flow of 70 ml/kg/min, after subjecting the lungs to 24H of cold ischemia to illicit a well-defined moderate degree of organ stress prone to lead to ischemia-reperfusion injury.[170,235-237] Roman *et al*., utilized a maximal perfusion flow of 50 ml/kg/min for 4H after 30 minutes of warm ischemia and 2H of CSP.[171] With regards to our oxygenation comparison (**Figure 15**), our results are in concordance with other studies that have reported stable and acceptable (>350 mm Hg) oxygenation indices, without

significance between acellular and cellular EVLP experimental groups.[99,156,170] Moreover, we note significantly improving trends of oxygenation only in the cellular based groups, similarly as published by Roman *et al*.[171] However, careful consideration should be noted with regards to oxygenation indices as a marker of lung evaluation during EVLP.[169] It is argued that a few oxygen molecules are needed to significantly increase the systemic serum PO_2 in an acellular/plasma-like perfusate, due to the lack of an oxygen carrier.[156] This may or may not be relevant for lung evaluation, reconditioning, and clinical eligibility for transplant suitability.[168]

With regards to mPAP and PVR (**Figure 16**), our results demonstrate significantly lower values for both hemodynamic parameters with the acellular group, compared to both cellular based perfusates. Moreover, significantly decreasing trends were noted for all groups over the course of EVLP. In accordance with these findings, other groups have reported higher PAP and PVR during cellular perfusion in porcine models and in clinical series.[154,170,173] The exact discrepancy in hemodynamics described by other groups are not only attributable to varying perfusion flow, but also, to the composition of the cellular perfusate. It is recognized that the cellular compartment within the cellular perfusate induces a higher perfusate viscosity, which can explain the significantly higher PAP and PVR between acellular and cellular EVLP.[238,239] As Becker and colleagues speculated, a higher PAP in the cellular based perfusates might result in less of an inherent ventilation-perfusion mismatch – as the difference between PAP and P_{Plat} decreases and eventually PAP exceeds P_{Plat} (**Figure 16A & 17A**).[170] Being aware of West's model,[240,241] the potential benefit of a moderately higher PAP with regards to overall lung perfusion when considering that marginal donor lungs, in clinical EVLP, usually present with increased airway pressures.[166,242]

Interestingly, over the years clinical EVLP has shifted from short term to prolonged ex vivo lung assessment; with initial EVLP indications serving primarily as a platform to assess donation after cardio-circulatory death (DCD) and extended criteria lungs.[99,159,166,204,205,243,244] Apart from organ reconditioning and the possibility of therapeutic approaches,[191,245,246] the advantage of prolonged EVLP lies in the platform's capability of revealing trends in functional lung parameters towards either improvement, stability, or deterioration. As such, clinical decision-making algorithms[166,167] have utilized these trends of hemodynamic (oxygenation indices) and aerodynamic (compliance) parameters as the basis for donor graft suitability for transplantation, after EVLP.[162,166,173,178,205,247,248] Our results demonstrate a unique significantly improving compliance trend with both the cellular based perfusates, $EVLP_R$ and $EVLP_B$ (**Figure 17B**). While with the acellular group ($EVLP_A$), a bimodal trend is noted with peak compliance reached after 7-hours of EVLP, only to decrease thereafter (**Figure 17B**). Moreover, $EVLP_R$ demonstrated the highest end of EVLP compliance, when compared to $EVLP_B$ and $EVLP_A$ (**Figure 17B**). These dynamic compliance trends are in concordance with the trends observed with their perspective plateau pressures – the acellular group demonstrating increasing P_{Plat} as EVLP is prolonged, while the cellular based perfusates have decreasing trends over time.

These findings are in agreement with some literature,[154,205,243] while contrary to what has been reported in the literature.[156,166,170,234] Loor *et al*., is the only other study to have investigated the effects between all three perfusates (acellular: mimicking STEEN solution, red blood concentrate and autologous blood); with the exception that they perfused swine lungs over 24-hours with the portable OCS Lung device. The OCS Lung device has its specialized perfusion protocol and OCS solution supplementation.[165] They are in agreement with our $EVLP_B$ compliance trend being stable and increasing over their EVLP run; however, their red blood concentrate group

appeared to deteriorate over EVLP. Moreover, their acellular group demonstrates faster deterioration of compliance over the first 6-hours of EVLP and significant visible edema – the acellular group could not pass 6-hour of EVLP.[234]

A possible explanation for the variation we observed with all three perfusate experimental groups and their compliance trends, compared to Loor and colleagues can be attributed to the difference between the perfusion protocols. We have elected for a more protective/lower perfusion flow, whether during the protective or evaluative phase (**Table 6B** – 30% and 50% CO, respectively). When compared to the OCS protocol's high perfusion flow, protective mode (~70% CO) and assessment mode (100% CO),[165,234] ss elucidated by the Toronto group, higher perfusion flows can be more susceptible in inducing greater hydrostatic edema. Thus, preceding a decrease in oxygenation, a significant deterioration in compliance and elevations in aerodynamic pressures have been reported as parenchymal edema increases.[155,156]

With regards to pro-inflammatory cytokine expression (TNFα, IL-6, IL-8), our study is unique since it captures the dynamic change over the entire duration of organ perfusion on EVLP, in a pre-clinical model. We report a similar trend between all three perfusate groups with regards to each cytokine (**Figure 18**). All three perfusates demonstrated a significantly increasing IL-6 and Il-8 concentration trend with time over the course of EVLP (**Figure 18B,C**); while only $EVLP_A$ demonstrating significantly higher IL-8 concentrations at the end of EVLP, compared to either cellular based perfusates (**Figure 18C**). Based on our knowledge, Roman *et al*. is the only other pre-clinical study that assessed the change in cytokine expression over time during EVLP, with a cellular and acellular based perfusate. However, as mentioned before, they conducted a shorter EVLP experiment where the porcine lungs underwent only 4-hours of EVLP. Nevertheless, Roman *et al*. is in concordance with our results reporting similar increasing trend of IL-6 and IL-

8 concentration over time for their acellular and cellular based groups, with no significant difference between the groups except with IL-8 – the acellular based experimental group demonstrated significantly higher concentration by the end of EVLP, when compared to either cellular based perfusates.[171] Moreover, Roman *et al.*, report significantly higher IL-8 concentrations in both perfusate and airway of the acellular group, compared to the cellular-based perfusates. Despite this study not conducting bronchoalveolar lavage samples, rising IL-8 perfusate can be utilized as marker of injury to the alveolar-capillary barrier. As reported by the Toronto group, increasing IL-8 airway/perfusate concentration ratio during ischemia-reperfusion correlates with early primary graft dysfunction in human lung transplantation.[85,249] Moreover, elevated IL-6 plasma levels as early as 48-hours after reperfusion during standard lung transplantation has been associated with primary graft dysfunction.[250] The increasing trend over time of IL-6 and IL-8 cytokine levels has been explained in the past by either the continuous production by stimulated IL-1 family, TNFα chemokine, or the overall decrease in cytokine absorption.[171] On the other hand, our results of TNFα trend and Roman *et al*. demonstrate the same interesting finding – unlike the other cytokines, TNFα concentrations appear to peak after 3-hours of EVLP, then decline over time for all three perfusates (**Figure 18A**).[171] Furthermore, we report $EVLP_B$ had significantly higher concentrations of TNFα compared to $EVLP_R$ and $EVLP_A$, at all time-points (**Figure 18A**), which was also reported by Roman *et al*.[171] The biphasic trend of TNFα has been reported by Oliver *et al*. and is attributed to the short half-life inherent with TNFα (~18.2 minutes). Oliver and colleagues attribute the short half-life to either the presence of either binding proteins or cellular metabolism.[251] Furthermore, Roman *et al*. report cellular based perfusates demonstrate a greater extravasation of monocytes (precursor for TNFα) from parenchymal tissue into the filter during EVLP. Controversy currently exists with regards to the benefit of

incorporating specialized cytokine[180,252,253] and leukocyte filters[158,171,227,254] during EVLP; thus, future studies are required to assess the effect these filters have in attenuating inflammatory cells during EVLP and whether it correlates with post-transplant outcomes.

Lung histology has been evaluated in different pre-clinical and clinical settings of EVLP. Cypel *et al*. observed less lung injury in transplanted porcine lungs after 12-hours of CSP and 12-hours of acellular EVLP compared to 24-hours of CSP alone.[254] Roman *et al*. assessed the ultrastructural architecture by electron microscopy for porcine lungs that underwent 2-hours of CSP followed by 4-hours of EVLP. They report no statistical difference in the degree of cell injury, when comparing acellular and two different cellular perfusate compositions. However, they do report that the acellular group demonstrated a higher incidence of edematous change, characterized by endothelial swelling and interstitial edema.[171] On the other hand, Becker *et al*. report largely preserved and minimal lung injury that was comparable in histology and ultrastructure architecture after prolonged (12-hours) EVLP and 24-hour cold ischemia with either an acellular or cellular based perfusate.[170] Our study demonstrates no significant difference in histopathology between the three perfusates, except for interstitial edema and interstitial inflammation (**Figure 20A,B,C,D,E**). The acellular perfusate had significantly higher interstitial edema score compared to either cellular based perfusates (**Figure 20D**). The cellular perfusates did not differ significantly. Moreover, only $EVLP_R$ had significantly lower interstitial inflammation compared to either $EVLP_A$ or $EVLP_B$ (**Figure 20E**).

Edema formation is identified as a key consequence during the manifestation of ischemia-reperfusion injury (IRI).[237] It is well recognized that the manifestation of edema formation has a typical sequence of events that begins with the disruption of the microscopic blood-alveolar barrier, followed by accumulation of edema in the interstitial compartment, then alveolar septal

edema, and with further aggravation leads to edema transgression into intra-alveolar air space.[51,255] The major contributing factors responsible for the pathogenesis of IRI, and inevitably edema formation, have been attributed to a hemodynamic imbalance favoring a pro-inflammatory environment – with a milieu of ongoing pro-inflammatory cytokine and chemokine released from the damaged vascular endothelial and alveolar epithelial layers causing further propagation of monocytic and neutrophilic activation/recruitment, and resulting in further capillary leakage and cell death.[51,54,256] Collectively, the histopathology finding (**Figure 20D**) and increasing IL-8 concentrations (**Figure 18C**) corroborate our findings of the staggering global edema formation of 49-58% more with an acellular perfusate strategy, compared to either cellular perfusate strategies after 12-hours of EVLP (**Figure 19**). Interestingly, $EVLP_B$ demonstrated non-significantly lower edema formation than $EVLP_R$ (**Figure 19**). Since all three perfusates had a similar baseline of osmolality, with the acellular perfusate having the greatest baseline oncotic pressure (**Table 5**), the difference in edema formation cannot be attributed to these factors. This finding of increased edema formation with an acellular EVLP technique, despite the utilization of the hyperoncotic STEEN solution, is in concordance with other reports.[173,210,234,257] As such, we theorize that the greater lung injury observed with an acellular based EVLP could be attributed to a) the lack of a closed left atrial technique, which Toronto claims that maintaining a left atrial pressure ~5 mmHg protects against lung edema/injury and improves lung function;[258] and/or b) the increasing sequestration of monocytes within lung parenchyma observed with acellular EVLP,[171] compared to the washout effect of monocytes observed with cellular based strategies.[171,172] Monocytes are capable of extravasating from the vascular bed to the alveolus and differentiating into macrophages and dendritic cells, which secrete inflammatory cytokines and biomarkers that perpetuate the deleterious inflammatory cascade of IRI.[54,58,172,259] Furthermore, the Toronto protocol is known to

exchange their acellular perfusate (STEEN solution) every 2-hours; thus, removing circulating inflammatory cytokines, minimizing continuous activation of parenchymal immune cells (monocytes, macrophages, or dendritic cells), and hence ongoing lung injury. The importance of minimizing cytokine aggregation during EVLP has been shown to correlate with better outcomes after lung transplantation, by the Toronto group,[249] and in pre-clinical settings.[252] On the contrary, despite the difficulty in obtaining autologous donor whole blood and the ethical considerations, whole blood maintains clotting factors and platelets within the plasma rich perfusate, which may mitigate early injury during EVLP; thus, allowing for lungs to be reconditioned safely beyond 12-hours, with minimal edema formation.[234,260] However, further investigations are needed to elucidate any discrepancy between $EVLP_R$ compared $EVLP_B$ and the plasma components that might further mitigate IRI.

Finally, we attempted to assess if there are any significant correlations between functional or inflammatory markers, which are perfusate specific. We report that cellular based perfusates show positive correlation with regards to compliance and oxygenation. While only an autologous whole blood strategy ($EVLP_B$) demonstrated a negative correlation with oxygenation and PVR. Moreover, $EVLP_B$ was the only perfusate strategy to show a negative correlation with regards to oxygenation and edema formation after 12-hours of EVLP. On the other hand, the acellular based strategy demonstrated a negative correlation with compliance and PVR, and with oxygenation and PVR. This is significant since other studies have reported that deteriorating lung compliance is an earlier indicator of graft dysfunction with an acellular EVLP strategy, than oxygenation in the evolution of acute lung injury.[156,168,261] These findings could help further improve current clinical decision-making algorithms,[166] and help identify reconditioned lungs that are suitable for transplantation after EVLP; while recognizing that depending on the perfusate strategy one

utilizes, some parameters should be heavily more weighted than others to identify deteriorating/improving trends during EVLP.

Study limitations: It cannot be excluded that applying different experimental conditions could generate differing results, regarding the comparison between acellular and cellular based EVLP strategies. We elected to minimize the cold ischemic insult on the lungs, to assess which perfusate strategy would be ideal when translating into utilizing a portable-custom designed EVLP platform in our future clinical settings. With our unique geographical isolation, our transplant centre will be electing to minimize cold ischemic preservation times by utilizing a portable EVLP platform to keep donor grafts under physiologic conditions, during the donor-recipient transport period to the centre. However, due to the vast aetiologies of insults encountered to donor grafts in clinical settings,[80] each insult etiology might require a specific adaptation of the EVLP protocol, including perfusate strategy. In this study, porcine lungs were processed for histology after EVLP to have a comprehensive understanding of the effect specific perfusate strategies have during ex vivo lung perfusion on the functional/macroscopic and microscopic levels. Thus, future studies will assess whether this study's findings translate into survival animal models, post-EVLP, and with human EVLP experiments.

In conclusion, this study has demonstrated the feasibility of utilizing a custom-designed portable EVLP platform to perfuse large animal lungs up to 12-hours. Furthermore, we have elucidated some inherent differences between the utilization of either an acellular, autologous whole blood, or red blood concentrate EVLP strategy. Demonstrating that with an open left atrial protocol, a cellular based perfusate is the ideal EVLP strategy to preserve lung compliance and minimize lung injury during ex vivo lung perfusion. Hence, future experimental and clinical studies should be aware that specific perfusate EVLP strategies require differing EVLP protocols,

components, and assessment criteria to safely recondition lungs on the platform. This will ensure that the appropriate evaluative parameters are being assessed, which will reliably predict organ health over extended EVLP and donor lung function after transplantation.

Chapter 5

Negative Pressure Ventilation Decreases Ventilator Induced Lung Injury during Normothermic Ex Vivo Lung Perfusion

5.1| Abstract

Introduction: Normothermic ex-vivo lung perfusion (EVLP) using positive pressure ventilation (PPV) and both acellular and red blood cell (RBC) based perfusate solutions have increased the rate of donor organ utilization. We sought to determine if a negative pressure ventilation (NPV) strategy would improve donor lung assessment during EVLP.

Materials and Methods: Thirty-two pig lungs were perfused ex-vivo for 12-hours in a normothermic state, allocated equally into 4 groups according to the mode of ventilation (PPV vs NPV) and perfusate composition (Acellular vs RBC). The impact of ventilation strategy on the preservation of six-unutilized human donor lungs was also evaluated. Physiologic parameters, cytokine profiles, lung injury, bullae and edema formation were compared between treatment groups.

Results: Perfused lungs demonstrated acceptable oxygenation (P/F ratio >350 mmHg) and physiological parameters. However, there was less generation of proinflammatory cytokines (TNFα, IL-6, and IL-8) in human and pig lungs perfused, irrespective of perfusate solution used, with NPV compared to PPV ($p<0.05$), and a reduction in bullae formation with an NPV modality ($p=0.02$). Pig lungs developed less edema with NPV ($p<0.01$), and EVLP using an acellular perfusate solution had greater edema formation, irrespective of ventilation strategy ($p=0.01$). Interestingly, human lungs perfused with NPV developed negative edema ("drying") ($p<0.01$) and lower composite acute lung injury ($p<0.01$).

Conclusions: Utilization of an NPV strategy during extended EVLP is associated with significantly less inflammation, and lung injury, irrespective of perfusate solution composition.

5.2| Introduction

Transplantation is an established therapy for end-stage lung failure. Despite a shortage of donor organs, the utilization rate of available organs is low (15%).[216,217] Normothermic ex vivo lung perfusion (EVLP) is an evolving technology that facilitates extended preservation, evaluation, and therapeutic intervention of donor lungs prior to transplantation.[155,157,158,162,219,262] Utilization of this technology has contributed to an increase in the number of suitable lungs available for transplantation.[74,158,167,203,219,263]

Current clinical EVLP protocols employ positive pressure ventilation (PPV) to preserve and evaluate donor lungs prior to transplantation;[158,159,162,167] however, there is a growing appreciation of the potential deleterious effects of ventilator-induced lung injury (VILI) associated with extended EVLP using PPV.[178-183] Alternatively, negative pressure ventilation (NPV) is a more physiologic method of ventilation used historically to treat respiratory failure.[184,185] A NPV ventilation strategy has theoretical advantages during EVLP, creating a negative intrathoracic pressure that is equally distributed over the pleural surface of the lungs relative to alveolar pressure, and uniform ventilation throughout the lung parenchyma.[188] NPV therefore eliminates donor lung exposure to the deleterious effects of PPV during EVLP and may improve donor lung preservation prior to transplantation. Therefore, we sought to investigate the impact of NPV on lung preservation during extended EVLP with acellular and red blood cell (RBC)-based perfusate solutions.

5.3| Materials and Methods

The Animal Care and Use Committee at the University of Alberta approved the experimental protocol. All animals received humane care in accordance to the "Principles of Laboratory Animal Care," formulated with the National Society for Medical research. Thirty-two

female domestic pigs (42 ± 5 kg) were allocated to four treatment groups according to the mode of ventilation (NPV vs PPV) and the composition of the perfusate solution (acellular vs RBC) (**Figure 21A**). In addition, the impact of ventilation mode on human lung preservation was investigated in six non-utilized human lungs (82 ± 5 kg) perfused with a RBC-based solution (**Figure 21A**). All lungs were perfused under normothermic conditions for 12 hours on one of two custom built EVLP platforms. A fully automated NPV-EVLP platform was developed and compared to a conventional PPV-EVLP platform.

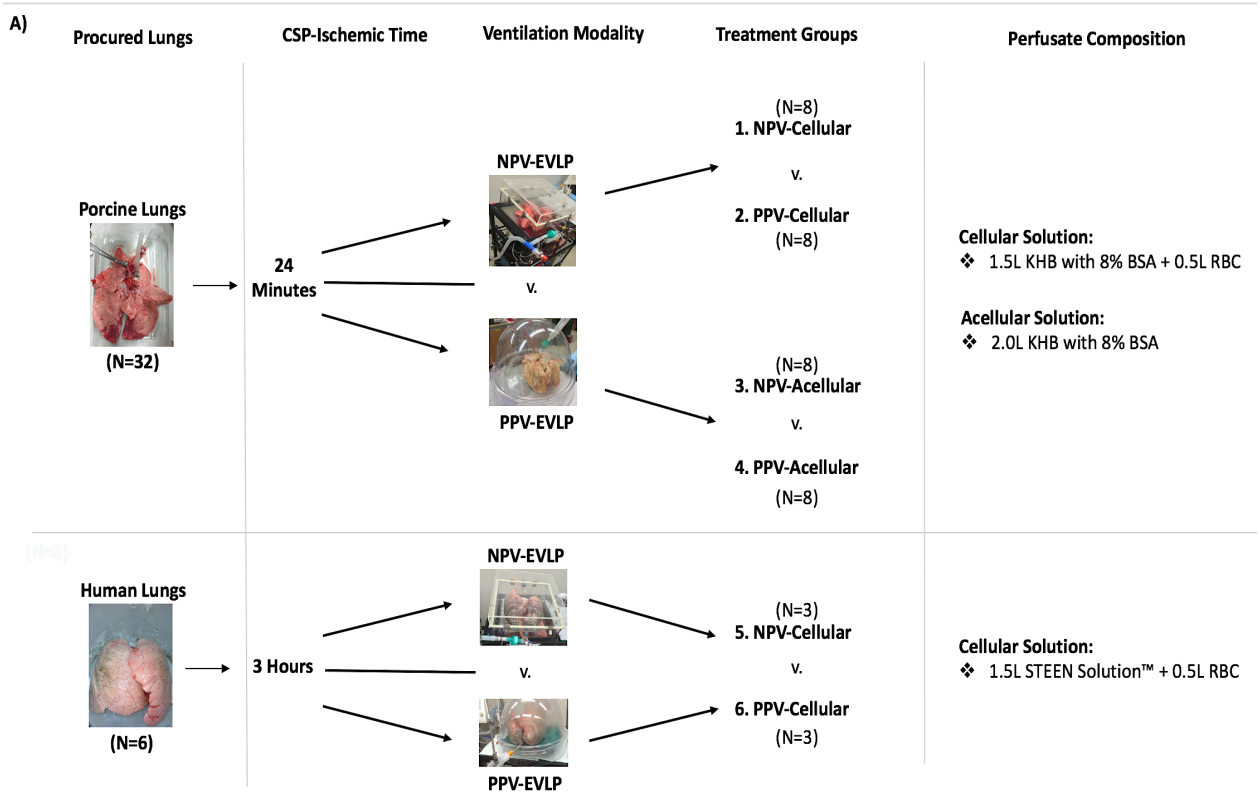

B)

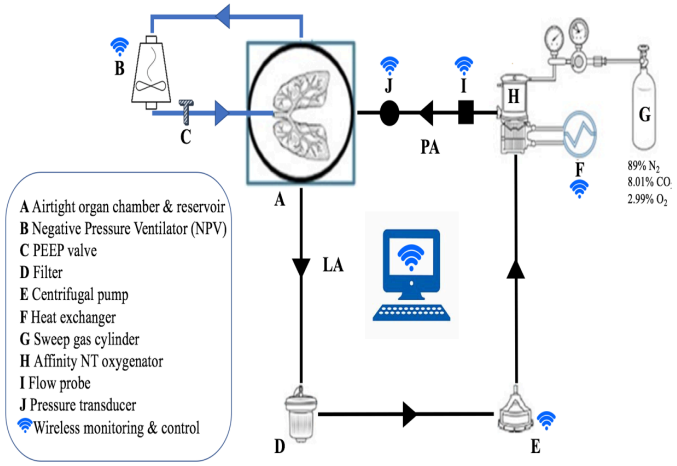

C)

Recorded Interface Parameters	Abbreviations	Units
1. Vascular Parameters:		
Left Atrial Pressure	LAP	mm Hg
Pulmonary Arterial Pressure	PAP	mm Hg
Pulmonary Vascular Resistance	PVR	dynes*s/cm^5
Pulmonary Arterial Flow	PA Flow	Litres/min (LPM)
2. Airway Parameters:		
Airway Pressure	Paw	cm H_2O
Intrathoracic Pressure	ITP	cm H_2O
Transpulmonary Gradient	TPG	cm H_2O
Airflow	Airflow	Litres/min (LPM)
Fraction of Inspired Oxygen	FiO_2	Percentage (%)
3. Ventilation Parameters:		
Expiratory Tidal Volume	Vte	ml
Inspiratory Tidal Volume	Vti	ml
Respiratory Rate	RR	breathe/min (bpm)
Minute Ventilation	MV	Litres/min (LPM)
Dynamic Compliance	Cdyn	ml/cm H_2O

Figure 21: (A) Representation of experimental protocol, **(B)** custom built NPV-EVLP platform schematic and **(C)** functional software interface recording.
(**A**) Porcine lungs (N=32) were randomly divided into 4 treatment groups based on ventilation strategy and perfusate composition: a) NPV-Cellular vs PPV-Cellular (N=8/group) and b) NPV-Acellular vs PPV-Acellular (N=8/group). While unutilized human lungs (N=6) compared NPV-Cellular (N=3) vs PPV-Cellular (N=3). Cold storage preservation (CSP) ischemic time for Porcine Lungs: 24.0 ± 5.0 minutes and Huma Lungs: 3.0 ± 0.8 hours (mean ± SEM). (**B**) NPV-EVLP schematic circuit. With the open left atrial system, oxygenated perfusate exits the lungs, drains naturally from the airtight organ chamber & reservoir (A), passes through an arterial line filter (D), pumped via a centrifugal pump (E) to the oxygenator/heat exchanger (H,F). Which in turn warms the perfusate to normothermia (computer controlled/adjusted) and deoxygenates it with a hypoxic gas mixture (G), prior to re-entering the lungs via the pulmonary arterial cannula for re-oxygenation. The microcontroller software (H) monitors and adjusts the centrifugal pump (F) in real time to maintain the desired PA flow (J). (**C**) Custom coded platform software interface: fully automated, monitors and records in real time - vascular, airway, and ventilation parameters.

5.3.1 **Perfusate Solutions**

5.3.1.1 Porcine Experiments:

The cellular perfusate solution was comprised of 1.5L of Krebs-Henseleit buffer (KHB) with 8% bovine serum albumin (BSA) + 0.5L of red blood cell concentrate (RBC).

The acellular perfusate solution was comprised of 2L KHB with 8% BSA.

The standard KHB solution was created fresh for each experiment and along with the 8% BSA (**Table 5**),[222-224] and was used to mimic the hyperoncotic pressure and buffered extracellular solution of the published proprietary STEEN Solution™ (XVIVO Perfusion, Gothenburg, Sweden).[162,225]

5.3.1.2 Human Experiments:

The cellular perfusate solution was comprised of 1.5L of STEEN Solution™ + 0.5L RBC. Cellular based perfusate solutions had autologous whole blood collected following donor (human or porcine) exsanguination, washed with 1L of 0.9% saline, and concentrated using the Sorin Xtra cell saver (Sorin Group Canada Inc., Burnaby, BC). The described volumes for the cellular groups provided a constant desired hemoglobin concentration of 40-50 g/liter or a hematocrit of 12-15%.

5.3.2 **Ex Vivo Lung Perfusion**

The NPV-EVLP and PPV-EVLP circuits were primed with 2 liters of the respective experimental perfusate (**Figure 21A**), 10,000 IU of heparin, 500 mg of methylprednisolone, and 3.375 g of piperacillin-tazobactam. The PPV-EVLP circuit had an organ chamber (XVIVO Perfusion, Gothenburg, Sweden), which emptied perfusate into a reservoir; while the NPV-EVLP circuit contained a custom-built airtight sealed organ chamber with an integrated reservoir. Both platforms utilize a centrifugal pump (Medtronic, Minneapolis, MN, USA) that drives continuous flow of perfusate from the reservoir, through a M27 PH.I.S.I.O adult arterial filter (Sorin Group Canada Inc., Burnaby, BC), a membrane de-oxygenator (Sorin PrimO_2X, Sorin Group Canada Inc., Burnaby, BC) and heat exchanger (PolyScience, Illinois, USA), and into the pulmonary artery (**Figure 21B**). Both platforms have a microcontroller with a custom software package that controls the desired pulmonary arterial flow and monitors corresponding physiologic parameters using a flow probe (BIO-Probe Transducer Model TX 40, Medtronic, Minneapolis), pressure transducers (Edwards Lifesciences, Dominican Republic), air pressure sensors and air flow meter. The interface software was used to construct real time Pressure/Volume and Flow/Volume loops during NPV experiments; and data collected and stored in real time, at 10s intervals (**Figure 21C**). Both platforms utilized compressed medical air and a hypoxic sweep gas mix (89% N_2, 8% CO_2, 3%

O_2) to maintain the pulmonary arterial PO_2 and PCO_2 within physiologic parameters.

5.3.2.1 PPV Platform:

Donor lung ventilation on the PPV platform (PPV-EVLP) was undertaken using a standard intensive care unit ventilator (SERVO-I, Maquet Critical Care AB, Solna, Sweden).

5.3.2.2 NPV Platform:

Donor lung ventilation on the NPV platform (NPV-EVLP) was undertaken using a custom-built turbine driven ventilator to change the air pressure within the sealed organ chamber (**Figure 21B**). The turbine and accompanying valve mechanism were used to create a negative pressure within the organ chamber to produce an inspired tidal volume. The unique platform also delivers continuous positive airway pressure, which is regulated with a positive-end-expiratory pressure (PEEP) valve (**Figure 21B**).

5.3.3 **Initiation of EVLP** (U of A Protocol)

Porcine donor lung procurement was undertaken as previously described.[226,264] Anesthesia was induced via an intramuscular injection of ketamine (20 mg/kg), atropine sulphate (0.05mg/kg) and xylazine (0.9mg/kg). Orotracheal intubation was established and general anesthesia was maintained with 1-3% isoflurane. A median sternotomy was performed, and the animal was anticoagulated with intravenous heparin (400 U/kg). A 2-stage venous cannula was placed into the right atrium, through which the animal was exsanguinated into a Sorin Xtra cell saver. The cardiectomy and bilateral pneumonectomy were then performed, the trachea was clamped at a peak airway pressure of 20 cm H_2O, and the lungs were explanted en bloc. Human donor lungs were obtained at the time of multiorgan retrieval according to accepted clinical standards.[74] Following organ procurement, the donor lungs were transferred to the PPV or NPV organ chamber according to the experimental protocol (**Figure 21A**). With both platforms designed to be portable,

reperfusion of porcine lungs commences in less than 30 minutes; therefore, they were subjected to minimum amount of cold ischemic time (**Figure 21A**). Both porcine and human lungs had the pulmonary artery cannulated and connected to the EVLP circuit, the left atrium left open to drain passively into the reservoir, the trachea was intubated with an endotracheal tube, and perfusion was initiated at 5% cardiac output and 22°C. Pulmonary arterial flow gradually was increased to 10% of predicted cardiac output (70 ml/kg/min) and then increased by increments of 10% predicted cardiac output every 20-minutes to achieve a flow of 30% predicted cardiac output by 1-hour of EVLP. During this time, the perfusate solution was gradually warmed to 37.5°C (Human) or 38°C (Porcine) (**Table 7**). Recruitment maneuvers were performed for the first 3-hours of EVLP by maintaining the PEEP at 7 cm H_2O with inspiratory holds performed every 30 minutes for three consecutive breaths (5-10 seconds/breath).

Table 7: Initiation of EVLP (NPV or PPV).

A)	**Perfusion Time (Minutes)**					
	0	10	20	20-40	40-50	60 (T1)
Perfusion Temperature (ºC)	20°C-25°C	25ºC-30ºC	32ºC	32ºC-34ºC	34ºC-36ºC	37.5ºC or 38ºC
PA Flow (% Cardiac Output, CO; CO = 70 ml/kg/min)	5%	10%	10%	20%	30%	30%
Ventilation	None	None	Initiate Preservation Mode			Recruitment Phase
Medical Gas Mixer	None	None	None	None	None	Start
Left Atrial Pressure (mm Hg)	0	0	0	0	0	0

NPV and PPV experiments utilized pressure-control ventilation and flow-controlled perfusion. Preservation mode ventilation was initiated once the perfusate temperature reached 32°C (**Table 7**). The desired preservation and evaluation modes of ventilations, and vascular pressure parameters are described in **Table 8**. Evaluation was conducted serially every 2 hours, for 5 minutes, with upper peak airway pressure limit set to 25 cm H_2O, and by raising preservation settings to the ventilation parameters described in **Table 8**. While for the majority of EVLP, lungs were maintained at standard routine preservation mode (**Table 8**). Sweep gas flow rate through the hollow fiber deoxygenator was titrated to maintain a physiologic pH of 7.35-7.45 and PCO_2 (35-50 mm Hg). Insulin (2.0 U/h) and glucose (1.0 g/h) were infused over the duration of EVLP. Data describing donor unutilized human lung characteristics is provided in **Table 9.**

Table 8: NPV and PPV ventilation strategy.

B)	**Ventilation Mode**	
	Preservation	**Evaluation**
Temperature (ºC)	37.5ºC (Human) or 38ºC (Porcine)	37.5ºC (Human) or 38ºC (Porcine)
Pulmonary Artery Flow	30% of estimated Cardiac Output; CO=70ml/kg/min	50% of estimated Cardiac Output; CO=70ml/kg/min
Ventilation Parameters:		
Mode	Pressure Control	Pressure Control
Desired Inspiratory Tidal Volume	6 ml/kg	10 ml/kg
Frequency	7-8 bpm	10-12 bpm
P_{AWP}	< 20 cm H_2O	< 25 cm H_2O
PEEP	7 cm H_2O	5 cm H_2O
FiO_2	21%	21%
Pressure Parameters:		
PAP	< 20 mm Hg	< 20 mm Hg
LAP	0 mm Hg	0 mm Hg
Medical gas mixer	89% N_2, 8% CO_2, 3% O_2	89% N_2, 8% CO_2, 3% O_2
Medical gas mixer (L/min) titrated to PCO_2	35-50 mm Hg	35-50 mm Hg
P_{AWP}: peak airway pressure; **PEEP**: positive end-expiratory pressure; **FiO_2**: fraction inspired of oxygen; **PAP**: mean pulmonary artery pressure; **LAP**: left atrial pressure; **PCO_2**: partial pressure of carbon dioxide in pulmonary arterial circulation		

Table 9: Unutilized human donor lung characteristics.

C)	Donor	Age (Years)	Donor Weight (Kg)	Sex	Type of Donor	CSP Ischemic Time (Hours)	Donor PO_2/FiO_2 (mm Hg)	Reason for EVLP
PPV-EVLP	1	72	80.0	M	DBD	1	190	Age: >64 Years & Poor Oxygenation (< 350 mm Hg)
	2	51	80	M	DBD	5	75	High Risk Donor & Poor Oxygenation (< 350 mm Hg)
	3	16	64.0	F	DBD	2	80	Poor Oxygenation & Aspiration (< 350 mm Hg)
NPV-EVLP	4	39	80	F	DBD	4	98	MRSA Pneumonia & Poor Oxygenation (< 350 mm Hg)
	5	65	100	M	DBD	2	170	Size Mismatch & Poor Oxygenation (< 350 mm Hg)
	6	55	85.0	M	DBD	6	145	Emphysematic, ABO Mismatch & Poor Oxygenation (< 350 mm Hg)

DBD: donation after brain-stem death; **CSP**: cold storage preservation at 4°C (Perfadex); **FiO_2** (100%): fraction inspired of oxygen; **PO_2**: partial pressure of arterial oxygen; **MRSA**: Methicillin-resistant Staphylococcus aureus.

With the NPV platform, to obtain the desired inspiratory tidal volumes, the pleural pressure was varied between a negative end-inspiratory pressure (EIP) and an end-expiratory pressure (EEP) that was slightly greater than airway pressure (P_{aw}). The transpulmonary air pressure gradient (TPG) was calculated as follows: $TPG = P_{aw} - EIP$ (**Figure 21C**).

5.3.4 **Organ Assessment**

5.3.4.1 Physiological Parameters:

Pulmonary artery pressure, pulmonary vascular resistance, dynamic compliance, peak airway pressure, and the ratio of partial pressure of oxygen in the pulmonary venous blood to the

percent oxygen in the inspired air were measured during the evaluative time points.

5.3.4.2 Inflammatory Markers:

Cytokine profiles (tumor necrosis factor-α, interleukin-6, and interleukin-8) were analyzed using enzyme-linked immunosorbent assay kits (R&D Systems, Minneapolis, MN, USA).

5.3.4.3 Lung Injury and Edema Formation:

Bullae formation observed during EVLP was counted via the established criteria (>1 cm in diameter).[265-267] All lungs were weighed before and after EVLP, and edema formation was calculated as a percentage of the initial organ weight (weight gain (%) = (End_{weight} (g) - $Start_{weight}$ (g)/ $Start_{weight}$ (g)) * 100%). Human peripheral lung tissue biopsies were collected following 12-hours of EVLP. Biopsies were fixed in 10% buffered formalin for 24 Hours, embedded in paraffin, sectioned at 5-μm thickness, stained by hematoxylin-eosin, and examined for pathological changes with light microscopy. A masked pulmonary pathologist graded the lung sections in a randomized fashion to assess the histopathological grading of acute lung injury as previously described.[232,233]

5.3.5 **Statistics**

All results are expressed as mean ± standard error and all statistical analyses were performed using SPSS (SPSS Inc., Chicago, USA). The Student *t* test was used to compare normally distributed continuous variables, chi-squared used for categorical variables, and repeated measures ANOVA for significance within groups, over time. Statistical significance was measured at $p<0.05$.

5.4| Results

5.4.1 Lung Oxygenation (PO_2/FiO_2 or P/F ratio)

Human and porcine lungs had acceptable criteria for lung oxygenation (P/F ratio > 350 mm Hg) during EVLP; but, did not differ significantly between perfusate composition and ventilation modalities at T11 (11 Hours of EVLP) (**Figure 22,** $p>0.05$). Only cellular based perfusates, irrespective of ventilation, demonstrated a statistically significant improvement in oxygenation over time (**Figure 22B**, $p<0.05$).

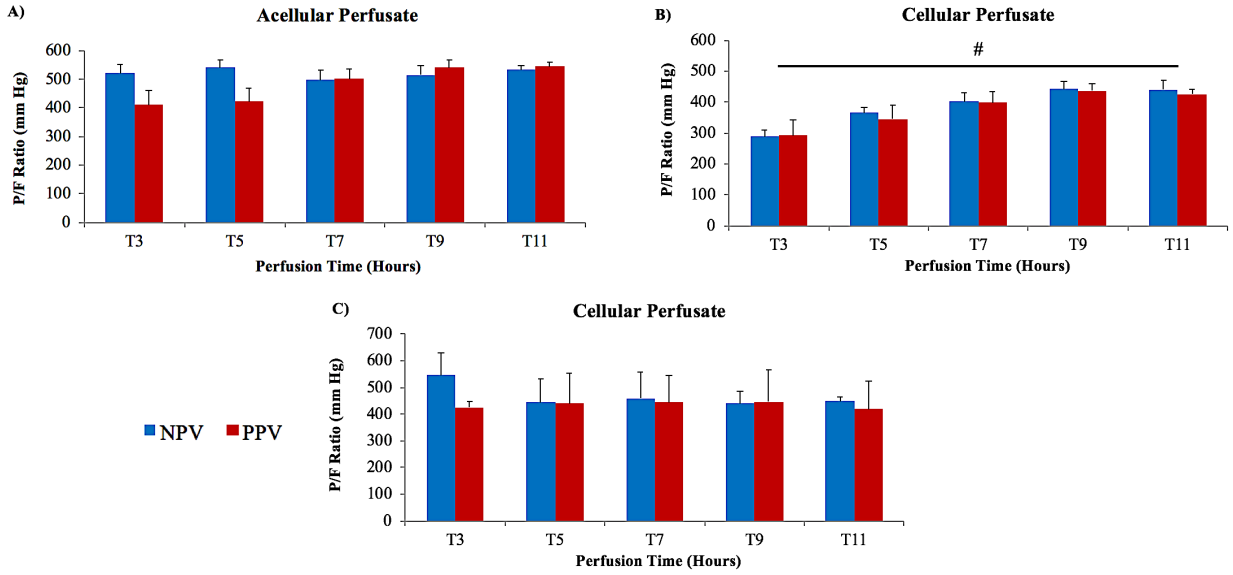

Figure 22: (A,B) Porcine and **(C)** human lung oxygenations (NPV and PPV strategies).
Acceptable porcine (A,B) and human (C) lung oxygenation. Results shown as mean ± SE. (**A-C**) No significant difference between perfusate groups and their ventilation modalities, for lung oxygenation at T11 (PO_2/FiO_2 or P/F ratio). (B) Only porcine lungs, with a cellular based perfusates (irrespective of ventilation) demonstrated a significant improvement in oxygenation over time ($^{\#}$**p < 0.05**).

5.4.2 Pulmonary Vascular Resistance (PVR) & mean Pulmonary Arterial Pressure (mPAP)

Porcine lungs demonstrated a significant decline in mPAP and PVR over time, for both perfusate and ventilation groups (**Figure 23A,B,D,E**, $p<0.05$). However, there was no statistically

significant difference between perfusate groups and their corresponding ventilation strategies at T11 (**Figure 23A,B,D,E**, p>0.05). There was no significant change in mPAP and PVR for human lungs, over time or at T11 (**Figure 23C,F**, p>0.05).

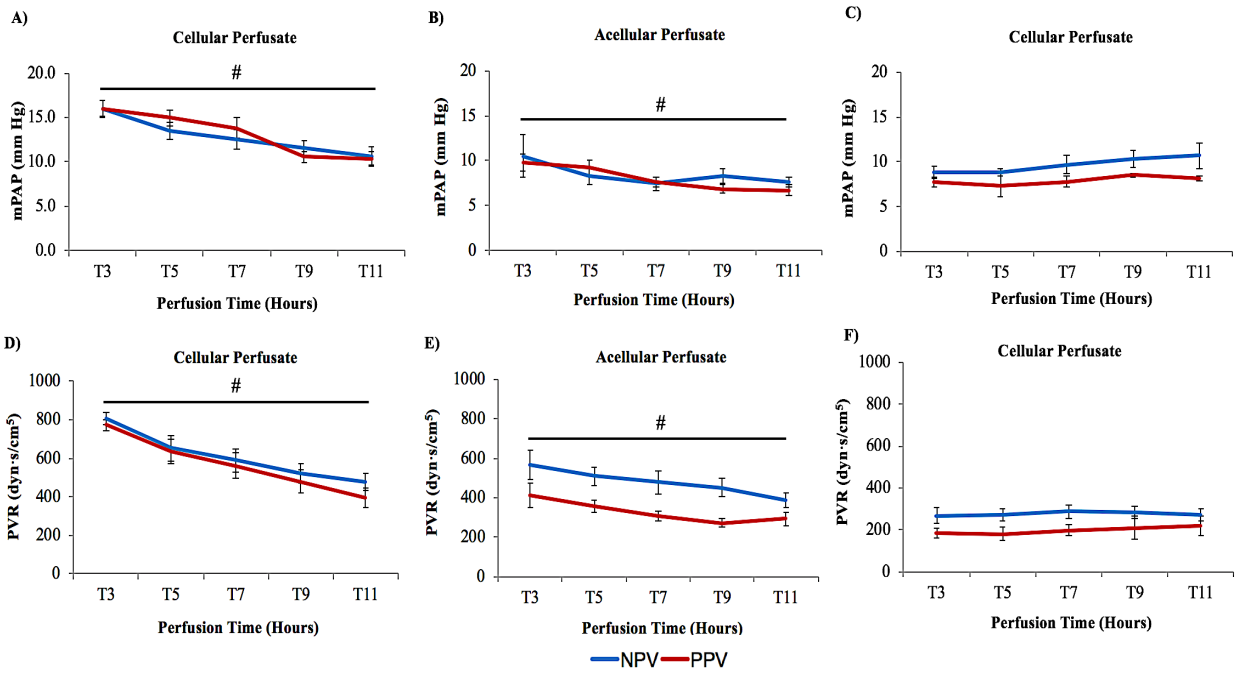

Figure 23: (A,B,D,E) Porcine and **(C,F)** human lungs mPAP and PVR (NPV and PPV strategies). Results shown as mean ± SE. There was a significant decline in mPAP and PVR over time in porcine lungs (A,B,D,E, $^{\#}$**p < 0.05**); but, not in human lungs (C,F, p > 0.05). **(A,B)** No statistically significant difference between both perfusate treatment groups at T11, irrespective of ventilation strategy (p > 0.05). **(D,E)** No significant difference was observed at T11 between both perfusate groups and ventilation strategies (p > 0.05). **(C,F)** No significant difference between groups at T11.

5.4.3 Dynamic Compliance (C_{dyn}) & Peak Airway Pressure (P_{AWP})

Porcine lungs demonstrated a significant improvement in compliance over time with the cellular based perfusate group (p<0.05); however, the same trend was not observed in the acellular group (p>0.05), irrespective of ventilation strategy (**Figure 24D,E**). In contrast, only Human NPV-Cellular lungs demonstrated significantly improving compliance over time (**Figure 24F,** p<0.05).

Between groups, there was a significant difference in dynamic compliance only for Porcine NPV-Cellular vs PPV-Cellular lungs at T11 (NPV-Cellular: 29.3 ± 1.6 ml/cm H_2O vs PPV-Cellular: & 24.5 ± 1.5 ml/cm H_2O, **Figure 24D**, $p<0.05$).

There was no significant difference in P_{AWP} between any of the perfusates and ventilation strategies (**Figure 24A-C**, $p>0.05$). However, only Porcine NPV-Cellular lungs showed significantly decreasing P_{AWP} over time (**Figure 24A**, $p<0.05$).

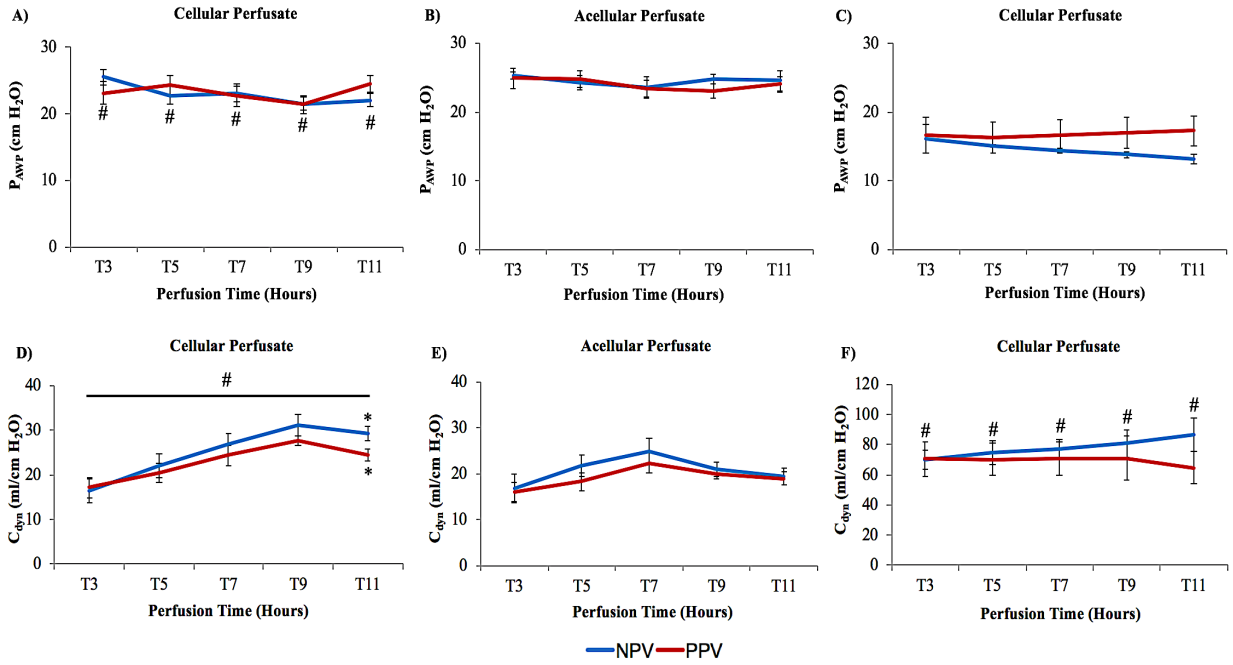

Figure 24: (A,B,D,E) Porcine and **(C,F)** human lung P_{AWP} and C_{dyn} (NPV and PPV strategies). Results shown as mean ± SE. **(A,B)** P_{AWP} did not differ significantly at T11 for both ventilation strategy and perfusate types ($p > 0.05$). Only NPV-Cellular had a significant decline in P_{AWP} over time (**$^{\#}p < 0.05$**). **(D)** There was a significant improvement in compliance over time in porcine lungs, both NPV and PPV (**$^{\#}p < 0.05$**). NPV-Cellular showing significantly higher lung compliance at T11, than PPV-Cellular (**$^{*}p < 0.05$**). **(E)** There was no significance between NPV and PPV dynamic compliance at T11, or over time with acellular based perfusate ($p > 0.05$). **(C)** Human lung peak airway pressure did not differ significantly at T11 and over time ($p > 0.05$). **(F)** Whereas dynamic compliance did not differ significantly at T11 between the ventilation modalities ($p > 0.05$), an NPV strategy had significantly improving compliance over time (**$^{\#}p < 0.05$**).

5.4.4 **Inflammatory Cytokine Analysis**

The NPV strategy was associated with significantly less cytokine production in porcine and human lungs, irrespective of perfusate (**Figure 25,** $p<0.05$).

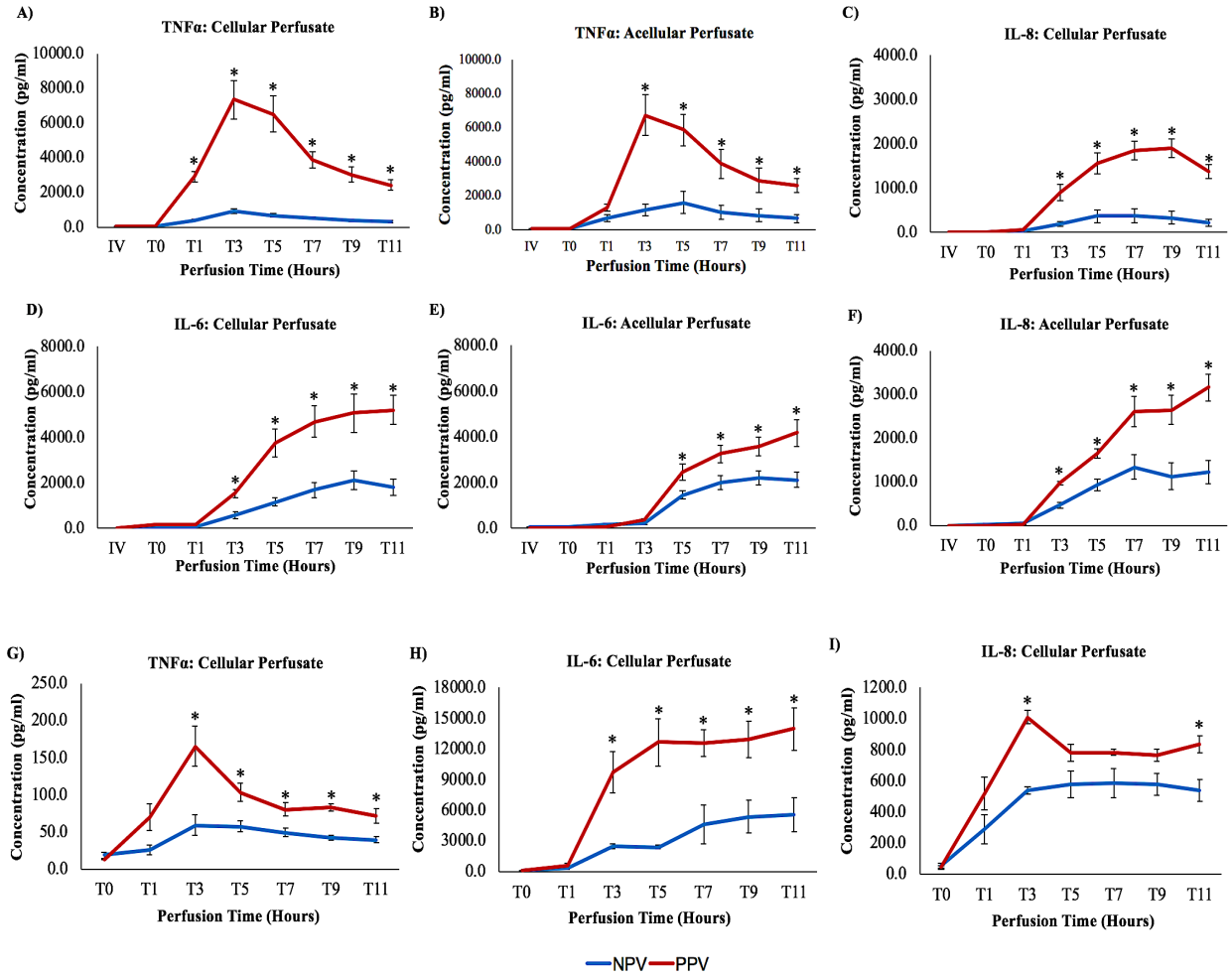

Figure 25: (A-F) Porcine and **(G-I)** human lung inflammatory expressions (NPV and PPV strategies). **NPV strategy demonstrated an overall decreased pro-inflammatory cytokine expression for both porcine (A-F) and human lungs (G-I).** **(A-F)** Analysis of pro-inflammatory cytokine accumulation throughout EVLP for porcine lungs showed significantly higher TNFα, IL-6, and IL-8 concentrations with a positive pressure ventilation strategy (PPV), irrespective of perfusate (***p < 0.05**). **(G-I)** Similarly, human lungs demonstrated significantly higher TNFα and IL-6 concentrations with a PPV strategy throughout EVLP; while only significantly higher IL-8 concentrations at T3 and T11, PPV vs. NPV (***p < 0.05**).

5.4.5 Lung Injury and Edema Formation

Among all porcine perfused lungs, there was 42% lower incidence of bullae formation with a NPV vs PPV strategy (**Figure 26A**, p=0.02). Perfused human lungs did not develop bullae, irrespective of ventilation strategy (data not shown). There was less edema formation (weight gain) in porcine lungs using an NPV strategy compared to a PPV strategy for both perfusates after 12 hours of EVLP (NPV-Cellular: 20.1 ± 4.1% vs PPV-Cellular: 39.0 ± 6.6%, p<0.01; NPV-Acellular: 40.4 ± 5.3% vs PPV-Acellular: 88.1 ± 11.0%, p<0.01; **Figure 26B**). Furthermore, an acellular based perfusate resulted in higher lung edema compared to a cellular based perfusate (**Figure 26B**, p<0.01**)**. Interestingly, with human lung perfusion, there was a drying effect (weight reduction) seen with an NPV strategy (NPV-Cellular: -8.0 ± 2.1% vs PPV-Cellular: 39.4 ± 5.7%, **Figure 26C**, p<0.01). Similarly, there was overall lower acute lung injury assessed by histopathology with an NPV strategy over PPV in human lungs (**Figure 27**).

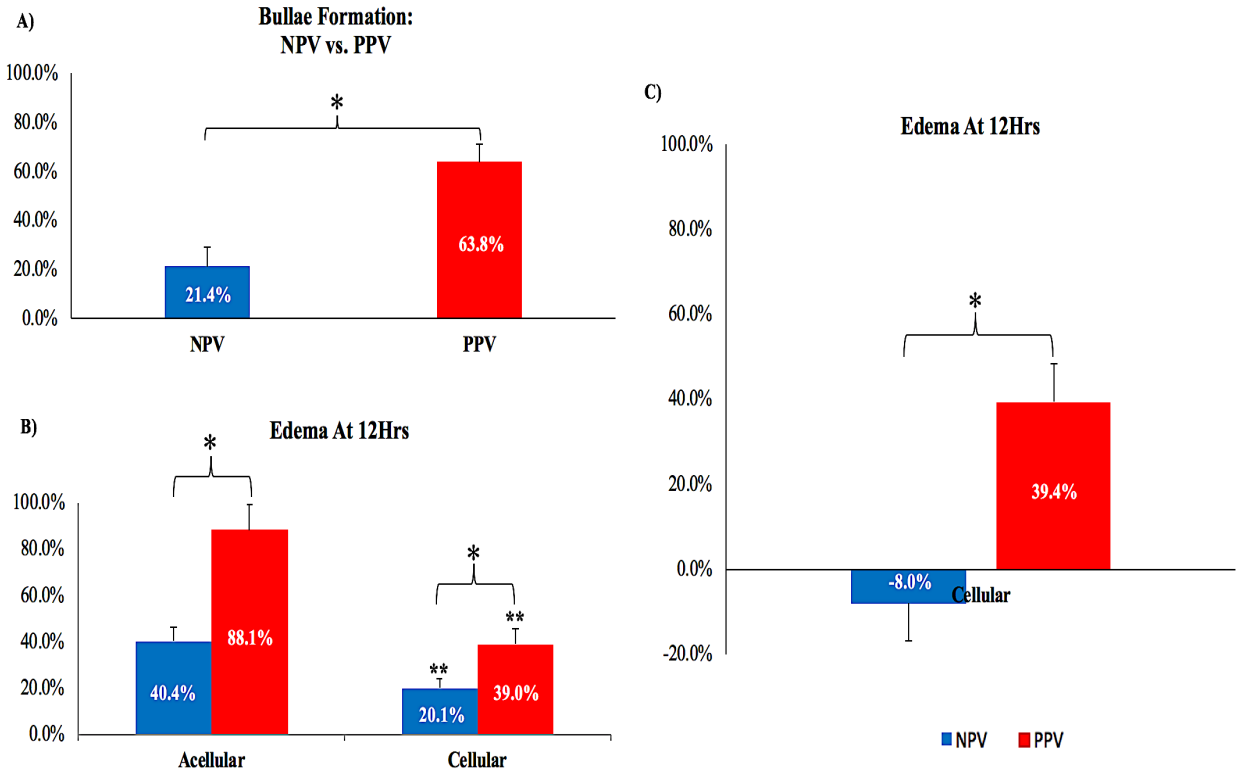

Figure 26: (A,B) Porcine lung bullae and edema formation and **(C)** human lung edema at 12-hours (NPV and PPV strategies).

Macroscopic evidence of decrease lung injury using NPV-EVLP and a 'drying' effect with human lungs treated with NPV-EVLP. Results shown as mean ± SE. (**A**) Bullae formation for total ventilated porcine lungs, comparing between the modes of ventilation, demonstrated 42% lower incidence of bullae formation when utilizing a negative pressure ventilation (***p = 0.02**). (**B**) Porcine lungs utilizing an NPV strategy showed overall less edema formation, irrespective of perfusate composition (***p < 0.01**). Moreover, an acellular based perfusate showed higher edema formation in both PPV-EVLP and NPV-EVLP compared to cellular based perfusate (****p = 0.01**). (**C**) Interestingly, with human lung perfusion there was a decrease in baseline weight gain due to a 'drying" effect with an NPV strategy (***p < 0.01**).

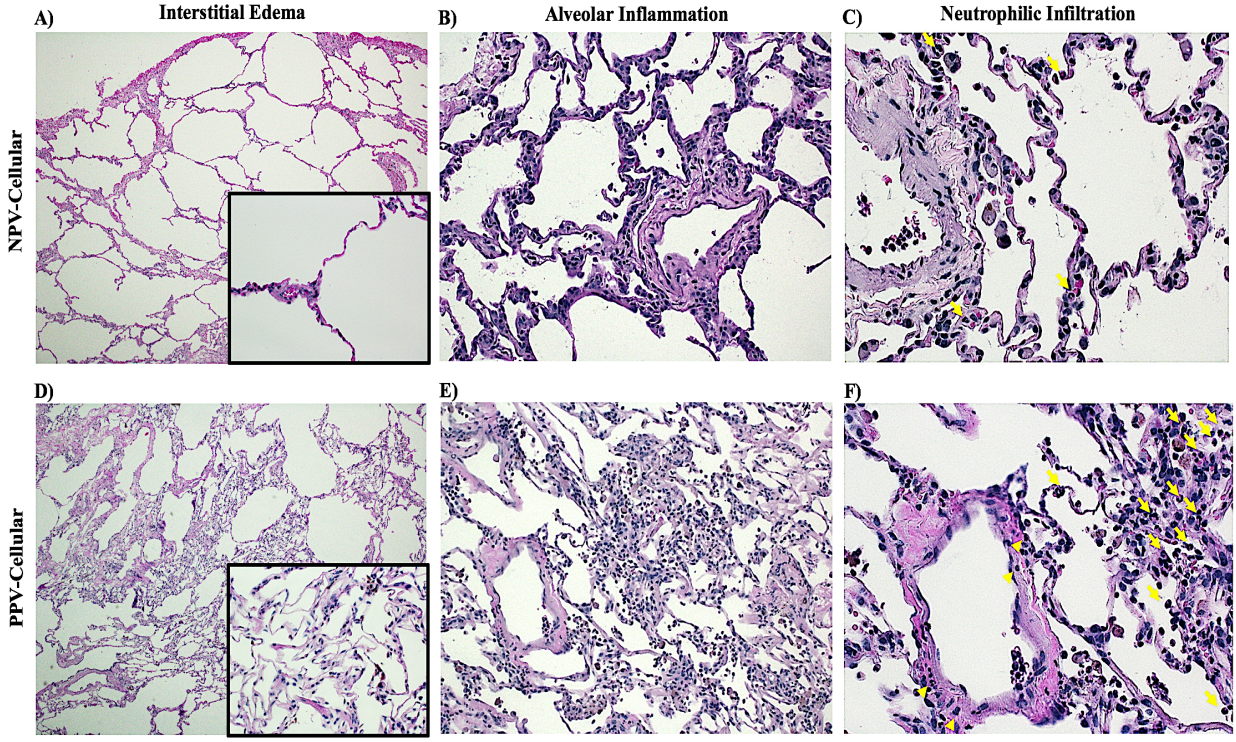

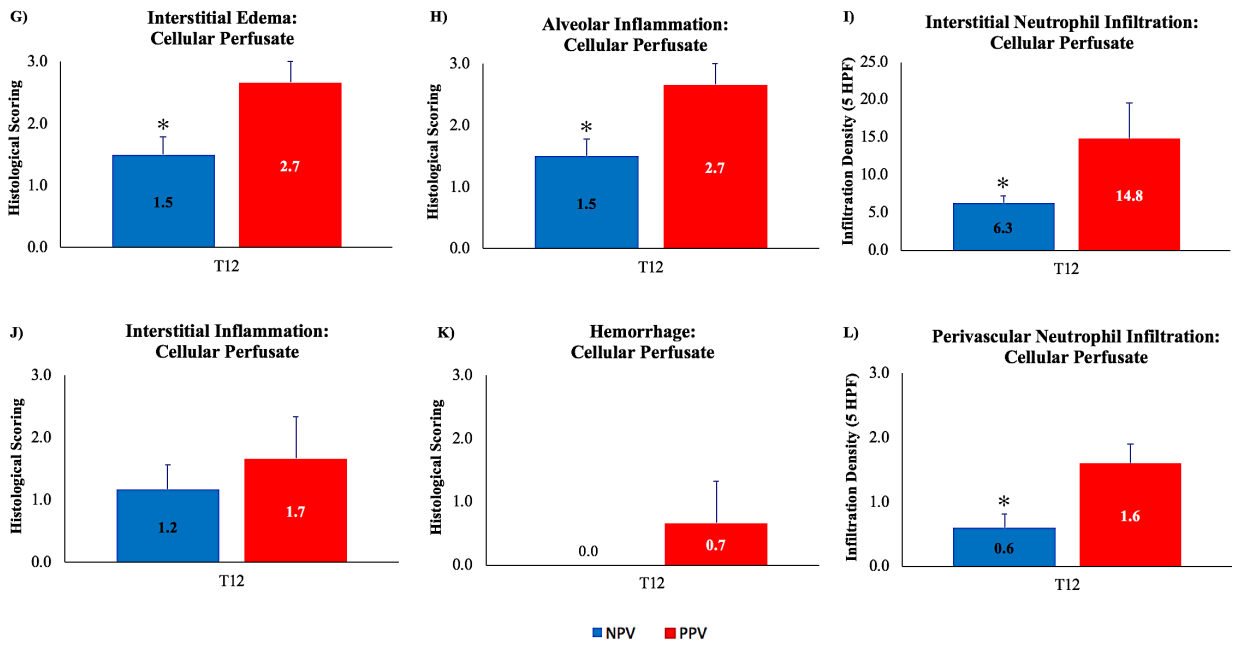

Figure 27: (A-F) Representative photomicrographs and **(G-L)** histopathology human lung injury scores after 12-hours of EVLP (NPV and PPV Strategies).
(A,D,G) Low magnification (4x) H&E staining with a 40x H&E micrograph inset, demonstrating less interstitial edema using an NPV strategy than a PPV strategy, for human lungs (***p < 0.05**). **(B,E,H)** Medium magnification (20x) H&E staining demonstrating less alveolar inflammation using an NPV strategy than a PPV strategy (***p < 0.05**). **(C,F,I,L)** High magnification (40x) H&E staining of human lungs, there were significantly higher neutrophilic infiltrates with a PPV strategy compared to an NPV strategy. Perivascular neutrophils represented with an arrow head without a tail, while interstitial neutrophils are represented with an arrow head with a tail: interstitial neutrophilic infiltration (***p < 0.05**) (I), and perivascular neutrophilic infiltration (***p < 0.05**), (L). **(J,K)** There was no difference in interstitial inflammation or hemorrhage ($p > 0.05$).

5.5| Discussion

As the value and potential risk associated with EVLP continues to be elucidated, there exists further opportunities to improve methodology and techniques to improve donor lung quality to mitigate deleterious effects of EVLP. Mechanical ventilation by Positive Pressure Ventilation (PPV) has the inherent risk of ventilator induced lung injury (VILI) during EVLP.[202,233,268]

Our results suggest NPV-EVLP may lead to less VILI and improved outcomes compared to PPV-EVLP. The NPV-EVLP platform provides stable and acceptable physiologic parameters over 12 hours as compared to a PPV-EVLP platform (**Figures 22-24**). There was superiority of an

NPV strategy by decreased production of pro-inflammatory cytokines (**Figure 25**), decreased incidence of bullae formation (**Figure 26A**), and decreased lung edema in both pig lungs (**Figure 26B**) and human lungs (**Figure 26C**) compared to PPV-EVLP. The benefit of NPV-EVLP was also observed by a decreased level of histopathologic finding of acute lung injury in human lungs (**Figure 27**).

As both acellular and cellular based perfusates are used clinically, we also tested both types of perfusates in NPV-EVLP and PPV-EVLP to discern whether a specific perfusate type was associated with improved lung quality based on the ventilator strategy. We found that both acellular and cellular based perfusates had very similar physiologic parameters during 12 hours of EVLP with both modalities of ventilation (**Figures 22-24**). Also, there were similar pro-inflammatory cytokine profiles with acellular and cellular based perfusates, with both types of perfusates being associated with decreased pro-inflammatory cytokine production using an NPV strategy (**Figure 25**). The only significant difference found with regards to perfusate was with respect to lung edema in pig lungs where acellular perfusate developed significantly more edema compared to cellular based perfusate for both NPV-EVLP and PPV-EVLP (**Figure 26B**). Based on these results, we used a cellular based perfusate for the six-human lung EVLP experiments, given the limited availability of human lungs to perform experiments with both types of perfusates (**Figure 26C**). Interestingly, both EVLP circuits had an open left atrium with excellent outcomes; with our data suggesting that a closed LA is not necessary in the context of NPV-EVLP.[258]

A finding of interest is the formation of bullae in juvenile pig EVLP experiments. The pigs used in our studies were domestic female pigs weighing an average of 42 kg (1-2 months of age). Consequently, the pig lungs demonstrate excessive elastance (poor compliance) leading to significant barotrauma and volutrauma even with protective ventilator settings. This was observed

by a significant level of bullae formation observed in PPV-EVLP compared to NPV-EVLP (**Figure 26A**). We appreciate that this is an inherent weakness of the pig model, as zero bullae was formed by either PPV or NPV strategies in any of the human lungs studied. Indeed, the sensitivity of the juvenile pig lungs to bullae formation during EVLP requires the most protective ventilatory strategy possible to avoid this damage, and NPV-EVLP greatly reduced the occurrence of bullae – supporting its further benefit to fragile marginal human lungs.

The human lung edema data suggests a significant finding that NPV-EVLP leads to a reduction in lung weight from baseline. As the human lungs were all from rejected donors with varying degrees of lung injury, it is promising that an NPV strategy allows for a potential therapeutic application simply by use of more physiologic ventilation to help reverse the state of lung edema that had occurred in the donor (**Figure 26C**).

Terragni *et al* (2016) reported the results of airway pressure-time curve (stress index) analysis of 14 patients undergoing lung transplantation after donor lungs were placed on EVLP.[268] They observed a significant reduction of post-operative mechanical ventilation, length of stay in the intensive care unit, and length of stay in-hospital for patients that received lungs that had "protected" ventilation during EVLP. The finding of potential ventilator induced sub-clinical deterioration of lung quality was shown by the lack of significant physiologic differences during EVLP of lungs ventilated by both "protected" and "non-protected" strategies where P/F ratios, dynamic compliance, and pulmonary vascular resistance were similar for both strategies. These finding are in support of our data, where both NPV-EVLP and PPV-EVLP showed excellent function throughout 12 hours of EVLP (**Figures 22-24**); yet, PPV-EVLP showed sub-clinical deterioration in quality (**Figures 25-27**). Furthermore, Mehaffey *et al* (2017) provided further evidence for VILI during EVLP in a pig model of donation after circulatory death (DCD),[233] and

found APRV to be less inflammatory than conventional PPV ventilation. Again, this study supports the finding of our results that PPV-EVLP may not be best suited for preservation and repair of injured lungs as seen by our human data of marginal human lungs that showed decreased edema formation using NPV (**Figure 26C**).

The porcine experiments employed a simplified perfusate lacking dextran 40. The rationale for this was a lack of evidence for benefit with regards to physiologic data during 12-hour EVLP. It is of relevance that all human lungs were perfused with proprietary STEEN solution, where dextran-40 is present. However, there is precedence for use of perfusates without dextran for extended EVLP.[269] Furthermore, the use of Low Potassium Dextran solutions in lung preservation is primarily predicated on Cold Static Preservation. At normothermic physiologic conditions, there is a lack of definitive evidence in the literature for the use of dextran in EVLP. Stig Steen and colleagues (1997) demonstrated no benefit for dextran in the heart.[270] As such, the use of dextran-40 specifically in EVLP requires further investigation, as we have demonstrated acceptable physiologic and functional outcomes during extended EVLP in a porcine model without dextran in the perfusate.

As the prevalence of EVLP as a preservation, evaluation, and therapeutic platform gains popularity, there is a potential that it will be used for the preservation of both marginal and standard criteria donors.[203,248,271-275] In part, a NPV strategy for EVLP has significant potential to mitigate PPV associated VILI. Slama *et al* (2017) have reported results of a randomized clinical trial examining the outcomes of standard criteria lungs placed on EVLP for 4-hours compared to lungs preserved by cold static storage alone. The authors suggest that two sets of standard criteria lungs perfused by EVLP, which did not meet physiologic criteria, could demonstrate the role of EVLP to detect standard criteria donor lungs that may result in otherwise unrecognized donor allograft

dysfunction. Though this is possible, however, an alternative explanation could be that even during a short course of 4-hours of PPV-EVLP, there was PPV-EVLP associated lung injury that led to donor lung edema formation – where VILI may have been a contributing factor.[248] Hence, these results point toward a need for further evaluation of current EVLP techniques to consider the potential of VILI that NPV-EVLP may ameliorate with further investigation.

Study limitations: Our study is limited as it is a proof of concept preclinical study. Large animal and clinical transplant studies are required in order to determine the impact of NPV-EVLP on post-transplant lung function and clinical outcomes. The use of non-commercial grade STEEN solution in the porcine experiments was required due to the significant cost of STEEN solution.

In conclusion, negative pressure ventilation during EVLP has limited the generation of pro-inflammatory cytokines, minimized the development of lung edema, and limited lung injury compared to conventional positive pressure ventilation.

Chapter 6

Summary and Future Directions

6.1| Summary and Limitations

It can be argued that the single most challenge facing lung transplantation is the shortage of suitable donor organs. Unlike other solid-organ transplantation, donor lung shortages are among the most severe, owing to the low utilization of donor organs. Primary graft dysfunction, following transplantation of an injured organ, is the major underlying reason for why centres have adopted a strict criteria list for deeming a donor lung suitable. This is justified due to donor lungs being particularly susceptible to injury from the sequalae of brain death and iatrogenic ICU care. Furthermore, this problem is compounded by the imprecise and subjective evaluation of potential donor lungs prior to transplantation. Current evaluation of donor lung graft relies on the combination of lung function (oxygenation), x-ray imaging, bronchoscopy, immunologic testing, and clinical judgement. While this method has been effective in identifying ideal lung graft, this ideal pool of lung grafts contributes 10-15% of potential donors. As a way to alleviate the low utilization rates, almost all lung transplant centers have begun to utilize extended criteria donor lungs. Unfortunately, this has brought its own challenges and complications, while making absolute cut-offs criteria for suitable versus non-suitable grafts a difficult consensus, when using the current standard lung evaluative techniques.

The University of Alberta Transplant Program has two major complications that further augment the shortage of suitable lung donor grafts and waitlist mortality rates – a) geographical isolation and b) large catchment area. Thus, to overcome these challenges our lab decided to build a custom-designed portable EVLP platform, with the hopes that one day the platform can move from a research setting to clinical application. Allowing for portable physiologic transport, assessment, and reconditioning of potential donors, without the limitation of borders – due to fear

of incremental injury from current prolonged cold ischemic preservation times and ischemia reperfusion.

This thesis began as a proof of concept to test the reproducibility and efficacy of our own PPV-EVLP platform – testing the optimal perfusate composition that would help establish a consistent, least damaging, extended EVLP therapeutic window of 12-hours. We demonstrated that the utilization of a cellular based perfusate, with a STEEN like solution, protects lung alveolar-endothelium integrity significantly more than the utilization of only an acellular solution. The fear that the addition of a blood product with extended EVLP runs might further augment edema formation and impact EVLP, was not evident in our results (Chapters 4). On the other hand, cellular based perfusates had some sort of a protective benefit – maybe the addition of oncotic pressure or inflammatory scavenger factors – which resulted in a surprising 50-60% less in edema formation than the use of an acellular perfusate. Some may argue that the importance of a closed left atrium might help in extended EVLP runs that utilize acellular perfusates; however, in a porcine study conducted by Nilsson *et al* (2017), they found that lung edema formation and decreased lung compliance were more pronounced in the acellular closed left atrium group versus cellular perfusate open left atrium group. Resulting in 3/10 lungs undergoing acellular closed left atrium EVLP to be terminated prematurely due to the onset of severe lung edema. Otherwise, there was no differences in oxygenation, other physiologic parameters, inflammatory production, ischemia/reperfusion injury, or histopathology between the EVLP techniques.[210] In chapter 4, we interestingly found that the use of cellular perfusate demonstrates trending improving compliance throughout EVLP, compared to the declining compliance of an acellular run. Moreover, only cellular perfusates had a significant positive compliance correlation with oxygenation. Further suggesting the importance of compliance trends during EVLP than oxygenation, as potentially

more accurate evaluative markers of evolving acute lung injury.[276,277] The first part of this thesis did indeed demonstrate the power and reproducibility of our custom-built EVLP platform and laid the foundation for the benefit of utilizing a cellular based perfusate, over an acellular perfusate, for extended EVLP runs. Furthermore, Chapter 4 raises the need for further investigations for more accurate physiologic markers of lung health on EVLP.

Chapter 5 builds on the protocol established in the chapter that precedes it, while bringing an exciting novel approach to further enhance the concept of EVLP. It is evident that to successfully preserve a lung, human or porcine, and provide the opportunity for the organ to be reconditioned ex vivo, one must pay close attention to the slow incremental re-warming/reperfusion early period; while serially recruiting the lungs during the early stages of the EVLP run. In addition, with protective ventilation strategies (5-7 ml/kg of body weight) and lower non-physiologic perfusate flows, it will ensure safe extended EVLP runs up to 6-12-hours. However, despite the agreed upon protective ventilation strategy utilized to minimize ALI/ARDS, all current EVLP protocols utilize standard positive pressure ventilation. The underlying physiology with PPV governs that air will always choose the path of least resistance; therefore, more potential for compliant alveoli to undergo barotrauma and VILI. Unfortunately, since most unutilized lung grafts have varying degree of injury and pathological aetiologies, they can be fragile and prone to further injury in an ex-vivo setting. Thus, a more protective ventilation strategy is required to prevent further injury during the EVLP reconditioning period. As such, we sought out to investigate, for the first time, the effect of negative pressure ventilation as a modality during extended EVLP. As predicted, VILI was significantly reduced with the utilization of a more protective ventilation modality (NPV-EVLP), irrespective of perfusate composition and human or porcine lungs. However, it was evident that the use of an acellular PPV-EVLP or NPV-EVLP still

produced significantly more edema formation than cellular PPV-EVLP or NPV-EVLP. For the first time in the literature of EVLP, pre-clinical or clinical, we demonstrate a promising finding that the utilization of NPV during extended 12-hours of EVLP develops negative edema or a drying effect, with unsuitable human organs.

The clinical significance of this finding and novel approach to EVLP ventilation can have major beneficial effect on the largest group of currently utilized lung donors, BDD. BDD lungs can be accompanied by an extensive pro-inflammatory milieu and neurogenic edema. Resulting in ongoing injury during standard cold ischemic transport and exacerbation of IRI. The utilization of an NPV strategy during human EVLP, not only provides a true physiologic mimicking preservation environment for the lungs ex-vivo, it acts as a natural therapeutic modality to decrease IRI. NPV-EVLP is capable of decreasing inflammation acquired at procurement and drying the lungs over 12-hours of EVLP. This is without the incorporation of any advance therapeutic measures such as drug, gene, or stem cell therapy. Furthermore, it may push the boundaries of EVLP reconditioning even further than 12-hours – permitting potentially safe 24-hour EVLP preservation/reconditioning windows. Thus, intercontinental organ donor retrieval, assessment, and reconditioning maybe be a future not too far in the horizon.

Limitation:

As this thesis was designed to establish a University of Alberta EVLP protocol, the studies performed have some limitations. The aim was to establish a proof of concept, with pre-clinical studies. Large animal and clinical re-transplantation studies are required to determine the impact of NPV-EVLP on post-transplant lung function and clinical outcomes. Also, the use of non-commercial grade STEEN solution in the porcine experiments was required, due to the significant

total cost associated with using STEEN solution – the total cost if STEEN solution was utilized for all the conducted porcine studies would equate to ~$80,000.

6.2| Future Directions

6.2.1 Re-Transplantation: Animal and Human Models

The fascinating aspect with regards to conducting an EVLP run, whether porcine or human lungs, is the opportunity to observe a "living" organ demonstrating dynamic in-situ physiology. EVLP as a platform is the closest modality scientist have to investigate any therapies, in an isolated setting. It truly provides valuable opportunities to push the scientific horizons in the field of pharmacotherapy, gene & stem-cell therapies, and organ/tissue bioengineering. Results obtained since the inception of EVLP in 2001, has shown quite the promising clinical translation.

Although most of the landmark work utilizing EVLP has been performed on lungs from humans or from large animals (e.g. porcine),[153,155,278] EVLP lungs from rodents have shown their significance and reproducibility.[279] The advantage of this model will help researchers rapidly test putative therapies, than in large animal models. In addition, rat clones make it possible for either more in-depth examination of immunologic outcomes or long-term post-transplant outcomes, without confounding factors of rejections.[181,202,279,280] However, despite demonstrating efficacy of proof-of-concepts in these models, translation of this evidence up to human studies at times falls short due to the inherent differences between the species. Multiple differences exist between human and rodent EVLP, including differing perfusion and ventilation techniques.[279] Moreover, extended (12-hour) stable normothermic EVLP rodent models still need to be developed to examine the effects of any therapeutic measures during extended EVLP. Since most pre-clinical/clinical EVLP investigations are pushing for extended reconditioning (6-12-hours).

On the other hand, in 2001 Dr. Stig Steen introduced EVLP as potential technique to possibly re-consider DCD donors. The report of the first successful human lung transplant case, after short-EVLP assessment and reconditioning (<1-hour) from a non-heart-beating donor, opened up the possibility of potential expansion of the gold standard limited donor pool (BDD).[219] One of the biggest disadvantages that transplant centers agree with regards to DCD lungs, is the insufficient evaluation time the retrieval team has to make a comprehensive reliable assessment of the graft. The deleterious effects of warm ischemia, compounded with asphyxiation and the unknown length of time of organ ischemia/hypoxia, forces transplant centers to elect for BDD organs. However, the advent of ex vivo assessment as a potential possibility opened up the avenue for experimentation. Dr. Stig Steen, published a landmark paper (2003) demonstrating promising post-transplant outcomes of twelve large porcine models with controlled-DCD injury: re-transplanted after 65-minutes of warm ischemia, 6-hours of cooling in-situ and assessment/reconditioning with EVLP.[162] This paper opened up the gates for experimental investigations to attempt to utilize EVLP to reverse lung injury in animal models of BDD and DCD.[281-284]

The mode of death for the lungs is pivotal in early allograft function. In a rodent DCD model comparing ventricular fibrillation and asphyxiation on an EVLP platform demonstrates that asphyxiation affects the lungs more severely than ventricular fibrillation. This has been attributed to the development of pulmonary edema, type II pneumocyte activation, and damage to alveolar wall.[285] Interestingly, there are reports of improved inflammatory profiles in DCD lungs, compared to BDD lungs, attributed to the avoidance of the cytokine storm seen in BDD.[286] As such, Cypel *et al* (2012) demonstrates in a 5-year retrospective study, 15-20% of lungs transplanted after EVLP reconditioning were procured from DCD donors and have similar short to mid-term outcomes in

survival rates, which are comparable with BDD lungs.[287] This paper and others demonstrated the potential of EVLP in resuscitating DCD lungs and accurately evaluating their suitability for transplantation. As such, DCD lung transplants are slowly increasing in volume in many transplant centers; while outcomes show promising comparison with the gold standard BDD lungs.[288,289]

Consequently, as it relates to University of Alberta Hospital Transplant Program, the combination of increasing acceptability for the utilization of DCD donor lungs and our custom-designed portable EVLP, will effectively complement the implementation of Bill 207 – the Human Tissue and Organ Donation Amendment Act of Alberta. The implementation of our portable NPV-EVLP platform with DCD donors will virtually increase the limited donor pool, and increase low donor utilization rates at the University of Alberta transplant program; thus, significantly improving the current waitlist mortality of the catchment area this transplant program serves.[204]

6.2.2 **EVLP: Potential Biomarkers**

In order to further refine EVLP protocols, the search for associated biomarkers of lung health/reconditioning status, remains to be under review. Lung tissue is known to be rich in lactate dehydrogenase, which catalyzes the conversion of pyruvate into lactate. One key finding in lung metabolism is the production of increasing levels of lactate.[290] In a porcine model, following standard human EVLP protocol with cellular perfusate, it was demonstrated that high glucose consumption demonstrated worse lung function and correlated with lung edema formation.[291] Clinically, plasma lactate concentrations are known to increase with severe hypoxemia, and generally thought to reflect hypoxic metabolism. Although lactate production and washout are a continuous process, lactate/pyruvate ratio and glucose levels during EVLP can be indicators for poor prognosis. However, the relationship between lactate production and post-transplant outcomes is unclear.[292] Lungs of patients with ALI will release lactate at a rate proportional to the

degree of injury.[290] The mechanism of lactate production by injured lungs may represent the ongoing deterioration of ongoing anaerobic metabolism, and direct pro-inflammatory biomarkers effecting pulmonary cells. With ongoing inflammation, glucose metabolism increases in both parenchymal and inflammatory cells infiltrating lung tissue.[290]

As described in previous chapters, the cellular characteristics of ALI include the loss of the alveolar-capillary integrity, excessive trans-epithelial neutrophil migration, and release of pro-inflammatory/cytotoxic mediators. Biomarkers involved in inflammation and coagulation cascades, found on both epithelium and endothelium, have been reported to be predictive of clinical morbidity and mortality. Furthermore, baseline and persistently elevated plasma levels of IL-6, IL-8, and TNF-α were strongly predicative of mortality.[51,293] Parsons and colleagues (2005) supported these findings in a large prospective study involving ARDS patients comparing lower versus higher tidal volumes. Despite positive pressure ventilator adjustments, higher plasma levels of IL-6 and IL-8 were independently associate with greater organ failure days, invasive intubation dependence, and predicted higher mortality.[51,294] Consequently, several aforementioned studies have demonstrated the attenuation capability with a more protective ventilation strategy – modulating the inflammatory response and decreasing VILI.[233,268]

The results presented in this thesis demonstrate potential enhancement of conventional PPV-EVLP with the utilization of our novel NPV-EVLP platform. As such, it will be critical to investigate post-transplant outcomes and inflammatory profile, after porcine or human lungs have undergone our NPV-EVLP reconditioning.

6.2.2.1 **Damage-associated molecular patterns**

Over the years, damage/danger-associate molecular patterns (DAMPs) have been an interest in organ transplantation due to the fascinating development in pre-clinical and clinical

research – elucidating the presence of a plethora of "danger/injury" signalling biomarkers (DAMPs) and their close association with endothelial dysfunction, ischemia-reperfusion injury (IRI), ALI/ARDS induction, and primary graft dysfunction.[33,181,214,295-307] Due to the complex nature of the interactions of DAMPs and the innate immune system, it is beyond the scope of this thesis to describe the detailed mechanisms of release and interactions of these biomarkers and the immune system. However, Hamilton *et al* (2017),[307] Land *et al* (2016),[300] Kuipers *et al* (2011),[181] and Bianchi (2007)[34] provide a combined, holistic, understanding of the consequence of DAMP propagations – from a cellular perspective, up to the tissue level.

In brief, DAMPs coined in early 2000s,[308] are endogenous molecules that can initiate and perpetuate a non-infectious sterile inflammatory response – eventually leading to the initiation of the innate immune response and the exacerbation of cellular dysfunction (**Figure 6**).[34,54] They are emitted under various conditions of major cell stress (e.g. shear stress) or tissue injury (e.g. brain death, organ preservation, and ischemia-reperfusion injury).[33,181,214,295-306] DAMPs are recognized either:

a) "Classically" via pattern recognition receptors (PRRs) found ubiquitously on various immune and non-immune cells (e.g. neutrophil, macrophage, dendritic cells, B-cells, epithelial cells, vascular and fibroblast cells) – toll-like receptors (TLRs), TLR2 and TLR4 best-known class, and the various DAMPs that activate them are summarized in **Figure 28**.[33,181,214,295-306]

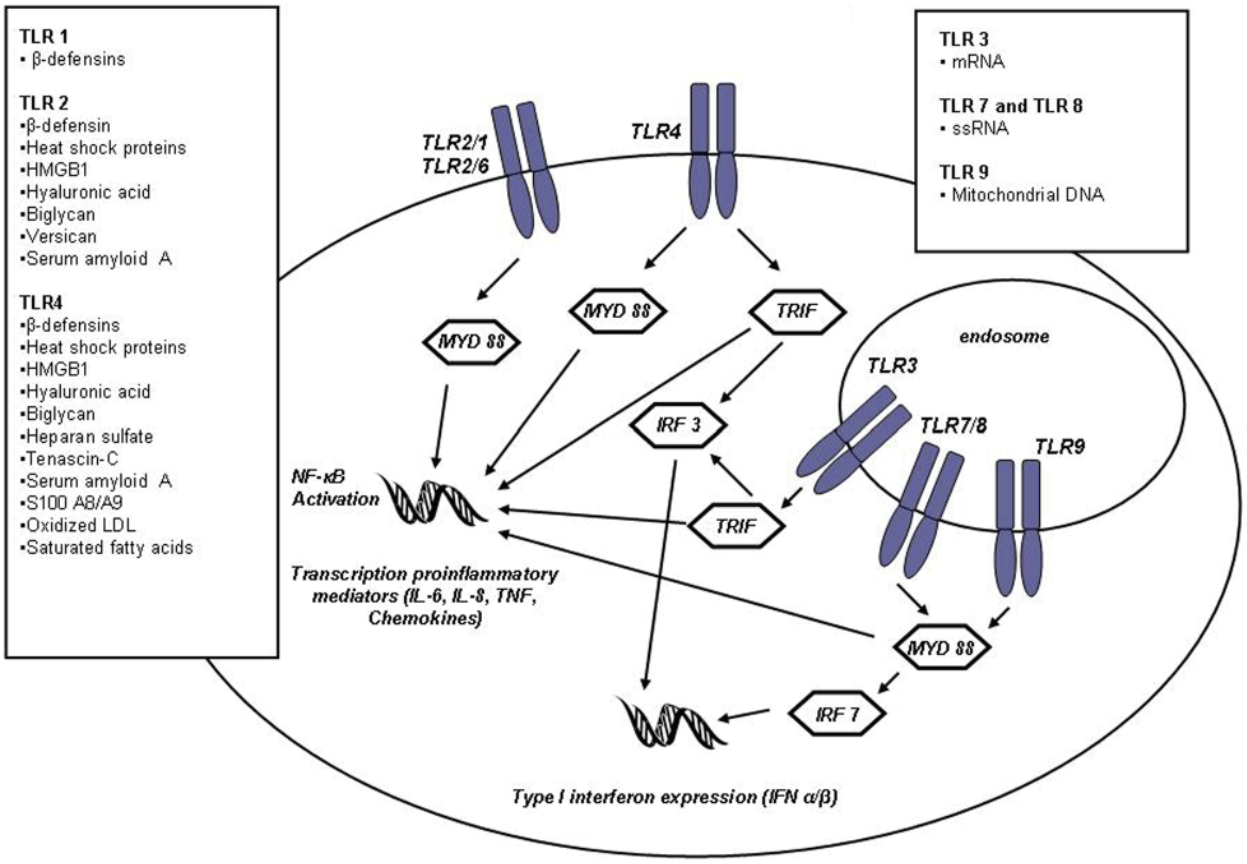

Figure 28: Interactions between DAMPs and TLRs. Adapted from Kuipers *et al.*[181]

b) "Non-classically" via specific cells (e.g. receptor for advanced glycation end products – RAGE). RAGE has been found to be highly expressed in lung tissue, especially on Type I pneumocytes.[33,181,214,295-306]

c) "Non-classically" via intracellular receptors (nucleotide-binding oligomerization domain-like receptors – NLRs). NLRP3 inflammasome, cryoporin, is one of many belonging to the NLR family and recognized to be activated in infection and tissue injury via the release of intracellular DAMPs (e.g. ATP, uric acid and DNA) and glycocalyx damage leading to soluble extracellular matrix components (e.g.

Glycosaminoglycans (GAGs) – hyaluronan fragments, dermatan sulfates, chondroitin sulfates, heparin, heparan sulfates, and biglycans).[34,181,300]

6.2.2.2 **Glycocalyx**

Another interesting area under investigation is the endothelial glycocalyx layer, EGL. A structure that has been reported to span a thickness of 0.5-3.0μm, plays the pivotal role of vascular protection and homeostasis in micro/microvasculature injury and repair. The EGL is situated at the luminal side of all blood vessels and acts as negatively charged mesh (**Figure 29**).

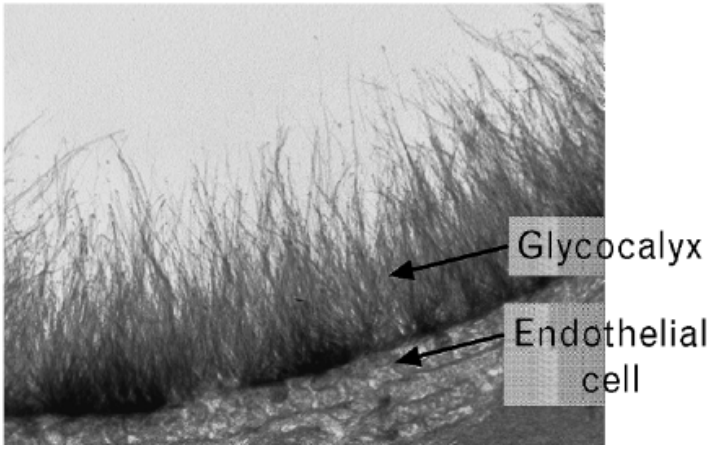

Figure 29: Electron microscopy of the endothelial glycocalyx layer. Adapted from Nieuwdorp *et al*.[309]

EGL obtains its negative charge and mesh like organization via glycoproteins (e.g. adhesion molecules – selectins, integrins and immunoglobulins) and proteoglycans. Proteoglycans have a protein core (e.g. syndecans, glypicans, versicans, biglycans) to which they are attached to negatively charged glycosaminoglycans (GAGs) side chains (**Figure 30**).[309,310]

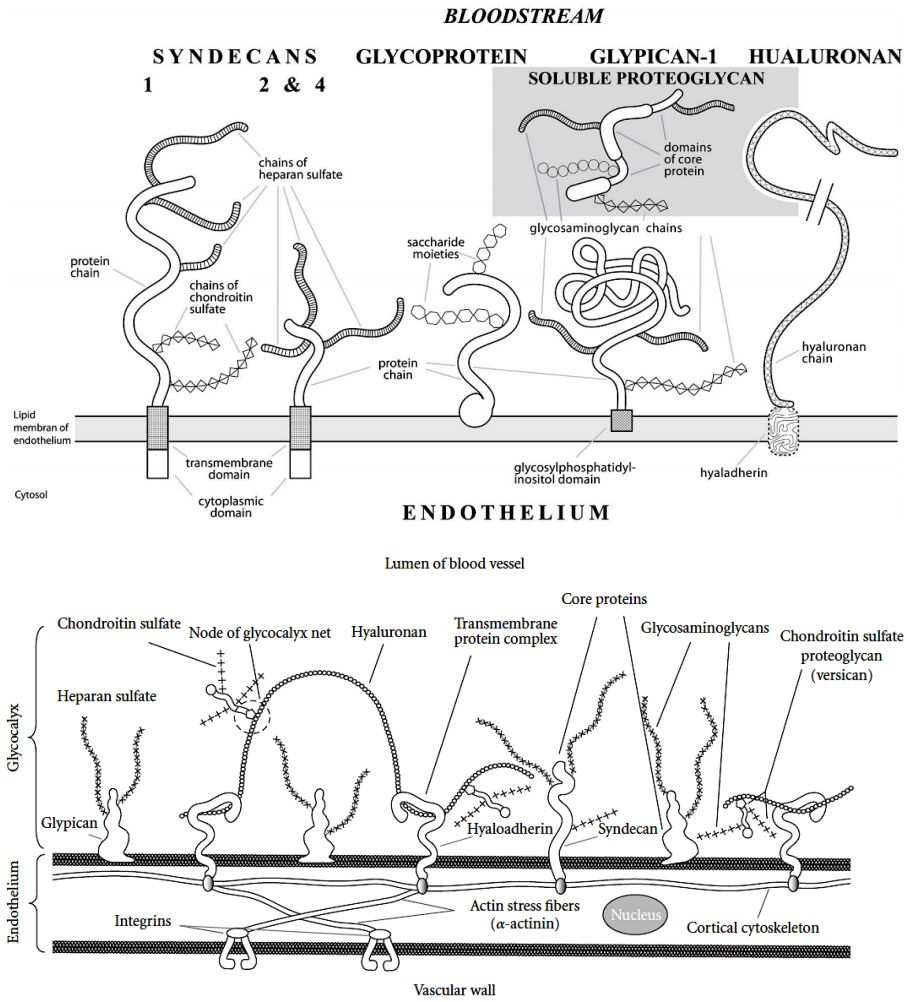

Figure 30: Schematic representation of the glycocalyx components. Adapted from Maksimenko.[311,312]

There are five types of GAG side chains – heparan sulphates, making up 50-90% of the EGL, and the remainder composed of hyaluronic acid (hyaluronate), dermatan sulfates, chondroitin sulfates, and keratin sulphates. Each GAG is expressed in varying concentration (based on the tissue origin) and covalently bound to core proteins. The exception, hyaluronan, the only GAG that does not contain any sulfates, is non-covalently bound to proteoglycan complexes in the EGL, and not to core proteins. Thus, hyaluronan, synthesized by hyaluronan synthases, are known to have high molecular weights allowing them to form a viscous solution with water. The volume of the glycocalyx depends on a balance between biosynthesis and the enzymatic or shear-

dependent shedding of its components. GAG side chain sulphation carried out by specific membrane-bound sulfotransferases, has been recognized as a pattern modified by time, physiology and pathophysiological stimuli. It has been demonstrated that changes in sulphation patterns affect protein binding and increase vascular permeability.[309-312]

From the standpoint of simple architecture, a healthy thick EGL will greatly exceed the length of apical-based selectins; as such, it has been proposed that in-vivo the glycocalyx forms a "cloak" like layer that conceals endothelial cell adhesion sites from passing neutrophils, leukocytes, and thrombocytes.[32] Furthermore, the EGL harbours a wide array of enzymes that might contribute to its vascular protective effect and prevention of endothelial dysfunction:[309-312]

I. Extracellular superoxide dismutase – an enzyme that converts oxygen radicals to hydrogen peroxides and is bound to heparan sulphate proteoglycans within the glycocalyx. Reduces oxidative stress and maintains nitric oxide bioavailability.

II. Endothelial nitric oxide synthase – increased blood shear stress on EGL results in nitric oxide production via this enzyme, which in turn dilates vessels and reduces stress. Hyaluronan has been reported to increase in concentration on the glycocalyx to help in response to shear stress.

III. Antithrombin III – an inhibitor of thrombin and activated factors IX and X. Its anticoagulant activity is enhanced by binding to heparan sulphate.

IV. Angiotensin converting enzyme – plays a vital role in the renin-angiotensin-aldosterone pathway.

Therefore, the negatively charged mesh of the glycocalyx acts as a macromolecular sieve – repelling negatively charged molecules, as well as white blood cells, red blood cells, and platelets. However, there is an intimate role between albumin (67 kDa) and the glycocalyx, which

exclude macromolecules larger than 70 kDa and negatively charged. Despite albumin having a net negative charge, it binds tightly to the glycocalyx due to its amphoteric nature – carrying some positive charge along the protein chain. This binding along with hyaluronan, maintains a finely balanced hydraulic conductivity across the vascular barrier.[310]

Various DAMPs have been associated with mechanical positive pressure ventilation injury, ischemia-reperfusion injury, and shear stress.[181,310] Specifically, low molecular weight hyaluronan, heparan sulfate proteoglycan, syndecan-4, heat shock protein (HSP72), S100A8/9/12 and high-mobility box group (HMGB-1) all have been shown to have significantly higher concentrations in bronchoalveolar lavage in ALI/ARDS patients and mice that underwent injurious mechanical ventilation.[313] Low molecular weight hyaluronan and hyaluronan synthase enzyme transcripts were found significantly elevated and localized in bronchoalveolar lavage from murine lung recipients that developed bronchiolitis obliterans syndrome.[304]

The majority of these DAMPs interact with TLR receptors and RAGE, which ultimately leads to the transcription of pro-inflammatory cytokines and chemokines production/release via downstream activation of MyD88 and NF-κB (**Figure 28**).[181,310] Conversely, blocking HMGB1 has shown significant reduction in neutrophil influx and TNFα concentration in bronchoalveolar lavage, improved oxygenation, limited microvascular permeability and reduction in IRI.[181,295,300,301] HSP70 expression due to injurious mechanical ventilation in rats have shown suppression of cytokine-induced IL-8 and TNFα expression in respiratory epithelial cells – ultimately demonstrating HSP70 induction attenuates downstream activation of NF-κB and decreases pro-inflammatory cytokine production, while improving lung compliance in ex vivo rat lungs pretreated with heat stress.[181,300]

Our lab began preliminary investigations of these various DAMPs in hopes to better understand their expression with lungs undergoing extended perfusion on EVLP platforms. We looked to compare ventilation modalities, NPV versus PPV, and perfusate composition on DAMP expressions/changes over extended (12-hours) EVLP. However, results are too preliminary to include, but further investigations are warranted since the literature demonstrates promising association of these biomarkers of cellular stress/injury and clinical outcome: the Toronto group report significant association of increasing sICAM-1 and sVCAM-1 perfusate levels during human EVLP reconditioning and recipient development of PGD 3 within 72-hours of post-transplant.[297]

EVLP will be a vital tool in preserving, assessing, and repairing injured donor lungs by providing an isolated therapeutic window for the glycocalyx to heal or undergo reconditioning pharmacotherapy.[181,310]

6.2.3 **EVLP: Potential Therapeutic Avenues**

6.2.3.1 **Von Willebrand Factor**

One of the major causes for allograft rejection after lung transplantation is the formation of a hypercoagulable state. As aforementioned, the increasing appreciation of the glycocalyx matrix and its components in the role of homeostasis and hemostasis has been extensively researched. von Willebrand Factor (vWF), is a blood glycoprotein expressed only on endothelial cells and megakaryocytes.[314] It acts as molecular bridge in the adhesion process between platelets and the sub-endothelium of injured vessels, in the formation of thrombus. In the subendothelial matrix, vWF has been reported to aggregate platelets via the interaction of vWF to specific platelet membrane glycoprotein Ib and glycoprotein IIb/IIIa. In the absence of injury, vWF does not appear to interact with circulating platelets.[314] Damage to the endothelium, via hypoxia or shear stress,

permits vWF to bind to constituents of subendothelial connective tissue, which enables vWF to bind to platelets with sufficient affinity – causing intravascular thrombus formation.

Furthermore, the endothelium is known to contain nitric oxide (NO), and prostacyclin – essential intrinsic antithrombotic factors. Research in xenotransplantation has shown that in states of hyperacute and acute vascular rejection, the anticoagulant endothelial surface is ruined and expresses pro-coagulant, adhesive phenotypes, and attenuation of NO production. Interestingly, NO was reported as a possible inhibitor of endothelial vWF secretion.[315]

As future possible directions, it will be interesting to investigate the effects of normothermic NPV-EVLP as a modality for physiologic organ preservation compared to the gold standard CSP, prior to transplantation. The purpose would be to determine the change in vWF expression (directly) or via NO attenuation (indirectly) over preservation time. Other biomarkers that might correspond to endothelial injury and loss of anticoagulant properties would be upregulation of heparin sulfate, adhesion molecules and tissue factor. Since these biomarkers have all shown facilitation of adhesion of leukocytes and platelets, and impairment of vasodilation – ultimately leading to organ dysfunction. It would be equally intriguing to test the effects of DDAVP and aurintricarboxylic acid (ATA) during NPV-EVLP, as potential antithrombotics.[316,317] Both have shown evidence to have such properties; while ATA has been reported to prolong graft survival in porcine-to-human ex vivo lung transplantation.[317] On the other hand, NO agonists utilized for stable angina and coronary vasospasm, such as molsidomine (non-nitrate), has shown that its active metabolite reduces reperfusion injury, preserves endothelial function, and improves ex vivo xenograft pulmonary function via a marked reduction in pulmonary vascular resistance.[315]

Parnian Alavi, a graduate student in the lab, has shown promising preliminary results of vWF mRNA levels significantly increasing with CSP organ preservation, while attenuation of

vWF mRNA during organ preservation on EVLP. As the lab progresses to animal transplantation models, it will be intriguing to correlate pre-transplantation vWF concentrations and post-transplant outcomes. Clinically, vWF-antigen plasma levels have been significantly shown to excellent predictor prognostic markers for pulmonary endothelial injury and the development of ALI/ARDS.[318,319]

6.2.3.2 **Drug Therapy**

EVLP is a powerful platform that has been utilized worldwide, since its inception in 2001 by Dr. Stig Steen, to investigate possible drug therapies to alleviate specific causes of known lung injuries. Some notable successes include the utilization of thrombolytics on EVLP by our lab,[189] and others,[245] for human donor lungs rejected due to the presence of a massive pulmonary emboli. The treated lungs were successfully reconditioned on EVLP, followed by successful transplantation with no thrombosis post-operation. Another possible intervention is the use of prophylactic broad-spectrum antibiotics and possibly anti-fungal to help reduce the infectious burden of donor lungs undergoing normothermic EVLP. Studies have shown that in human donor lungs rejected for transplantation due to clinical concerns of infectious etiology, showed significant quantitative decrease in bacterial load in bronchoalveolar lavage (BAL), when treated with high dose of broad-spectrum antibiotics during EVLP.[190,320] Moreover, lungs treated with broad-spectrum antibiotics demonstrated significant improvement in oxygenation, compliance, reduced pulmonary vascular resistance, and perfusate endotoxin levels after 12-hours of EVLP strongly correlated with perfusate levels of TNF-α, IL-1β and macrophage inflammatory proteins.[190] Interestingly, when some of the same infectious marginal donor lungs were subjected to anti-fungal treatment on EVLP versus being reconditioned on EVLP without anti-fungal treatment, the yeast load increased over time for the untreated human lungs – six treated lungs were ultimately

transplanted into patients, all of whom survived to hospital discharge, and only one mortality at 11 months.[320]

Other targeted drug therapies include the use of adenosine A2A receptor agonist, salbutamol, and prophylactic surfactant inhalation during EVLP reconditioning. The addition of Adenosine A2A receptor agonist in the perfusate during EVLP of porcine DCD lungs, lead to successful treatment of ischemia-reperfusion injury and better post-transplant outcomes than control-EVLP porcine DCD lungs.[284,321] On the other hand, salbutamol inhalation therapy during EVLP has exhibited protective effects in DCD lungs treated, by enhancing alveolar fluid clearance and attenuating acute lung injury – reduction in PAP, improved oxygenation and lung mechanics, were reported in treated group compared to placebo.[283,322] Finally, prophylactic surfactant inhalation has been studied shown to decrease PVR, improve compliance, and decrease mRNA expression of IL-6 and IL-6/IL-10 ratios.[278]

Future studies should investigate the reproducibility of these therapeutic endeavours on NPV-EVLP, with survival injured animal models and rejected donor human lungs. Emphasis should be placed not only on seeking reproducibility, but better therapeutic delivery modalities. Ultimately, as we gain better understanding on various pathological cellular mechanism for lung injury and continue to refine various known therapeutic delivery tools, NPV-EVLP will be the ultimate platform aiding in our progression toward precision medicine.

6.2.3.3 **Gene Therapy**

Gene therapy is a promising strategy towards a future of personalized medicine. Engineering donor lungs to alleviate some of the damage that ensues at organ procurement, will hopefully have a significant impact on post-transplant graft outcomes (primary or secondary). As

such, EVLP is a promising platform, which various gene therapy investigations can be evaluated under isolated physiologic conditions.

Over the last decade, there has been significant advances in gene therapy understanding, research applications and various vector delivery modalities. One commonly studied modality are viral vector gene therapies, such as adeno-associated virus. Adenoviral gene therapy are attractive candidates for efficient gene delivery in-vivo because of their low immunogenic potential, reduced oncogenic risk from host-genome integration, and well characterized serotype specificity.[323] The Toronto group have demonstrated significant studies elucidating the potential safety and efficacy of adenoviral gene therapy delivery, on their EVLP platform, for both porcine lung survival studies and in pre-clinical marginal human lungs.[191,324] Overall, when compared, porcine lungs treated with human IL-10 gene therapy via intra-tracheal adenoviral delivery to lungs undergoing standard EVLP or only prolonged CSP, the Toronto group found superior immediate post-transplant lung function, detectable plasma levels of human IL-10, significantly improved oxygenation, overall less pro-inflammatory markers, and no signs of systematic toxicity, throughout all post-transplant follow-up days.[324] Moreover, in the non-transplanted marginal human studies, injured lungs treated ex vivo with intra-tracheal IL-10 gene therapy, compared to reconditioning with standard EVLP, exhibited improved lung function to potentially being classified as suitable for transplantation – EVLP adenoviral human IL-10 treated lungs showed significant improvement in oxygenation and pulmonary vascular resistance, a favorable shift from pro-inflammatory to anti-inflammatory cytokine expression, and recovery of alveolar-endothelial barrier integrity, compared to standard EVLP.[191]

These two papers provided the encouraging bases for the potential impact of incorporating gene therapy during extended EVLP for Sayed Himmat's project (PhD student in the lab). Sayed's

project investigates the potential anti-inflammatory and cytoprotective properties that adiponectin (bioactive peptide) has been reported to exhibit on pulmonary vascular endothelium and airway epithelium. Adiponectin enhances nitric oxide generation, attenuates production of reactive oxygen species, reduces vascular smooth muscle cell proliferation and TNF-α induced leukocyte-endothelium adhesiveness – overall, reducing the primary state of endothelial dysfunction.[325-327] Preliminary porcine investigations have shown feasibility of intravascular delivery of adenoviral gene transduction on our EVLP platform. As the project grows, it will hopefully investigate any vector-associated inflammation comparison between acellular PPV-EVLP versus cellular PPV-EVLP, marked differences with the switch to a more protective ventilation strategy (NPV-EVLP), and the effects of adenoviral adiponectin gene therapy EVLP (pre-clinical and porcine survival models).

Another interesting development has been in the field of recombinant DNA technology. Initiating in the 1970s, it marked a new era for biology.[323] For the first time, molecular biologists had the capabilities to manipulate DNA molecules – allowing them to study genes and exploit them to develop novel medicine and biotechnology. However, as this fascinating field continued to flourish, and technology enhanced, recent advances in genome engineering technologies (CRISPER-Cas9) have sparked an entirely new realm of possibilities in biological research.[323] Clustered regularly interspaced short palindromic repeats (CRISPER) and Cas9 (commonly used nuclease-encoding gene) is a system that acts as an RNA-mediate adaptive immune system found in bacteria and archaea.[323] Together, CRISPER-Cas9 act to protect the host bacterial/archaea cell from invading foreign DNA elements.[328] Originally, genome manipulation breakthrough was reported by Capecchi (1989) demonstrating gene targeting via homologous recombination.[329] This technique drastically advanced many areas of biological research, since it facilitated the generation

of knock-in and knock-out animal models. Nevertheless, although homologous recombination-mediated gene targeting produced highly precise alterations, the desired recombination events occurred extremely infrequently.[329] This presented obvious challenges for large-scale applications of gene-targeting experiments. Thus, with the discovery and understanding of CRISPER-Cas9 applicability in recent years, the challenges once faced with homologous recombination mediated gene manipulation were easily circumvented. Rather than only studying DNA excised out of the context of the genome, researchers can now directly edit or modulate (inhibit/activate) the function of DNA sequences in their endogenous context; with surgical precision and efficiency, in a variety of eukaryotic and mammalian species.[323,330]

Scientists now are capable of creating mouse models of human diseases faster than before, they can study individual genes quicker, and easily change multiple genes in cells at once to study their interactions. Soni *et al* (2018) utilized in-vivo silencing of IRAK-M in mouse lung vascular endothelial cells, using CRISPER-Cas9 system, and demonstrated that prevention of A20 and vascular endothelial cadherin expression at endothelial adheren junctions augmented lung vascular leak. Thus, suggesting that genetic targeting of endothelial A20 is a potential therapeutic strategy to restore endothelial barrier integrity in the setting of ALI.[331]

As such, one can imagine the unprecedented possibilities of CRISPER utilization with extended EVLP. A genetic disorder, such as cystic fibrosis, can be rapidly modeled in animal models, and utilized in an isolated EVLP platform to assess various therapies. Moreover, various lung injury models can have their pathogenesis elucidated, on a genomic level, and establish causal linkages between genetic variations/manipulations and biological phenotypes. Consequently, molecular evaluation on EVLP will be imperative in progressing our understanding of various mechanisms involved in the pathogenesis/repair of lung injury, primary graft dysfunction, and

breaking down any previous barriers with regards to “unrepairable” donor grafts – EVLP gene reconditioning is truly a futuristic, but foreseeable, realm of vast therapeutic possibilities.

6.2.4 NPV-EVLP: A New Frontier

6.2.4.1 Expanding the Therapeutic Window (24-Hours)

As reported in chapter 5, it was exciting to see our custom-designed portable NPV-EVLP platform showing significant attenuation of edema, inflammation, and bullae formation in our porcine studies; while similar significant reduction in pro-inflammatory cytokines with the unutilized rejected human BDD lungs, compared to PPV-EVLP reconditioned organs. Moreover, trends of improving compliance were observed with human reconditioned lungs on NPV-EVLP. What makes NPV-EVLP an exciting breakthrough in the field of EVLP is a) it represents the first truly feasible protective ventilation strategy that mimics in-situ physiologic conditions, b) NPV inducing less VILI than the utilization of PPV during EVLP, and c) it is the first-time negative edema, a drying effect, is exhibited with porcine or rejected injured human lungs undergoing EVLP.

Therefore, this exciting finding led us to attempt to push the reconditioning window to 24 hours. To our surprise, we were able to perfuse two cellular based unutilized BDD human lungs up to 24-hours with minimal edema gain, stable/promising physiologic parameters (oxygenation, PAP, PVR, and dynamic compliance). These preliminary results have demonstrated that 24-hour EVLP is a possibility when a protective ventilation strategy such as negative pressure is utilized. Moreover, the utilization of a portable NPV-EVLP platform, which can safely preserve/recondition human lungs for 24-hours, introduces the potential capability of intercontinental organ donor retrieval between transplant centres worldwide – no longer will geographical limitations be a challenge facing the current shortage in organ donation.

With NPV-EVLP pushing the limits of the therapeutic window into new boundaries, graduate students to come will have the means to test future pharmaceutical, cell, and gene therapies on injured porcine models and rejected human donor organs – assessing their expression under ex vivo conditions, possible iatrogenic effects, and real-time functional repair over the span of 24-hours. However, re-transplantation of these NPV-EVLP reconditioned organs will be the next step, in order to demonstrate any clinical translational effects.

6.2.4.2 **Tissue Bioengineering**

In recent years, scientists from various disciplines (surgical, medical, and biomedical engineering) have collaborated to investigate an alternative solution(s) for the current shortage of donor lung grafts and the ever-increasing waitlist mortality rate; which haunts patients facing end-stage lung disease and in-need for a lung transplantation. To circumvent this barrier, the theory of ex vivo lung evaluation of "unsuitable" allograft donors – albeit recoverable – was brought to clinical reality.[153,154] In parallel, progress in the science-fiction realm of whole organ bioengineering, witnessed several milestones in our understanding in reproducible decellularization, viable recellularization, and in-vivo perfusion;[194,332] with a major milestone occurring in 2010, when two separate labs published their successful experience in generating transplantable rodent lung grafts after in-vitro bioengineering lungs in a bioreactor (**Figure 31**).[332,333]

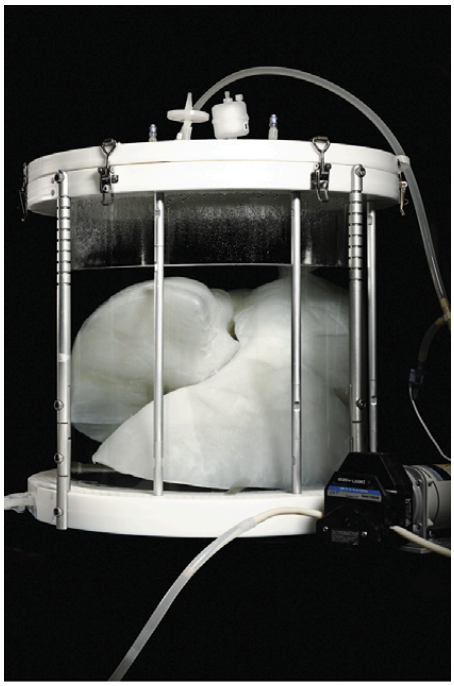

Figure 31: Human lungs undergoing decellularization in a bioreactor. Adapted from Gilpin *et al.*[334]

In brief, autologous bioengineered lungs are derived from the recipient's own cells, which would provide a viable tissue graft that is syngeneic. However, the necessary steps to create a this syngeneic tissue graft, in-vitro and in-vivo, is meticulous and has been under refinement over the recent years.[194,269,332,335] The first step in creating a whole-organ scaffold requires specific decellularization detergents, which will generate an acellular matrix scaffold that retains the hierarchical branching structures of the airway and vasculature.[193,195,332,334] This acellular scaffold provides the foundation for recellularization with selected primary animal and human cell lines.[195,332,334-336] However, to create a functioning in-vitro/ex-vivo airway and vascularized lung scaffold, time and an isolated environment is needed to mimic the biological, mechanical, and chemical environment experienced in-vivo by the organ. Hence, the refinement of bioreactors, by exploration of successful EVLP platforms, has progressed the development of bioreactors not only to serve as a means to administrate decellularization detergents; but, adequate prolonged times for

the recellularization process to come to fruitfulness under physiologic perfusion and ventilation conditions.[269,332,337]

In today's world, the dawn of 3D-bioprinting in-vitro scaffold material, has advanced the field of regenerative medicine and tissue engineering. As one can envision, the vast barriers facing current lung transplantation – donor organ shortage, ethical issues regarding which patient receives which organ first, and chronic lung allograft dysfunction – can be bypassed and deemed a "problem of the past." Until recently, the biggest limiting factor in tissue engineering over the years has been producing adequate vascularized scaffolded tissues, which demonstrated functioning in-vivo viability and without dysfunctional formation of pulmonary edema.[338] In 2017, Dorrello *et al*, successfully sought out to address the need for functional vascularized lung scaffolds, since intact vascular network is critical for maintaining the blood-gas barrier, allowing proper graft function, and supporting the regenerative cells. They developed an airway-specific approach to remove pulmonary epithelium, while demonstrating preservation and functioning vascular endothelium, extracellular matrix, other supporting cell types, and trends of improving lung compliance in an ex vivo/in-vitro rodent model. Their paper signifies a paramount milestone towards a step closer to producing fully functioning bioengineered lungs for transplantation (large animal model or humans).[335]

August 1, 2018, Nichols *et al*,[339] publishes promising results for the first whole single lung bioengineered and transplanted successfully in a survival porcine model. Five single lungs were utilized as the source of autologous cells used to bioengineer each respective donor's acellular lung scaffold. Over 30-days of bioreactor culturing, decellularization-recellularization, four successful respective syngeneic bioengineered single lungs were created and autotransplanted. Recipient survival, autograft bioengineered lung vascular and parenchymal tissue development, graft

rejection, and microbiome reestablishment were assessed in autografted animals after 10-hours, 2-weeks, 1 month, and 2-months of transplantation. Interestingly, viable vascularity was reported as early as 2-weeks, while formation of alveolar tissue was observed in all animals. There were no indications of transplant rejection; while bioengineered lungs continued to develop post-transplantation and did not require addition of exogenous growth factors to drive cell proliferation or lung and vascular tissue development, in-situ. Furthermore, the sterile bioengineered lungs demonstrated seeded and colonization by the bacterial biome of the native lung. However, the autografted lungs were not capable of respiration. Each pig continued to breathe via the native, non-bioengineered lung.[339] Nonetheless, this is a major milestone towards creating functioning artificial lungs that oxygenate in large animals, and aiding to translate this to clinical settings. Theoretically, any human donor lungs (suitable or marginal), could be utilized as scaffolds that can have the recipient's autologous cells seeded to create a healthy viable autogenic graft.[338] Eventually, instead of relying on the need for a donor graft, computer aided 3D-bioprinting of stable, extensive, pre-vascularized scaffolds will be a reality not too far in the future.[340-343]

Future approaches may involve performing these processes in parallel. Bioreactors aiding to progress regenerative medicine and tissue engineering; while NPV-EVLP is utilized as a modality to assess, evaluate, and provide further reconditioning of bioengineered lungs (over 24-hours), prior to re-transplantation in humans. Having the capability of organ-on-a-chip platforms, will make the process of bench-to-bedside more rapidly accessible, cost-effective, and facilitate in the transcending of humanity, in the field of lung transplantation.[344]

6.2.4.3 **Artificial Intelligence: The Lung Whisperer**

The coining of "artificial intelligence" (AI) was first termed by John McCarthy in 1955, defining it as "the science and engineering of making intelligent machines."[345] However, the definition of AI proposed by the online version of Merriam Webster Dictionary includes:[346]

I. A branch of computer science dealing with simulation of intelligent behavior in computers;

II. The capability of a machine to imitate intelligent human behavior.

On the other hand, the term *Medicine* is defined as "the science and art dealing with the maintenance of health and the prevention, alleviation, or cure of disease."[347] Breaking down the basics, AI can be divided into two main categories:[348]

I. Specific/narrow AI – Most commonly utilized and incorporated in autonomous vehicles, computer-aided medical diagnostics, proving mathematical theorems, playing board games (Chess or Go), search engines (Google search), online assistants (Siri and Alexa), image recognition in photographs, and spam filtering. Utilizes step-by-step teaching and directed establishment of layered neuronal networks to acquire information, recognize patterns, and perform an outcome.

II. Generalized/strong AI – AI that is capable of combining all the narrow AI skills, but learning to perform any desired output task, from autonomous reinforcement learning, without pre-programming/teaching, from raw heterogenous inputted data. Artificial general intelligence will possess true "intelligence", since one algorithm/system is adaptable to learn any raw data from any discipline. Facilitating greater efficiency, accuracy and reliability in the process of acquisition,

interpretation, and decision performance. General intelligence is among the field's long-term goals.[349]

In the early days of AI in medicine, the most challenging aspect was modeling of knowledge and of reasoning techniques for the purpose of supporting tasks as diagnosis, therapy, monitoring, and prognosis.[350,351] Despite this remaining a challenging research topic, the information explosion of the Internet, cloud computing, and big-data platforms have brought a drastic shift in focus from "knowledge-intensive" to "data-intensive" applications; and from systems that advise to systems that provide ad-hoc information during decision-based (intelligent) tasks.[348,350,352] As such, research over the years has attempted to develop algorithms/systems that help AI exploit the ever expanding heterogenous volume of data in various domains.

Big data has been reported as a primary driver towards precision medicine.[352,353] However, without having systems in-place to analyze that data, AI cannot transform this heterogenous data into clinically relevant knowledge. As such, machine learning (deep learning) has been developed and refined over the years.[345,348,351,353-357] Machine learning (ML), and its related systems, is a major branch of AI. Machine learning is the essence of machine intelligence – utilizing modern computers and mathematic algorithms to build models based on available data sets, in which the model itself can improve with experience. Machine learning can recognize complex combinations of variables, and reliably predict an outcome or exquisitely perform an action with the newly acquired knowledge.[345,348,351,353-357] Therefore, one can imagine how powerful of a tool ML can be when utilized to analyze current challenges facing lung transplantation and providing possible remedial models, with reliable scenario-based predictive outcomes.

Some notable application of AI in medicine include Watson, AI developed by IBM intended to play Jeopardy, was found to have a highly concordant (93%) treatment

recommendations for Oncology, when compared to multidisciplinary tumor board human experts.[358] Moreover, Watson was utilized in Tokyo to help doctors unravel a puzzling patient presentation, and make the diagnosis for the doctors within only 10 minutes. Watson accurately diagnosed the rare leukemia by cross-referencing and analyzing data from tens of millions of oncology papers from research institutes all over the world; while cross-referencing the patient's genetic data with its own database.[359] Other sectors that AI has demonstrated surprising outcomes is in image recognition strategies for disciplines that utilize image diagnostic tools such as ophthalmology, dermatology, pathology, and radiology. In recent studies, AI has been trained, using deep neural networks (ML), to make diagnoses on 2D images of skin cancer,[360] and diabetic retinopathy.[361] When compared with professional dermatologists and ophthalmologists, AI performed on par, and in some cases, slightly better than their human counterparts. In the realm of clinical guidelines, AI with varying ML algorithms was compared with the most widely accepted clinical guidelines for the American College of Cardiology/American Heart Association. The AI was tasked to identify people who are at risk of a cardiovascular event within 10-years; thus, would benefit from preventive treatment. All ML algorithms significantly improved accuracy of cardiovascular risk prediction compared to gold-standard current clinical guidelines. Therefore, AI can help increase the number of patients who would benefit from preventive treatment, while avoiding unnecessary treatment of others.[362] AI even demonstrated highly significant predictive accuracy for postoperative seizure-free outcomes for patient with mesial temporal lobe epilepsy undergoing epileptic surgery, compared to inferences from clinical variables.[363] Furthermore, the implementation of narrow AI has also made encouraging advances in the fields of genomics, epigenomics, proteomics, and drug therapy.[345,348,364-367]

Deep learning (ML) has transformed many important subfields of AI, one of which includes computer vision. Computer vision is particularly interesting and relevant to the incorporation of AI with our NPV-EVLP platform, since it is an interdisciplinary field that deals with how computers can be augmented to gaining high-level understanding from digital images or videos. The utilization of AI with computer vision will demonstrate tasks that include acquiring, processing, analyzing and understanding digital images to inform decisions.[348,368] The research for machine vision has been under investigation since 1993,[369] with various breakthroughs since then in computer-aided-diagnostic 3D imaging (MRI and CT) in detecting various diseases in the field of radiology and retinal diseases – in a timely and precise manner.[368-375]

As one can foresee, the integration and utility of narrow AI with NPV-EVLP will truly create a revolutionary machine/platform in the field of *Ex Vivo Lung Perfusion* – ultimately, ushering an unprecedented era for humans suffering from debilitating lung diseases, and providing them with personalized *Medicine*. As science and technology continue to progress in parallel directions, it will be feasible to aim to incorporate "*vision*" (motion-based camera and infrared), real time perfusate *monitoring/analysis* (inter/intra-circuit oximeter, capnography, electrolyte, and glucose) and *deep learning* to the current novel NPV-EVLP machine. However, with such upgrades the NPV-EVLP platform will evolve to become an *intelligent* platform – dynamically precise with its adaptive capability to maintain the ideal physiologic ex-situ reconditioning environment. Moreover, this intelligent platform will work at an efficiency and cost-effectiveness never seen before; while continuously providing the scientist/operator with enhancing suggestions that the machine or human can execute. To initiate this powerful platform, the scientist needs only to press one button – "Start Ventilation."

With over 267, 840 seconds (>740 hours) worth of functional physiologic data accumulated from the projects included in this thesis – corresponding serial evaluative measurements (arterial blood gases, perfusate molecular, and cellular analysis), tissue histopathology, and graduate students yet to come who will surely add to the NPV-EVLP dataset – one hopes to witness the evolution of NPV-EVLP from machine to the ultimate *Lung Whisperer*.

Figure 32: The *Lung Whisperer* – NPV-EVLP.

6.3| Concluding Remarks

To summarize, we have discussed the basics of anatomy and physiology, to varying degrees of detail. Explored a deeper understanding of lung mechanics, molecular/cellular physiology, and the immune response; while focusing greater attention on immunology. When one takes a moment to realize the myriad of potential foreign particles this organ encounters on a daily basis, there is no doubt that the lungs, and all its intricate cellular components, act as the body's frontline immunity. Hence, laying the foundation for cellular physiology helped elucidate the fundamental properties behind some common clinical manifestations of varying lung pathological aetiologies.

After a global review of varying domains concerning lung transplantation – history, indications, the burden, current preservation techniques, and the inception of EVLP – the stage was set to illuminate EVLP as a promising revolutionary platform in the field of lung transplantation; but more importantly, for patients and their families that endure increasing waiting lists, and the fear that their beloved might end up as a number on the dreaded mortality list.

As such, knowing that the University of Alberta Mazankowski institute carries a heavy burden and high expectations to address a geographical catchment area of more than 6 million km^2 and 7 million Canadians, of which some suffer from end-stage lung disease, the establishment of our own EVLP model was inevitable. The first project was tailored to establish a reproducible PPV-EVLP model, with our own custom-designed, portable, platform. This feat on its own brought with it quite the memorable journey – personal challenges, unsuccessful perfusions, many teaching lessons, and gradual platform iterations. However, the first time we succeeded in conducting a 12-hour perfusion, brought with it Hope. Thus, our own EVLP strategy (U of A protocol) was conceived and its refinement was established with every passing successful extended EVLP run. The more one perfused each unique lung, the clearer it became the variations expressed by the

organ when subjected to varying perfusates. Consequently, we sought out to investigate the dilemma of the *optimal perfusate*, which had the literature split for almost a decade. This dilemma was introduced when our neighbours in Toronto argued and established a reproducible acellular technique for extended PPV-EVLP, in 2008. Interestingly, with our protocol and portable PPV-EVLP platform our results demonstrated promising findings for the utility of a physiologic, cellular, perfusate – considerably less lung injury after 12-hours, represented by global lung edema and histopathology. Hence, the promising finding of the benefit in optimizing the perfusate strategy for lungs undergoing the harsh/foreign environment of PPV-EVLP, further inspired us to seek out a more physiologic ventilation modality.

Despite the literature remaining incongruent with regards to the optimal perfusate, they are in unanimity with the mode of ventilation during EVLP – the utilization of positive pressure ventilation via a standard intensive care unit ventilator. Thus, we sought out to create an extended EVLP platform that utilizes a truly physiologic *ventilation modality* – our custom-built NPV-EVLP truly is a first of its kind. Observing its potential to induce an overall noteworthy decrease in ventilator induced lung injury, with either a cellular or acellular based perfusate strategy; furthermore, a first-time reporting of a *drying effect* after injured rejected human donor lungs were subjected to 12-hours of NPV-EVLP, drew quite the international interest at the 37th ISHLT Annual Scientific Meeting. As briefly noted, preliminary human data with the utilization of NPV-EVLP, without any therapeutic additives or software enhancements, has shown promising extension for safe dynamic preservations up to 24-hours. This is significant, since this "window" between procurement and transplantation provides better opportunity for pharmacological, cellular, and genetic therapies to repair injured grafts; while providing the transplant surgeon with

reliable real-time objective functional performance and graft viability, in response to the utilized reconditioning modality.

In closing, NPV-EVLP will hopefully usher a new era to the field of *Ex Vivo Lung Perfusion*. One can truly envision the impact this machine will have on the future of lung transplantation. NPV-EVLP truly is a versatile platform which will aid in the transcending of our understanding in molecular & cellular physiology, pathophysiology, and repair mechanisms. Accordingly, as this novel platform gains greater global credibility, it surely is bound to evolve towards a more sophisticated *intelligent* platform. Consequently, future scientific theories will only be limited by the imagination of the scientist.

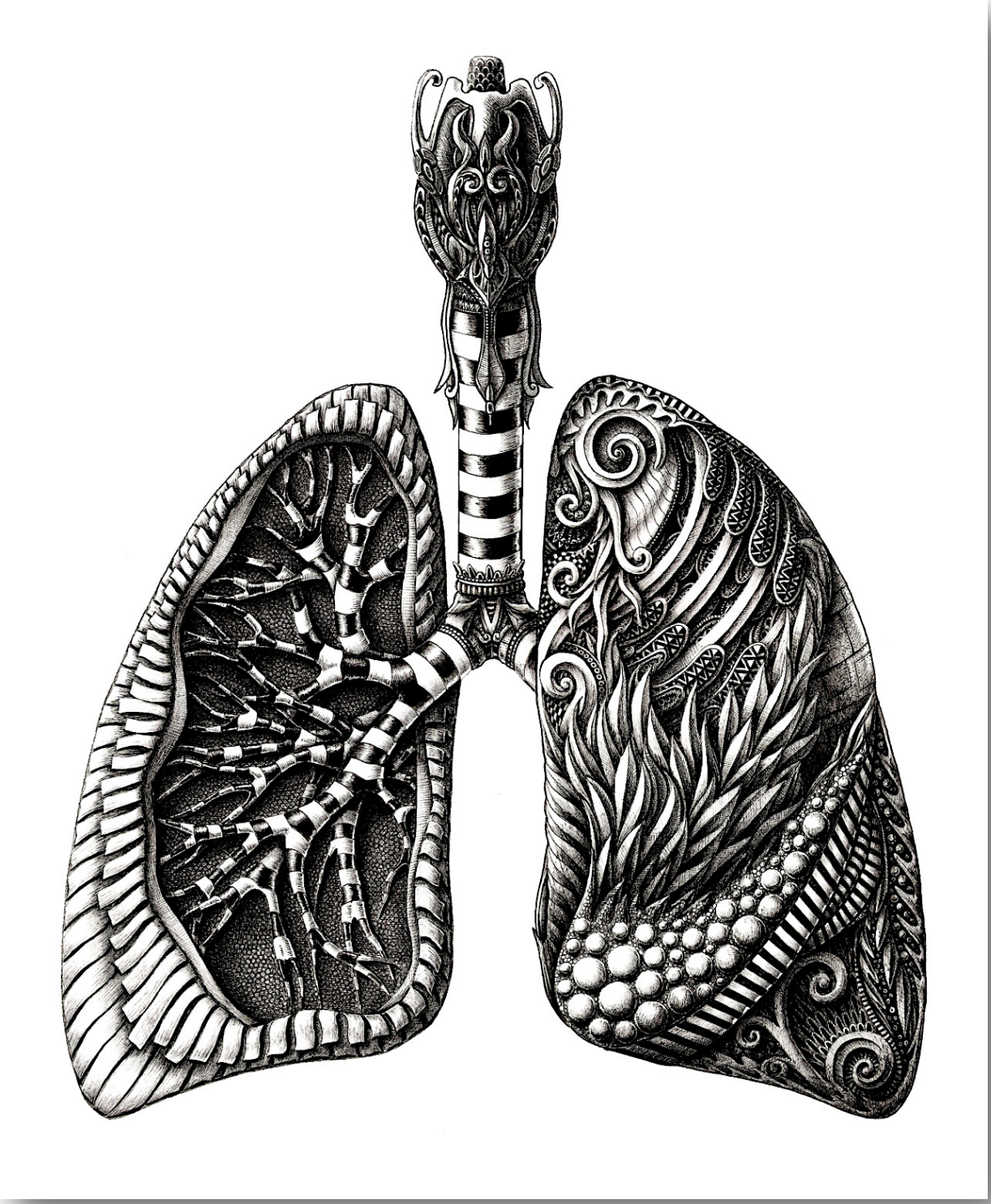

"Never doubt that a small group of thoughtful, concerned citizens, can change the world. Surely, it is the only thing that ever has." – *Margaret Mead*

Bibliography

1. Van De Graaff KM. Schaum's outline of human anatomy and physiology. In: Rhees RW, Palmer SL, eds. 4th ed. ed. New York: McGraw-Hill; 2014.
2. Widmaier EP, Raff, Hershel., Strang, Kevin T. Vander's human physiology: the mechanisms of body function. In: Fourteenth edition. ed.2014.
3. Sarafoleanu C, Mella C, Georgescu M, Perederco C. The importance of the olfactory sense in the human behavior and evolution. *Journal of Medicine and Life.* 2009;2(2):196-198.
4. Ignatavicius DD, Workman ML, Blair M, Rebar CR, Winkelman C. *Medical-surgical nursing: patient-centered collaborative care.* 2016.
5. Wikipedia. Respiratory System. 2017; https://en.wikipedia.org/wiki/Respiratory_system. Accessed June 10, 2017.
6. Netter FH. Atlas of Human Anatomy. In: 6th ed. Philadelphia, PA: Saunders/Elsevier; 2014.
7. Hall JE, Guyton, Arthur C. Guyton and Hall textbook of medical physiology. In. 12th ed. Philadelphia, PA: Saunders/Elsevier; 2011.
8. Stacy KM. Pulmonary Anatomy and Physiology. 2015; https://clinicalgate.com/pulmonary-anatomy-and-physiology/. Accessed June 20, 2017.
9. Celis EA. Lung Anatomy. 1994-2017; http://emedicine.medscape.com/article/1884995-overview#a2. Accessed June 15, 2017.
10. Armstrong JD, Gluck EH, Crapo RO, Jones HA, Hughes JM. Lung tissue volume estimated by simultaneous radiographic and helium dilution methods. *Thorax.* 1982;37(9):676-679.
11. Staub NC. Pulmonary edema. *Physiological Reviews.* 1974;54:678-811.
12. Krishnan S. Respiratory System. 2017; https://www.studyblue.com/#flashcard/view/13120379. Accessed June 15, 2017.
13. West JB. Respiratory physiology: the essentials. In: 9th ed. ed. Philadelphia: Wolters Kluwer Health/Lippincott Williams & Wilkins; 2012.
14. Culbertson WR, Tanner DC, Christensen SC. *Anatomy and Physiology Study Guide for Speech and Hearing.* Vol Second edition. San Diego: Plural Publishing, Inc; 2013.
15. Thompson JM, Gertrude K. McFarland, Jane E. Hirsch, and Susan Martin Tucker. Mosbys clinical nursing. In: 5th ed. St. Louis: MO: Mosby; 2002: https://nursekey.com/pulmonary-anatomy-and-physiology/. Accessed June 20, 2017.
16. Des Jardins TR. Cardiopulmonary anatomy & physiology: essentials of respiratory care. In. 6th ed. ed. Clifton Park, NY :: Delmar Cengage Learning; 2013.
17. Rees HC. Assessment of the Respiratory System. 2016; https://nursekey.com/assessment-of-the-respiratory-system-3/. Accessed June 20, 2017.
18. Atkinson JJ, Adair-Kirk TL, Kelley DG, deMello D, Senior RM. Clara cell adhesion and migration to extracellular matrix. *Respiratory Research.* 2008;9(1):1.
19. Crapo JD, Barry BE, Gehr P, Bachofen M, Weibel ER. Cell Number and Cell Characteristics of the Normal Human Lung. *American Review of Respiratory Disease.* 1982;126(2):332-337.
20. Hans-Ulrich Kauczor HCS, Eckhard Mayer, Franz Schweden, Hans H. Schild, and Manfred Thelen. Spiral CT of Bronchial Arteries in Chronic Thromboembolism. *Computer Assisted Tomography.* 1994;18(6):855-861.

21. Nowak K, Kamler M, Bock M, et al. Bronchial Artery Revascularization Affects Graft Recovery after Lung Transplantation. *American Journal of Respiratory and Critical Care Medicine.* 2002;165(2):216-220.
22. Parker JC, Cave CB, Ardell JL, Hamm CR, Williams SG. Vascular tree structure affects lung blood flow heterogeneity simulated in three dimensions. *Journal of Applied Physiology.* 1997;83(4):1370-1382.
23. Qureshi MU, Vaughan GDA, Sainsbury C, et al. Numerical simulation of blood flow and pressure drop in the pulmonary arterial and venous circulation. *Biomechanics and modeling in mechanobiology.* 2014;13(5):1137-1154.
24. Huang W, Yen RT, McLaurine M, Bledsoe G. Morphometry of the human pulmonary vasculature. *Journal of Applied Physiology.* 1996;81(5):2123-2133.
25. Dawson CA. Role of pulmonary vasomotion in physiology of the lung. *Physiological Reviews.* 1984;64(2):544-616.
26. Rhodin JAG. Microscopic anatomy of the pulmonary vascular bed in the cat lung. *Microvascular Research.* 1978;15(2):169-193.
27. Rippe B, Parker JC, Townsley MI, Mortillaro NA, Taylor AE. Segmental vascular resistances and compliances in dog lung. *Journal of Applied Physiology.* 1987;62(3):1206-1215.
28. Abman SH, Chatfield BA, Hall SL, McMurtry IF. Role of endothelium-derived relaxing factor during transition of pulmonary circulation at birth. *American Journal of Physiology - Heart and Circulatory Physiology.* 1990;259(6):H1921-H1927.
29. Ganong WF. Review of medical physiology. In: Barman SM, Barrett KE, Boitano S, Brooks HL, Ganong WF, eds. 24th ed. New York, N.Y.: McGraw-Hill Education LLC.; 2012.
30. Razani B. Pulmonary Blood Flow Distribution. 2010-2015; http://www.pathwaymedicine.org/pulmonary-blood-flow-distribution. Accessed Sept 9, 2017.
31. Wikipedia. Innate Immune System. 2017; https://en.wikipedia.org/wiki/Innate_immune_system. Accessed September 10, 2017.
32. Schmidt EP, Lee WL, Zemans RL, Yamashita C, Downey GP. On, Around, and Through: Neutrophil-Endothelial Interactions in Innate Immunity. *Physiology.* 2011;26(5):334-347.
33. Tolle LB, Standiford TJ. Danger-associated molecular patterns (DAMPs) in acute lung injury. *J Pathol.* 2013;229(2):145-156.
34. Bianchi ME. DAMPs, PAMPs and alarmins: all we need to know about danger. *J Leukoc Biol.* 2007;81(1):1-5.
35. Kumar H, Kawai T, Akira S. Pathogen recognition by the innate immune system. *Int Rev Immunol.* 2011;30(1):16-34.
36. Takeda K, Akira S. Toll-like receptors in innate immunity. *Int Immunol.* 2005;17(1):1-14.
37. Takeda K, Akira S. Toll-like receptors. *Curr Protoc Immunol.* 2015;109:14 12 11-10.
38. Kreisel D, Goldstein DR. Innate immunity and organ transplantation: focus on lung transplantation. *Transpl Int.* 2013;26(1):2-10.
39. Hardison SE, Brown GD. C-type lectin receptors orchestrate antifungal immunity. *Nat Immunol.* 2012;13(9):817-822.
40. Inohara, Chamaillard, McDonald C, Nunez G. NOD-LRR proteins: role in host-microbial interactions and inflammatory disease. *Annu Rev Biochem.* 2005;74:355-383.

41. Burberry A, Zeng MY, Ding L, et al. Infection mobilizes hematopoietic stem cells through cooperative NOD-like receptor and Toll-like receptor signaling. *Cell Host Microbe.* 2014;15(6):779-791.
42. Guo H, Callaway JB, Ting JP. Inflammasomes: mechanism of action, role in disease, and therapeutics. *Nat Med.* 2015;21(7):677-687.
43. Eisenacher K, Krug A. Regulation of RLR-mediated innate immune signaling--it is all about keeping the balance. *Eur J Cell Biol.* 2012;91(1):36-47.
44. Loo YM, Gale M, Jr. Immune signaling by RIG-I-like receptors. *Immunity.* 2011;34(5):680-692.
45. Pattabhi S, Wilkins CR, Dong R, et al. Targeting Innate Immunity for Antiviral Therapy through Small Molecule Agonists of the RLR Pathway. *J Virol.* 2015;90(5):2372-2387.
46. Li L, Li Y, Ijaz M, Shahbaz M, Lian Q, Wang F. Review on complement analysis method and the roles of glycosaminoglycans in the complement system. *Carbohydr Polym.* 2015;134:590-597.
47. Reddy YN, Siedlecki AM, Francis JM. Breaking down the complement system: a review and update on novel therapies. *Curr Opin Nephrol Hypertens.* 2017;26(2):123-128.
48. Hoornaert CJ, Le Blon D, Quarta A, et al. Concise Review: Innate and Adaptive Immune Recognition of Allogeneic and Xenogeneic Cell Transplants in the Central Nervous System. *Stem Cells Transl Med.* 2017;6(5):1434-1441.
49. Chambers DC, Yusen RD, Cherikh WS, et al. The Registry of the International Society for Heart and Lung Transplantation: Thirty-fourth Adult Lung And Heart-Lung Transplantation Report-2017; Focus Theme: Allograft ischemic time. *J Heart Lung Transplant.* 2017;36(10):1047-1059.
50. Caronia JR. Restrictive Lung Disease. 2017; https://emedicine.medscape.com/article/301760-overview. Accessed September 13, 2017.
51. Johnson ER, Matthay MA. Acute Lung Injury: Epidemiology, Pathogenesis, and Treatment. *Aerosol Medicine and Pulmonary Drug Delivery.* 2010;23(4):243-252.
52. Ashbaugh DG, Bigelow DB, Petty TL, BE L. Acute respiratory distress in adults. *Lancet (London, England).* 1967;2:319-323.
53. Bernard GR, Artigas A, Brigham KL, et al. Report of the American-European Consensus conference on acute respiratory distress syndrome: definitions, mechanisms, relevant outcomes, and clinical trial coordination. Consensus Committee. *J Crit Care.* 1994;9:72-81.
54. Thompson BT, Chambers RC, Liu KD. Acute Respiratory Distress Syndrome. *N Engl J Med.* 2017;377(6):562-572.
55. Ferguson ND, Fan E, Camporota L, et al. The Berlin definition of ARDS: an expanded rationale, justification, and supplementary material. . *Intensive Care Medicine.* 2012;38:1573-1582.
56. Katzenstein AL, Bloor CM, AA L. Diffuse alveolar damage — the role of oxygen, shock, and related factors: a review. *Am J Pathol.* 1976;85:209-228.
57. Aggarwal NR, King LS, D'Alessio F. Diverse macrophage populations mediate acute lung inflammation and resolution. *Am J Physiol Lung Cell Mol Physiol.* 2014;306:L709-L725.
58. Matthay M, Zimmerman G. Acute lung injury and the acute respiratory distress syndrome: four decades of inquiry into pathogenesis and rational management. *Am J Respir Cell Mol Biol.* 2005;33:319-327.

59. Dos Santos C, Okutani D, Hu, P. Differential gene profiling in acute lung injury identifies injury-specific gene expression *Critical Care Medicine.* 2009;36(3):855-865.
60. Grigoryev D, Cheranova D, Chaudhary S, Heruth D, Zhang, LQ, , Ye S. Identification of new biomarkers for Acute Respiratory Distress Syndrome by expression-based genome-wide association study. *BMC Pulmonary Medicine.* 2015;15:95.
61. Jeyaseelan S, Chu H, Young S, Worthen G. Transcriptional profiling of lipopolysaccharide-induced acute lung injury. *Infection and Immunity.* 2004;72(12):7247-7256.
62. Yamane M, Liu M, Kaneda H, Uhlig S, Waddell T, Keshavjee S. Reperfusion-induced gene expression profiles in rat lung transplantation. *American Journal of Transplantation.* 2005;5(9):2160-2169.
63. Cooper J, Pearson F, Patterson G, et al. Technique of successful lung transplantation in humans. *J Thorac Cardiovasc Surg.* 1987;93(2):173-181.
64. Konstantinov I. A mystery of Vladimir P. Demikhov: the 50th anniversary of the first intrathoracic transplantation. *Ann Thorac Surg.* 1998;65(4):1171-1177.
65. H M. Note preliminarie sur la greffe total du poumon chez le chien. *C R Acad Sci III.* 1950;231(1176-7).
66. Hardy JD, Webb WR, Dalton ML J, Walker GR J. Lung Homotransplantation in Man. *JAMA* 1963;186:1065-1074.
67. Derom F, Barbier F, Ringoir S, et al. Ten-month survival after lung homotransplantation in man. *J Thorac Cardiovasc Surg.* 1971;61(6):835-846.
68. Calne RY, White DJ, Thiru S, et al. Cyclosporin A in patients receiving renal allografts from cadaver donors. *Lancet (London, England).* 1978;2(8104-5):1323-1327.
69. Goldberg M, Lima O, Morgan E, et al. A comparison between cyclosporin A and methylprednisolone plus azathioprine on bronchial healing following canine lung autotransplantation. *J Thorac Cardiovasc Surg.* 1983;85(6):821-826.
70. Patterson GA, Cooper JD, Goldman B, et al. Technique of successful clinical double-lung transplantation. *Ann Thorac Surg.* 1988;45(6):626-633.
71. Gross CR, Savik K, Bolman RM r, MI H. Long-term health status and quality of life outcomes of lung transplant recipients. *Chest.* 1995;108(6):1587-1593.
72. Lanuza DM, Lefaiver C, Mc Cabe M, Farcas G, Garrity E, Jr. Prospective study of functional status and quality of life before and after lung transplantation. *Chest.* 2000;118(1):115-122.
73. Israni A. K., Zaun D., Bolch C., et al. OPTN/SRTR 2015 Annual Data Report: Deceased Organ Donation. *American Journal of Transplantation.* 2017;17(S1):503-542.
74. Munshi L, Keshavjee S, Cypel M. Donor management and lung preservation for lung transplantation. *The Lancet Respiratory Medicine.* 2013;1(4):318-328.
75. Andreasson AS, Dark JH, Fisher AJ. Ex vivo lung perfusion in clinical lung transplantation--state of the art. *Eur J Cardiothorac Surg.* 2014;46(5):779-788.
76. Jeremie R, Marcelo C. Ex vivo lung perfusion. *Clinical Transplantation.* 2016;30(3):183-194.
77. Thabut G, Mal H, Cerrina J, et al. Graft Ischemic Time and Outcome of Lung Transplantation. *American Journal of Respiratory and Critical Care Medicine.* 2005;171(7):786-791.
78. Orens JB, Boehler A, Perrot Md, et al. A review of lung transplant donor acceptability criteria. *The Journal of Heart and Lung Transplantation.* 2003;22(11):1183-1200.

79. Snell GI, Paraskeva M Fau - Westall GP, Westall GP. Donor selection and management. *Semin Respir Crit Care Med.* 2013;34(03):361-370.
80. Yeung JC, Keshavjee S. Overview of clinical lung transplantation. *Cold Spring Harb Perspect Med.* 2014;4(1):a015628.
81. Wijdicks EF, Varelas PN, Gronseth GS, Greer DM, American Academy of N. Evidence-based guideline update: determining brain death in adults: report of the Quality Standards Subcommittee of the American Academy of Neurology. *Neurology.* 2010;74(23):1911-1918.
82. Takada M, Nadeau KC, Hancock WW, et al. Effects of explosive brain death on cytokine activation of peripheral organs in the rat. *Transplantation.* 1998;65(12):1533-1542.
83. Lopau K, Mark J, Schramm L, Heidbreder E, Wanner C. Hormonal changes in brain death and immune activation in the donor. *Transpl Int.* 2000;13 Suppl 1:S282-285.
84. Avlonitis VS, Fisher AJ, Kirby JA, Dark JH. Pulmonary transplantation: the role of brain death in donor lung injury. *Transplantation.* 2003;75(12):1928-1933.
85. De Perrot M, Sekine Y, Fischer S, et al. Interleukin-8 release during ischemia-reperfusion correlates with early graft function in human lung transplantation. *J Heart Lung Transplant.* 2001;20(2):175-176.
86. De Perrot M, Sekine Y, Fischer S, et al. Interleukin-8 release during early reperfusion predicts graft function in human lung transplantation. *Am J Respir Crit Care Med.* 2002;165(2):211-215.
87. Fisher AJ, Donnelly SC, Hirani N, et al. Elevated levels of interleukin-8 in donor lungs is associated with early graft failure after lung transplantation. *Am J Respir Crit Care Med.* 2001;163(1):259-265.
88. Kaneda H, Waddell TK, de Perrot M, et al. Pre-implantation multiple cytokine mRNA expression analysis of donor lung grafts predicts survival after lung transplantation in humans. *Am J Transplant.* 2006;6(3):544-551.
89. Smith M. Physiologic changes during brain stem death--lessons for management of the organ donor. *J Heart Lung Transplant.* 2004;23(9 Suppl):S217-222.
90. Marshall VC. Pathophysiology of brain death: effects on allograft function. *Transplant Proc.* 2001;33(1-2):845-846.
91. Pratschke J, Wilhelm MJ, Kusaka M, et al. Brain death and its influence on donor organ quality and outcome after transplantation. *Transplantation.* 1999;67(3):343-348.
92. Novitzky D, Wicomb WN, Rose AG, Cooper DK, Reichart B. Pathophysiology of pulmonary edema following experimental brain death in the chacma baboon. *Ann Thorac Surg.* 1987;43(3):288-294.
93. Barklin A. Systemic inflammation in the brain-dead organ donor. *Acta Anaesthesiol Scand.* 2009;53(4):425-435.
94. Tracey KJ. Physiology and immunology of the cholinergic antiinflammatory pathway. *J Clin Invest.* 2007;117(2):289-296.
95. Hoeger S, Bergstraesser C, Selhorst J, et al. Modulation of brain dead induced inflammation by vagus nerve stimulation. *Am J Transplant.* 2010;10(3):477-489.
96. Scaffidi P, Misteli T, Bianchi ME. Release of chromatin protein HMGB1 by necrotic cells triggers inflammation. *Nature.* 2002;418(6894):191-195.
97. Akira S. Mammalian Toll-like receptors. *Curr Opin Immunol.* 2003;15(1):5-11.

98. Rostron AJ, Cork DM, Avlonitis VS, Fisher AJ, Dark JH, Kirby JA. Contribution of Toll-like receptor activation to lung damage after donor brain death. *Transplantation.* 2010;90(7):732-739.
99. Ingemansson R, Eyjolfsson A, Mared L, et al. Clinical transplantation of initially rejected donor lungs after reconditioning ex vivo. *Ann Thorac Surg.* 2009;87(1):255-260.
100. Norris S. Organ Donation and Transplantation in Canada. *Ottawa: Library of Parliament.* 2018:1-23.
101. Canadian Organ Replacement Register [CORR], CIHI. Annual Statistics on Organ Replacement in Canada: Dialysis, Transplantation and Donation, 2007 to 2016. In: CIHI Snapshot; 2017:1-9.
102. Ipsos-Reid. Views Toward Organ and Tissue Donation and Transplantation. 2010; https://www.ipsos.com/en-ca/majority-51-canadians-have-decided-donate-organs-after-death-just-27-those-who-wish-donate-have. Accessed November 16, 2017.
103. Cision. Organ donation and transplantation streamlined in new national system - Canadian Blood Services Patient/donor registries and $35 million in new funding will save lives. 2007; https://www.newswire.ca/news-releases/organ-donation-and-transplantation-streamlined-in-new-national-system---patientdonor-registries-and-35-million-in-new-funding-will-save-lives-536520231.html. Accessed November 16, 2017.
104. CIHI. 2012 E-Statistics Report On Transplants, Waiting Lists And Donors Type. 2016; https://www.cihi.ca/en/2012-e-statistics-report-on-transplants-waiting-lists-and-donors. Accessed November 14, 2017.
105. Kootstra G, Kievit J, Nederstigt A. Organ donors: heartbeating and non-heartbeating. *World J Surg.* 2002;26(2):181-184.
106. Steinbrook R. Organ donation after cardiac death. *N Engl J Med.* 2007;357(3):209-213.
107. A definition of irreversible coma. Report of the Ad Hoc Committee of the Harvard Medical School to Examine the Definition of Brain Death. *JAMA.* 1968;205(6):337-340.
108. Beecher HK. A definition of irreversible coma. 1968. *Int Anesthesiol Clin.* 2007;45(4):113-119.
109. Egan TM, Lambert CJ, Jr., Reddick R, Ulicny KS, Jr., Keagy BA, Wilcox BR. A strategy to increase the donor pool: use of cadaver lungs for transplantation. *Ann Thorac Surg.* 1991;52(5):1113-1120; discussion 1120-1111.
110. Ulicny KS, Jr., Egan TM, Lambert CJ, Jr., Reddick RL, Wilcox BR. Cadaver lung donors: effect of preharvest ventilation on graft function. *Ann Thorac Surg.* 1993;55(5):1185-1191.
111. Alessandrini F. Experimental researches on heart and lung preservation. *Acta Biomed Ateneo Parmense.* 1994;65(3-4):59-73.
112. Alessandrini F, D'Armini AM, Roberts CS, Reddick RL, Egan TM. When does the lung die? II. Ultrastructural evidence of pulmonary viability after "death". *J Heart Lung Transplant.* 1994;13(5):748-757.
113. Date H, Matsumura A, Manchester JK, Cooper JM, Lowry OH, Cooper JD. Changes in alveolar oxygen and carbon dioxide concentration and oxygen consumption during lung preservation. The maintenance of aerobic metabolism during lung preservation. *J Thorac Cardiovasc Surg.* 1993;105(3):492-501.
114. Egan TM. Non-heart-beating donors in thoracic transplantation. *J Heart Lung Transplant.* 2004;23(1):3-10.

115. Keshavjee SH, Yamazaki F, Yokomise H, et al. The role of dextran 40 and potassium in extended hypothermic lung preservation for transplantation. *J Thorac Cardiovasc Surg.* 1992;103(2):314-325.
116. Van Raemdonck DE, Rega FR, Neyrinck AP, Jannis N, Verleden GM, Lerut TE. Non-heart-beating donors. *Semin Thorac Cardiovasc Surg.* 2004;16(4):309-321.
117. Kootstra G, Daemen JH, Oomen AP. Categories of non-heart-beating donors. *Transplant Proc.* 1995;27(5):2893-2894.
118. Sanchez-Fructuoso AI, Prats D, Torrente J, et al. Renal transplantation from non-heart beating donors: a promising alternative to enlarge the donor pool. *J Am Soc Nephrol.* 2000;11(2):350-358.
119. Dark JH. Lung transplantation from the non-heart beating donor. *Transplantation.* 2008;86(2):200-201.
120. Dark JH. Lung transplantation from donation after cardiocirculatory death: the end of the golden era? *Eur J Cardiothorac Surg.* 2016;49(1):53-54.
121. Mason DP, Murthy SC, Gonzalez-Stawinski GV, et al. Early experience with lung transplantation using donors after cardiac death. *J Heart Lung Transplant.* 2008;27(5):561-563.
122. Kang CH, Anraku M, Cypel M, et al. Transcriptional signatures in donor lungs from donation after cardiac death vs after brain death: a functional pathway analysis. *J Heart Lung Transplant.* 2011;30(3):289-298.
123. de Perrot M, Weder W, Patterson GA, Keshavjee S. Strategies to increase limited donor resources. *Eur Respir J.* 2004;23(3):477-482.
124. Snell GI, Griffiths A, Levvey BJ, Oto T. Availability of lungs for transplantation: exploring the real potential of the donor pool. *J Heart Lung Transplant.* 2008;27(6):662-667.
125. Ware LB, Wang Y, Fang X, et al. Assessment of lungs rejected for transplantation and implications for donor selection. *Lancet.* 2002;360(9333):619-620.
126. Bhorade SM, Vigneswaran W, McCabe MA, Garrity ER. Liberalization of donor criteria may expand the donor pool without adverse consequence in lung transplantation. *J Heart Lung Transplant.* 2000;19(12):1199-1204.
127. Botha P, Trivedi D, Weir CJ, et al. Extended donor criteria in lung transplantation: impact on organ allocation. *J Thorac Cardiovasc Surg.* 2006;131(5):1154-1160.
128. Kron IL, Tribble CG, Kern JA, et al. Successful transplantation of marginally acceptable thoracic organs. *Ann Surg.* 1993;217(5):518-522; discussion 522-514.
129. Lardinois D, Banysch M, Korom S, et al. Extended donor lungs: eleven years experience in a consecutive series. *Eur J Cardiothorac Surg.* 2005;27(5):762-767.
130. Pierre AF, Sekine Y, Hutcheon MA, Waddell TK, Keshavjee SH. Marginal donor lungs: a reassessment. *J Thorac Cardiovasc Surg.* 2002;123(3):421-427; discussion, 427-428.
131. Sundaresan S, Semenkovich J, Ochoa L, et al. Successful outcome of lung transplantation is not compromised by the use of marginal donor lungs. *J Thorac Cardiovasc Surg.* 1995;109(6):1075-1079; discussion 1079-1080.
132. Gabbay E, Williams TJ, Griffiths AP, et al. Maximizing the utilization of donor organs offered for lung transplantation. *Am J Respir Crit Care Med.* 1999;160(1):265-271.
133. Christie JD, Sager JS, Kimmel SE, et al. Impact of primary graft failure on outcomes following lung transplantation. *Chest.* 2005;127(1):161-165.

134. Snell GI, Yusen RD, Weill D, et al. Report of the ISHLT Working Group on Primary Lung Graft Dysfunction, part I: Definition and grading-A 2016 Consensus Group statement of the International Society for Heart and Lung Transplantation. *J Heart Lung Transplant.* 2017;36(10):1097-1103.
135. Daud SA, Yusen RD, Meyers BF, et al. Impact of immediate primary lung allograft dysfunction on bronchiolitis obliterans syndrome. *Am J Respir Crit Care Med.* 2007;175(5):507-513.
136. de Perrot M, Liu M, Waddell TK, Keshavjee S. Ischemia-reperfusion-induced lung injury. *Am J Respir Crit Care Med.* 2003;167(4):490-511.
137. Suzuki Y, Cantu E, Christie JD. Primary graft dysfunction. *Semin Respir Crit Care Med.* 2013;34(3):305-319.
138. Zhao M, Fernandez LG, Doctor A, et al. Alveolar macrophage activation is a key initiation signal for acute lung ischemia-reperfusion injury. *Am J Physiol Lung Cell Mol Physiol.* 2006;291(5):L1018-1026.
139. de Perrot M, Young K, Imai Y, et al. Recipient T cells mediate reperfusion injury after lung transplantation in the rat. *J Immunol.* 2003;171(10):4995-5002.
140. Fiser SM, Tribble CG, Long SM, et al. Lung transplant reperfusion injury involves pulmonary macrophages and circulating leukocytes in a biphasic response. *J Thorac Cardiovasc Surg.* 2001;121(6):1069-1075.
141. de Perrot M, Bonser RS, Dark J, et al. Report of the ISHLT Working Group on Primary Lung Graft Dysfunction part III: donor-related risk factors and markers. *J Heart Lung Transplant.* 2005;24(10):1460-1467.
142. Van Raemdonck D, Hartwig MG, Hertz MI, et al. Report of the ISHLT Working Group on primary lung graft dysfunction Part IV: Prevention and treatment: A 2016 Consensus Group statement of the International Society for Heart and Lung Transplantation. *J Heart Lung Transplant.* 2017;36(10):1121-1136.
143. Boasquevisque CH, Yildirim E, Waddel TK, Keshavjee S. Surgical techniques: lung transplant and lung volume reduction. *Proc Am Thorac Soc.* 2009;6(1):66-78.
144. de Perrot M, Fischer S, Liu M, et al. Prostaglandin E1 protects lung transplants from ischemia-reperfusion injury: a shift from pro- to anti-inflammatory cytokines. *Transplantation.* 2001;72(9):1505-1512.
145. Keshavjee SH, Yamazaki F, Cardoso PF, McRitchie DI, Patterson GA, Cooper JD. A method for safe twelve-hour pulmonary preservation. *J Thorac Cardiovasc Surg.* 1989;98(4):529-534.
146. Oto T, Griffiths AP, Rosenfeldt F, Levvey BJ, Williams TJ, Snell GI. Early outcomes comparing Perfadex, Euro-Collins, and Papworth solutions in lung transplantation. *Ann Thorac Surg.* 2006;82(5):1842-1848.
147. Gohrbandt B, Simon AR, Warnecke G, et al. Lung Preservation With Perfadex or Celsior in Clinical Transplantation: A Retrospective Single-Center Analysis of Outcomes. *Transplantation.* 2015;99(9):1933-1939.
148. Van Raemdonck DE, Jannis NC, Rega FR, De Leyn PR, Flameng WJ, Lerut TE. Extended preservation of ischemic pulmonary graft by postmortem alveolar expansion. *Ann Thorac Surg.* 1997;64(3):801-808.
149. Kayano K, Toda K, Naka Y, Pinsky DJ. Identification of optimal conditions for lung graft storage with Euro-Collins solution by use of a rat orthotopic lung transplant model. *Circulation.* 1999;100(19 Suppl):II257-261.

150. Lee JC, Christie JD. Primary graft dysfunction. *Proc Am Thorac Soc.* 2009;6(1):39-46.
151. Carrel A, Lindbergh CA. The Culture of Whole Organs. *Science.* 1935;81(2112):621-623.
152. Jirsch DW, Fisk RL, Couves CM. Ex vivo evaluation of stored lungs. *Ann Thorac Surg.* 1970;10(2):163-168.
153. Steen S, Sjoberg T, Pierre L, Liao Q, Eriksson L, Algotsson L. Transplantation of lungs from a non-heart-beating donor. *Lancet.* 2001;357(9259):825-829.
154. Steen S, Liao Q, Wierup PN, Bolys R, Pierre L, Sjoberg T. Transplantation of lungs from non-heart-beating donors after functional assessment ex vivo. *Ann Thorac Surg.* 2003;76(1):244-252.
155. Cypel M, Yeung JC, Hirayama S, et al. Technique for prolonged normothermic ex vivo lung perfusion. *The Journal of heart and lung transplantation : the official publication of the International Society for Heart Transplantation.* 2008;27(12):1319-1325.
156. Yeung JC, Cypel M, Machuca TN, et al. Physiologic assessment of the ex vivo donor lung for transplantation. *The Journal of heart and lung transplantation : the official publication of the International Society for Heart Transplantation.* 2012;31(10):1120-1126.
157. Cypel M, Keshavjee S. The clinical potential of ex vivo lung perfusion. *Expert review of respiratory medicine.* 2012;6(1):27-35.
158. Cypel M, Yeung JC, Liu M, et al. Normothermic ex vivo lung perfusion in clinical lung transplantation. *The New England journal of medicine.* 2011;364(15):1431-1440.
159. Steen S, Ingemansson R, Eriksson L, et al. First human transplantation of a nonacceptable donor lung after reconditioning ex vivo. *Ann Thorac Surg.* 2007;83(6):2191-2194.
160. Mulloy DP, Stone ML, Crosby IK, et al. Ex vivo rehabilitation of non-heart-beating donor lungs in preclinical porcine model: delayed perfusion results in superior lung function. *J Thorac Cardiovasc Surg.* 2012;144(5):1208-1215.
161. Van Raemdonck D, Neyrinck A, Cypel M, Keshavjee S. Ex-vivo lung perfusion. *Transpl Int.* 2014;28(6):643-656.
162. Steen S, Liao Q, Wierup PN, Bolys R, Pierre L, Sjöberg T. Transplantation of lungs from non–heart-beating donors after functional assessment ex vivo. *The Annals of Thoracic Surgery.* 2003;76(1):244-252.
163. Machuca TN, Cypel M, Keshavjee S. Advances in lung preservation. *Surg Clin North Am.* 2013;93(6):1373-1394.
164. Sanchez PG, D'Ovidio F. Ex-vivo lung perfusion. *Curr Opin Organ Transplant.* 2012;17(5):490-495.
165. Warnecke G, Moradiellos J, Tudorache I, et al. Normothermic perfusion of donor lungs for preservation and assessment with the Organ Care System Lung before bilateral transplantation: a pilot study of 12 patients. *The Lancet.* 2012;380(9856):1851-1858.
166. Cypel M, Yeung JC, Machuca T, et al. Experience with the first 50 ex vivo lung perfusions in clinical transplantation. *J Thorac Cardiovasc Surg.* 2012;144(5):1200-1206.
167. Sanchez PG, Davis RD, D'Ovidio F, et al. The NOVEL Lung Trial One-Year Outcomes. *The Journal of Heart and Lung Transplantation.* 2014;33(4):S71-S72.
168. Sanchez PG, Bittle GJ, Burdorf L, Pierson RN, 3rd, Griffith BP. State of art: clinical ex vivo lung perfusion: rationale, current status, and future directions. *J Heart Lung Transplant.* 2012;31(4):339-348.

169. Lowe K, Alvarez DF, King JA, Stevens T. Perivascular fluid cuffs decrease lung compliance by increasing tissue resistance. *Crit Care Med.* 2010;38(6):1458-1466.
170. Becker S, Steinmeyer J, Avsar M, et al. Evaluating acellular versus cellular perfusate composition during prolonged ex vivo lung perfusion after initial cold ischaemia for 24 hours. *Transpl Int.* 2015;29(1):88-97.
171. Roman M, Gjorgjimajkoska O, Neil D, et al. Comparison between cellular and acellular perfusates for ex vivo lung perfusion in a porcine model. *J Heart Lung Transplant.* 2015;34(7):978-987.
172. Stone JP, Sevenoaks H, Sjoberg T, Steen S, Yonan N, Fildes JE. Mechanical removal of dendritic cell-generating non-classical monocytes via ex vivo lung perfusion. *J Heart Lung Transplant.* 2014;33(8):864-869.
173. Wallinder A, Ricksten SE, Hansson C, et al. Transplantation of initially rejected donor lungs after ex vivo lung perfusion. *J Thorac Cardiovasc Surg.* 2012;144(5):1222-1228.
174. Slutsky AS, Ranieri VM. Ventilator-Induced Lung Injury. *New England Journal of Medicine.* 2013;369(22):2126-2136.
175. Bellani G, Guerra L, Musch G, et al. Lung regional metabolic activity and gas volume changes induced by tidal ventilation in patients with acute lung injury. *Am J Respir Crit Care Med.* 2011;183(9):1193-1199.
176. Terragni PP, Filippini C, Slutsky AS, et al. Accuracy of plateau pressure and stress index to identify injurious ventilation in patients with acute respiratory distress syndrome. *Anesthesiology.* 2013;119(4):880-889.
177. Terragni PP, Rosboch G, Tealdi A, et al. Tidal hyperinflation during low tidal volume ventilation in acute respiratory distress syndrome. *Am J Respir Crit Care Med.* 2007;175(2):160-166.
178. Fisher A, Andreasson A, Chrysos A, et al. An observational study of Donor Ex Vivo Lung Perfusion in UK lung transplantation: DEVELOP-UK. *Health Technology Assessment (Winchester, England).* 2016;20(85):1-276.
179. Andreasson AS, Karamanou DM, Gillespie CS, et al. Profiling inflammation and tissue injury markers in perfusate and bronchoalveolar lavage fluid during human ex vivo lung perfusion. *European journal of cardio-thoracic surgery : official journal of the European Association for Cardio-thoracic Surgery.* 2017;51(3):577-586.
180. Sadaria MR, Smith PD, Fullerton DA, et al. Cytokine expression profile in human lungs undergoing normothermic ex-vivo lung perfusion. *The Annals of Thoracic Surgery.* 2011;92(2):478-484.
181. Kuipers MT, van der Poll T, Schultz MJ, Wieland CW. Bench-to-bedside review: Damage-associated molecular patterns in the onset of ventilator-induced lung injury. *Critical Care.* 2011;15(6):235-235.
182. Plataki M, Hubmayr RD. The physical basis of ventilator-induced lung injury. *Expert review of respiratory medicine.* 2010;4(3):373-385.
183. Ricard JD, Dreyfuss D, Saumon G. Ventilator-induced lung injury. *The European Respiratory Journal Supplement.* 2003;42:2s-9s.
184. Gunn W. Iron lungs save lives; cure for infantile paralysis. *Calcutta medical review.* 1946;13:9.
185. Aschenbrenner R, Donhardt A, Foth K. Permanent artificial respiration in the iron lung; report on experiences with 105 respirator paralyzed poliomyelitis patients from 1947 to 1952. *Munchener medizinische Wochenschrift (1950).* 1953;95(27):748-751; contd.

186. Gorham J. A medical triumph: the iron lung. *Respir Ther.* 1979;9(1):71-73.
187. Kenneth E. The iron lung and other equipment. 2011; http://amhistory.si.edu/polio/howpolio/ironlung.htm. Accessed June 20th, 2018.
188. Grasso F, Engelberts D, Helm E, et al. Negative-Pressure Ventilation. *American Journal of Respiratory and Critical Care Medicine.* 2008;177(4):412-418.
189. Luc JG, Bozso SJ, Freed DH, Nagendran J. Successful repair of donation after circulatory death lungs with large pulmonary embolus using the lung organ care system for ex vivo thrombolysis and subsequent clinical transplantation. *Transplantation.* 2015;99(1):e1-2.
190. Nakajima D, Cypel M, Bonato R, et al. Ex Vivo Perfusion Treatment of Infection in Human Donor Lungs. *Am J Transplant.* 2016;16(4):1229-1237.
191. Cypel M, Liu M, Rubacha M, et al. Functional repair of human donor lungs by IL-10 gene therapy. *Sci Transl Med.* 2009;1(4):4ra9.
192. Moore GE. Cramming more components onto integrated circuits. *Electronics.* 1965;38(8):1-6.
193. Badylak SF, Taylor D, Uygun K. Whole-organ tissue engineering: decellularization and recellularization of three-dimensional matrix scaffolds. *Annu Rev Biomed Eng.* 2011;13:27-53.
194. Ott HC, Matthiesen TS, Goh SK, et al. Perfusion-decellularized matrix: using nature's platform to engineer a bioartificial heart. *Nat Med.* 2008;14(2):213-221.
195. Ren X, Tapias LF, Jank BJ, Mathisen DJ, Lanuti M, Ott HC. Ex vivo non-invasive assessment of cell viability and proliferation in bio-engineered whole organ constructs. *Biomaterials.* 2015;52:103-112.
196. Wilson JG, Liu KD, Zhuo H, et al. Mesenchymal stem (stromal) cells for treatment of ARDS: a phase 1 clinical trial. *Lancet Respir Med.* 2015;3(1):24-32.
197. Ren X, Ott HC. On the road to bioartificial organs. *Pflugers Arch.* 2014;466(10):1847-1857.
198. Gennai S, Monsel A, Hao Q, Park J, Matthay MA, Lee JW. Microvesicles Derived From Human Mesenchymal Stem Cells Restore Alveolar Fluid Clearance in Human Lungs Rejected for Transplantation. *Am J Transplant.* 2015;15(9):2404-2412.
199. Walter J, Ware LB, Matthay MA. Mesenchymal stem cells: mechanisms of potential therapeutic benefit in ARDS and sepsis. *Lancet Respir Med.* 2014;2(12):1016-1026.
200. Mordant P, Nakajima D, Kalaf R, et al. Mesenchymal stem cell treatment is associated with decreased perfusate concentration of interleukin-8 during ex vivo perfusion of donor lungs after 18-hour preservation. *J Heart Lung Transplant.* 2016;35(10):1245-1254.
201. Konishi S, Gotoh S, Tateishi K, et al. Directed Induction of Functional Multi-ciliated Cells in Proximal Airway Epithelial Spheroids from Human Pluripotent Stem Cells. *Stem Cell Reports.* 2016;6(1):18-25.
202. Tane S, Noda K, Shigemura N. Ex Vivo Lung Perfusion: A Key Tool for Translational Science in the Lungs. *Chest.* 2017;151(6):1220-1228.
203. Warnecke G, Van Raemdonck D, Massard G, et al. (182) - The INSPIRE Lung International Trial Evaluating the Impact of Portable Ex-vivo Perfusion Using the Organ Care System (OCS™) Lung Technology on Routine Lung Transplant Outcomes. *The Journal of Heart and Lung Transplantation.* 2014;33(4, Supplement):S72.
204. Bozso S, Vasanthan V, Luc JGY, Kinaschuk K, Freed D, Nagendran J. Lung transplantation from donors after circulatory death using portable ex vivo lung perfusion.

Canadian Respiratory Journal : Journal of the Canadian Thoracic Society. 2015;22(1):47-51.
205. Warnecke G, Van Raemdonck D, Smith MA, et al. Normothermic ex-vivo preservation with the portable Organ Care System Lung device for bilateral lung transplantation (INSPIRE): a randomised, open-label, non-inferiority, phase 3 study. *The Lancet Respiratory Medicine.* 2018.
206. Warnecke G, Van Raemdonck D, Kukreja J, et al. (354) - Negative Impact of Ischemia on Short and Long Term Outcomes in Standard Criteria Double Lung Transplants Prospective Evidence from the OCS Lung INSPIRE International Trial Results. *The Journal of Heart and Lung Transplantation.* 2018;37(4, Supplement):S147.
207. Cantu E, Diamond JM, Suzuki Y, et al. Quantitative Evidence for Revising the Definition of Primary Graft Dysfunction after Lung Transplant. *Am J Respir Crit Care Med.* 2018;197(2):235-243.
208. Meyer KC, Raghu G, Verleden GM, et al. An international ISHLT/ATS/ERS clinical practice guideline: diagnosis and management of bronchiolitis obliterans syndrome. *Eur Respir J.* 2014;44(6):1479-1503.
209. Van Raemdonck D, Warnecke G, Kukreja J, et al. The EXPAND Lung International Trial to Evaluate the Safety and Effectiveness of the Portable Organ Care System (OCS™) Lung for Recruiting, Preserving and Assessing Expanded Criteria Donor Lungs for Transplantation. *The Journal of Heart and Lung Transplantation.* 2014;33(4):S17-S18.
210. Nilsson T, Gielis JF, Slama A, et al. Comparison of two strategies for ex vivo lung perfusion. *J Heart Lung Transplant.* 2017.
211. Loor G, Howard BT, Spratt JR, et al. Prolonged EVLP Using OCS Lung: Cellular and Acellular Perfusates. *Transplantation.* 2016.
212. Hartert M, Senbaklavaci Ö, Gohrbandt B, Fischer BM, Buhl R, Vahl C-F. Lung Transplantation: a Treatment Option in End-Stage Lung Disease. *Deutsches Ärzteblatt International.* 2014;111(7):107-116.
213. Yusen RD, Edwards LB, Kucheryavaya AY, et al. The registry of the International Society for Heart and Lung Transplantation: thirty-first adult lung and heart-lung transplant report--2014; focus theme: retransplantation. *J Heart Lung Transplant.* 2014;33(10):1009-1024.
214. Tao JQ, Sorokina EM, Vazquez Medina JP, et al. Onset of Inflammation With Ischemia: Implications for Donor Lung Preservation and Transplant Survival. *Am J Transplant.* 2016;16(9):2598-2611.
215. Van Raemdonck D. Thoracic organs: current preservation technology and future prospects; part 1: lung. *Curr Opin Organ Transplant.* 2010;15(2):150-155.
216. Snell GI, Griffiths A, Levvey BJ, Oto T. Availability of lungs for transplantation: exploring the real potential of the donor pool. *The Journal of heart and lung transplantation : the official publication of the International Society for Heart Transplantation.* 2008;27(6):662-667.
217. Botha P. Extended donor criteria in lung transplantation. *Current opinion in organ transplantation.* 2009;14(2):206-210.
218. Machuca TN, Cypel M. Ex vivo lung perfusion. *J Thorac Dis.* 2014;6(8):1054-1062.
219. Steen S, Sjoberg T, Pierre L, Liao Q, Eriksson L, Algotsson L. Transplantation of lungs from a non-heart-beating donor. *Lancet (London, England).* 2001;357(9259):825-829.

220. Sanchez P DRDoFWMCPCE, III, et al. Normothermic Ex Vivo Lung Perfusion as an Assessment of Marginal Donor Lungs—the NOVEL lung trial. *J Heart Lung Transplant.* 2013;32:1053-2498.
221. Warnecke G, Van Raemdonck D, Massard G, et al. The INSPIRE Lung International Trial Evaluating the Impact of Portable Ex-vivo Perfusion Using the Organ Care System (OCS™) Lung Technology on Routine Lung Transplant Outcomes. *The Journal of Heart and Lung Transplantation.*33(4):S72.
222. Mattison L, Spratt J, Howard B, et al. A Simplified Model for the Assessment of Ex Vivo Lung Perfusion Methodologies and Treatments1. *Journal of Medical Devices.* 2016;10(2):020960-020960-020962.
223. Park E-S, Kang D-H, Yang M-K, et al. Cordycepin, 3′-Deoxyadenosine, Prevents Rat Hearts from Ischemia/Reperfusion Injury Via Activation of Akt/GSK-3β/p70S6K Signaling Pathway and HO-1 Expression. *Cardiovascular Toxicology.* 2014;14(1):1-9.
224. Stowe DF, Camara AK, Heisner JS, Aldakkak M, Harder DR. Low-flow perfusion of guinea pig isolated hearts with 26 degrees C air-saturated Lifor solution for 20 hours preserves function and metabolism. *J Heart Lung Transplant.* 2008;27(9):1008-1015.
225. Steen S. Evaluation and preservation solution. In: Google Patents (US7255983 B2); 2007.
226. Emaminia A, LaPar DJ, Zhao Y, et al. Adenosine A2A Agonist Improves Lung Function During Ex Vivo Lung Perfusion. *The Annals of Thoracic Surgery.* 2011;92(5):1840-1846.
227. Luc JGY, Aboelnazar NS, Himmat S, et al. A Leukocyte Filter Does Not Provide Further Benefit During Ex Vivo Lung Perfusion. *ASAIO J.* 2017;63(5):672-678.
228. Fuller A, Mitchell G, Mitchell D. Non-thermal signals govern selective brain cooling in pigs. *J Comp Physiol B.* 1999;169(8):605-611.
229. Gronert GA. Malignant hyperthermia. *Anesthesiology.* 1980;53(5):395-423.
230. Hanneman SK, Jesurum-Urbaitis JT, Bickel DR. Comparison of methods of temperature measurement in swine. *Laboratory Animals.* 2004;38:297-306.
231. RCI. Temperature and Humidity Index for Pigs. 1957; https://www.heatstress.info/LostProduction/Wherefarmedanimalsbirdsaremostcomfortable/PigTHI.aspx. Accessed June 18, 2018.
232. Matute-Bello G, Downey G, Moore BB, et al. An official American Thoracic Society workshop report: features and measurements of experimental acute lung injury in animals. *Am J Respir Cell Mol Biol.* 2011;44(5):725-738.
233. Mehaffey JH, Charles EJ, Sharma AK, et al. Airway pressure release ventilation during ex vivo lung perfusion attenuates injury. *J Thorac Cardiovasc Surg.* 2017;153(1):197-204.
234. Loor G, Howard BT, Spratt JR, et al. Prolonged EVLP Using OCS Lung: Cellular and Acellular Perfusates. *Transplantation.* 2017;101(10):2303-2311.
235. Fischer S, Maclean AA, Liu M, et al. Dynamic changes in apoptotic and necrotic cell death correlate with severity of ischemia-reperfusion injury in lung transplantation. *Am J Respir Crit Care Med.* 2000;162(5):1932-1939.
236. Keshavjee S, Zhang XM, Fischer S, Liu M. Ischemia reperfusion-induced dynamic changes of protein tyrosine phosphorylation during human lung transplantation. *Transplantation.* 2000;70(3):525-531.

237. Knudsen L, Boxler L, Muhlfeld C, et al. Lung preservation in experimental ischemia/reperfusion injury and lung transplantation: a comparison of natural and synthetic surfactants. *J Heart Lung Transplant.* 2012;31(1):85-93.
238. Murray JF, Karp RB, Nadel JA. Viscosity effects on pressure-flow relations and vascular resistance in dogs' lungs. *J Appl Physiol.* 1969;27(3):336-341.
239. Nihill MR, McNamara DG, Vick RL. The effects of increased blood viscosity on pulmonary vascular resistance. *Am Heart J.* 1976;92(1):65-72.
240. Glenny RW, Bernard S, Robertson HT, Hlastala MP. Gravity is an important but secondary determinant of regional pulmonary blood flow in upright primates. *Journal of Applied Physiology.* 1999;86(2):623-632.
241. West JB, Dollery CT, Naimark A. Distribution of blood flow in isolated lung; relation to vascular and alveolar pressures. *Journal of Applied Physiology.* 1964;19(0021-8987 (Print)):713.
242. Wallinder A, Ricksten SE, Silverborn M, et al. Early results in transplantation of initially rejected donor lungs after ex vivo lung perfusion: a case-control study. *Eur J Cardiothorac Surg.* 2014;45(1):40-44; discussion 44-45.
243. Bozso S, Freed D, Nagendran J. Successful transplantation of extended criteria lungs after prolonged ex vivo lung perfusion performed on a portable device. *Transpl Int.* 2015;28(2):248-250.
244. Sanchez PG, Bittle GJ, Williams K, et al. Ex vivo lung evaluation of prearrest heparinization in donation after cardiac death. *Annals of Surgery.* 2013;257(3):534-541.
245. Inci I, Yamada Y, Hillinger S, Jungraithmayr W, Trinkwitz M, Weder W. Successful lung transplantation after donor lung reconditioning with urokinase in ex vivo lung perfusion system. *Ann Thorac Surg.* 2014;98(5):1837-1838.
246. Yeung JC, Wagnetz D, Cypel M, et al. Ex vivo adenoviral vector gene delivery results in decreased vector-associated inflammation pre- and post-lung transplantation in the pig. *Molecular therapy : the journal of the American Society of Gene Therapy.* 2012;20(6):1204-1211.
247. Gomez-de-Antonio D, Campo-Canaveral JL, Crowley S, et al. Clinical lung transplantation from uncontrolled non-heart-beating donors revisited. *J Heart Lung Transplant.* 2012;31(4):349-353.
248. Slama A, Schillab L, Barta M, et al. Standard donor lung procurement with normothermic ex vivo lung perfusion. A prospective randomized clinical trial. *The Journal of Heart and Lung Transplantation.* 2017.
249. Machuca TN, Cypel M, Yeung JC, et al. Protein expression profiling predicts graft performance in clinical ex vivo lung perfusion. *Annals of Surgery.* 2015;261(3):591-597.
250. Hoffman SA, Wang L, Shah CV, et al. Plasma cytokines and chemokines in primary graft dysfunction post-lung transplantation. *Am J Transplant.* 2009;9(2):389-396.
251. Oliver JC, Bland LA, Oettinger CW, et al. Cytokine kinetics in an in vitro whole blood model following an endotoxin challenge. *Lymphokine Cytokine Res.* 1993;12(2):115-120.
252. Iskender I, Cosgun T, Arni S, et al. Cytokine filtration modulates pulmonary metabolism and edema formation during ex vivo lung perfusion. *J Heart Lung Transplant.* 2018.
253. Kakishita T, Oto T, Hori S, et al. Suppression of inflammatory cytokines during ex vivo lung perfusion with an adsorbent membrane. *Ann Thorac Surg.* 2010;89(6):1773-1779.

254. Cypel M, Rubacha M, Yeung J, et al. Normothermic ex vivo perfusion prevents lung injury compared to extended cold preservation for transplantation. *Am J Transplant.* 2009;9(10):2262-2269.
255. Steinmeyer J, Becker S, Avsar M, et al. Cellular and acellular ex vivo lung perfusion preserve functional lung ultrastructure in a large animal model: a stereological study. *RESPIRATORY RESEARCH.* 2018;19(1):238.
256. Barker CE, Ali S, O'Boyle G, Kirby JA. Transplantation and inflammation: implications for the modification of chemokine function. *Immunology.* 2014;143(2):138-145.
257. Nilsson T, Hansson C, Wallinder A, et al. Hemofiltration in ex vivo lung perfusion-a study in experimentally induced pulmonary edema. *J Thorac Cardiovasc Surg.* 2016;151(2):570-575 e571.
258. Linacre V, Cypel M, Machuca T, et al. Importance of left atrial pressure during ex vivo lung perfusion. *J Heart Lung Transplant.* 2016;35(6):808-814.
259. Losa Garcia JE, Rodriguez FM, Martin de Cabo MR, et al. Evaluation of inflammatory cytokine secretion by human alveolar macrophages. *Mediators Inflamm.* 1999;8(1):43-51.
260. Price LC, McAuley DF, Marino PS, Finney SJ, Griffiths MJ, Wort SJ. Pathophysiology of pulmonary hypertension in acute lung injury. *Am J Physiol Lung Cell Mol Physiol.* 2012;302(9):L803-815.
261. Vasanthan V, Nagendran J. Compliance trumps oxygenation: Predicting quality with ex vivo lung perfusion. *The Journal of thoracic and cardiovascular surgery.* 2015;150(5):1378-1379.
262. Wierup P, Haraldsson Å, Nilsson F, et al. Ex Vivo Evaluation of Nonacceptable Donor Lungs. *The Annals of Thoracic Surgery.* 2006;81(2):460-466.
263. Valenza F, Rosso L, Coppola S, et al. Ex vivo lung perfusion to improve donor lung function and increase the number of organs available for transplantation. *Transplant International.* 2014;27(6):553-561.
264. Luc JG, Aboelnazar NS, Himmat S, et al. A Leukocyte Filter Does Not Provide Further Benefit During Ex Vivo Lung Perfusion. *ASAIO J.* 2017.
265. Collins J SE. *Chest radiology: the essentials.* 2nd ed. ed. Philadelphia :: Wolters Kluwer Health/Lippincott Williams & Wilkins; 2008.
266. Stern EJ, Frank MS. CT of the lung in patients with pulmonary emphysema: diagnosis, quantification, and correlation with pathologic and physiologic findings. *American Journal of Roentgenology.* 1994;162(4):791-798.
267. Wiese ER. Bulla of the lung. *Chest.* 1946;12(3):238-241.
268. Terragni PP, Fanelli V, Boffini M, et al. Ventilatory Management During Normothermic Ex Vivo Lung Perfusion: Effects on Clinical Outcomes. *Transplantation.* 2016;100(5):1128-1135.
269. Charest JM, Okamoto T, Kitano K, et al. Design and validation of a clinical-scale bioreactor for long-term isolated lung culture. *Biomaterials.* 2015;52:79-87.
270. Ingemansson RB, A.; Bolys, R.; Sjoberg, T.; and Steen, S. Effect of Flush-Perfusion on Vascular Endothelial and Smooth Muscle Function. *Ann Thorac Surg.* 1997;64:1075-1081.
271. Ardehali A, Warnecke G, Van Raemdonck D, et al. (164) - Impact of OCS Lung Portable EVLP on Pulmonary Function and Bronchiolitis Obliterans in Standard Lung Transplant

Recipients - Prospective Evidence from the OCS Lung INSPIRE Trial Patients. *The Journal of Heart and Lung Transplantation.* 2016;35(4, Supplement):S69.
272. Warnecke G, Haverich A, Massard G, et al. 322 The INSPIRE International Lung Trial with the Organ Care System Technology (OCS™). *The Journal of Heart and Lung Transplantation.* 2012;31(4, Supplement):S115.
273. Warnecke G, Van Raemdonck D, Kukreja J, et al. (19) - Mid and Long-Term Clinical Results of OCS Lung INSPIRE International Trial. *The Journal of Heart and Lung Transplantation.* 2016;35(4, Supplement):S15-S16.
274. Warnecke G, Van Raemdonck D, Smith M, et al. (242) - The Organ Care System (OCS™) Lung INSPIRE International Trial Results. *The Journal of Heart and Lung Transplantation.* 2015;34(4, Supplement):S96.
275. Warnecke G, Weigmann B, Van Raemdonck D, et al. The INSPIRE International Lung Trial with the Organ Care System Technology (OCS™). *The Journal of Heart and Lung Transplantation.* 2013;32(4, Supplement):S16.
276. Sanchez PG, Rajagopal K, Pham SM, Griffith BP. Defining quality during ex vivo lung perfusion: The University of Maryland experience. *The Journal of thoracic and cardiovascular surgery.* 2015;150(5):1376-1377.
277. Vasanthan V, Nagendran J. Compliance trumps oxygenation: Predicting quality with ex vivo lung perfusion. *J Thorac Cardiovasc Surg.* 2015;150(5):1378-1379.
278. Roman MA, Nair S, Tsui S, Dunning J, Parmar JS. Ex vivo lung perfusion: a comprehensive review of the development and exploration of future trends. *Transplantation.* 2013;96(6):509-518.
279. Noda K, Shigemura N, Tanaka Y, et al. Successful prolonged ex vivo lung perfusion for graft preservation in rats. *Eur J Cardiothorac Surg.* 2014;45(3):e54-60.
280. Noda K, Tane S, Haam SJ, et al. Targeting Circulating Leukocytes and Pyroptosis During Ex Vivo Lung Perfusion Improves Lung Preservation. *Transplantation.* 2017;101(12):2841-2849.
281. Meers CM, Tsagkaropoulos S, Wauters S, et al. A model of ex vivo perfusion of porcine donor lungs injured by gastric aspiration: a step towards pretransplant reconditioning. *J Surg Res.* 2011;170(1):e159-167.
282. Charles EJ, Huerter ME, Wagner CE, et al. Donation After Circulatory Death Lungs Transplantable Up to Six Hours After Ex Vivo Lung Perfusion. *Ann Thorac Surg.* 2016;102(6):1845-1853.
283. Kondo T, Chen F, Ohsumi A, et al. beta2-Adrenoreceptor Agonist Inhalation During Ex Vivo Lung Perfusion Attenuates Lung Injury. *Ann Thorac Surg.* 2015;100(2):480-486.
284. Wagner CE, Pope NH, Charles EJ, et al. Ex vivo lung perfusion with adenosine A2A receptor agonist allows prolonged cold preservation of lungs donated after cardiac death. *The Journal of Thoracic and Cardiovascular Surgery.* 2016;151(2):538-546.
285. Yamada T, Chen F, Sakamoto J, et al. 509: Injury of Donor Lungs from Donation after Cardiac Death in Various Settings; Investigation by RT-PCR and Pathology. *The Journal of Heart and Lung Transplantation.* 2010;29(2):S166.
286. Cypel M, Yeung JC, Keshavjee S. Novel approaches to expanding the lung donor pool: donation after cardiac death and ex vivo conditioning. *Clin Chest Med.* 2011;32(2):233-244.
287. Cypel M, Pierre A, Yasufuku K, et al. 5 Years Experience with Lung Donation after Cardiac Death. *The Journal of Heart and Lung Transplantation.* 2012;31(4):S116.

288. Cypel M, Keshavjee S. Strategies for safe donor expansion: donor management, donations after cardiac death, ex-vivo lung perfusion. *Curr Opin Organ Transplant.* 2013;18(5):513-517.
289. Cypel M, Yeung JC, de Perrot M, et al. Ex Vivo Lung Perfusion in Clinical Lung Transplantation - The HELP Trial. *The Journal of Heart and Lung Transplantation.* 2010;29(2):S88.
290. Iscra F, Gullo A, Biolo G. Bench-to-bedside review: Lactate and the lung. *Critical Care.* 2002;6(4):327-329.
291. Valenza F, Rosso L, Pizzocri M, et al. The Consumption of Glucose During Ex Vivo Lung Perfusion Correlates With Lung Edema. *Transplantation Proceedings.* 2011;43(4):993-996.
292. Koike T, Yeung JC, Cypel M, et al. Kinetics of lactate metabolism during acellular normothermic ex vivo lung perfusion. *J Heart Lung Transplant.* 2011;30(12):1312-1319.
293. Meduri GU, Kohler G, Headley S, Tolley E, Stentz F, Postlethwaite A. Inflammatory cytokines in the BAL of patients with ARDS. Persistent elevation over time predicts poor outcome. . *Chest.* 1995;108:1303-1314.
294. Parsons PE, Eisner MD, Thompson BT, et al. Lower tidal volume ventilation and plasma cytokine markers of inflammation in patients with acute lung injury. *Crit Care Med.* 2005;33(1-6):230-232.
295. Asavarut P, Zhao H, Gu J, Ma D. The role of HMGB1 in inflammation-mediated organ injury. *Acta Anaesthesiol Taiwan.* 2013;51(1):28-33.
296. Ding HS, Yang J, Chen P, et al. The HMGB1-TLR4 axis contributes to myocardial ischemia/reperfusion injury via regulation of cardiomyocyte apoptosis. *Gene.* 2013;527(1):389-393.
297. Hashimoto K, Cypel M, Kim H, et al. Soluble Adhesion Molecules During Ex Vivo Lung Perfusion Are Associated With Posttransplant Primary Graft Dysfunction. *American Journal of Transplantation.* 2017.
298. Land W, Schneeberger H, Schleibner S, et al. The beneficial effect of human recombinant superoxide dismutase on acute and chronic rejection events in recipients of cadaveric renal transplants. *Transplantation.* 1994;57(2):211-217.
299. Land WG. Transfusion-Related Acute Lung Injury: The Work of DAMPs. *Transfus Med Hemother.* 2013;40(1):3-13.
300. Land WG, Agostinis P, Gasser S, Garg AD, Linkermann A. Transplantation and Damage-Associated Molecular Patterns (DAMPs). *Am J Transplant.* 2016;16(12):3338-3361.
301. Mukhopadhyay S, Hoidal JR, Mukherjee TK. Role of TNFalpha in pulmonary pathophysiology. *Respir Res.* 2006;7:125.
302. Rahbar E, Cardenas JC, Baimukanova G, et al. Endothelial glycocalyx shedding and vascular permeability in severely injured trauma patients. *J Transl Med.* 2015;13:117.
303. Shadi Shafaghi EM, Azizollah Abbasi Dezfuli, Hoda Gudarzi, Kambiz Sheikhy,, Zahra Ansari Aval BF, Habib Emami, Fatemeh Sadat Hosseini-Baharanchi,, Najafizadeh aK. Normothermic Ex Vivo Lung Perfusion in Brain-dead Donors Reduces Inflammatory Cytokines and Toll-like Receptor Expression. *Iran Journal Allergy Asthma Immunology.* 2016;15(5):340-354.

304. Todd JL, Wang X, Sugimoto S, et al. Hyaluronan contributes to bronchiolitis obliterans syndrome and stimulates lung allograft rejection through activation of innate immunity. *Am J Respir Crit Care Med.* 2014;189(5):556-566.
305. Van Den Berg BM, Nieuwdorp M, Stroes ES, Vink H. Glycocalyx and endothelial (dys) function: from mice to men. *Pharmacol Rep.* 2006;58 Suppl:75-80.
306. Weber DJ, Allette YM, Wilkes DS, White FA. The HMGB1-RAGE Inflammatory Pathway: Implications for Brain Injury-Induced Pulmonary Dysfunction. *Antioxid Redox Signal.* 2015;23(17):1316-1328.
307. Hamilton BC, Kukreja J, Ware LB, Matthay MA. Protein biomarkers associated with primary graft dysfunction following lung transplantation. *Am J Physiol Lung Cell Mol Physiol.* 2017;312(4):L531-L541.
308. Seong SY, Matzinger P. Hydrophobicity: an ancient damage-associated molecular pattern that initiates innate immune responses. *Nat Rev Immunol.* 2004;4(6):469-478.
309. Nieuwdorp M, Meuwese MC, Vink H, Hoekstra JB, Kastelein JJ, Stroes ES. The endothelial glycocalyx: a potential barrier between health and vascular disease. *Curr Opin Lipidol.* 2005;16(5):507-511.
310. Alphonsus CS, Rodseth RN. The endothelial glycocalyx: a review of the vascular barrier. *Anaesthesia.* 2014;69(7):777-784.
311. Maksimenko AV. Translational research into vascular wall function: regulatory effects of systemic and specific factors. *Journal of Translational Science.* 2017;3(3).
312. Maksimenko AV, Turashev AD. No-reflow phenomenon and endothelial glycocalyx of microcirculation. *Biochemistry Research International.* 2012;2012(2090-2255 (Electronic)):10.
313. Held HD, Boettcher S, Hamann L, Uhlig S. Ventilation-induced chemokine and cytokine release is associated with activation of nuclear factor-kappaB and is blocked by steroids. *Am J Respir Crit Care Med.* 2001;163(3 Pt 1):711-716.
314. Horvath B, Hegedus D, Szapary L, et al. Measurement of von Willebrand factor as the marker of endothelial dysfunction in vascular diseases. *Exp Clin Cardiol.* 2004;9(1):31-34.
315. Park HS, Kim JE, You HJ, et al. Beneficial effect of a nitric oxide donor in an ex vivo model of pig-to-human pulmonary xenotransplantation. *Xenotransplantation.* 2015;22(5):391-398.
316. Kim HK, Kim JE, Wi HC, et al. Aurintricarboxylic acid inhibits endothelial activation, complement activation, and von Willebrand factor secretion in vitro and attenuates hyperacute rejection in an ex vivo model of pig-to-human pulmonary xenotransplantation. *Xenotransplantation.* 2008;15(4):246-256.
317. Pfeiffer S, Zorn GL, 3rd, Zhang JP, et al. Hyperacute lung rejection in the pig-to-human model. III. Platelet receptor inhibitors synergistically modulate complement activation and lung injury. *Transplantation.* 2003;75(7):953-959.
318. El Basset Abo El Ezz AA, Abd El Hafez MA, El Amrousy DM, El Momen Suliman GA. The predictive value of Von Willebrand factor antigen plasma levels in children with acute lung injury. *Pediatr Pulmonol.* 2017;52(1):91-97.
319. Ware LB, Conner ER, Matthay MA. von Willebrand factor antigen is an independent marker of poor outcome in patients with early acute lung injury. *Crit Care Med.* 2001;29(12):2325-2331.

320. Andreasson A, Karamanou DM, Perry JD, et al. The effect of ex vivo lung perfusion on microbial load in human donor lungs. *J Heart Lung Transplant.* 2014;33(9):910-916.
321. LaPar DJ, Laubach VE, Emaminia A, et al. Pretreatment strategy with adenosine A2A receptor agonist attenuates reperfusion injury in a preclinical porcine lung transplantation model. *J Thorac Cardiovasc Surg.* 2011;142(4):887-894.
322. Valenza F, Rosso L, Coppola S, et al. beta-adrenergic agonist infusion during extracorporeal lung perfusion: effects on glucose concentration in the perfusion fluid and on lung function. *J Heart Lung Transplant.* 2012;31(5):524-530.
323. Hsu Patrick D, Lander Eric S, Zhang F. Development and Applications of CRISPR-Cas9 for Genome Engineering. *Cell.* 2014;157(6):1262-1278.
324. Machuca TN, Cypel M, Bonato R, et al. Safety and Efficacy of Ex Vivo Donor Lung Adenoviral IL-10 Gene Therapy in a Large Animal Lung Transplant Survival Model. *Hum Gene Ther.* 2017;28(9):757-765.
325. Joseph M Rutkowski1 NH, Qiong A Wang1, William L Holland1, Jonathan Y Xia1 and Philipp E Scherer1,2*. Differential transendothelial transport of adiponectin complexes. *Cardiovascular Diabetology.* 2014;13(47):1-14.
326. Ouedraogo R, Gong Y, Berzins B, et al. Adiponectin deficiency increases leukocyte-endothelium interactions via upregulation of endothelial cell adhesion molecules in vivo. *J Clin Invest.* 2007;117(6):1718-1726.
327. Vaiopoulos AG, Marinou K, Christodoulides C, Koutsilieris M. The role of adiponectin in human vascular physiology. *Int J Cardiol.* 2012;155(2):188-193.
328. Barrangou R, Fremaux C, Deveau H, et al. CRISPR provides acquired resistance against viruses in prokaryotes. *Science.* 2007;315(5819):1709-1712.
329. Capecchi MR. Altering the genome by homologous recombination. *Science.* 1989;244(4910):1288-1292.
330. Damian M, Porteus MH. A crisper look at genome editing: RNA-guided genome modification. *Mol Ther.* 2013;21(4):720-722.
331. Soni D, Wang DM, Regmi SC, et al. Deubiquitinase function of A20 maintains and repairs endothelial barrier after lung vascular injury. *Cell Death Discov.* 2018;4:60.
332. Petersen TH, Calle EA, Zhao L, et al. Tissue-engineered lungs for in vivo implantation. *Science.* 2010;329(5991):538-541.
333. Ott HC, Clippinger B, Conrad C, et al. Regeneration and orthotopic transplantation of a bioartificial lung. *Nat Med.* 2010;16(8):927-933.
334. Gilpin SE, Guyette JP, Gonzalez G, et al. Perfusion decellularization of human and porcine lungs: Bringing the matrix to clinical scale. *The Journal of Heart and Lung Transplantation.* 2014;33(3):298-308.
335. Dorrello NV, Guenthart BA, O'Neill JD, et al. Functional vascularized lung grafts for lung bioengineering. *Sci Adv.* 2017;3(8):e1700521.
336. Ren X, Moser PT, Gilpin SE, et al. Engineering pulmonary vasculature in decellularized rat and human lungs. *Nature Biotechnology.* 2015;33:1097.
337. Gilpin SE, Charest JM, Ren X, Ott HC. Bioengineering Lungs for Transplantation. *Thorac Surg Clin.* 2016;26(2):163-171.
338. Kottamasu P, Herman I. Engineering a microcirculation for perfusion control of ex vivo–assembled organ systems: Challenges and opportunities. *Journal of Tissue Engineering.* 2018;9:1-16.

339. Nichols JE, La Francesca S, Niles JA, et al. Production and transplantation of bioengineered lung into a large-animal model. *Science Translational Medicine.* 2018;10.
340. Li J, Regli WC, Sun W. An approach to integrating shape and biomedical attributes in vascular models. *Computer-Aided Design.* 2007;39(7):598-609.
341. Nam J, Starly B, Darling A, Sun W. Computer Aided Tissue Engineering for Modeling and Design of Novel Tissue Scaffolds. *Computer-Aided Design and Applications.* 2004;1(1-4):633-640.
342. Sun W, Darling A, Starly B, Nam J. Computer-aided tissue engineering: overview, scope and challenges. *Biotechnol Appl Biochem.* 2004;39(Pt 1):29-47.
343. Sun W, Starly B, Darling A, Gomez C. Computer-aided tissue engineering: application to biomimetic modelling and design of tissue scaffolds. *Biotechnol Appl Biochem.* 2004;39(Pt 1):49-58.
344. Knowlton S, Yenilmez B, Tasoglu S. Towards Single-Step Biofabrication of Organs on a Chip via 3D Printing. *Trends Biotechnol.* 2016;34(9):685-688.
345. Hamet P, Tremblay J. Artificial intelligence in medicine. *Metabolism.* 2017;69:S36-S40.
346. Merriam-Webster. "Artificial Intelligence". 2018; https://www.merriam-webster.com/dictionary/artificialintelligence. Accessed August 26, 2018.
347. Merriam-Webster. "Medicine". 2018; https://www.merriam-webster.com/dictionary/medicine. Accessed August 26, 2018.
348. Williams AM, Liu Y, Regner KR, Jotterand F, Liu P, Liang M. Artificial intelligence, physiological genomics, and precision medicine. *Physiol Genomics.* 2018;50(4):237-243.
349. Silver D, Schrittwieser J, Simonyan K, et al. Mastering the game of Go without human knowledge. *Nature.* 2017;550:354.
350. Combi C. Editorial from the new Editor-in-Chief: Artificial Intelligence in Medicine and the forthcoming challenges. *Artificial Intelligence in Medicine.* 2017;76:37-39.
351. Patel VL, Shortliffe EH, Stefanelli M, et al. The coming of age of artificial intelligence in medicine. *Artif Intell Med.* 2009;46(1):5-17.
352. Chang AC. Big data in medicine: The upcoming artificial intelligence. *Progress in Pediatric Cardiology.* 2016;43:91-94.
353. Alanazi HO, Abdullah AH, Qureshi KN. A Critical Review for Developing Accurate and Dynamic Predictive Models Using Machine Learning Methods in Medicine and Health Care. *J Med Syst.* 2017;41(4):69.
354. Putzer D, Klug S, Moctezuma JL, Nogler M. The use of time-of-flight camera for navigating robots in computer-aided surgery: monitoring the soft tissue envelope of minimally invasive hip approach in a cadaver study. *Surg Innov.* 2014;21(6):630-636.
355. Ramesh AN, Kambhampati C, Monson JR, Drew PJ. Artificial intelligence in medicine. *Ann R Coll Surg Engl.* 2004;86(5):334-338.
356. Miller PL. The evaluation of artificial intelligence systems in medicine. *Comput Methods Programs Biomed.* 1986;22(1):5-11.
357. Negrete-Martinez J. From artificial intelligence to the teaching of medicine. *Gac Med Mex.* 1977;113(8):385-386.
358. Somashekhar SP, Sepulveda MJ, Puglielli S, et al. Watson for Oncology and breast cancer treatment recommendations: agreement with an expert multidisciplinary tumor board. *Ann Oncol.* 2018;29(2):418-423.

359. Magazine AS. IBM's Watson Detected Rare Leukemia In Just 10 Minutes. 2016; https://www.asianscientist.com/2016/08/topnews/ibm-watson-rare-leukemia-university-tokyo-artificial-intelligence/. Accessed August 26, 2018.
360. Esteva A, Kuprel B, Novoa RA, et al. Dermatologist-level classification of skin cancer with deep neural networks. *Nature.* 2017;542(7639):115-118.
361. Gulshan V, Peng L, Coram M, et al. Development and Validation of a Deep Learning Algorithm for Detection of Diabetic Retinopathy in Retinal Fundus Photographs. *JAMA.* 2016;316(22):2402-2410.
362. Weng S, Reps J, Kai J, Garibaldi J, Qureshi N. Can machine learning improve cardiovascular risk prediction using routine clinical data? . *PLoS One* 2017;12(4):e0174944.
363. Gleichgerrcht E, Munsell B, Bhatia S, et al. Deep learning applied to whole-brain connectome to determine seizure control after epilepsy surgery. *Epilepsia.* 2018.
364. Holder LB, Haque MM, Skinner MK. Machine learning for epigenetics and future medical applications. *Epigenetics.* 2017;12(7):505-514.
365. Libbrecht MW, Noble WS. Machine learning applications in genetics and genomics. *Nat Rev Genet.* 2015;16(6):321-332.
366. Kelchtermans P, Bittremieux W, De Grave K, et al. Machine learning applications in proteomics research: how the past can boost the future. *Proteomics.* 2014;14(4-5):353-366.
367. Dasta JF. Application of artificial intelligence to pharmacy and medicine. *Hosp Pharm.* 1992;27(4):312-315, 319-322.
368. Colyer SL, Evans M, Cosker DP, Salo AIT. A Review of the Evolution of Vision-Based Motion Analysis and the Integration of Advanced Computer Vision Methods Towards Developing a Markerless System. *Sports Medicine - Open.* 2018;4(1):24.
369. Sonka M, Hlavac V, Boyle R. 3D Vision. In: Sonka M, Hlavac V, Boyle R, eds. *Image Processing, Analysis and Machine Vision.* Boston, MA: Springer US; 1993:373-421.
370. De Fauw J, Ledsam JR, Romera-Paredes B, et al. Clinically applicable deep learning for diagnosis and referral in retinal disease. *Nature Medicine.* 2018.
371. Bluemke DA. Radiology in 2018: Are You Working with AI or Being Replaced by AI? *Radiology.* 2018;287(2):365-366.
372. Wang Y, Qiu Y, Thai T, Moore K, Liu H, Zheng B. A two-step convolutional neural network based computer-aided detection scheme for automatically segmenting adipose tissue volume depicting on CT images. *Comput Methods Programs Biomed.* 2017;144:97-104.
373. Dilsizian SE, Siegel EL. Artificial intelligence in medicine and cardiac imaging: harnessing big data and advanced computing to provide personalized medical diagnosis and treatment. *Curr Cardiol Rep.* 2014;16(1):441.
374. Yang S, Nam Y, Kim MO, Kim EY, Park J, Kim DH. Computer-aided detection of metastatic brain tumors using magnetic resonance black-blood imaging. *Invest Radiol.* 2013;48(2):113-119.
375. Nakayama R, Watanabe R, Namba K, et al. An improved computer-aided diagnosis scheme using the nearest neighbor criterion for determining histological classification of clustered microcalcifications. *Methods Inf Med.* 2007;46(6):716-722.